

Imperial College London
National Heart and Lung Institute
Vascular Sciences Section

**The transcription factor ERG mediates multiple
endothelial signalling pathways required for
angiogenesis**

Aarti Shah

Supervisor: Professor Anna Randi
Co-supervisor: Dr Graeme Birdsey

This thesis is submitted to Imperial College London for the
degree of Doctor of Philosophy (PhD)

Declaration of originality

I, Aarti Shah, confirm that the work presented in this thesis is my own. Where information has been derived from other sources, I confirm that this has been indicated in the thesis.

The copyright of this thesis rests with the author and is made available under a Creative Commons Attribution Non-Commercial No Derivatives licence. Researchers are free to copy, distribute or transmit the thesis on the condition that they attribute it, that they do not use it for commercial purposes and that they do not alter, transform or build upon it. For any reuse or redistribution, researchers must make clear to others the licence terms of this work.

For my Family

Abstract

ERG is a crucial regulator of endothelial gene expression and controls endothelial functions including cell survival and monolayer permeability. Previous studies indicate a role for ERG in angiogenesis and vascular development, however the pathways through which ERG controls angiogenesis are unclear. Transcriptome profiling comparing ERG-positive and ERG-deficient endothelial cells has previously shown that ERG controls a network of genes that are essential to angiogenesis. This analysis identified genes involved in the Wnt, Notch and Angiopoietin1/Tie2 signalling pathways as candidate ERG targets.

ERG has been shown to drive expression of the junction molecule vascular endothelial (VE)-cadherin, which binds β -catenin, a crucial mediator of Wnt signalling, at the cell membrane. Here, I show that ERG controls β -catenin stability, by driving expression of both VE-cadherin and the Wnt receptor Frizzled-4- the balance of which regulates β -catenin localisation and activity. ERG promotes angiogenesis via Wnt/ β -catenin signalling, since activation of Wnt signalling with lithium chloride, which stabilises β -catenin, corrects the angiogenic defect in ERG-deficient endothelial cells.

The Notch signalling pathway is critical for promoting vascular quiescence and I demonstrate that ERG controls Notch signalling by regulating the levels of two Notch ligands, Delta like ligand (Dll)-4 and Jagged-1, with reported opposing roles in the vasculature. ERG simultaneously drives expression of pro-quiescent Dll4 and represses expression of pro-angiogenic Jagged-1, which has been shown to antagonize Dll4-mediated signalling.

The Angiopoietin1/Tie2 pathway, also connected to the Wnt and Notch pathways, is a regulatory growth factor system essential for vessel maturation and quiescence. The results from this thesis suggest that ERG mediates growth factor Angiopoietin-1-dependent signals and ERG is required for Angiopoietin-1-induced Notch and Wnt signalling.

Thus, ERG is able to integrate with three signalling pathways controlling vascular growth and stability - Wnt, Notch, Angiopoietin1/Tie2- which may function downstream of ERG to regulate blood vessel patterning during angiogenesis.

Publications arising from this thesis

Birdsey, G.M.^{*}, **Shah, A.V.^{*}**, Dufton, N., Reynolds, L.E., Osuna Almagro, L., Yang, Y., Aspalter, I.M., Khan, S.T., Mason, J.C., Dejana, E., Göttgens, B., Hodivala-Dilke, K., Gerhardt, H., Adams, R.H. and Randi, A.M. (2015). The endothelial transcription factor ERG promotes vascular stability and growth through Wnt/ β -catenin signaling. *Dev Cell* 32, 82-96. (see Appendix 2)

^{*} Co-first author

Shah, A.V., Birdsey, G.M., Pitulescu, M., Yang, Y., Osuna Almagro, L., Mason, J.C., Adams, R.H. and Randi, A.M. (2014). Angiopoietin-1 modulates endothelial cell function and gene expression via the transcription factor ERG (*manuscript in preparation*).

Acknowledgments

I would like to thank the National Heart and Lung Institute Foundation and British Heart Foundation for funding this research and to Professor Dorian Haskard for providing laboratory research facilities in the BHF Vascular Sciences department.

I would like to express my special appreciation and gratitude to my supervisor, Professor Anna Randi, for her superb supervision, guidance and encouragement. She has been a tremendous mentor and I have learnt a great deal from Anna both scientifically and professionally. I was very lucky to benefit from her rich expertise and constructive comments that built my scientific proficiency. The joy and enthusiasm she has for science was contagious and motivational for me, even during tough times in the PhD pursuit. I would like to thank her for encouraging me and for allowing me to grow as a research scientist.

Special thanks goes to Dr Graeme Birdsey, or so-called ‘Google ERG’, for his supervision and guidance in the lab. He is consistently patient and always willing to help, which I feel very lucky to have benefitted from during my time in the group. I have enjoyed the opportunity to learn from his knowledge and experience. I am grateful for his friendship and am very proud of the paper we have published together.

I would also like to acknowledge Professor Elisabetta Dejana, Professor Ralf Adams and Dr Holger Gerhardt for their scientific collaboration, advice and technical expertise.

I am especially grateful to past and present members of the group for providing a special environment to work in and making my time in the lab so enjoyable. When things weren’t going smoothly, I was so thankful to have been surrounded by good friends who made it much easier to keep going. I would like to thank Richard Starke, for being my lab bay buddy and his daily entertainment in the lab; Koralia Paschalaki for her positive outlook and endless encouragement; Neil Dufton, for his guidance, humour, fun facts and grumpiness; Lourdes Osuna Almagro for her support, gossiping and ‘floopy’ moments, Youwen Yang for his concern and advice, Koval Smith and Luke ‘Lennie’ Payne for making my final year so enjoyable by goofing around and putting the world to rights; Silvia Martin Almedina for her laughter, support and happy

personality, Nicky Dryden for her calm demeanour and humour, Andrea Sperone for his guidance and friendly nature.

I would also like to express thanks to all my colleagues at Hammersmith, in particular, Professor Justin Mason, Dr Joe Boyle and Mike Johns for the helpful discussions and technical expertise; Danuta Mahiouz for her support and I am especially grateful to Hayley Mylroie, Nicky Ambrose, Amalia De Luca, Niall Burke, Karl Lawrence, Mikhael Caga-Anan, Enrico Tombetti and Ignasi Moran Castany for their friendship, support and for being my stress release.

Thank you to Paras for his love, understanding, and faithful support. He has always believed in me and has offered reassurance throughout these three years. A heartfelt thank you goes to my wonderful parents, who have given me the strength to reach for the stars. I am extremely fortunate to receive so much love and unwavering support from them in all my pursuits, which is the foundation of my achievements. From an early age they instilled in me a desire to learn and without their sacrifices, support and guidance I would not be where I am today. To dad, my hero, who didn't get to see me finish my PhD, but whose love is still my guide and is always at my side. To mum, my rock, my inspiration, whom I'd be lost without.

Table of Contents

Abstract	5
Publications arising from this thesis	6
Acknowledgments	7
Table of contents	9
List of figures	14
List of tables	18
Abbreviations	19
1. Chapter 1: Introduction	22
1.1 The vascular system	23
1.2 Mechanisms of angiogenesis	26
1.2.1 Cellular and molecular mechanisms involved in vessel sprouting	29
1.2.2 Cellular and molecular mechanisms involved in vascular stability	31
1.2.2.1 Endothelial cell junctions maintain vessel integrity	32
1.2.2.2 Pericyte recruitment to the endothelium stabilises vessels	36
1.3 Transcriptional pathways regulating gene expression in angiogenesis	37
1.4 ETS family of transcription factors	38
1.4.1 Structure of the ETS transcription factors	38
1.4.2 Expression and biological functions of the ETS transcription factors....	41
1.4.3 ETS factors in the endothelium	41
1.5 ETS related gene ERG	43
1.5.1 Expression of ERG	43
1.5.2 ERG genomic structure and isoforms	44
1.5.3 DNA binding activity of ERG and domains of the ERG protein	46
1.5.4 ERG binding partners	48
1.5.5 Dysregulation of ERG in cancer	48
1.5.6 ERG and its role in the endothelium: lineage specification and homeostasis.....	50
1.5.6.1 ERG and its role in EC differentiation	50
1.5.6.2 ERG and its function in EC homeostasis	50
1.5.6.3 ERG as a repressor of inflammation	51
1.5.7 Regulation of vascular development and angiogenesis by ERG	53

1.5.7.1 ERG is required for vascular development	53
1.5.7.2 ERG controls postnatal retinal angiogenesis	55
1.5.7.3 Endothelial deletion of ERG impairs tumour angiogenesis and growth.....	55
1.5.7.4 ERG regulates vessel formation and stability in Matrigel angiogenesis models	56
1.5.7.5 ERG is required for vascular development in the zebrafish	56
1.6 Future perspectives	57
2. Chapter 2: Materials and Methods	58
2.1. HUVEC isolation	59
2.2 Cell culture	59
2.3 Delivery of ERG-specific antisense oligonucleotides in HUVEC	59
2.4 Pharmacological/ growth factor <i>in vitro</i> cell treatments	60
2.5 DLL4 stimulation of endothelial cells	61
2.6 Isolation of mouse lung endothelial cells	61
2.7 Adenovirus amplification and titration	61
2.8 Adenoviral transduction of HUVEC	61
2.9 RNA isolation from HUVEC and mouse tissue	62
2.10 First-Strand cDNA synthesis	62
2.11 Quantitative real-time PCR	63
2.12 Agarose Gel Electrophoresis	64
2.13 Immunofluorescence analysis of HUVEC	64
2.14 Immunofluorescence of mouse retina tissue	65
2.15 Immunoblotting	66
2.15.1 Preparation of total cell lysates	66
2.15.2 Preparation of nuclear and cytosolic cell fraction lysates	66
2.15.3 Sodium Dodecyl Sulphate Polyacrylamide Gel Electrophoresis	66
2.16 Co-immunoprecipitation assays	67
2.17 Chromatin immunoprecipitation- qPCR	68
2.18 Plasmids	70
2.19 Plasmid construction	70
2.19.1 PCR Amplification and Digestion	70
2.19.2 Cloning and Vector Preparation	71

2.20 Transfections	71
2.21 Luciferase assays	71
2.22 Chromatin immunoprecipitation- sequencing	72
2.23 Bioinformatics analysis	73
2.24 Gene set enrichment analysis	73
2.25 Gene ontology analysis	74
2.26 Fibrin gel bead assay	74
2.26.1 Quantification of sprouts <i>in vitro</i>	74
2.27 BrdU <i>in vitro</i> proliferation assay	74
2.28 Apoptosis assay	75
2.29 Data analysis	75
3. Chapter 3: ERG controls multiple pathways required for vessel growth and stability: Wnt/β-catenin pathway.....	76
3.1 Introduction	77
3.1.1 Wnt signalling	77
3.1.2 β -catenin: a mediator of cell adhesion and canonical Wnt signalling in EC	77
3.1.3 Wnt/ β -catenin signalling in the vasculature	81
3.2 Results	84
3.2.1 ERG regulates β -catenin junctional localisation in confluent EC	84
3.2.2 ERG regulates β -catenin protein expression	86
3.2.3 Endothelial Wnt/ β -catenin signalling requires ERG	89
3.2.4 ERG controls downstream β -catenin target gene expression in human and mouse EC	91
3.2.5 ERG regulates β -catenin degradation	97
3.2.6 ERG regulates β -catenin stability partly through VE-cadherin	97
3.2.7 ERG regulates β -catenin stability partly through Wnt-dependent mechanisms	103
3.2.8 ERG drives expression of the Wnt receptor Frizzled-4	107
3.2.8.1 Endothelial expression of Frizzled-4 is regulated by ERG <i>in vitro</i> and <i>in vivo</i>	107
3.2.8.2 ERG binds to the Fzd4 promoter	109
3.2.8.3 ERG transactivates the Fzd4 promoter in EC	114

3.2.8.4 Frizzled-4 overexpression in ERG-deficient EC partially rescues Wnt3a activation of β -catenin transcriptional activity	118
3.2.9 ERG regulates β -catenin nuclear localisation in sparse EC	120
3.2.10 ERG controls cell proliferation and survival through Wnt signalling...	122
3.2.11 ERG-dependent angiogenesis requires Wnt signalling	124
3.2.12 Pharmacological stabilisation of β -catenin rescues vascular defects in <i>Erg</i> ^{EC-KO} mice	126
3.2.13 ERG interacts with β -catenin in HUVEC	129
3.3 Discussion and Future Work	131

4. Chapter 4: ERG controls multiple pathways required for vessel growth

and stability: Notch pathway	138
4.1 Introduction	139
4.1.1 Notch signalling	139
4.1.2 Notch signalling in the vasculature	143
4.1.2.1 Regulation of arteriovenous identity by Notch signalling	144
4.1.2.2 Role of Notch signalling in vessel sprouting	145
4.2 Results	148
4.2.1 ERG controls Notch signalling in EC	148
4.2.2 ERG represses expression of Jagged-1 mRNA and protein <i>in vitro</i> and <i>in vivo</i>	150
4.2.3 ERG binds to the Jagged-1 promoter	152
4.2.4 ERG represses Jagged-1 promoter activity	152
4.2.5 Jagged-1 induction following ERG inhibition is repressed by NFKB inhibitor	155
4.2.6 ERG is required for Dll4 mRNA and protein expression in EC	157
4.2.7 ERG binds to the Dll4 promoter	159
4.2.8 ERG transactivates the Dll4 promoter	159
4.2.9 β -catenin does not cooperate with ERG to regulate Dll4 expression	162
4.2.10 ERG binds to putative Dll4 enhancer regulatory regions	164
4.2.11 ERG and Notch signalling cooperate to control Dll4 expression	166
4.2.12 ERG represses expression of Sox17 in EC	171
4.2.13 ERG repression of Sox17 is not Notch-dependent	171
4.3 Discussion and Future Work	175

5. Chapter 5: ERG controls multiple pathways required for vessel growth and stability: Angiopoietin-1/Tie2 pathway	182
5.1 Introduction	183
5.1.1 Ang1/Tie2 signalling in the vasculature	183
5.2 Results	186
5.2.1 ERG controls expression of the Angiopoietin receptor Tie2 in human and mouse EC	186
5.2.2 Expression of Tie2 is controlled by an ERG-dependent enhancer	188
5.2.3 Angiopoietin-1 promotes canonical Wnt and Notch signalling through ERG	191
5.2.4 Ang1 induction of Dll4 requires ERG	195
5.2.5 Ang1 increases ERG binding to Dll4 regulatory regions in confluent cells	197
5.2.6 Ang1 induces Dll4 through a PI3K–Akt–ERG signal axis	200
5.3 Discussion and Future work	205
6 Final Summary and Discussion	210
6.1 ERG regulation of Wnt, Notch and Ang1/Tie2 angiogenesis pathways	210
6.2 Control of ERG transcriptional activity	211
6.3 ERG as an integrating hub for interconnected pathways	213
References	215
Appendix 1: Birdsey, Shah, et al. (2015). The endothelial transcription factor ERG promotes vascular stability and growth through Wnt/ β -catenin signaling. <i>Dev Cell</i>	231
Appendix 2: Permission for third party copyright works	247

List of Figures

Chapter One

Figure 1.1 Development of the vasculature occurs through vasculogenesis and angiogenesis	24
Figure 1.2 Model of angiogenesis	27
Figure 1.3 An angiogenic sprout consists of endothelial tip and stalk cells	30
Figure 1.4 Endothelial cell junction organisation and adhesion proteins	33
Figure 1.5 VE-cadherin domain organization and VE-cadherin mediated protein interactions within endothelial intercellular junctions	35
Figure 1.6 Structure of the ETS domain and pointed domain of ETS1	39
Figure 1.7 Structure and domains of ETS factor proteins	40
Figure 1.8 Phylogenetic tree of human ETS transcription factors	42
Figure 1.9 Structure of the human ERG gene	45
Figure 1.10 Schematic diagram of the functional domains of ERG-2	47
Figure 1.11 Transcriptome profiling of control versus ERG GeneBloc-treated HUVEC	52
Figure 1.12 ERG is required for vascular development, angiogenesis and tumour growth	54

Chapter Three

Figure 3.1 Canonical Wnt/ β -catenin signalling in the endothelium.....	80
Figure 3.2 ERG is required for β -catenin localisation at endothelial cell junctions..	85
Figure 3.3 ERG regulates β -catenin protein expression	87
Figure 3.4 β -catenin mRNA expression is unaffected by ERG inhibition	88
Figure 3.5 β -catenin transcriptional activity is controlled by ERG	90
Figure 3.6 ERG regulates β -catenin target gene expression <i>in vitro</i> and <i>in vivo</i>	92
Figure 3.7 ERG is required for N-cadherin mRNA and protein expression	93
Figure 3.8 ERG regulates blood brain barrier permeability and expression of Claudin-3 and Plvap	95
Figure 3.9 Gene set enrichment analysis demonstrates significant correlation between genes regulated by ERG and β -catenin	96
Figure 3.10 MG132 proteosomal degradation inhibitor treatment ablates ERG inhibition-induced β -catenin degradation	98

Figure 3.11 Control GFP and VE-cadherin-GFP adenovirus transduction of HUVEC	99
Figure 3.12 ERG controls β -catenin stability partially through VE-cadherin	101
Figure 3.13 ERG controls β -catenin stability through both a VE-cadherin- and Wnt- dependent mechanism	102
Figure 3.14 ERG regulates genes involved in control of β -catenin degradation	105
Figure 3.15 Treatment of ERG-deficient EC with the Wnt ligand Wnt3a was unable to rescue β -catenin expression	106
Figure 3.16 ERG regulates Frizzled-4 expression	108
Figure 3.17 Post-translational modifications of the core histones affect DNA accessibility	111
Figure 3.18 ERG binds to the Fzd4 promoter	112
Figure 3.19 ERG binds to the Fzd4 promoter R1 in HUVEC	113
Figure 3.20 Generation of Fzd4-pGl4 luciferase construct	116
Figure 3.21 ERG transactivates the Frizzled-4 promoter	117
Figure 3.22 Fzd4 overexpression in ERG-deficient EC partly rescues Wnt3a activation of β -catenin transcriptional activity	119
Figure 3.23 ERG is required for β -catenin expression in sparse HUVEC	121
Figure 3.24 ERG regulates cell proliferation and survival through Wnt/ β -catenin signalling	123
Figure 3.25 ERG regulates angiogenesis through Wnt/ β -catenin signalling	125
Figure 3.26 Pharmacological inhibition of β -catenin degradation with LiCl rescues vascular defects in <i>Erg</i> ^{EC-KO} yolk sacs <i>in vivo</i>	127
Figure 3.27 Inhibition of β -catenin degradation with LiCl treatment rescues Wnt signalling in <i>Erg</i> ^{EC-KO} yolk sacs <i>in vivo</i>	128
Figure 3.28 ERG interacts with β -catenin and Wnt3a induces ERG expression	130
Figure 3.29 Proposed model for ERG regulation of vascular growth and stability through Wnt/ β -catenin signalling	132

Chapter Four

Figure 4.1 Protein structure of the vertebrate DSL family of ligands	141
Figure 4.2 Overview of Notch signal transduction	142
Figure 4.3 Regulation of vessel sprouting by Dll4 and Jagged-1	147
Figure 4.4 ERG regulates endothelial Notch signalling	149

Figure 4.5 ERG represses Jagged-1 expression	151
Figure 4.6 ERG binds to the Jagged-1 promoter in EC	153
Figure 4.7 ERG represses Jagged-1 promoter activation in resting EC	154
Figure 4.8 Upregulation of Jagged-1 after ERG deletion is repressed by the NF- κ B inhibitor BAY-117085	156
Figure 4.9 ERG is required for Dll4 expression in EC	158
Figure 4.10 ERG binds to the Dll4 promoter	160
Figure 4.11 ERG overexpression transactivates the Dll4 promoter	161
Figure 4.12 β -catenin does not cooperate with ERG to regulate Dll4 expression	163
Figure 4.13 ERG binds to putative regulatory enhancer regions of Dll4	165
Figure 4.14 ERG interacts with endogenous Notch intracellular domain in HUVEC	167
Figure 4.15 Notch signalling contributes to ERG regulation of Dll4	168
Figure 4.16 Notch signalling regulates ERG levels in EC	170
Figure 4.17 ERG represses Sox17 mRNA expression in EC	172
Figure 4.18 <i>In vitro</i> and <i>in vivo</i> ERG inhibition increases Sox17 protein expression	173
Figure 4.19 ERG repression of Sox17 expression in HUVEC is not Notch- dependent	174
Figure 4.20 Schematic of a model of ERG regulation of Notch signalling in EC	176

Chapter Five

Figure 5.1 Vascular stabilisation by Angiopoietin-1	184
Figure 5.2 ERG regulates Tie2 expression in EC	187
Figure 5.3 ERG binds a putative enhancer region within the 1 st intron of the Tie2 locus	189
Figure 5.4 ChIP-qPCR validates ERG binding within R1 of the Tie2 locus	190
Figure 5.5 ERG is required for Ang1 regulation of Wnt signalling	192
Figure 5.6 ERG is required for Ang1 regulation of Notch signalling	193
Figure 5.7 Ang1 treatment increases ERG expression in a dose-dependent manner	194
Figure 5.8 ERG is required for Ang1 regulation of Dll4	196
Figure 5.9 Ang1 induces Dll4 expression through increased binding of ERG	198
Figure 5.10 Ang1 induction of Dll4 in confluent HUVEC is mediated by ERG.....	199

Figure 5.11 ERG induces Dll4 transactivation through the PI3K/AKT pathway	202
Figure 5.12 Ang1 induces increased binding of ERG to the Dll4 locus through the PI3K/AKT pathway	203
Figure 5.13 Ang1 induces β -catenin occupancy at Dll4 enhancers	204
Figure 5.14 Model for how Ang1/Tie2 signal induces Dll4 expression through ERG	206

List of Tables

Chapter Two

Table 2.1 Oligonucleotides used for qPCR	63
Table 2.2 Oligonucleotides used in ChIP-qPCR	69
Table 2.3 Oligonucleotides used for generating promoter constructs	71

Chapter Three

Table 3.1 Table of ChIP-seq histone post-translational modification markers and their functional association	111
---	-----

Abbreviations

aa: amino acid
Ad.GFP: adenovirus encoding for control GFP tag
Ad.VEC-GFP: adenovirus encoding for GFP-tagged VE-cadherin
AF: alexa fluor
Ang: angiopoetin
AJ: adherens junction
AP-1: activator protein-1
APC: adenomatous polyposis coli
BAEC: bovine aortic endothelial cells
BBB: blood brain barrier
bp: base pairs
BrdU: bromodeoxyuridine
cEC-het: constitutive endothelial-specific heterozygous knockout
cEC-KO: constitutive endothelial-specific knockout
ChIP: chromatin immunoprecipitation
ChIP-seq: chromatin immunoprecipitation- sequencing
CLDN: claudin
DACT: Dapper antagonist of catenin
DAVID: Database for Annotation, Visualization and Integrated Discovery
DLL4: delta like ligand 4
DMSO: dimethyl sulfoxide
DSL: delta/serrate/lag
DTT: dithiothreitol
DVL: dishevelled
E: embryonic age
EBS: ETS binding site
EC: endothelial cells
ECGF: endothelial cell growth factor
ECM: extra cellular matrix
EDB: ETS DNA binding domain
EDTA: ethylenediaminetetraacetic acid
EMSA: electrophoretic mobility shift assay
ENCODE: encyclopaedia of DNA elements
ERG: ETS related gene
Erk: extracellular signal-regulated kinase
ESET: ERG associated protein with a SET domain
ETA: ETS transcriptional activation domain
ETS: E26 transformation specific
EWS: Ewing's sarcoma
EZH2: enhancer of zeste homolog 2
FBS: foetal bovine serum
FITC: fluorescein isothiocyanate

FLI-1: friend leukaemia virus integration 1
FOX: forkhead
FUS: fused in sarcoma
FZD: frizzled
g: gravity
GAPDH: glyceraldehyde-3-phosphate dehydrogenase
GB: Genebloc
GFP: green fluorescent protein
GSEA: gene set enrichment analysis
GSK3: glycogen synthase kinase-3
GTP: guanosine triphosphate 198
h: hour
H3K4me1: monomethylated histone H3 at lysine 4
H3K4me3: trimethylated histone H3 at lysine 4
H3K27ac: acetylated histone H3 at lysine 27
HAT: histone acetyltransferase
HBSS: hanks' balanced salt solution
HDAC: histone deacetylase
HES: Hairy/Enhancer of Split
HEY: Hes-related proteins
HRP: horseradish peroxidase
HUVEC: human umbilical vein endothelial cells
ICAM: intercellular adhesion molecule
iEC-KO: inducible endothelial-specific knockout
Ig: immunoglobulin
IKK: inhibitor of κ B kinase
IL: interleukin
IP: immunoprecipitation
JAG: jagged
kDa: kilodalton
KDR: kinase insert domain receptor
KLF: kruppel-like factor
LEF: lymphoid enhancer binding factor
LPS: lipopolysaccharide
mAbs: monoclonal antibodies
MAPK: mitogen activated protein kinase
Mbp: megabase pair
min: minutes
MOI: multiplicity of infection
NES: normalised enrichment score
NF- κ B: nuclear factor kappa B
NICD: notch intracellular domain
NOS: NO synthase
NRARP: Notch-regulated ankyrin repeat protein

NRT: negative regulatory transcriptional activation domain
pAbs: polyclonal antibodies
PCR: polymerase chain reaction
PECAM: platelet endothelial cell adhesion molecule
PFU: plaque forming units
PLVAP: plasmalemma vesicle associated protein
PMA: phorbol 12-myristate 13-acetate
PNT: pointed domain
qPCR: quantitative real time polymerase chain reaction
r: recombinant
SDS-PAGE: sodium dodecyl sulphate polyacrylamide gel electrophoresis
secs: seconds
SEM: standard error of mean
Seq: sequencing
SET: suppressor of variegation, enhancer of zest and trithorax
siCtrl: control mismatch antisense oligonucleotides/ siRNA
siERG: antisense oligonucleotides/ siRNA targeting ERG
TAD: transactivation domain
TCF: T-cell factor
TGF: transforming growth factor
TJ: tight junction
TMPRSS2: transmembrane protease, serine 2
TNF: tumour necrosis factor
TSS: transcription start site
UCSC: University of California, Santa Cruz
UTR: untranslated region
VEGF: vascular endothelial growth factor
VEGFR: vascular endothelial growth factor receptor
vSMC: vascular smooth muscle cells
VWF: von Willebrand factor
ZO-1: zonula occludens-1

Chapter One

Introduction

1. INTRODUCTION

1.1 The vascular system

The importance of the vascular system is demonstrated by its early emergence during development. The vascular circulatory system, consisting of the heart, blood, and blood vessels, is the first functional organ system formed during vertebrate embryogenesis. It is essential for controlling a range of physiological processes including the delivery of oxygen and nutrients to rapidly growing tissues with high metabolic demand. The vasculature is also crucial in the removal of waste products, facilitating rapid deployment of immune responses to sites of infection, and in maintaining blood pressure. Further organogenesis during development is totally dependent on the delivery of oxygen and nutrients facilitated by a functional circulatory system, and major defects in the developing vasculature lead to early embryonic lethality.

Formation of the vascular system occurs primarily through two main mechanisms, vasculogenesis and angiogenesis. In the embryo, the de novo formation of vessels, defined as vasculogenesis, occurs via the assembly of mesoderm-derived endothelial precursors called angioblasts (Figure 1.1). Angioblasts aggregate to form multi-cellular structures called blood islands and later differentiate into endothelial cells (EC) that coalesce into cords to establish a primitive vascular plexus (Figure 1.1). The dorsal aorta and the cardinal vein are the first vessels to form during embryonic development through vasculogenesis. New vessel branches emanate from the nascent primary vascular plexus, through a cellular process of angiogenesis, namely the growth of new blood vessels from pre-existing blood vessels, which allows for the subsequent sprouting and expansion of this network (Figure 1.1).

Blood vessels form a hierarchical network of arteries, veins and capillaries and for the circulatory system to efficiently function as a closed loop; it depends on these two discrete yet interconnected networks of arterial and venous vessels. Functionally, arteries carry oxygenated blood away from the heart under high pressure while veins return deoxygenated blood to the heart at a lower pressure, with the pulmonary vasculature being the exception.

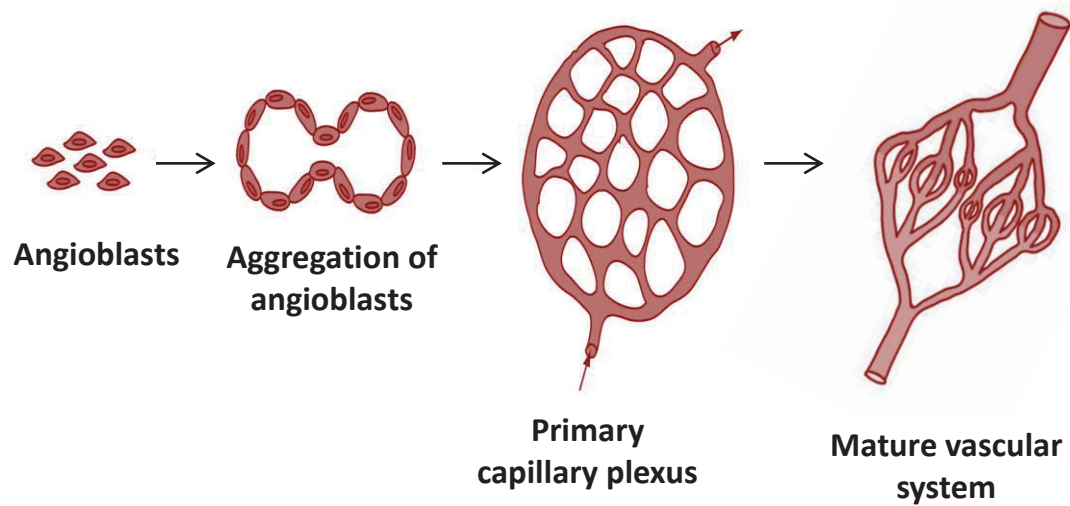


Figure 1.1 Development of the vasculature occurs through vasculogenesis and angiogenesis. During early embryonic development, mesodermal cells differentiate into endothelial precursor cells or angioblasts and form aggregates of blood islands. Vasculogenesis involves the differentiation of angioblasts into endothelial cells. Coalescence of blood islands leads to the formation of honeycomb-shaped primary capillary plexi in the yolk sac and the embryo proper. Angiogenesis is responsible for the remodelling and expansion of this network.

Blood vessels are composed of two interacting cell types. Endothelial cells line the luminal surface of the vessel wall, and perivascular cells—referred to as pericytes, vascular smooth muscle cells or mural cells—envelop the surface of the blood vessel. Endothelial cells are key functional players in the induction of angiogenesis and in maintaining blood vessel homeostasis. The endothelium forms an interface between circulating blood and the rest of the vessel wall. Thus, endothelial cells line the entire circulatory system, from the heart to the smallest capillaries, and control the passage of materials into and out of the bloodstream. Perivascular cells comprise pericytes, which wrap around small vessels such as capillaries, and vascular smooth muscle cells (vSMCs), which are found around bigger vessels such as arteries and veins.

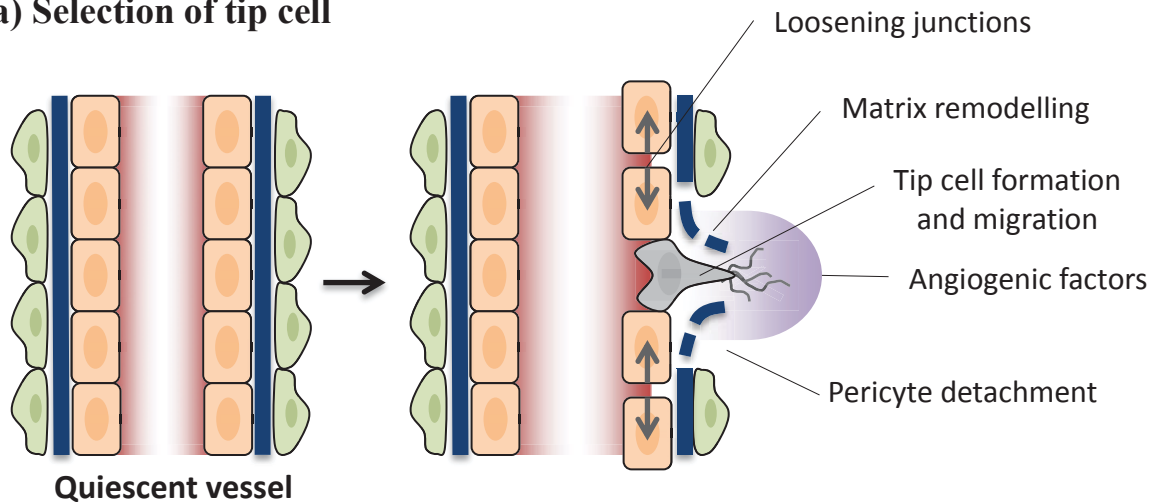
1.2 Mechanisms of angiogenesis

Angiogenesis requires precise coordination of cellular events and a host of signalling molecules, which upon interaction with specific receptors, are known to play a crucial role in activating and modulating vessel formation. Angiogenesis is key in many physiological processes including during development, reproduction and wound repair. Under these conditions, angiogenesis is a tightly regulated process. In a healthy adult, vessels are quiescent and rarely form new branches. However, EC retain high plasticity to sense and respond to angiogenic signals.

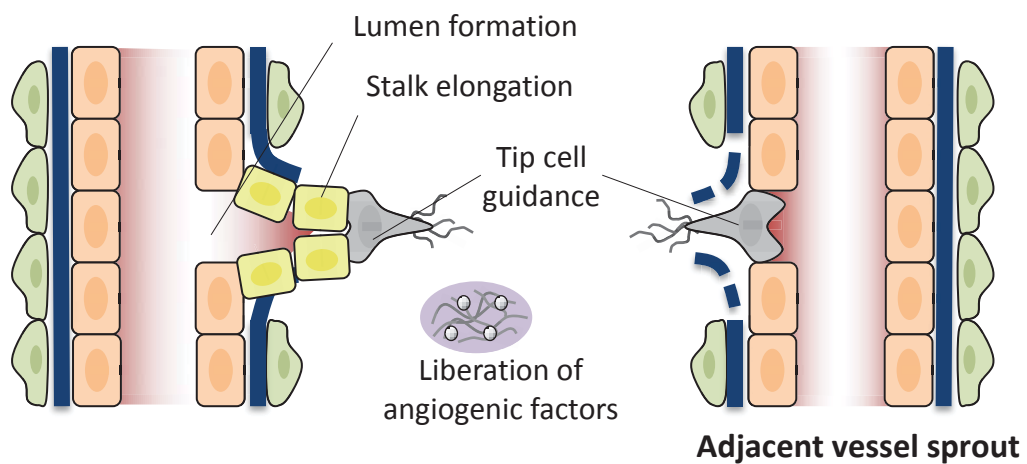
Angiogenesis also plays an important role in many diseases (reviewed in Carmeliet, 2003). Inadequate blood vessel growth and defective function result in ischemia in diseases such as myocardial infarction, stroke, and neurodegenerative disorders. On the other hand, excessive vessel growth contributes to the progression of cancer growth, inflammatory disorders, and eye disease (reviewed in Carmeliet, 2003). Angiogenesis is therefore a putative target for therapy. Therapeutic application of angiogenesis inhibitors to block vascular supply is currently under intense clinical investigation, however efficacy issues pose unresolved challenges. A greater understanding of the biology of vascular growth may translate into new targets for treatment, which may overcome the current limitations of pro- and anti-angiogenic medicine.

Angiogenesis in its strictest sense refers specifically to sprouting angiogenesis, which involves a range of cellular and morphogenetic events. Although vessel growth can occur via other mechanisms, such as the splitting of pre-existing vessels through intussusception or the stimulation of vessel expansion by circulating precursor cells (Fang and Salven, 2011; Makanya et al., 2009), I will focus here on sprouting angiogenesis, which is proposed to account for a significant proportion of vessel growth. Angiogenesis requires tight regulation of processes such as cell proliferation, differentiation, migration, matrix adhesion and cell-cell signalling during vessel morphogenesis (Figure 1.2). Several elegant studies have provided crucial insights into the mechanistic model of vessel formation and the morphogenetic events and molecular mechanisms mediating the process, which will be described in detail below (Adams and Alitalo, 2007; Carmeliet and Jain, 2011; Eilken and Adams, 2010; Phng and Gerhardt, 2009).

a) Selection of tip cell



b) Stalk elongation and tip cell guidance



c) Endothelial quiescence resolution

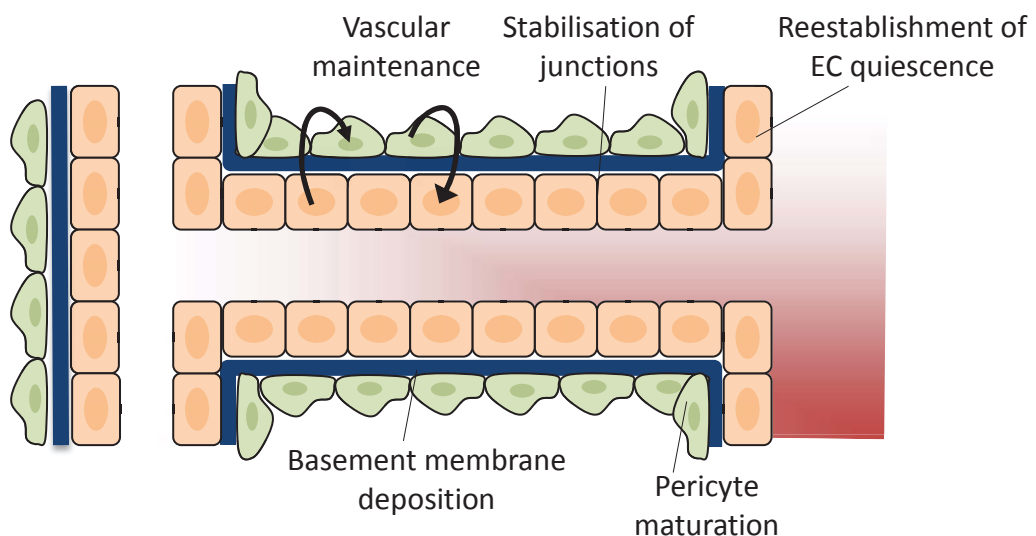


Figure 1.2 Model of angiogenesis. (A) On initiation of an angiogenic response by pro-angiogenic factors, an endothelial cell tip cell is selected (Dll4 and Jagged-1) to lead the nascent sprout. Tip-cell formation requires local basement membrane degradation, pericyte detachment and modulation and loosening of endothelial cell junctions. (B) Tip cells navigate in response to guidance signal gradients and adhere to the extracellular matrix to migrate. Stalk cells behind the tip cell proliferate (Wnt), elongate and support the growth of the sprouting vessel. The fusion of adjacent sprouts establishes a perfused neovessel. Proliferating stalk cells recruit pericytes (Ang1/Tie2) and deposit basement membranes. (C) Following vessel fusion, lumen formation allows perfusion of the neovessel, and promotes maturation processes such as stabilisation of cell junctions (VE-cadherin), deposition of basement membrane and pericyte attachment, which act to reestablish vascular quiescence (Notch) and produce vascular maintenance signals (image reproduced from Carmeliet and Jain, 2011, with permission of the rights holder, Nature Publishing Group) .

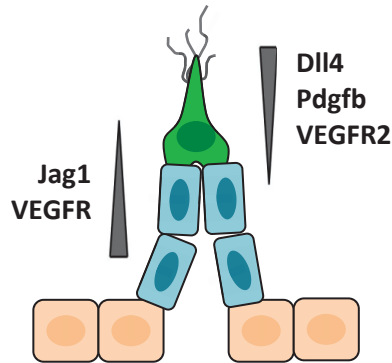
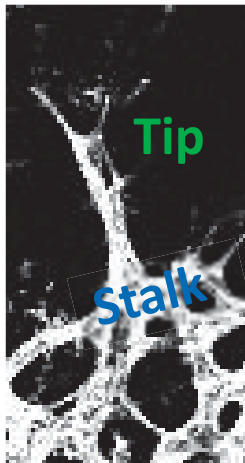
1.2.1 Cellular and molecular mechanisms involved in vessel sprouting

A nascent vascular sprout comprises different subpopulations of EC, which assume different morphologies and specialised functions (Gerhardt et al., 2003). When a quiescent vessel senses a pro-angiogenic stimulus, such as vascular endothelial growth factor (VEGF), released by a hypoxic, inflammatory or tumour cell, it causes a selected activated endothelial cell to acquire motile and invasive behaviour and to extend filopodia in a polarised manner (Figure 1.2 A). These EC, known as tip cells, drive the formation of new sprouts and guide their migration into an avascular tissue. The adjacent neighbouring cells that trail the tip cell within the vascular sprout assume subsidiary positions and divide to support sprout elongation so that blood vessels grow in length and diameter (Figure 1.2 B). These cells are referred to as stalk cells. Stalk cells, unlike tip cells, form and line the vascular lumen.

Tip and stalk cells also display distinct gene expression profiles, with tip cells expressing increased levels of the Notch ligand delta like ligand 4 (Dll4), platelet-derived growth factor subunit B, vascular endothelial growth factor receptor (VEGFR)-2 and VEGFR3 compared to stalk cells (Figure 1.3) (Tammela et al., 2008; Siekmann and Lawson, 2007; Claxton and Fruttiger, 2004; Lu et al., 2004; Gerhardt et al., 2003). Mechanistically, a feedback loop between VEGF signalling and Notch signalling promotes this specification of EC into tip and stalk cells in a single nascent sprout (Eilken and Adams, 2010; Phng and Gerhardt, 2009). During sprouting, endothelial junctions are plastic and dynamically modulated to allow endothelial cell migration (Figure 1.2 A). When a tip cell of a newly developing sprout contacts the adjacent sprout, these two sprouts form anastomotic connections, resulting in the fusion of the vessels.

The differences in cell morphology and gene expression suggest that endothelial tip and stalk cells have specialized functions. Indeed, as discussed in more detail below, tip cells function to guide the migration of nascent blood vessels into an avascular tissue so that an organized vessel network is formed. Stalk cells proliferate more frequently so that blood vessels grow in length and diameter. In addition, stalk cells undergo positional rearrangements within a vessel to form lumen (Figure 1.3).

The control of vascular patterning can be attributed to attractive cues such as VEGF-A, which during vascular development is required for chemotaxis and



Endothelial tip cell:

- Extends filopodia
- Induced by VEGF-A
- Specialised for migration
- Rarely proliferate
- Lack a lumen

Endothelial stalk cell:

- Induced by Notch signalling
- Proliferate in response to VEGF
- Establish adherens junctions
- Form vascular lumen
- Deposit basement membrane

Figure 1.3 An angiogenic sprout consists of endothelial tip and stalk cells. A confocal image of vascular sprouts from a postnatal day 6 mouse retina (left panel). Endothelial tip cells (green) project filopodia and lead stalk cells (blue) in a sprouting vessel. The retina has been stained with Isolectin-B4, which recognizes endothelial cells as well as microglial cells. A simplified cartoon of a tip cell (green) with many filopodia and trailing stalk cells (blue) lining the vessel lumen (middle panel). Tip and stalk cells are molecularly different: tip cells express Dll4, Pdgfb and VEGFR2 more strongly than stalk cells. Stalk cells express Jagged-1 (Jag1) and VEGFR1 more strongly than tip cells. Tip and stalk cells are also functionally different (right panels).

differentiation of angioblasts, endothelial cell proliferation, vasculogenesis and angiogenic remodelling. Inactivation of a single VEGF-A allele in mice results in early embryonic lethality (embryonic day (E)11-12) as a result of deficient endothelial cell development and lack of vessels (Carmeliet et al., 1996; Ferrara et al., 1996). The generation of an extracellular gradient of VEGF-A is essential for directed migration of endothelial cells during vessel patterning and in the developing retina, astrocytes in hypoxic regions of the retina are the source of VEGF-A production. Disruption of this VEGF-A gradient or ectopic activation of VEGFR2 results in defective tip cell filopodia formation and inhibits directed endothelial tip cell migration (Gerhardt et al., 2003).

1.2.2 Cellular and molecular mechanisms involved in vascular stability

Once a functional vascular network is established, the endothelium must resume its quiescent or phalanx state, where sprouting and cell proliferation signals are dampened (Figure 1.2 C). Instead, signals that maintain vascular homeostasis and promote endothelial quiescence are turned on to stabilize the nascent vessels. Vessel stability is achieved through the re-established adhesion and junctional integrity between interconnected endothelial cells and the recruitment of pericytes, which ensheath the vessel and are necessary for its stabilisation.

1.2.2.1 Endothelial cell junctions maintain vessel integrity

Endothelial intercellular junctions are crucial for maintaining vascular integrity. EC junctions are organised into two main distinct adhesion structures including adherens and tight junctions (Figure 1.4). These junctional complexes comprise a network of adhesion proteins that are linked to the cytoskeleton and intracellular signalling molecules. However, multiple adhesion proteins are able to cluster at cell-cell contacts but do not form adherens or tight junctions complexes, such as platelet endothelial cell adhesion molecule (PECAM) and intercellular adhesion molecule (ICAM)-2 (Figure 1.4). Adherens junctions are primarily important for controlling permeability and thus vessel integrity, whereas tight junctions are implicated in the regulation of the passage of ions and solutes through the paracellular route (Bazzoni and Dejana, 2004) and thus maintaining the barrier functions of endothelial cells (Wallez and Huber, 2008). The organization of tight and adherens junctions vary along the vascular tree depending on the functional needs of the vessel. For instance, tight junctions are particularly abundant and complex in the brain microcirculation where there is a need to strictly control permeability (Dejana, 2004).

In EC, members of the cadherin family of adhesion proteins regulate formation of adherens junctions. EC highly express two members of the cadherin family: vascular endothelial (VE)-cadherin, which is selectively expressed in EC, and neuronal (N)-cadherin, which is also expressed in other cell types such as neural cells and smooth muscle cells (Bazzoni and Dejana, 2004). VE-cadherin is a calcium-dependent adhesion protein mediating homophilic cell adhesion, and linking the site of the junction to the actin cytoskeleton. VE-cadherin-based adherens junctions are a crucial determinant of vascular integrity both in developing and existing vessels. During angiogenesis, EC undergo dynamic rearrangement upon extracellular stimuli while continuously reorganizing cell-cell junctions and maintaining barrier function at the same time. This coordination is to a great extent regulated by VE-cadherin, which is crucial in the maintenance of nascent vessels. This has been shown in multiple *in vivo* studies where disruption of VE-cadherin function in the developing or established adult vasculature results in severe vascular defects caused by vessel collapse, regression, cell detachment and apoptosis, leading to extensive haemorrhages (Dejana et al., 2008; Crosby et al., 2005; Carmeliet et al., 1999; Corada et al., 1999). Furthermore genetic

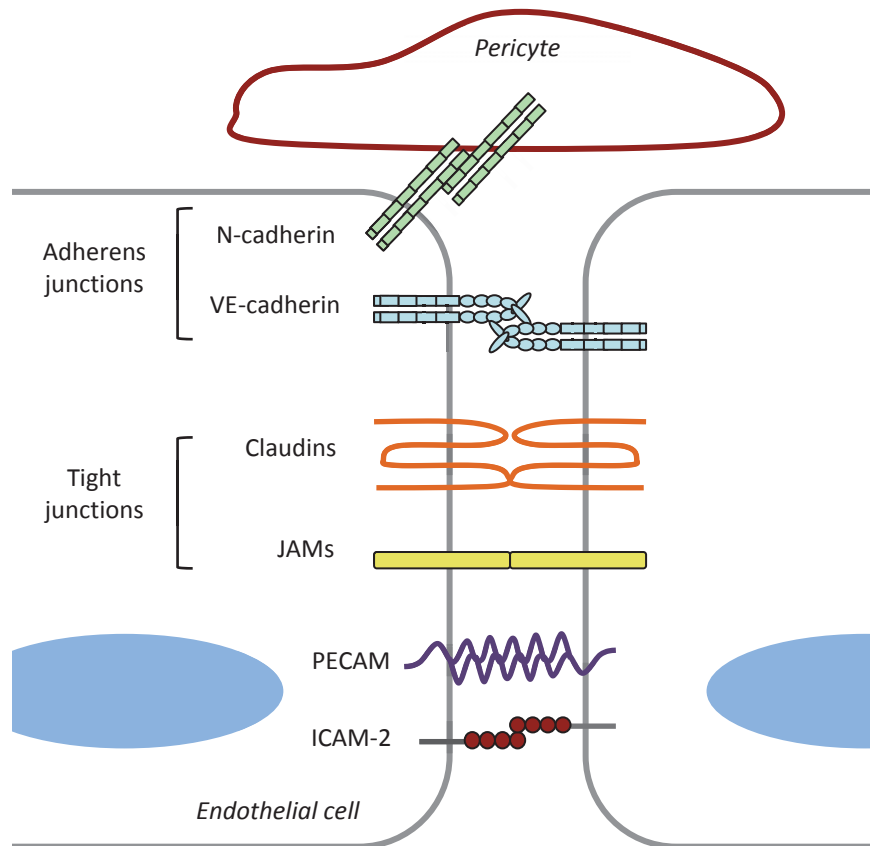


Figure 1.4 Endothelial cell junction organisation and adhesion proteins. Junctional structures maintain the integrity of the endothelium. EC express cell-type-specific transmembrane adhesion proteins, such as VE-cadherin at adherens junctions and members of the Claudin family at tight junctions. Many components of adherens or tight junctions such as α - and β -catenin interact directly or indirectly with actin filaments. Multiple adhesion proteins are able to cluster at cell-cell contacts but do not form adherens or tight junctions complexes, such as PECAM and ICAM2. EC also express N-cadherin, which mediates binding to pericytes (image reproduced from Dejana, 2004, with permission of the rights holder, Nature Publishing Group).

deletion of *Cdh5*, encoding VE-cadherin, in mouse embryos causes embryonic lethality at E9.5 due to defects in vessel remodelling (Carmeliet et al., 1999).

Through its cytoplasmic tail, VE-cadherin interacts with cytoskeletal and signalling proteins that anchor junctions to the actin cytoskeleton and transfer signals intracellularly (Figure 1.5). These intercellular junctions provide attachment sites and importantly relay intracellular signals that control many endothelial cell functions. The intracellular cytoplasmic domain of VE-cadherin contains binding sites for catenins, such as β -catenin (Wallez and Huber, 2008) (Figure 1.5), which is a well-studied example of a junctional protein that can also shuttle from the membrane to the nucleus to influence transcription; this will be discussed in detail in Chapter 3. Within its role as a structural component of adherens junctions, β -catenin also interacts with α -catenin, which binds to several actin-binding proteins including zonula occludens-1 (ZO-1). The indirect association between VE-cadherin and the actin cytoskeleton is necessary for junction stabilization and to provide strength to the junction and cell-cell interaction (Figure 1.5). Accordingly, a truncated form of VE-cadherin that lacks the cytoplasmic binding domain for β -catenin caused changes in cell permeability as a result of defective junction cohesion (Navarro et al., 1995). Histamine, tumour necrosis factor (TNF)- α and VEGF induce tyrosine phosphorylation of VE-cadherin and β -catenin. This phosphorylation of AJ proteins parallels increases in permeability in cell culture systems (Dejana et al., 2008).

It is commonly accepted that contact inhibition of cell proliferation is at least partially mediated by the establishment of cadherin-based junctions. Endothelial cell division is inhibited when cells are plated onto a substrate containing the VE-cadherin extracellular domain (Caveda et al., 1996), indicating that VE-cadherin engagement limits endothelial cell proliferation. Furthermore, VEGF transduces a survival signal to EC through a VE-cadherin-dependent mechanism. This signal is mediated by the PI3-kinase/Akt pathway and requires VE-cadherin association with VEGFR2 (Carmeliet et al., 1999).

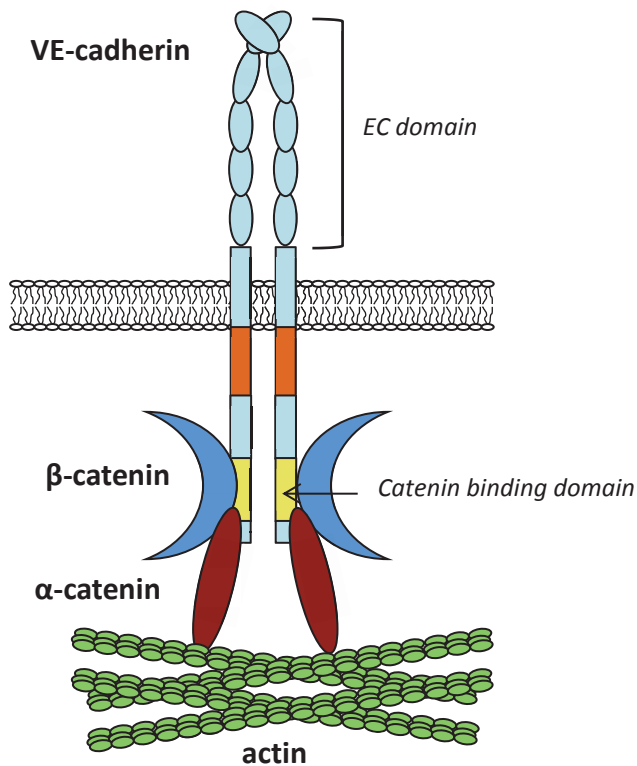


Figure 1.5 Schematic diagram of VE-cadherin domain organization and VE-cadherin mediated protein interactions within endothelial intercellular junctions. VE-cadherin comprises 5 cadherin repeats in the extracellular (EC) domain. The intracellular cytoplasmic portion of VE-cadherin includes the ‘catenin binding domain’ that interacts with β -catenin. β -catenin is thought to indirectly mediate assembly of actin-based adhesive structures, as β -catenin also binds α -catenin, which interacts with several actin-binding proteins (image reproduced from Vincent et al., 2004).

1.2.2.2 Pericyte recruitment to the endothelium stabilises vessels

Although vessel stability is primarily regulated by EC, which boast intrinsic cellular mechanisms to sense environmental cues and modulate blood vessels accordingly, recently vascular mural cells have gained increasing attention as key regulators of vessel stability, maturation and remodelling, in part through control of the endothelial phenotype. Pericytes surrounding endothelial cells are embedded within the basement membrane of blood microvessels (Armulik et al., 2005). Pericyte contractile forces can function as a scaffold for vessels, and these mural cells also synthesize and promote assembly of basement membrane components (Davis and Senger, 2005). Pericytes differ from their vSMC counterparts by their localization to blood vessels, their morphology and to a certain extent, their marker expression. Pericytes are found around blood capillaries, pre-capillary arterioles, post-capillary venules and collecting venules where they project long cytoplasmic processes that wrap around the capillary wall. Pericytes often contact several EC, which suggests they may function to facilitate cell communication and coordinate adjacent EC responses. However, vSMCs usually localize to bigger vessels such as arteries and vein where they are arranged to mediate vascular tone and contraction (Armulik et al., 2005).

A direct pericyte–endothelial contact is established via membrane invaginations extending from either cell type at sites where the basement membrane is absent, forming so called peg–socket contacts, which contain junction complexes. N-cadherin-based adherens junctions are located to peg–socket contacts and studies applying an *in vivo* injection of anti–N-cadherin antibody into chick brain (Gerhardt et al., 2000) or *in vivo* siRNA in Matrigel plugs (Paik et al., 2004) suggest the functional importance for N-cadherin in these contacts.

Pericyte coverage of vessel area ranges from approximately 10% to 50%, depending on the vascular bed (Armulik et al., 2005). The microvessels within the CNS have the highest pericyte coverage. In the brain, pericytes together with the cerebral microvasculature, astrocytes, pericytes and neurons, constitute a "neurovascular unit". Recent studies have shown a key role for pericytes in the integration of endothelial and astrocyte functions at these neurovascular units, and importantly, in the regulation of the blood brain barrier (Armulik et al., 2010; Daneman et al., 2010).

The functional importance of pericyte recruitment to EC was evident in mouse genetic studies where signalling pathways controlling the recruitment of mural cells to the vessel wall, such as that of Angiopoietin (Ang)-1/ Tyrosine kinase with immunoglobulin-like and EGF-like domains (Tie)-2, have been disrupted. In quiescent adult vasculature, Ang1 secreted from pericytes induces activation of the endothelium-specific receptor tyrosine kinase Tie2 in endothelial cells to maintain mature blood vessels by enhancing vascular integrity and endothelial survival. Mice lacking Ang1 or Tie2 are embryonic lethal and die between E10.5–E12.5, attributable to defective vascular integrity, reduced pericyte coverage and therefore, compromised vascular function (Suri et al., 1996; Dumont et al., 1994).

1.3 Transcriptional pathways regulating gene expression in angiogenesis

By considering vascular morphogenesis as a series of connected, but overlapping, events, it becomes clear that a strict temporal and spatial regulation of cell signalling pathways and downstream gene expression are required within a developing vessel for proper assembly to occur. The list of endothelial signalling pathways involved in modulating the formation of a new vessel is constantly growing. Importantly, most of these pathways require the dynamic regulation of gene expression in EC, which depend on a complex network of transcriptional regulators. The transcriptional mechanisms through which the expression of the genes within the signalling cascades are activated and maintained or repressed in endothelial cells remain important questions in vascular biology. In addition, how growth factors influence the array of transcription factors involved in the endothelial gene expression program remains to be fully elucidated. The transcription factors that regulate angiogenesis have been a focus of active research for several years, and many players in the endothelial transcriptional program have been identified, including the E-26 transformation specific (ETS) family of transcription factors, which I will focus on in this thesis.

1.4 ETS family of transcription factors

1.4.1 Structure of the ETS transcription factors

All ETS factors share a highly conserved 85 amino acid DNA binding domain (ETS domain) that binds to the DNA core consensus sequence 5'GGA(A/T)3' (Oikawa and Yamada, 2003); further specificity in binding is defined by the flanking bases. The highly conserved ETS domain (Figure 1.6) contains three α -helices and four stranded β -sheets forming a winged helix-turn-helix structure, where interaction with the major groove of DNA is facilitated by the third α -helix (Figure 1.6). The ETS factor family can be divided into subfamilies consistent with the homology of their ETS domain and the presence of other conserved domains (Figure 1.7). Another conserved domain shared by a number of ETS factors is the approximate 80 amino acid pointed domain (Figure 1.6-1.7), which has been shown to function as a site of interaction with kinases, transcriptional co-regulators, and involved in dimerisation with other ETS transcription factors (Seidel and Graves, 2002; Sharrocks, 2001; Lacronique et al., 1997).

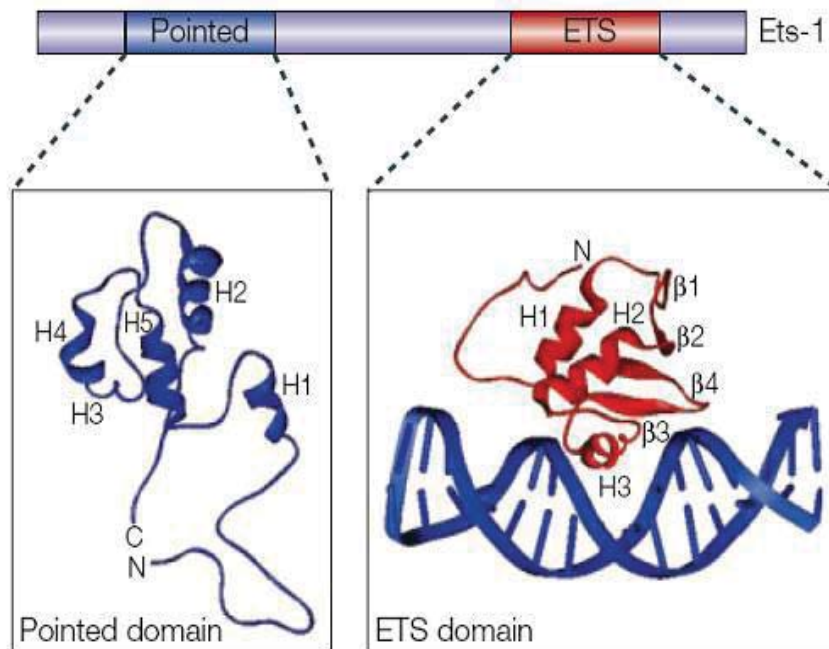


Figure 1.6 Structure of the ETS domain and pointed domain of ETS1. The location of helices (H) and β -strands (β) within the structures of the pointed domain (blue) and ETS domain (red) of ETS1 are shown (image reproduced from Sharrocks, 2001, with permission of the rights holder, Nature Publishing Group).

Human ETS family

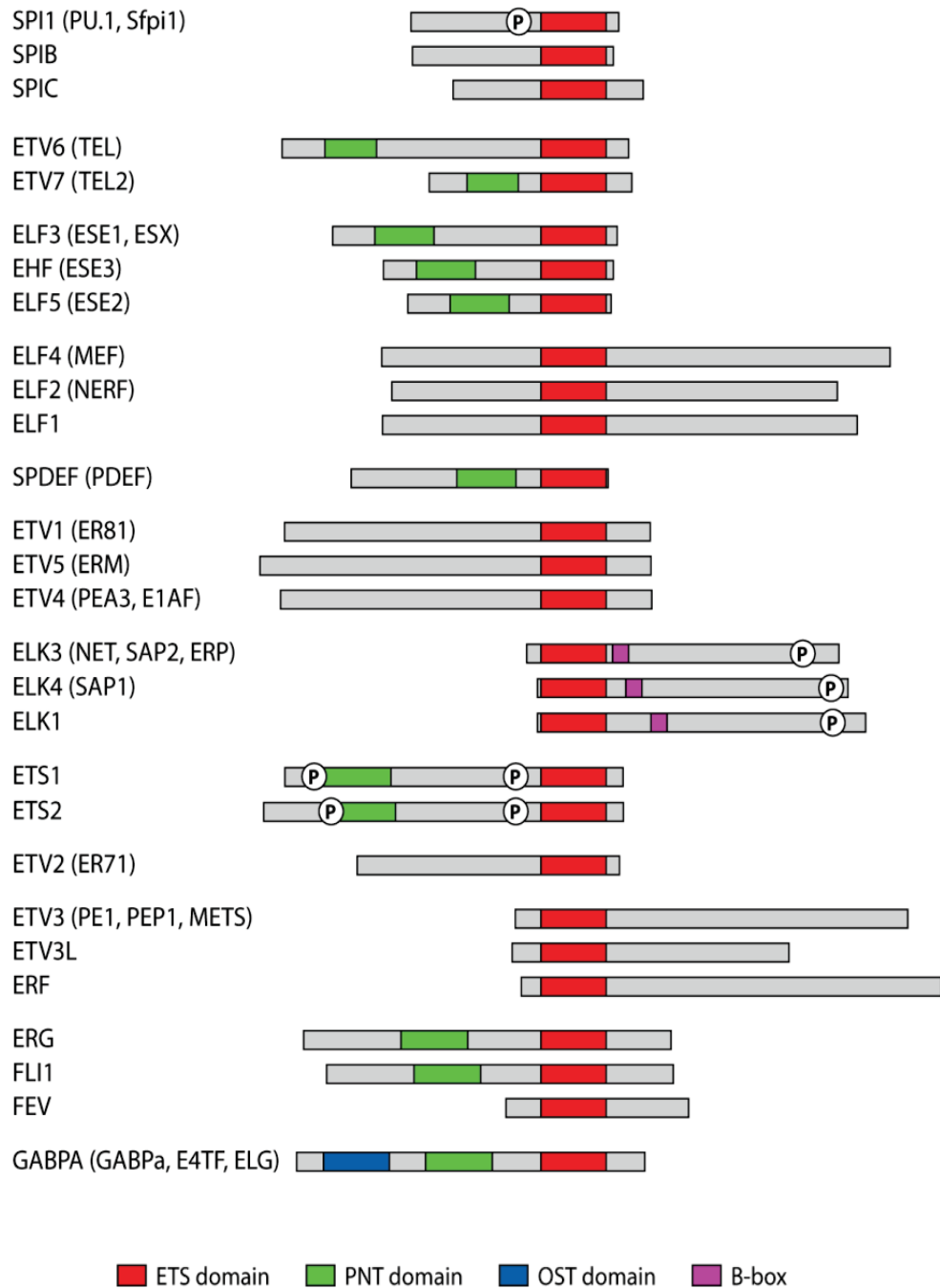


Figure 1.7 Structure and domains of ETS factor proteins. Boxes identify the ETS family structural domains, including DNA-binding ETS domain (red), Pointed (PNT) domain (green), OST domain (blue), and B-box (magenta) of the ETS factors. The circled P depicts a phosphorylated residue (image reproduced from Hollenhorst et al., 2011).

1.4.2 Expression and biological functions of the ETS transcription factors

So far, approximately 30 members of the ETS transcription factor family have been identified in mammalian cells, two thirds of which are expressed ubiquitously in adult tissue (Figure 1.8). ETS proteins have been estimated to bind between 5 and 15% of gene promoters (Hollenhorst et al., 2011). ETS factors can act as transcriptional activators or repressors or both, depending on the target gene or activity of the cell. The activity of many ETS factors is regulated by signal transduction cascades, which alter their sub-cellular localisation, DNA binding activity, or transcriptional activity through post-translational modification. Chromatin immunoprecipitation sequencing (ChIP-seq) studies have shown a degree of redundancy in ETS factor binding at sites not associated with any regulatory regions; however, greater enrichment of ETS factors has been shown for binding sites near transcription start sites of specific target genes (Wei et al., 2010). A number of composite binding sites for ETS factors with other transcription factors have been identified, including FOXC/ETS and AP-1/ETS composite sites (De et al., 2008; Moulton et al., 1994).

ETS factors regulate the expression of a variety of genes and mediate diverse cellular functions such as cell growth, differentiation, proliferation, survival, cell-cell and cell-matrix interactions (reviewed in Oikawa and Yamada, 2003). They are also important in the regulation of processes that include haematopoiesis, angiogenesis and inflammation. Several ETS factors also act as protooncogenes, including ETS-1, ETS-2, PU-1 (SPI1), FLI-1, ERG and TEL (ETV6) (Seth and Watson, 2005), and are therefore implicated in the pathogenesis of several different types of cancer.

1.4.3 ETS factors in the endothelium

At least 19 ETS factors have been shown to date to be expressed in human EC at some point during development, and have been shown to be required for endothelial lineage differentiation and homeostasis. ETS factors are central to the transcriptional systems controlling EC gene expression as all characterized endothelial promoters and enhancers contain multiple ETS DNA-binding motifs, which can be bound by more than one ETS family member (reviewed in Randi et al., 2009; De Val and Black, 2009). Several studies support a role for ETS factors in the regulation of endothelial-specific gene expression. Consensus ETS binding motifs have been identified within the promoters of several endothelial-restricted genes, including von Willebrand factor

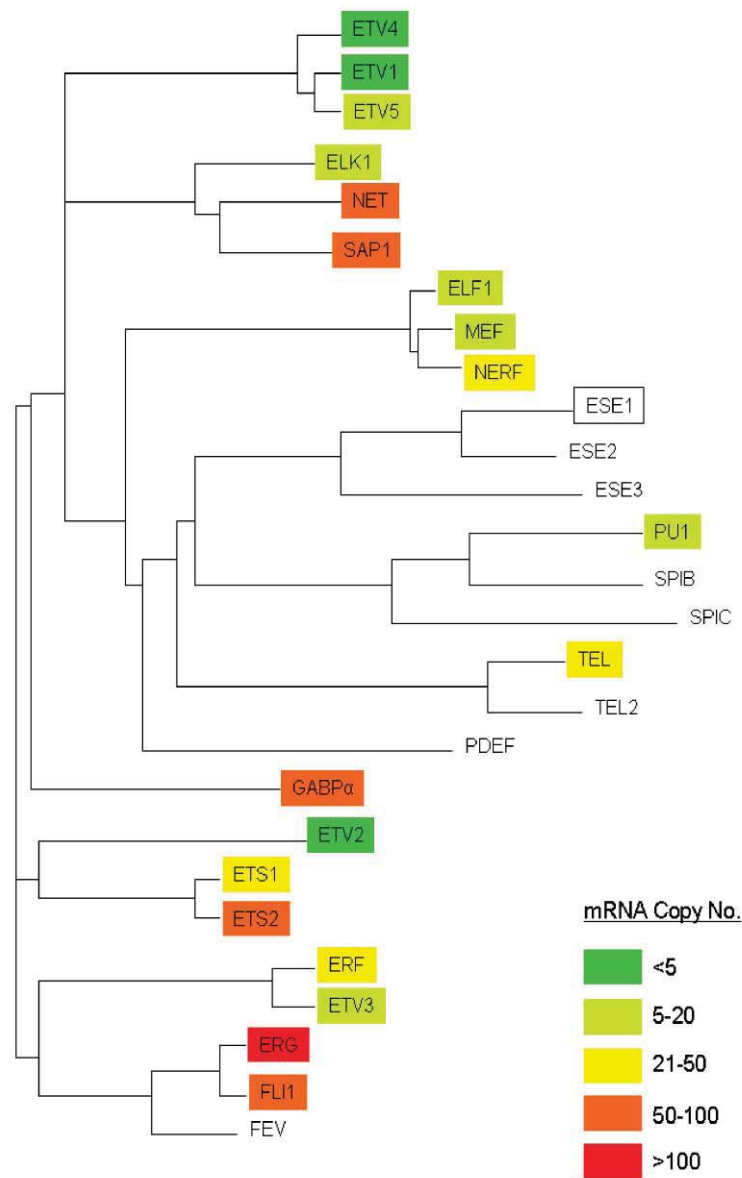


Figure 1.8 Phylogenetic tree of human ETS transcription factors. Phylogenetic tree showing the evolutionary relationship between different ETS factor family members, based on the relative conservation of the ETS domain, linking members with closely homologous amino acid sequences. The horizontal branch lengths represent predicted evolutionary distance. ETS genes expressed in HUVEC with mRNA levels above 1 copy per cell are highlighted. The ETS transcription factor with the highest expression levels in human umbilical vein endothelial cells is ERG (image reproduced from Hollenhorst et al., 2007, under the Creative Commons BY-NC License; <http://creativecommons.org/licenses/by-nc/4.0/>).

(VWF), VEGFR1, VEGFR2, TIE1, TIE2, endothelial nitric oxide synthase, and VE-cadherin. Many ETS factors are expressed in the vasculature of several organisms during development, and both gain and loss-of-function studies in mice and zebrafish have shown a key role for ETS proteins during vascular development (reviewed in Randi et al., 2009). In the adult, several endothelial ETS factors have been shown to regulate angiogenesis (Dejana et al., 2007).

1.5 ETS related gene ERG

1.5.1 Expression of ERG

ETS related gene (ERG) is the most highly expressed ETS factor in differentiated quiescent EC (Hollenhorst et al., 2004). Although ERG expression progressively decreases in the developing zebrafish vasculature, ERG remains highly expressed in EC of most adult tissues in the mouse and human (Yuan et al., 2009; Vlaeminck-Guillem et al., 2000; Baltzinger et al., 1999). ERG is also endogenously expressed in megakaryocytes (Rainis et al., 2005), chondrocytes (Iwamoto et al., 2000) and premature T and B-lymphocytes (Anderson et al., 1999). ERG is expressed in the nucleus of resting cells and so far there is no evidence of ERG localisation and function in the cytoplasm.

In the developing mouse embryo, ERG is expressed in EC and in pre-cartilage and haematopoietic tissues, but not in the epithelium or lymphocytes (Mohamed et al., 2010). A recent study reported enriched isoform-specific expression of ERG during embryonic development in the chondrocytes and vasculature (Vijayaraj et al., 2012). Additionally, ERG expression has been reported in the myocardium of E8.5 mouse embryos (Schachterle et al., 2012). The mediators of constitutive ERG expression have not been identified; however, multiple studies have shown that ERG protein is downregulated after stimulation with the inflammatory stimuli TNF- α and lipopolysaccharide (LPS) (Yuan et al., 2009; McLaughlin et al., 1999). Little is known about the post-translational modifications of ERG in endothelial cells. In myeloblast cells, ERG is phosphorylated on a serine residue by an activator of the protein kinase C pathway (Murakami et al., 1993); in transmembrane protease, serine 2 (TMPRSS2)-ERG fusion positive VCaP cells, ERG is phosphorylated at serine-81 and -215, by both I κ B and Akt kinases (Singareddy et al., 2013).

1.5.2 ERG genomic structure and isoforms

The ERG gene maps to the reverse strand of chromosome 21 (21q.22.2) (Rao et al., 1987). Up to nine Erg isoforms, which generate transcripts from a gene encoding 17 exons, have been identified to date. The intron/exon structure of the nine isoforms is shown in Figure 1.9 and their expression is dependent on alternative splicing, polyadenylation sites or initiation codons. Of these 9 transcripts, Erg-1, Erg-2, Erg-3 (p55), Erg-4 (p49), and Erg-5 (p38) encode for functional proteins that bind DNA (Prasad et al., 1994; Duterque-Coquillaud et al., 1993; Reddy and Rao, 1991). Erg-7 and Erg-8 are predicted to form functional proteins as they have open reading frames, whereas Erg-6 and Erg-9 are assumed to be non-functional (Owczarek et al., 2004). Reverse transcriptase-PCR analysis of isoforms using specific primers indicates Erg-3 and Erg-5, are expressed in the endothelium (Hewett et al., 2001); nevertheless, PCR analysis from our group suggests Erg-2 may also be expressed in the endothelium (unpublished data). As of yet, no differences in the activity of these different isoforms have been identified.

The human ERG gene has at least 2 recognized promoters (distal and proximal) separated by approximately 165 kilo base pairs (kb) (Thoms et al., 2011). A region 85 kb downstream of the transcription start site has been identified as an ERG enhancer, which is active during normal haematopoiesis and in T-cell acute lymphoblastic leukaemia cells. ERG has been shown to positively regulate its own expression via the +85 enhancer in these cells (Thoms et al., 2011). However, no endothelial-specific ERG enhancer has been identified so far.

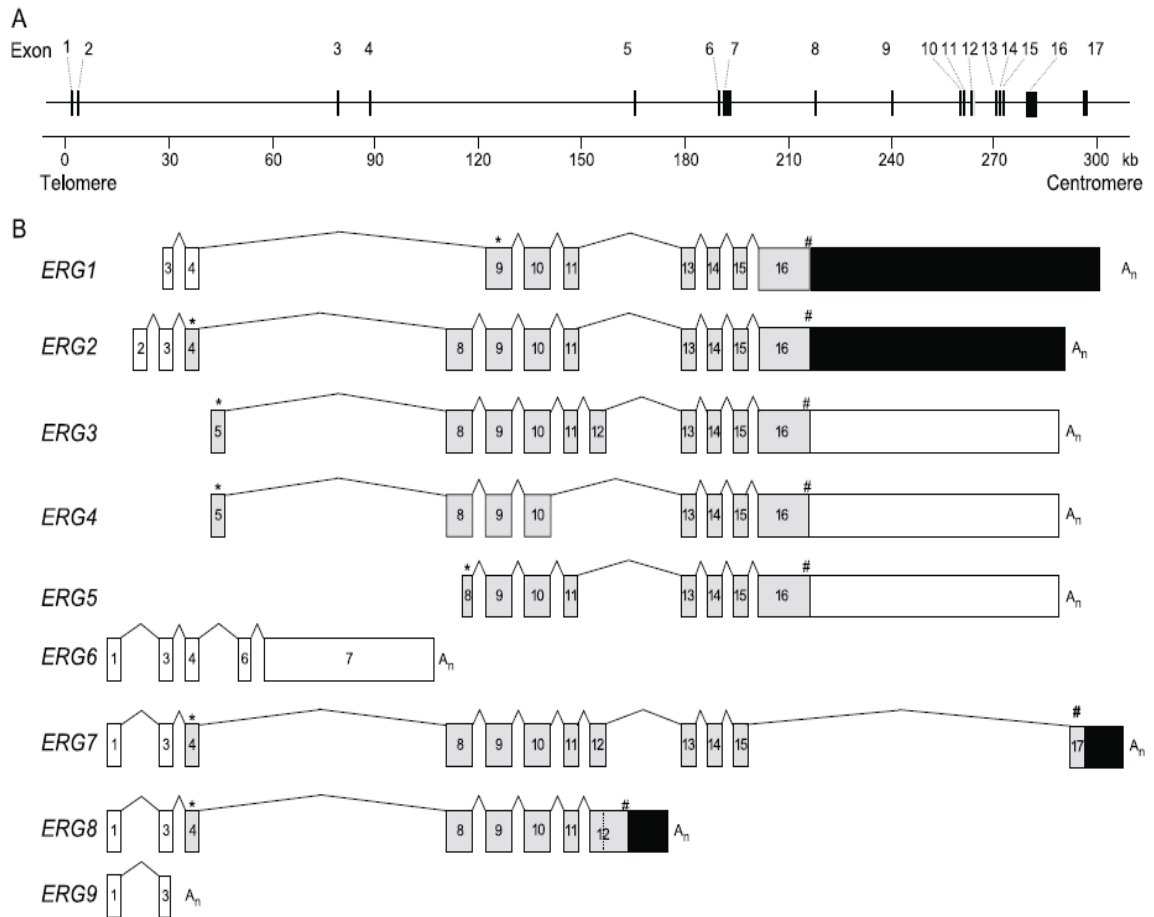


Figure 1.9 Structure of the human ERG gene. (A) Schematic representation of the ERG gene. Exons are indicated by black boxes, and numbered starting from the 5' exon. (B) Structure of alternative transcripts encoded by the ERG gene. Start codons are indicated by an asterisk (*) and stop codons are indicated by a hash (#). Open reading frames are shown in black boxes, the 5'UTRs and 3'UTRs in white boxes, and the transcribed exons in grey boxes (image reproduced from Owczarek et al., 2004, with permission of the rights holder, Elsevier).

1.5.3 DNA binding activity of ERG and domains of the ERG protein

Analysis of deletion mutants has led to the characterization of ERG protein domains mediating DNA binding and transcriptional activation (Siddique et al., 1993). The ETS domain is located in the C-terminus of ERG and as with other ETS factor family members, the ERG ETS domain is essential for DNA binding. ERG and its closest related ETS factor, FLI1, share a highly homologous ETS DNA-binding domain (Figure 1.7). Since a degree of specificity is conferred by bases flanking the core (GGAA/T) motif, multiple studies using various techniques have investigated the specific ERG extended DNA binding consensus sequence. Early studies using EMSA assays identified specific ERG consensus sequences as (C/G)(C/a)GGAA(G/a)T (Murakami et al., 1993) or (A/C)GGAAG (Duterque-Coquillaud et al., 1993). Further genome-wide studies using ChIP-seq, characterized the sequences AGGA(A/t)(G/A) (Wilson et al., 2010) or (C/a/g)(A/C)GGAA(G/A/c) (Wei et al., 2010) as specific ERG consensus sequences. Interestingly, a recent study has shown, by using a variety of biophysical methods, that ERG DNA-binding is allosterically regulated by autoinhibitory regions both N- and C-terminally adjacent to the ETS domain (Regan et al., 2013).

ERG also possesses a second structured domain known as the pointed (PNT) domain, which is conserved in eleven other ETS factors (Figure 1.7). The ERG PNT domain comprises four α -helices and a short α -helix (Hollenhorst et al., 2011). Carrere et al., 1998 suggested a role for the PNT domain in mediating protein-protein interactions and homo/hetero-dimerisation (Carrere et al., 1998). Whilst no function for the ERG PNT domain has yet been reported, deletion of the domain has been shown to result in a 70% decrease in ERG-2 transcriptional activity (Siddique et al., 1993). The PNT domain can, in other ETS proteins, oligomerize and alter DNA-binding affinity (Green et al., 2010). Deletion and homology analysis of the ERG-2 protein showed that ERG also contains a C-terminal transcriptional activation (CTA) domain, which is also conserved in FLI-1, and this domain is repressed by a negative regulatory transcriptional activation (NRT) domain (Siddique et al., 1993) (Figure 1.10).



Figure 1.10 Schematic diagram of the functional domains of ERG-2. ETA, ERG/ETS transcriptional activation domain. NRT, negative regulatory transcriptional activation domain. EDB, ETS DNA binding domain. CTA, carboxyterminal transcriptional activation domain. Numbers indicate amino acid residues of ERG-2.

1.5.4 ERG binding partners

Transcriptional regulation is controlled by interactions between nuclear proteins. Protein-protein interactions can be involved in regulation of DNA binding ability, regulation of transcriptional activity and turnover of transcription factors. Technologies such as two hybrid interactive screens have identified many novel proteins as ERG partners and here I will review some of the protein-protein interactions that have been identified.

Carrere et al. reported that the ERG proteins form homo and hetero-dimeric complexes *in vitro* (Carrere et al., 1998). The authors identified 2 domains involved in ERG dimerization: the ETS domain and a domain within the amino-terminal of the protein containing the pointed domain. Furthermore, ERG can also form heterodimers with some other ETS factors, including FLI-1, ETS-2 and PU-1 (Carrere et al., 1998). The ERG ETS domain also mediates interaction with c-Jun to form a ternary complex with c-Fos and c-Jun (Camuzeaux et al., 2005; Verger et al., 2001; Carrere et al., 1998).

A yeast two-hybrid screen performed using the full-length *Xenopus* Erg protein as bait identified three proteins that physically interacted with ERG: the *xenopus* homeobox transcription factors Xvent-2 and Xvent-2B and *xenopus* small nuclear RNP C protein (Deramaudt et al., 1999). Yang et al. screened a yeast two-hybrid cDNA library constructed from mouse haematopoietic cells using the amino-terminal region of ERG as bait (Yang et al., 2002). This study showed that ERG interacted with UBC9, a ubiquitin-conjugating enzyme and with ESET (ERG associated protein with a suppressor of variegation, enhancer of zest and trithorax domain), which is a histone H3-specific methyltransferase (Yang et al., 2002). Co-immunoprecipitation studies have also shown that ERG is able to associate with the transcription factor KLF2 (Meadows et al., 2009). These experiments did not demonstrate direct physical interaction between ERG and KLF2, but they did place the two proteins in the same complex.

1.5.5 Dysregulation of ERG in cancer

ERG is of particular interest for its role in the pathogenesis of a range of cancers. Chromosomal translocations that result in the expression of oncogenic ERG fusion proteins have been identified in Ewing sarcoma, leukaemia and prostate cancer

and abnormal ERG expression levels have also been linked to prostate cancers.

In Ewing's sarcoma and acute myeloid leukaemia, chromosomal translocations cause ERG to fuse with RNA binding proteins EWS and FUS respectively, producing a chimeric protein (Shing et al., 2003; Sorensen et al., 1994; Peter et al., 1996). The EWS and FUS genes are closely related and contain conserved domains (Delattre et al., 1992). The most common fusions in EWS actually occur between EWS and FLI-1 (85%), while the EWS/Erg fusion has a 5-10% occurrence rate. In EWS, ERG fusions result in replacement of the C-terminus of EWS by the DNA-binding domain of ERG and loss of endogenous ERG promoter activity consequently, causing dysregulation of ERG and its target genes (Barr and Meyer, 2010).

ERG fusion genes are also observed in prostate cancer. Studies have shown that more than 50% of human prostate cancer over-express ERG, where a chromosomal translocation between TMPRSS2 and ERG is induced by exposure to androgens and DNA damage. Strikingly, these two genes are both encoded on chromosome 21 but are located 3 Mbp apart. This TMPRSS2/ERG fusion causes aberrant transactivation of ERG, regulated by the androgen responsive TMPRSS2 promoter (Tomlins et al., 2005). However, how the fusion products regulate prostate cancer remains unclear. Tomlins et al. showed that over-expression of ERG increases cell invasion (Tomlins et al., 2008). Interestingly, Yu et al. implicate ERG activation of the Polycomb group protein EZH2, as important to cancer progression (Yu et al., 2010).

Increasing evidence implicates Wnt signalling as a critical downstream pathway that is important for ERG-mediated tumourigenesis (Wu et al., 2013; Gupta et al., 2010). Wu et al. reported that ERG directly binds to and regulates various genes at different levels of the Wnt signalling cascade (Wu et al., 2013). An earlier study by Gupta et al. demonstrated that expression of the Wnt receptor Frizzled-4 (Fzd4) was positively regulated by ERG (Gupta et al., 2010).

1.5.6 ERG and its role in the endothelium: lineage specification and homeostasis

1.5.6.1 ERG and its role in EC differentiation

ERG regulates the expression of multiple EC genes with roles in crucial endothelial functions such as cell survival, cell migration and junction stability. Importantly, data from our group and several other groups using *in vitro* and *in vivo* models indicate that ERG is a key regulator of angiogenesis and vascular development; these studies will be discussed in detail in section 1.5.7. A further line of evidence for the key role ERG plays in endothelial biology comes from developmental studies of differentiation of embryoid bodies, which show that ERG is required for the differentiation of embryonic stem cells along the endothelial lineage (Nikolova-Krstevski et al., 2009). Moreover, ERG drives the expression of genes that define the endothelial lineage, such as VWF and endoglin (Pimanda et al., 2006; McLaughlin et al., 2001; Schwachtgen et al., 1997). Interestingly, a recent study has shown that constitutive expression of ERG and FLI1 in combination with TGF β pathway inhibition is sufficient to reprogram non-vascular amniotic cells into stable vascular endothelial cells (Ginsberg et al., 2012).

1.5.6.2 ERG and its function in EC homeostasis

ERG also plays a key role in maintaining junction integrity through its transcriptional regulation of multiple junction molecules. ERG binds and transactivates the promoter of the endothelial junctional adhesion molecules VE-cadherin (Birdsey et al., 2008), claudin-5 (Yuan et al., 2012) and ICAM-2 (McLaughlin et al., 1999). ERG is also required for EC survival, partly via a pathway involving VE-cadherin and endothelial junction integrity (Birdsey et al., 2008). ERG is also implicated in the transcriptional regulation of VEGFR1 (Wakiya et al., 1996) and VEGFR2 (Meadows et al., 2009). Work by our group and others show that ERG regulates the endothelial cytoskeleton through the transcriptional regulation of HDAC6 (Birdsey et al., 2012) and of the GTPase RhoJ (Yuan et al., 2011). Additionally, scratch wound assays and single cell imaging have shown a role for ERG in EC migration, as inhibition of ERG decreases the speed and distance at which human umbilical vein EC (HUVEC) migrate and results in a reduction of lamellipodia formation (Birdsey et al., 2012).

1.5.6.3 ERG as a repressor of inflammation

Increasing evidence supports a role for ERG in the modulation of vascular inflammation. As discussed previously, ERG is regulated by pro-inflammatory stimuli, suggesting that its regulation may be critical during inflammatory processes. Transcriptome profiling of control and ERG-depleted HUVEC (Birdsey et al., 2012) showed that ERG inhibition significantly decreased expression levels of 1511 genes, consistent with the role of ERG as a transcriptional activator (Figure 1.11). Interestingly, expression levels of 1138 genes were also significantly increased following ERG inhibition, supporting a role for ERG in repressing transcription of these genes in quiescent EC. ERG has been previously shown to maintain the endothelium in an anti-inflammatory state, by repressing expression of ICAM-1 and interleukin (IL)-8 (Dryden et al., 2012; Sperone et al., 2011; Yuan et al., 2009) and inhibiting leukocyte adhesion *in vitro* (Yuan et al., 2009). ICAM-1 repression by ERG was due to inhibition of NF- κ B p65 binding to the promoter, suggesting a direct mechanism of interference (Dryden et al., 2012). Gene set enrichment analysis of ERG and NF- κ B-dependent genes identified by microarray, coupled with chromatin immunoprecipitation analysis, revealed that in fact this mechanism is common to other pro-inflammatory genes, including IL-8 (Dryden et al., 2012).

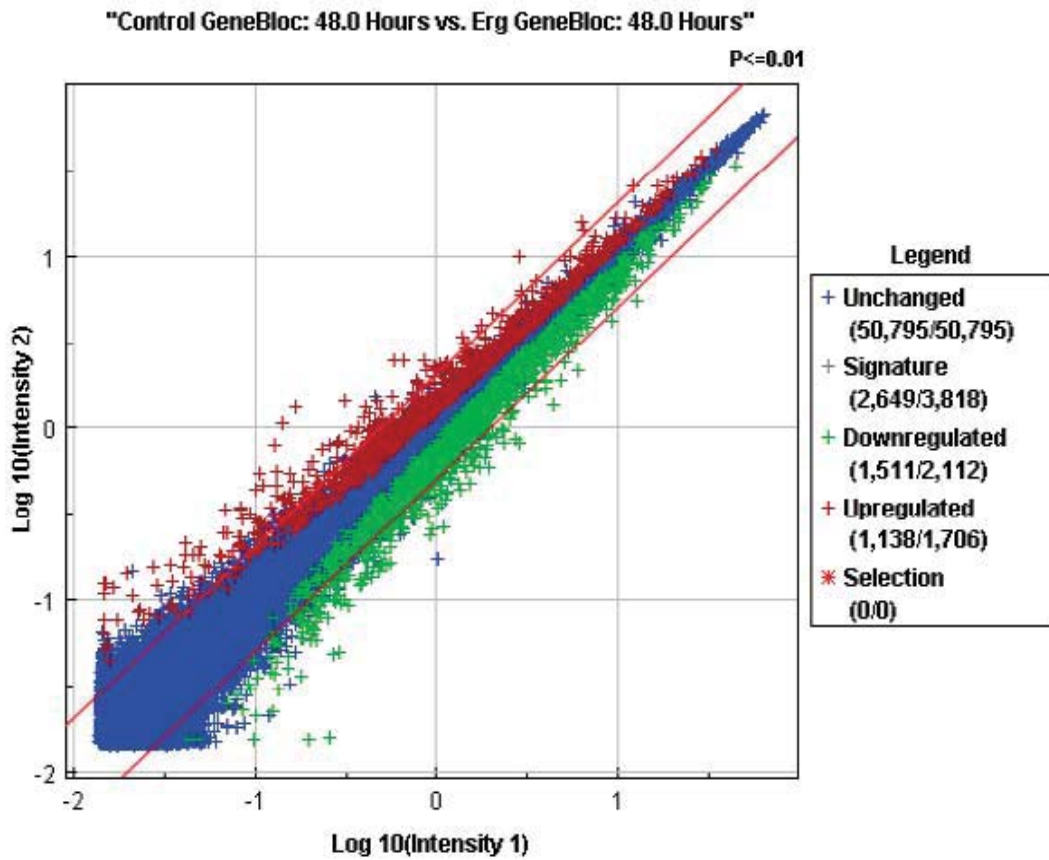


Figure 1.11 Transcriptome profiling of control versus ERG GeneBloc-treated HUVEC. Microarray intensity plot showing the expression values of genes that are significantly different between HUVEC treated with control or ERG GeneBloc for 48 hours (Birdsey et al., 2012). Red crosses represent genes significantly up-regulated, green crosses represent genes significantly down regulated following ERG inhibition and blue crosses represent genes that are unchanged. One-way ANOVA, $p < 0.01$ (image from Dr. G Birdsey).

1.5.7 Regulation of vascular development and angiogenesis by ERG

As discussed, angiogenesis involves the co-ordination of a number of cellular processes such as EC migration, cell-cell interactions and survival; all of which are regulated in part by ERG (Birdsey et al., 2012; Birdsey et al., 2008), pointing to a role for ERG in angiogenesis. Here, I summarise several *in vivo* and *in vitro* model systems that have been used to provide key insights into the role of ERG in vascular development and angiogenesis.

1.5.7.1 ERG is required for vascular development

The dysregulation of blood vessel formation generally has major consequences for normal development, as organogenesis is critically dependent on blood supply (reviewed in Carmeliet, 2003). In our group, we have used genetic lineage-specific deletion in mice to show that ERG is required for vascular development. Constitutive endothelial-specific deletion of ERG was achieved by breeding floxed *Erg* mice with mice expressing the *Cre* transgene under the control of the Tie2 promoter and enhancer (Kisanuki et al., 2001; for methods and details of mouse characterisation and phenotype see Appendix 1). We have shown that constitutive homozygous deletion of endothelial ERG in the mouse embryo (*Erg*^{EC-KO}) causes embryonic lethality between E10.5 and E11.5, with severe vascular disruption. Analysis of the yolk sacs from *Erg*^{EC-KO} embryos showed a reduction in perfused large vessels, consistent with defects in vascular remodelling (Figure 1.12 A). These observations are in line with a recent report by Vijayaraj et al., where global deletion of a subset of ERG isoforms, shown to be predominantly endothelial, resulted in vascular defects and lethality (Vijayaraj et al., 2012). *In vivo* studies also point to a regulatory role for ERG during murine haematopoiesis (Taoudi et al., 2011; Loughran et al., 2008). In these studies, mice carrying a single point mutation in the DNA-binding domain of ERG, inhibiting ERG transactivation, showed multiple defects in definitive haematopoiesis and a failure to sustain self-renewal of haematopoietic stem cells.

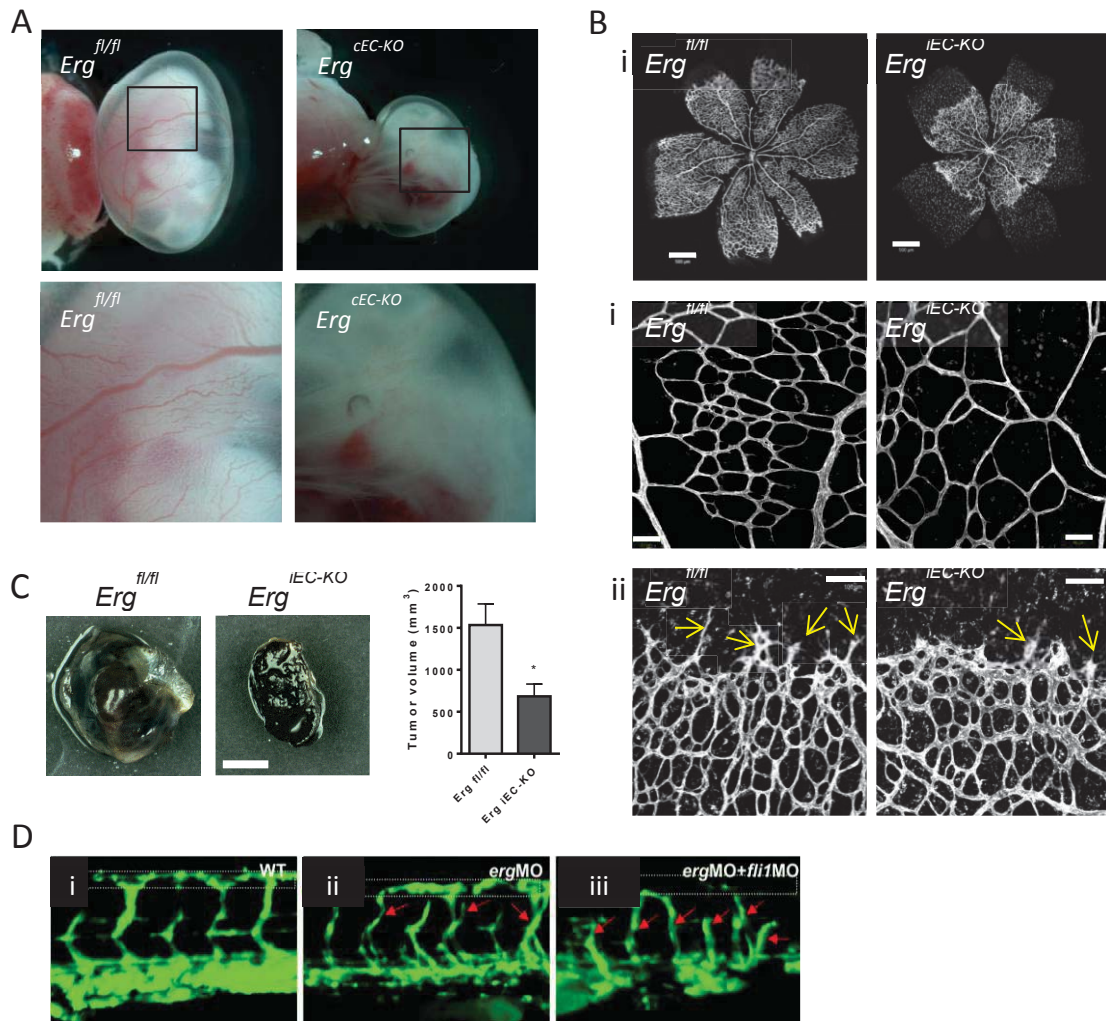


Figure 1.12 ERG is required for vascular development, angiogenesis and tumour growth. (A) Transmitted light microscopy of the yolk sac surrounding E10.5 embryos reveals a decrease in yolk sac vascularisation in *Erg^{cEC-KO}* embryos, compared to *Erg^{fl/fl}* controls. (B) Following tamoxifen treatment, retinas from P6 *Erg^{iEC-KO}* and *Erg^{fl/fl}* mice were stained with isolectinB4 to label the endothelium. Confocal tile scans of retinas show a reduction in (i) the overall extent of the vascular plexus, (ii) the number of vascular branches and (iii) numbers of EC sprouts at the angiogenic front in retinas from *Erg^{iEC-KO}* mice compared to controls. (C) Representative images of B16F0 tumours which were grown for 14 days on adult *Erg^{iEC-KO}* and *Erg^{fl/fl}* mice, scale bar, 2 mm; tumour volume was quantified (images reproduced from Birdsey, Shah et al., 2015, under the Creative Commons BY license; <http://creativecommons.org/licenses/by/3.0/>). (D) Confocal microscopy of *flk1:gfp-gata1:dsRed* transgenic embryos at 72 hours post-fertilisation injected with *erg* and *fli1* morpholinos. (ii) *Erg* morpholino (*ergMO*) results in disruption to intersomitic vessel formation (ISV; red arrows) during zebrafish development. (iii) Double knockdown by *ergMO* and *fli1MO* gave more severely disorganized ISV patterning (red arrows) (image reproduced from Liu and Patient, 2008, with permission of the rights holder, Wolters Kluwer Health).

1.5.7.2 ERG controls postnatal retinal angiogenesis

To circumvent the issue of embryonic lethality, our group also bred floxed *Erg* mice with mice carrying tamoxifen-inducible Cre recombinase under the control of the *Cdh5* promoter (*Cdh5*(PAC)-iCreERT2; Wang et al., 2010), to delete ERG expression at specific times after birth (for methods and details of mouse characterisation and phenotype see Appendix 1). Mouse retinas become vascularized postnatally through sprouting angiogenesis and have therefore recently gained popularity as a model system to study angiogenesis. As vessels develop in a central to peripheral manner, vessels at the migrating front of the developing plexus are less mature compared to more central vessels and there is therefore a spatial separation of different aspects of angiogenesis. Using this approach, we show that ERG is required for angiogenesis in the developing retina of newborn mice (Figure 1.12 B) (Birdsey, Shah et al., 2015). ERG deficiency causes increased vessel regression and reduced pericyte recruitment, confirming that ERG controls vascular stability, thus demonstrating an *in vivo* role for endothelial ERG in physiological angiogenesis (Birdsey, Shah et al., 2015). Furthermore, a marked reduction in VE-cadherin expression and junctional localization was also observed in the retinal vasculature of *Erg*^{iEC-KO} mice, demonstrating that loss of endothelial ERG leads to a disruption of cell-cell junctions *in vivo* (Birdsey, Shah et al., 2015).

1.5.7.3 Endothelial deletion of ERG impairs tumour angiogenesis and growth

In order to determine whether ERG is involved in pathological angiogenesis, our group investigated the requirement for ERG during tumour growth and neovascularisation. To induce tumour formation, B16 melanoma cells were subcutaneously injected into *Erg*^{fl/fl} and *Erg*^{iEC-KO} mice, which had previously been treated with tamoxifen. At day 14, the B16 skin melanoma tumours were significantly reduced in size from *Erg*^{iEC-KO} mice compared to controls (Figure 1.12 C; Birdsey, Shah et al., 2015). Histological staining of blood vessels within the B16 melanoma tumours revealed a significant decrease in vessel density in the mutant mice, which correlated with the decrease in tumour density following *Erg* deletion (Birdsey, Shah et al., 2015). This study confirmed that endothelial ERG is involved in tumour angiogenesis and tumour growth.

1.5.7.4 ERG regulates vessel formation and stability in Matrigel angiogenesis models

In vitro inhibition of ERG has been shown to result in a decreased ability of HUVEC to form tube-like structures when grown on Matrigel matrix (McLaughlin et al., 2001). Furthermore, the *in vivo* Matrigel plug assay has validated the requirement for ERG in formation of neovessels in mice and complemented the *in vitro* Matrigel studies (Birdsey et al., 2008). ERG inhibition resulted in a significant decrease in vascularization of the plugs and significantly more apoptotic cells than control. Interestingly, by measuring the vascular permeability of new vessels using two different sized dextran tracers, we recently showed that over-expression of ERG can reduce permeability and promote VEGF-induced angiogenesis *in vivo* (Birdsey, Shah et al., 2015).

1.5.7.5 ERG is required for vascular development in the zebrafish

Blood vessel development in zebrafish follows a spatiotemporally conserved pattern (Isogai et al., 2003). Loss of function studies in zebrafish embryos showed that ERG was required for efficient vascular development and maintaining vessel integrity, since treatment with an ERG antisense morpholino caused defective intersomitic vessel patterning and haemorrhage in the head (Figure 1.12 D; Liu and Patient, 2008). Moreover, double knockdown of both ERG and FLI-1 in the zebrafish caused a more severe phenotype than the individual knockdowns, suggesting an additive requirement for both these ETS factors (Figure 1.12 D; Liu and Patient, 2008).

1.6 Future perspectives

Numerous studies have examined the signalling molecules involved in angiogenesis, and it is well established that growth factors such as VEGF and their receptors are critical cell non-autonomous regulators of nascent blood vessel formation (Ferrara, 2004). However, the cell autonomous transcriptional regulatory networks through which the expression of genes downstream of growth factor receptors and the receptor genes themselves are activated and maintained in EC remain important questions in vascular biology. Additionally, how signalling pathways influence the transcription factors networks involved in the endothelial gene expression program remains to be fully elucidated.

Current anti-angiogenic therapies are primarily aimed at blocking the pro-angiogenic growth factor VEGF and other signalling pathways (Ferrara, 2004). In line with this, in ischemic diseases VEGF is being trialled for therapeutic angiogenesis applications. However, VEGF has been shown to induce the formation of unstable and highly permeable vessels *in vivo* (Reginato et al., 2011), giving rise to local oedema and inefficient tissue perfusion. It is attractive to speculate that targeting key endothelial transcription factors may be an alternative approach for modulating angiogenesis and vessel stability. As we unravel the transcriptional networks, upstream signalling pathways, and chromatin modifications involved in vessel growth, new molecular hubs, which coordinate multiple endothelial pathways and modulate vessel growth, should emerge.

One such candidate is the transcription factor ERG: transcriptome profiling comparing ERG-positive and ERG-deficient EC shows changes in the expression of genes associated with the multiple signalling pathways (Birdsey et al., 2012), including the Wnt and Notch cascades, that control vascular growth and stability, suggesting that this ETS factor may be essential for the growth and stabilisation of newly formed vascular sprouts as well as maintaining mature, established vessels. The work in this thesis focuses on the interplay among transcription factors and signalling molecules and investigates ERG's mechanism of action in regulating the vasculature.

Chapter Two
Materials and Methods

2. MATERIALS AND METHODS

2.1. HUVEC isolation

Human umbilical cord veins were washed twice with 20 ml Hank's Balanced Salt Solution (HBSS; Sigma) and incubated with 0.5 mg/ml Collagenase-A (Roche) in 20 ml HBSS at 37° C and 5% CO₂ for 8 mins. The cell suspension was centrifuged at room temperature for 10 min at 306 g. The supernatant was discarded and the cell pellet was resuspended in 5 ml complete M199 medium (Sigma), and transferred to a 1 % gelatin precoated-T25 flask (Corning). The following day the M199 medium was changed and Human Umbilical Vein EC (HUVEC) were passaged after reaching confluence.

2.2 Cell culture

HUVEC were routinely grown in M199 medium supplemented with 20 % Fetal Bovine Serum (FBS; Sigma-Aldrich), 1 U/ml penicillin, 0.1 mg/ml streptomycin, 2mM L-glutamine, 30 µg/ml Endothelial Cell Growth Factor (ECGF, Sigma), 10 U/mL heparin (CP Pharmaceutical) at 37 °C and 5 % CO₂, in plates pre-coated with 1% gelatin (Sigma). Cells were cultured in 75 cm² flasks (Corning) and passaged every 3-4 days by trypsinization: cells were washed twice with HBSS, incubated with 0.5 mg/ml trypsin in EDTA (MP Biomedicals) for 2 min at 37 °C and 5 % CO₂ and resuspended in M199 growth medium. HUVEC were used between passage 3 and 4.

Human skin fibroblasts were purchased from the European Collection of Cell Cultures (ECACC) and maintained in M199 supplemented with 10 % FBS at 37 °C and 5 % CO₂. Skin fibroblasts between P2 and P10 were used for all experiments.

2.3 Delivery of ERG-specific antisense oligonucleotides in HUVEC

Human ERG expression was inhibited using either ERG GeneBloc antisense oligonucleotides (McLaughlin et al., 2001) or siRNA against ERG; both denoted as siERG in the text. In parallel, a Control GeneBloc antisense or AllStars Negative Control siRNA was used, which are denoted as siCtrl. These approaches have been extensively characterized in previous studies (Birdsey et al., 2012; Birdsey et al., 2008; McLaughlin et al., 2001). For delivery into HUVEC, cells were seeded the day before transfection at a density of 1×10^5 cells per well of a 35-mm 6-well dish in endothelial

growth medium (EGM-2; Lonza), to form 60 to 80% confluent cultures at time of transfection. 24 h after seeding, cells were transfected with GeneBloc (GB; final concentration, 100 nM) and lipid AtuFect01 (final concentration, 1 µg/mL; Silence Therapeutics) prepared at 5 times concentration in OptiMEM medium (Invitrogen) at 37°C for 30 min. After mixing, the lipid-GB mixture was added to each well of HUVEC containing EGM-2 and incubated for 24 or 48 h. In some experiments Ctrl or ERG siRNA were used (final concentration, 20 nM) and were mixed with AtuFect01 as above.

2.4 Pharmacological/ growth factor *in vitro* cell treatments

HUVEC (1×10^5 cells per well) were seeded in a 35-mm diameter, 6-well dish in EGM-2. 24 h after seeding, HUVEC were transfected with 100 nM ERG or control GB for 24 or 48 h and pharmacologically treated with the proteosomal inhibitor MG132 (Calbiochem) (10 µM) or 200 ng/ml rWnt3a (R&D systems) for 6 h. HUVEC were treated overnight with lithium chloride (10 mM, Sigma). Control groups were treated with the respective vehicles. Cells were lysed and subjected to immunoblotting.

HUVEC placed on 100 µg/mL type 1 collagen (BD Biosciences)-coated dishes at densities of 2,000 cells cm² and 40,000 cells cm² were cultured for 24 h to obtain sparse and confluent cell densities, respectively. After starvation in M199 containing 1% BSA for 6 h, the cells were stimulated with human Ang1* (kindly provided by Regeneron Pharmaceuticals, Inc.) as described in the figures. Ang1* is a recombinant version of Ang1 (Davis et al., 1996) with a modified NH₂-terminus where the first 77 amino acids of human Ang1 have been replaced with the first 73 residues of Ang2 and amino acid replacement of cysteine 245 to a serine residue. In some experiments, cells were pre-treated in the presence of 20 µM LY294002 (Cell Signaling Technology), or 8 µM Akt inhibitor IV (Calbiochem) for 30 min.

For inhibition of NF-κB in HUVEC with BAY 11-7085, HUVEC (1×10^5 cells/well) were seeded onto 1 % gelatin-coated 6-well plates in EGM-2 and transfected with Ctrl or ERG siRNA 24 h later. 24 h post-transfection, cells were treated with BAY 11-7085 (5 µM, Sigma) diluted in DMSO and incubated for a further 24 h. Cells were treated with 10 ng/ml TNF-α for the final 6 h.

2.5 DLL4 stimulation of endothelial cells

Lyophilized recombinant human or mouse DLL4 was purchased from R&D Systems and reconstituted at 100 mg/ml in PBS containing 0.1% bovine serum albumin. For stimulation of cultured endothelial cells, DLL4 was immobilized by coating culture dishes with 500 mg/ml DLL4 in PBS for 1 h at room temperature or overnight at 4 °C.

2.6 Isolation of mouse lung endothelial cells (Neil Dufton)

Primary mouse lung endothelial cells were isolated from the lungs of control *Erg^{fl/fl}* and *Erg^{cEC-het}* mice. Lungs were minced using GentleMACS C tubes and GentleMACS Dissociator (Miltenyi Biotec), digested with 0.1% collagenase type I (Invitrogen, UK), and sieved through a 70 µm-pore cell strainer (BD Falcon). EC were selected by magnetic immunosorting (Dynabeads; Invitrogen) with a negative sort for FcγRII/III receptor-positive macrophages and a positive sort for ICAM-2-positive endothelial cells. Cells were cultured in EGM-2 media (Lonza), in flasks precoated with a mixture of 0.1% gelatin (Sigma), PureCol (Invitrogen) and human plasma fibronectin (Chemicon).

2.7 Adenovirus amplification and titration

Adenovirus was amplified in human embryonic kidney (HEK) 293A cells and purified using the AdenoX™ virus purification kit (Clontech) following the manufacturer's instructions. Briefly, HEK 293A cells were grown in 175 cm² tissue culture flasks (BD falcon) until confluent. Cells were infected with 200 µl adenovirus and incubated for 5 days or until cytopathic effects are seen. The adenovirus was then purified from the cells using the kit components and eluted in a volume of 3 ml. Adenoviral titre was then determined using the Adeno-X Rapid titre kit following the manufacturer's instructions.

2.8 Adenoviral transduction of HUVEC

The volume of GFP-tagged control and VE-cadherin adenovirus used to infect the cells was calculated using the formula; number of infected cells x desired multiplicity of infection (MOI) = Total plaque forming units (PFU) needed / PFU/ ml = ml virus.

HUVEC either seeded at 5×10^4 cells on gelatin-coated 13-mm diameter glass coverslips or at 1×10^5 cells in a 6-well dish were transduced with GFP-tagged adenovirus (VE-cadherin [VEC]-GFP and GFP; kindly provided by F. William Lusinskas, Harvard Medical School, Boston, MA). After 48 h, cells were transfected with ERG or control GB (100 nM). 48 h later, cells on coverslips were fixed and stained for immunofluorescence microscopy or samples were collected for subcellular fractionation and immunoblotting.

2.9 RNA isolation from HUVEC and mouse tissue

Mouse yolk sacs and brains were immediately placed in RNALater (Qiagen) after removal from animals and kept at 4 °C. Mouse tissues were homogenized using QiaShredder (Qiagen). Mouse tissues, primary lung EC and HUVEC were harvested with 350 µl RLT buffer (Qiagen) containing 3.5 µl 2-mercaptoethanol. The lysate was passed 5 times through a blunt 20-gauge needle (0.9 mm diameter) fitted to an RNase-free syringe. 1 volume of 70 % ethanol was added to the homogenized lysate. The sample was transferred to an RNeasy spin column (Qiagen) placed in a 2 ml collection tube, and centrifuged for 15 seconds at 8000 x g. The flow-through was discarded. 350 µl Buffer RW1 (Qiagen) was added to the RNeasy spin column. The column was centrifuged for 15 sec at 8000 g, and the flow-through was discarded. DNase I (Qiagen) diluted in RNase-free water was added to 70 µl Buffer RDD (Qiagen), and added to the RNeasy spin column membrane. After 15 min 350 µl Buffer RW1 (Qiagen) was added to the RNeasy spin column. The column was centrifuged for 15 seconds at 8000 g, and the flow-through was discarded. 500 µl Buffer RPE (Qiagen) was added to the RNeasy spin column. The column was centrifuged for 2 min at 8000 g, and placed in a new 2 ml collection tube. 50 µl RNase-free water (Qiagen) was added to the spin column membrane. The column was centrifuged for 1 min at 8000 g to elute the RNA. The purity and the concentration of the RNA were analyzed using a NanoDrop ND-1000 spectrophotometer.

2.10 First-Strand cDNA synthesis

1 µg total RNA was added to 1 µl oligodT and 1 µl 10 mM dNTP mix (Invitrogen) and the final volume of the reaction was made up to 13 µl with water. The reaction was heated to 65 °C for 5 min and incubated on ice for at least 1 min. 4 µl 5X First-Strand Buffer (Invitrogen), 1 µl 0.1M Dithiothreitol (DTT), and 1 µl of

SuperScript III Reverse Transcriptase (Invitrogen) were added to the mixture. The reaction was incubated at 50 °C for 60 min and inactivated by heating it to 70 °C for 15 min.

2.11 Quantitative real-time PCR (qPCR)

5 µl of 1:50 pre-diluted template cDNA was amplified using PerfeCTa SYBR Green Fastmix (Quanta Biosciences), 0.4 µM forward primer, 0.4 µM reverse primer and 5.5 µl H₂O. The cycling conditions comprised DNA denaturation for 3 min at 95 °C and amplification repeated for 40 cycles at 95 °C for 15 sec and 60 °C for 45 seconds. All PCR efficiencies were above 95 %. Real-time PCR were performed using Bio-Rad CFX96 thermocycler. The results were analysed using Bio-Rad CFX Manager Software version 2.0.

Table 2.1 Oligonucleotides used for qPCR

Primers		Oligonucleotide Sequences
<i>AXIN2</i> (human)	Forward	5'- CATTTCCTCCGAGAACCCACCGCC -3'
	Reverse	5'- TGTGGCGGCTCTCCAACCTCCA -3'
<i>Axin2</i> (mouse)	Forward	5'- GGTCCTGGCAACTCAGTAACA -3'
	Reverse	5'- CTCATGTGAGCCTCCTCTCTTTT -3'
<i>CTNNB1</i> (β-catenin; human)	Forward	5'- TCGGTGAGCAGGGTGCCATTC -3'
	Reverse	5'- CATGCGGACCCCCTCCACAA -3'
<i>Ctnnb1</i> (β-catenin; mouse)	Forward	5'- GTCAGTGCAGGAGGCCG -3'
	Reverse	5'- CAGGTCAGCTTGAGTAGCCA -3'
<i>Cldn3</i> (mouse)	Forward	5'- GAGTGCTTTTCTGTGGCG -3'
	Reverse	5'- TCCCTGATGATGGTGTGGC -3'
<i>CCND1</i> (Cyclin D1; human)	Forward	5'- TCAAGTGTGACCCGACTGCCT -3'
	Reverse	5'- GCCTGGCGCAGGCTTGACT -3'
<i>Ccnd1</i> (Cyclin D1; mouse)	Forward	5'- GCGTACCCTGACACCAATCT -3'
	Reverse	5'- CACAGACCTCCAGCATCCAG -3'
<i>DACT1</i> (human)	Forward	5'- ACAGTCGGCCTAGCTCAGGGTT -3'
	Reverse	5'- TGCAGATTTGGGGCAACCATCTGA -3'
<i>DLL4</i> (human)	Forward	5'- CTGGCCGACGCTGTGAGGTG -3'
	Reverse	5'- GGCAAGCCACGGGGAATC -3'
<i>Dll4</i> (mouse)	Forward	5'- TTTGCTCTCCCAGGGACTCT -3'
	Reverse	5'- AGGCTCCTGCCTTATACCTCT -3'
<i>ERG</i> (human)	Forward	5'- GGAGTGGGCGGTGAAAGA -3'
	Reverse	5'- AAGGATGTCGGCGTTGTAGC -3'
<i>Erg</i> (mouse)	Forward	5'- CCGGATACTGTGGGGATGAG -3'
	Reverse	5'- TCTGCGCTCATTTGTGGTCA -3'
<i>FZD4</i> (human)	Forward	5'- GCTCCAGCCAGCTGCAGTTCT -3'
	Reverse	5'- CGCATGGGCCAATGGGGATGT -3'
<i>Fzd4</i> (mouse)	Forward	5'- TTCGGGGACGAGGAGGAG -3'
	Reverse	5'- ACCGAACAAAGGAAGAACTGC -3'
<i>GAPDH</i> (human)	Forward	5'- CAAGGTCATCCATGACAACCTTTG -3'
	Reverse	5'- GGGCCATCCACAGTCTTCTG -3'

<i>GSK3B</i> (human)	Forward	5'- GGACTAAGGTCTTCCGACCC -3'
	Reverse	5'- GGATGGTAGCCAGAGGTGGA -3'
<i>HES1</i> (human)	Forward	5'- AATTCCCTCGTCCCCGGTGGCT -3'
	Reverse	5'- CTTGGAATGCCGCGAGCTATCTT -3'
<i>HEY1</i> (human)	Forward	5'- TCGGCTCTAGGTTCCATGTCCCC -3'
	Reverse	5'- AGCTTAGCAGATCCCTGCTTCTCAA -3'
<i>Hprt</i> (mouse)	Forward	5'- GTTAAGCAGTACAGCCCCAAAATG -3'
	Reverse	5'- TCAAGGGCATATCCAACAACAAAC -3'
<i>JAG1</i> (human)	Forward	5'- GTTTCGCCTGGCCGAGGTCC -3'
	Reverse	5'- GTGGGCAACGCCCGTGTCT -3'
<i>Jag1</i> (mouse)	Forward	5'- CTGCTTGAATGGGGGTCACT -3'
	Reverse	5'- GCAGCTGTCAATCACTTCGC -3'
<i>CDH2</i> (N-cadherin; human)	Forward	5'- TGGTGAAATCGCATTATGCAAGA -3'
	Reverse	5'- TGCAGTTGCTAAACTTCACATTG -3'
<i>Cdh2</i> (N-cadherin; mouse)	Forward	5'- GCTTCAGGCGTCTGTGGAG -3'
	Reverse	5'- CTGTCCCTTCGTGCACATCCT -3'
<i>NRARP</i> (human)	Forward	5'- GCGCTGCACCAGTCGGTCAT -3'
	Reverse	5'- GCCGCGTACTTCGCCTTGGT -3'
<i>CDKN1A</i> (p21; human)	Forward	5'- CACTCAGAGGAGGCGCCATGT -3'
	Reverse	5'- CGCTGTCCACTGGGCCGAAG -3'
<i>Plvap</i> (mouse)	Forward	5'- CCCTCCACCCATTGATCCAG -3'
	Reverse	5'- CAGCAGGGTTGACTACAGGG -3'
<i>SOX17</i> (human)	Forward	5'- CCCC AAGGCTAGCTTCCGAT -3'
	Reverse	5'- CTGCTCATGGCTCTCCAGAC -3'
<i>Sox17</i> (mouse)	Forward	5'- GAACGCTTTCATGGTGTGGG -3'
	Reverse	5'- CACGACTTGCCAGCATCT -3'
<i>TCF1</i> (human)	Forward	5'- TTCTTGGCAGAAGGTGGCAT -3'
	Reverse	5'- AGGCAGCTGTCATTCTTGGA -3'
<i>Tcf1</i> (mouse)	Forward	5'- GTAAGGTCCACGGTGTACGG -3'
	Reverse	5'- TACTTGGTGTAAAGGCCGCAG -3'
<i>TEK</i> (Tie2; human)	Forward	5'- TGTGCTGTTCTTCTTGCCT -3'
	Reverse	5'- GCACCTTCCACAGTTCCAGA -3'
<i>Tek</i> (Tie2; mouse)	Forward	5'- TTTCTCCTTGCCGCCAACTT -3'
	Reverse	5'- TTTCTCCTTGCCGCCAACTT -3'

2.12 Agarose Gel Electrophoresis

PCR products were run on an agarose (Sigma) gel (% specified in figures) in Tris-Acetate-EDTA (TAE) buffer and ethidium bromide (Invitrogen) was added at a final concentration of 0.5 µg/ml. Gels were loaded with sample DNA and 6x loading dye alongside a 100 bp DNA molecular weight ladder (New England BioLabs) and run at 100 volts until the DNA sample had migrated a sufficient distance through the gel. The gel was visualized under 365 nm UV light and images recorded using a UVP gel documentation imaging system.

2.13 Immunofluorescence analysis of HUVEC

HUVEC (5×10^4 cells) were grown on gelatin-coated 13-mm diameter glass coverslips and treated with either 100nM ERG or control GB for 48 h. In some

experiments, 100 nM of FITC-conjugated GeneBlocs were used. HUVEC were fixed in ice-cold methanol for 10 min and stained using the following primary antibodies: rabbit anti-ERG (1:400; Santa Cruz Biotechnology), goat anti-VE-cadherin (1:200; Santa Cruz Biotechnology) and mouse anti-active- β -catenin (1:200; Upstate-Millipore). Secondary antibodies were anti-mouse Alexa Fluor (AF) 488, anti-mouse AF 555, anti-rabbit AF 488, anti-rabbit AF 546, anti-goat AF 546, streptavidin AF 633 (1:500; all from Invitrogen); biotinylated anti-mouse IgG (1:200; Vector Laboratories, Peterborough, UK). Nuclei were visualized using either TOPRO-3 or DAPI (1:500; Invitrogen). All antibody incubations were performed at room temperature for 15 min in PBS containing 3% BSA. Coverslips were mounted onto glass slides using VectorShield (Vector Laboratories). Images were captured using a Carl Zeiss LSM510 META confocal microscope.

2.14 Immunofluorescence of mouse retina tissue

Mice were injected intraperitoneally (IP) with Tamoxifen (50 μ g per mouse; Sigma) at postnatal (P) day 1, P2 and P3 before eyes were collected at P6. Retinas were isolated from P6 mice and fixed in 3 % paraformaldehyde (PFA) in PBS for 30 min at room temperature and were then blocked in 3 % BSA, 0.2 % Triton X-100 in PBS for 2 h. Retinas were incubated overnight at 4 °C in primary antibody to Sox17 (1:200, R&D systems) diluted in 0.5 % BSA, 0.25 % Tween-20 in PBS. Retinas were washed in PBS containing 0.1 % Tween-20 (PBST) three times for 15 min each. Primary antibodies were followed by incubation with anti-goat IgG AF 546 (1:500, Invitrogen), diluted in 1 % BSA, 0.5 % Tween-20 for 2 h at room temperature. Following washes in PBST, retinas were post-fixed in 3 % PFA for 15 min. Retinas were equilibrated in PBLEC (1 % Tween-20, 0.1 mM CaCl₂, 0.1 mM MgCl₂, 0.1 mM MnCl₂ in PBS) and then incubated with biotinylated isolectin B4 (1:250, Vector Labs) diluted in PBLEC overnight at 4 °C. Retinas were washed in PBST and incubated with streptavidin-AF 633 (1:500, Invitrogen) diluted in PBLEC for 2 h at room temperature followed by washing in PBST. Retinas were mounted in Fluoromount G (Southern Biotech). Confocal microscopy was carried out on a LSM510 META (Carl Zeiss). Images were analysed with Volocity (PerkinElmer).

2.15 Immunoblotting

2.15.1 Preparation of total cell lysates

Cells were washed twice with 2 ml ice-cold PBS, and whole cell protein lysates were prepared from HUVEC using 100 μ l CelLytic reagent (Sigma) supplemented with protease inhibitor cocktail (SIGMA) (1:100). Lysates were centrifuged for 15 min at 2000 *g* at 4°C. Supernatants were processed for SDS-PAGE.

2.15.2 Preparation of nuclear and cytosolic cell fraction lysates

Subcellular fractionation of cells into cytoplasmic and nuclear extracts was performed using the Nuclear Extract kit (Active Motif) according to the manufacturer's instructions. Cells were washed with ice-cold PBS/Phosphatase inhibitors, harvested by scraping, centrifuged at 53 *g* for 5 min at 4 °C. The cell pellet was resuspended in 500 μ l hypotonic buffer and incubated for 15 min on ice. 25 μ l detergent was added and the suspension was vortexed and then centrifuged at 14000 *g* for 30 seconds at 4°C. The supernatant, which constituted the cytoplasmic fraction, was collected. The nuclear pellet was resuspended in 50 μ l complete lysis buffer, vortexed and incubated on ice on a rocking platform for 30 min. After vortexing, the suspension was centrifuged at 14000 *g* for 10 min at 4°C, and the pellet discarded.

2.15.3 Sodium Dodecyl Sulphate Polyacrylamide Gel Electrophoresis (SDS-PAGE)

Immunoblotting was carried out using 10 to 30 μ g of total cell lysate. When nuclear and cytoplasmic lysates were prepared, 5 μ g of lysates were used. Protein concentration of the lysates was determined with Precision Red reagent (Universal Biologicals): the adsorbance of the samples was obtained with Synergy HT spectrophotometer (BIO-TEK) at 600 nm wavelength. Samples were added to NuPAGE® LDS Sample Buffer (4 \times ; Invitrogen) containing 0.7 M 2-mercaptoethanol and heated for 10 min at 70 °C.

Proteins were separated by SDS-polyacrylamide gel electrophoresis (PAGE) and transferred to polyvinylidene difluoride (PVDF) membrane (Immobilon-P, Millipore). PVDF membranes were either blocked with PBS milk (PBS with 5 % low-fat milk) for 1 h at room temperature, and probed with antibodies diluted in PBS-T

(PBS with 0.1% Tween-20), or blocked in TBS-T BSA (TBS with 5 % w/v BSA; 0.1 % Tween-20) for 1 h at room temperature and probed with antibodies diluted in TBS-T BSA overnight at 4 °C.

Immunoblots were labelled with the following primary antibodies: anti-active β -catenin (1:1000; Upstate-Millipore), anti-AKT (1:1000; Cell Signaling Technology), anti-phospho-AKT (1:1000; Cell Signaling Technology), anti-ERG (1:500; Santa Cruz Biotechnology), anti-Fzd4 (1:1000; Santa Cruz Biotechnology), anti-Dll4 (1:500; R&D systems), anti-GAPDH (1:10,000; Millipore), anti-GFP (1:1000; Santa Cruz Biotechnology), anti-HDAC1 (1:1000; Abcam), anti-tubulin (1:10,000; Sigma-Aldrich), anti-Jag1 (1:1000; Santa Cruz Biotechnology), anti-N-cadherin (1:1000; Cell Signaling), anti-NICD (1:500; Cell Signaling), anti-Sox17 (1:1000; R&D systems), anti-Tie2 (1:1000; BD Biosciences) and anti-VE-cadherin (1:1000; BD Biosciences). Primary antibodies were detected either using fluorescently labelled secondary antibodies (1:10,000): goat anti-rabbit IgG DyLight 680 and goat anti-mouse IgG Dylight 800 (Thermo Scientific). Detection and quantification of fluorescence intensity were performed using an Odyssey® CLx imaging system (LI-COR Biosciences, Lincoln) and Odyssey® 2.1 software. In some instances, HRP-conjugated secondary antibodies were used for chemiluminescence detection (ECL™; Amersham™ GE Healthcare) and Kodak®BioMax® Light Film (Sigma), where protein levels were quantified by densitometry and normalized against loading controls.

2.16 Co-immunoprecipitation assays (Lourdes Osuna Almagro and Silvia Martin Almedina)

For immunoprecipitations, cells were lysed in buffer (20 mM Tris [pH 7.5], 0.5 % Triton, Phenylmethanesulfonyl Fluoride and Protease Inhibitor Cocktail; Sigma, UK) containing 150 mM Sodium Chloride. Either 2 μ g ERG rabbit polyclonal IgG (H-95; sc-28680, Santa Cruz Biotechnology) or negative control rabbit IgG antibody in buffer (#7074; Millipore, UK) was incubated with protein A sepharose beads (Sigma, UK) on an end-to-end rotator for 2 h at 4 °C. The antibody-protein A sepharose complexes were then incubated with pre-cleared cellular lysates for at least 2.5 h or overnight at 4 °C. Immunocomplexes were collected, washed three times in lysis buffer and 10 μ l of SDS loading buffer was added to the sepharose beads. The protein samples were denatured at 100°C for 5 min, and resolved by SDS-PAGE. Immunoblots were labelled

with the following primary antibodies: anti-active β -catenin (Upstate-Millipore), anti-ERG (Santa Cruz Biotechnology), anti-NICD (Cell signalling). Primary antibodies were detected using anti-mouse or anti-Protein A HRP-conjugated secondary antibodies and bands were visualised using ECL chemiluminescence detection.

2.17 Chromatin immunoprecipitation- qPCR

Chromatin immunoprecipitation (ChIP) was performed using ChIP-IT (Active Motif, Rixensart, Belgium) as previously described (Birdsey et al., 2008). HUVEC previously transfected with siCtrl or siERG, or untreated HUVEC, were grown to confluence in 15 cm diameter tissue culture plates and were fixed for 10 min with formaldehyde (to a final concentration of 1 %) in basal M199 media on a shaker at 60 rpm. Plates were rinsed with 10 ml PBS followed by a glycine solution for 5 mins to stop the fixation reaction. After one further rinse with ice-cold PBS, cells were collected into a 15 ml Falcon tube using 6 ml PBS containing 30 μ l PMSF, then pelleted by centrifugation for 10 mins at 720 g and 4 °C.

The supernatant was removed and the cell pellet was then resuspended in 1 ml ice-cold lysis buffer (Active Motif) containing 5 μ l PIC (Active Motif) and 5 μ l PMSF (Active Motif) and incubated on ice for 30 mins. The cells were homogenized using an ice-cold Dounce homogeniser to aid nuclei release. The homogenised cell sample was centrifuged for 10 min 2400 g at 4°C to pellet the nuclei. The pellet was then resuspended in 350 μ l shearing buffer (Active Motif) supplemented with 1.75 μ l PMSF.

Chromatin was sheared by sonication for 4 cycles of 30 secs on 30 secs off at 4 °C using a Bioruptor water bath sonicator (Diagenode), resulting in DNA fragments of 500–1000 bp in size. The sheared chromatin was then centrifuged at 18,000 g for 10 mins at 4 °C and the supernatant containing the sheared chromatin was used immediately or stored at -80 °C.

100 μ l of sheared chromatin was added to a siliconised microcentrifuge tube containing 25 μ l protein G magnetic beads (Active Motif), 20 μ l ChIP buffer 1 (Active Motif), 1 μ l protease inhibitor cocktail, 3 μ g of antibody (anti-ERG from Santa Cruz Biotechnology, anti-cleaved Notch1 (anti-NICD) from Cell Signaling, anti- β -catenin from BD Biosciences; or rabbit or mouse IgG control) and dH₂O to give a final volume of 200 μ l. Immunoprecipitation reaction was incubated overnight on a rotator at 4 °C.

The antibody and chromatin complexes bound to magnetic beads were separated from the chromatin solution using a magnet. Beads were then washed once with 800 μ l ChIP buffer 1 and twice with 800 μ l ChIP buffer 2 (Active Motif). Chromatin was then eluted from the washed beads by adding 50 μ l of elution buffer AM2 (Active Motif), and incubating on an end-to-end rotator for 15 mins at room temperature. 50 μ l of reverse cross-linking buffer (Active Motif) was then added to eluted chromatin and beads. The eluted chromatin was removed from the beads using a magnet to allow the beads to pellet to the side of the tube and the supernatant collected. An “input DNA” sample was processed by adding 88 μ l of ChIP buffer 2 and 2 μ l 5 M NaCl to 10 μ l of sheared chromatin. This and the immunoprecipitated chromatin samples were incubated at 95 °C for 15 mins to reverse the cross-links. 2 μ l of proteinase K was then added and samples were incubated at 37 °C for 1 h to digest proteins.

Immunoprecipitated DNA was then used as template for qPCR using primers specific for specific genomic loci to amplify a region containing putative ERG-binding sites. Oligonucleotide sequences are listed below. To determine the specificity of the ERG chromatin interactions, PCR amplification was also carried out with primers downstream of the promoter in a region that should not interact with transcription factors (Ctrl). Data are represented as the percentage of immunoprecipitated template compared to the total input sample, relative to negative control IgG.

Table 2.2 Oligonucleotides used for ChIP-qPCR

Primers		Oligonucleotide Sequences
<i>DLL4</i> -16 enhancer	Forward	5'- TCATTCAAAGCTCGGCCCT -3'
	Reverse	5'- TGATGCCCTGCGCTAGATTT -3'
<i>DLL4</i> -12 enhancer	Forward	5'- TCCCACGCCCTCTATGAGTA -3'
	Reverse	5'- GCAGGACATCACAGCGTTTC -3'
<i>DLL4</i> R1 promoter	Forward	5'- GGGAACACGAGGCCAAGAG -3'
	Reverse	5'- CTGTCTAATCCTGGGGCTGC -3'
<i>DLL4</i> int3 enhancer	Forward	5'- GTTTCCTGCGGGTTATTTTT -3'
	Reverse	5'- CTTTCAAAGGAGCGGAAT -3'
<i>DLL4</i> +14 enhancer	Forward	5'- GGGGTTGTGCAGAAGGAGAA -3'
	Reverse	5'- TTTTCCCTACCCCTGACCA -3'
<i>DLL4</i> Ctrl exon 11	Forward	5'- CTCAGGGCAGTGTGTTGGAA -3'
	Reverse	5'- CTCGAGGTTGTGGAGATGGG -3'
<i>FZD4</i> R1 promoter	Forward	5'- TTTAGAAACCGTGTCCCCGAG -3'
	Reverse	5'- GTCTCGCGCTCTGATTTCT -3'
<i>FZD4</i> Ctrl 3'UTR	Forward	5'- GCCAATCTGGGGGACTTTCA -3'
	Reverse	5'- TTCAGGGCATGTGTAGCAGG -3'

<i>JAG1</i> R1	Forward	5'- GAGCACGCCCTCTCATGAAT -3'
	Reverse	5'- GCCGCAGGTAACACAATGAC -3'
<i>JAG1</i> R2	Forward	5'- GGGTGGGAAGGAAGATGGGTG -3'
	Reverse	5'- AGTGCACCCCATTAGAGCAC -3'
<i>JAG1</i> R3	Forward	5'- ACTCCATGGCGGTTACCTTG -3'
	Reverse	5'- CGGCTGCCAACACAATTACC -3'
<i>JAG1</i> Ctrl 3'UTR	Forward	5'- CCTGACAGAGGGATGGAGGA -3'
	Reverse	5'- AGGGAATCAAGGCTCCCCTA -3'
<i>TIE2</i> R1 enhancer	Forward	5'- GGGACCCACACTTCCAACAA -3'
	Reverse	5'- TTTGGTATCAGCAGGGCTGG -3'
<i>TIE2</i> Ctrl 3'UTR	Forward	5'- TTTCCTGGCATGGGAGACC -3'
	Reverse	5'- TTTCCTGGCATGGGAGACC -3'

2.18 Plasmids

The human Jagged-1 promoter cloned into a pGL3 Luciferase Reporter Vector was kindly provided by Chris Hughes, University of California. The pcDNA-ERG-2 expression plasmid was provided by Graeme Birdsey, Imperial College London. The Notch-regulated luciferase reporter genes TP1 was from U. Zimmer-Strobl. TOPFLASH (luciferase reporter with TCF/LEF binding sites) or FOPFLASH (luciferase reporter with mutated TCF/LEF-binding sites) plasmids were a gift from Marc van de Wetering and Hans Clevers, Hubrecht Institute, Utrecht, The Netherlands. pGL4.10[luc2] (Promega, Madison, USA) Firefly Luciferase empty vector, lacking a promoter sequence, was used as a control. pGL4.73[hRluc/TK] (Promega) Renilla luciferase vector was used as an internal control in the luciferase assay. pGL4.13 [luc2/sv40] (Promega) was used as a parallel control to measure transfection efficiency.

2.19 Plasmid construction

2.19.1 PCR Amplification and Digestion

Primers were designed to amplify a 1000-bp fragment of the Dll4 promoter sequence (1kb upstream of the transcription start site) from human genomic DNA. NheI and HindIII restriction sites were included at the 5' end of the forward and reverse primers (see Table 2.3 for oligonucleotide sequences), respectively, to maintain the promoter orientation while cloning into the NheI and HindIII site of the Firefly luciferase reporter vector, pGL4.10 [luc2] (Promega). PCR reactions were cleaned up by using the Qiaquick Minispin column (Qiagen) and digested with NheI and HindIII.

pLightSwitchProm-Fzd4 luciferase reporter plasmid, containing the Fzd4 promoter sequence 1.1 kb upstream of the transcription start site (purchased from

SwitchGear, Active Motif), was digested with restriction enzymes SacI and HindIII to extract the 1.1 kb insert of the Fzd4 promoter.

Table 2.3 Oligonucleotides used for generating promoter constructs

Primers		Oligonucleotide Sequences
<i>Dll4</i> promoter	Forward (NheI)	5'-ACGTGCTAGCGGGCCAGAACCTCATTACC-3'
	Reverse (Hind III)	5'-ACGTAAGCTTCGCCGCTACTGAAACCTG-3'
<i>Fzd4</i> promoter	Forward (NheI)	5'-ACGTGCTAGCTACTCAGCACAGGCACACAG-3'
	Reverse (Hind III)	5'-ACGTAAGCTTTTGGGCATCTTGGTCACGTT-3'

2.19.2 Cloning and Vector Preparation

Firefly luciferase reporter vector, pGL4.10 [luc2] (Promega Madison USA) was digested with restriction enzymes NheI and HindIII or SacI and HindIII and the *Dll4* or *Fzd4* promoter digested products were ligated upstream to the luciferase gene into the pGL4 backbone. The ligated plasmid was then transformed into DH5 α competent bacterial cells and colonies were picked after plating each transformation reaction. Each colony was then grown as an overnight culture in LB broth containing 100 μ g/ml ampicillin for selection. Plasmids were purified by using the Qiagen plasmid mini prep kit and Qiagen Endotoxin free maxiprep kit for use in luciferase assays. Correct insertion was confirmed by sequencing of the plasmid using forward and reverse primers from the 5' and 3' region of the insert.

2.20 Transfections

HUVEC were seeded at 1×10^5 per well in EGM-2 medium (Lonza) on a gelatin-coated 6-well plate and 24 h later transfected with Genejuice transfection reagent (Merck Chemicals), as recommended. Cells were incubated with 9 μ l of GeneJuice, 1 μ g luciferase plasmid and/or 1 μ g of expression plasmid and 1 μ g of pGL4-Renilla for 24 h.

2.21 Luciferase assays

Reporter assays in HUVEC were performed with the Dual-Luciferase Reporter Assay System (Promega) and a Synergy HT microplate reader. 24 h after co-transfection with the luciferase reporters, expression plasmids and the constitutive

Renilla luciferase reporter pGL4.74hRluc/TK (Promega) HUVEC were lysed and reporter assays were performed in triplicate.

For siRNA experiments, cells were transfected with 20 nM ERG or control siRNAs and after 24 h transfected with the luciferase reporters and the constitutive Renilla luciferase reporter. For experiments in which Notch activity was induced by DLL4, transfected HUVEC were replated on DLL4-coated dishes 6 h after plasmid transfections. Luciferase activity was measured after an additional 24 h. For TOPFLASH/FOPFLASH experiments, 24 h after transfection, cells were treated for 6 h before preparation of lysates with Wnt3a, Wnt5a or control conditioned-medium derived from L cells and diluted 1:1 with endothelial cell growth medium (Liebner et al., 2008). The activation of TCF/ β -catenin-mediated transcription was defined by the ratio of TOPFLASH/FOPFLASH luciferase activity. In some experiments, cells were also co-transfected with 1 μ g pCMV6-Fzd4 expression construct (OriGene Technologies, Rockville, MD). The ratio of luciferase signal to renilla signal from each transfection was determined to control for well-to-well variation in transfection efficiency.

2.22 Chromatin immunoprecipitation-sequencing (ChIP-seq; Youwen Yang)

HUVEC were cultured according to standard protocols and ChIP-seq was performed as described by Wilson et al. 2010. ERG ChIP was performed using a polyclonal antibody from Santa Cruz (SC-354). HUVEC were fixed using 1 % formaldehyde to crosslink the proteins to the DNA and for each ChIP, 10-20 million cells were harvested. Cells were then lysed and the chromatin was sonicated to a final size of 500-1000 base pairs. ERG and negative control IgG antibodies were coupled to magnetic beads (Invitrogen) by overnight incubation at 4 °C. After this incubation, chromatin was then added to the antibody-coupled beads and DNA-protein complexes were immunoprecipitated overnight at 4 °C. Four chromatin immunoprecipitations, corresponding to one batch of chromatin, were pooled for each library preparation. The control input library sample was chromatin that was reverse cross-linked, phenol extracted, and purified using a Qiagen PCR cleanup column. The libraries for input, negative control IgG and ERG samples were prepared using a TruSeq ChIP-seq kit (Illumina) as per the manufacturer's instructions. Briefly, the four ChIPs were blunted, phosphorylated, and then ligated to library adapters. These products were then

sequenced on the Illumina HiSeq 2000. Sequence reads were mapped to the human reference genome hg19 using MACS (Feng et al., 2012), converted to a density plot, and displayed as UCSC genome browser custom tracks.

2.23 Bioinformatics analysis

Genome-wide ChIP-seq data for H3K4me1, H3K27ac, H3K4me3 histone modifications and RNA polymerase II occupancy in HUVEC were obtained from the 'ENCODE histone modification tracks' of the UCSC Genome Browser (<http://genome.ucsc.edu>). These tracks are produced by the Broad and Bernstein laboratories as part of the ENCODE project and are released for public use. Human and Mouse sequences were aligned using ClustalW2 analysis software (<http://www.ebi.ac.uk/Tools/msa/clustalw2/>) using default settings (Larkin et al., 2007; Goujon et al., 2010).

2.24 Gene set enrichment analysis (Graeme Birdsey)

Gene set enrichment analysis (GSEA) was carried out using Gene Set Enrichment Analysis Software (GSEA, version 2) (<http://www.broad.mit.edu/gsea>; Subramanian et al., 2005). The query dataset were the genes identified as being down-regulated following 24 h ERG inhibition in HUVEC (Birdsey et al., 2012), which were compared against genes identified by transcriptome analysis of 24 h β -catenin inhibition in human pulmonary artery endothelial cells (Alastalo et al., 2011). GSEA ranks the raw data from the ERG-regulated gene set, and compares this with the β -catenin-regulated gene set. If the β -catenin data overlaps at the top or the bottom of the ERG ranked data, as opposed to being distributed evenly across it, it suggests there is a correlation. The green line in the graphical output represents the normalized enrichment score. The enrichment score is determined by calculating a cumulative sum along the ERG ranked data; i.e. each time a gene is present in both datasets (represented by a vertical black line in the graphical output) the cumulative sum increases; when an ERG-regulated gene is not a β -catenin-regulated gene, the cumulative sum decreases. The size of the relative increase or decrease in the cumulative sum is greater for genes, which are the most up or down-regulated and therefore at the extreme ends of the ERG ranked data. The cumulative sum score is then normalised to correct for the gene set size to give the normalised enrichment score (NES).

2.25 Gene ontology analysis

The Database for Annotation, Visualization and Integrated Discovery (DAVID; Huang et al., 2009) was used to identify over-represented gene ontology (GO) categories. The functional clustering tool within DAVID was used to group together GO annotations that have similar gene members and assign an enrichment score (ES). We used an ES > 1.3 (which corresponds to P < 0.05) to identify genes that may be over-represented in particular annotation categories.

2.26 Fibrin gel bead assay

HUVEC treated with control or ERG siRNA in the presence or absence of LiCl (10 mM), were mixed with Cytodex 3 microcarrier beads (GE Healthcare) at a concentration of 400 cells per bead in 1.5 ml of EGM-2 medium. Beads with cells were shaken gently every 20 min during a 4 h incubation at 37 °C and 5 % CO₂. After incubating, cell-coated beads were transferred to a 25 cm² tissue culture flask (Corning) and left overnight in 5 ml of EGM-2 medium at 37 °C and 5 % CO₂. The following day, cell-coated beads were washed 3 times with 1 ml of EGM-2 and resuspended at a concentration of 200 cell-coated beads/ml in 2.5 mg/ml of fibrinogen (Sigma) in PBS supplemented with 0.15 units/ml of aprotinin (Sigma). 500 µl of fibrinogen/bead solution was added to 0.625 units of thrombin (Sigma) in one well of a 24-well plate. Fibrinogen/bead solution was allowed to clot for 5 min at room temperature and then at 37 °C and 5 % CO₂ for 20 min. 20,000 skin fibroblasts were plated on top of the clot in 1 ml of EGM-2. Medium and treatment were renewed every other day.

2.26.1 Quantification of sprouts *in vitro*

For quantification of *in vitro* sprouting, images of beads were captured on an IX70 Olympus microscope with a 10X objective. Images were then analysed using ImageJ; the number of sprouts per bead was determined and sprout length was measured in arbitrary units using the NeuronJ plugin. A minimum of 20 beads were counted for each experimental group.

2.27 BrdU *in vitro* proliferation assay

BrdU incorporation was determined *in vitro* using a BrdU proliferation ELISA kit (Roche) according to the manufacturer's instructions. HUVEC were transfected with

control or ERG siRNA for 8 h in a 6-well plate and then plated in a 96-well plate at a density of 5000 cells/100 μ l/well in M199 with 10 % FBS. After an overnight treatment with LiCl (10 mM, Sigma), cells were labelled using 10 μ M BrdU per well and incubated for 4 h at 37 °C. After incubation, culture media was removed, the cells were fixed, and the DNA was denatured by adding FixDenat reagent. Cells were incubated at room temperature with an anti-BrdU-POD antibody for 90 min. The antibody conjugate was removed; the cells were washed and incubated with the substrate solution at room temperature for approximate 15 min. When colour development was sufficient for photometric detection, 25 μ l 1M H₂SO₄ stop solution was added to each well and incubated on a shaker at 300 rpm for 1 min. The reaction product was quantified by measuring the absorbance using a Synergy HT microplate reader at 450 nm with a reference wavelength of 690 nm.

2.28 Apoptosis assay

HUVEC were seeded at a density of 1×10^4 per well in 100 μ l EGM-2 medium (Lonza) on a gelatin-coated white-walled 96-well tissue culture plate and 24 h later transfected with control or ERG siRNA. Apoptosis was quantified by measuring caspase 3 and 7 activation at 48 hr, using Caspase-Glo 3/7 Assay (Promega) according to manufacturer's instructions. Plates containing cells were removed from the incubator and allowed to equilibrate to room temperature for 30 min. 100 μ l of Caspase-Glo 3/7 reagent was added to each well in a 1:1 ratio and the plate was placed on a shaker at 300–500 rpm for 30 seconds and incubated at room temperature for 2 h. Luminescence was measured in a Bio-Tek Synergy HT multidetection microplate reader.

2.29 Data analysis

Data shown are representative of at least three experiments (unless otherwise stated) and are expressed as the mean \pm standard error of the mean (SEM). Data were plotted and analysed with a relevant statistical test, where stated, using GraphPad Prism 5.0 (Graph Pad Software, CA, USA). Differences were considered significant with a P value <0.05 .

Chapter Three

ERG controls multiple pathways required for vessel growth and stability: Wnt/ β -catenin pathway

3. ERG controls multiple pathways required for vessel growth and stability: Wnt/ β -catenin pathway

3.1 Introduction

3.1.1 Wnt signalling

Over the last decade, our understanding of the Wnt signalling cascades has increased significantly through the identification of cell surface receptors for Wnt ligands and by deciphering a network of intracellular transduction components. A feature of the Wnt signalling network is its high complexity, containing numerous components and being subject to many regulatory and crosstalk mechanisms. Wnt signalling is a highly conserved cellular communication system that has been shown to play important roles both in normal development and in the pathogenesis of a variety of diseases, including cancer (reviewed in Clevers, 2006). Its mediated effects are diverse, ranging from proliferation, apoptosis, migration, polarization, to stem cell maintenance and differentiation.

Wnt factors are evolutionally conserved, secreted, cysteine-rich glycoproteins. They couple to and signal through seven transmembrane-spanning G-protein-coupled receptors of the Frizzled (Fzd) family. At least 19 Wnt ligands and 10 Fzd homologs are expressed in mammals (reviewed in Clevers and Nusse, 2012). Wnt ligands can signal through multiple pathways depending on the specific Wnt-Fzd interaction and the presence of co-receptors such as LRP5/6 (Tamai et al., 2000; Bhanot et al., 1996). Moreover, secreted antagonists, including Dickkopf homologues (Dkk) and secreted frizzled-related protein families (sFRPs) can regulate the Wnt-signalling output (Bovolenta et al., 2008; Glinka et al., 1998). The distinct Wnt cascades are often referred to as the canonical or Wnt/ β -catenin pathway and the non-canonical, which includes Wnt/calcium signalling and the planar cell polarity (PCP) pathways. Here I shall discuss the canonical Wnt signalling pathway, which is the best-characterised cascade. The central mediator of this signalling pathway is the protein β -catenin.

3.1.2 β -catenin: a mediator of cell adhesion and canonical Wnt signalling in EC

β -catenin is a multifunctional protein that can either act as a scaffold between VE- and N-cadherins and the actin cytoskeleton, stabilising cell-cell adhesion and tissue integrity, or as a transcriptional co-regulator for the T cell factor/lymphoid

enhancer-binding factor (TCF/LEF) transcription factor complex (Figure 3.1), where it drives the expression of genes involved in multiple cellular functions including cell proliferation, differentiation and survival, as well as tight junction proteins and pericyte signals (reviewed in Reis and Liebner, 2013; Dejana, 2010). Conflicting literature exists on the understanding of the interplay between the junctional and signalling β -catenin pathways; it is still unclear whether these two processes act together or independently.

In the absence of a canonical Wnt signal, accumulation of cytoplasmic β -catenin is prevented by a multiprotein degradation complex that targets β -catenin for rapid phosphorylation and ubiquitin-mediated proteosomal degradation (Figure 3.1 A) (Aberle et al., 1997). Within this multiprotein degradation complex, Axin and the tumour suppressor adenomatous polyposis coli (APC) function as a scaffold to bring glycogen synthase kinase-3 (GSK3) within the proximity of its target, β -catenin. GSK3 phosphorylates the β -catenin NH2 terminus, which acts as a recognition signal for the E3-ubiquitin ligase b-TrCP. Consequently, the transcriptional repressors Groucho/TLE are bound to LEF1/TCF transcription factors, thus downstream Wnt target gene expression is repressed.

Activation of canonical Wnt signalling through the binding of a Wnt ligand to the Frizzled receptor complex increases levels of cytoplasmic β -catenin, transiently, by activating and recruiting Dishevelled (Dvl) to the membrane, which in turn blocks the GSK3-mediated phosphorylation of β -catenin (Figure 3.1 B). Wnt-induced β -catenin stabilisation and accumulation in the cytoplasm promotes its translocation into the nucleus, where it displaces the transcriptional repressors Groucho/TLE from their binding to TCF/LEF1 and activates target gene expression (Figure 3.1 B). The TCF/ β -catenin complex targets many genes that promote the cell cycle and simultaneously regulates transcription of some members of the Notch signalling pathway, establishing reciprocal interactions between Wnt and Notch signals.

Importantly, as mentioned previously β -catenin can bind to cadherins and this pool of β -catenin tethered to the cadherin complex at the junctions, is protected from degradation (Figure 3.1). However, in sub-confluent or angiogenic endothelium, where VE-cadherin is not engaged and junctions are partially dismantled, binding of β -catenin to the cadherin tail is decreased by phosphorylation, thus β -catenin dissociates from

junctions and translocates to the nucleus. This has been shown in work on VE-cadherin null endothelial cells or in sparsely plated EC in culture, which displayed increased nuclear β -catenin and signalling (Taddei et al., 2008). Cadherins can therefore tether β -catenin to the junctions and in this way indirectly modulate downstream Wnt signalling. The translocation of β -catenin into the nucleus in sparse cells, however, would require cytoplasmic β -catenin to be prevented from degradation via Wnt signals. Therefore for a cell to be able to respond to pro-quiescence or pro-angiogenic stimuli directing β -catenin to the junction or nucleus respectively, it would require both the VE-cadherin and Wnt signalling pathway to be effective.

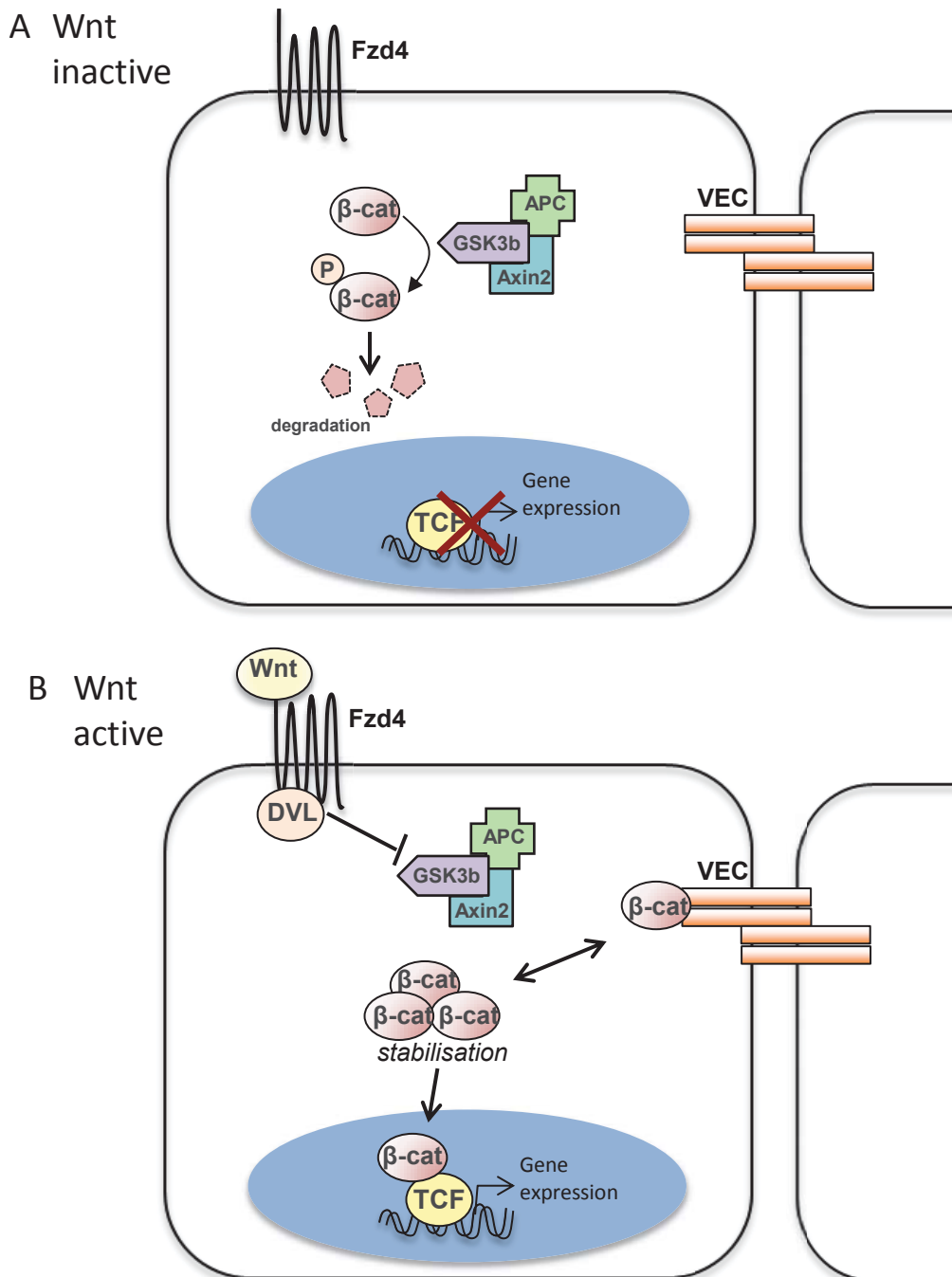


Figure 3.1 Canonical Wnt/ β -catenin signalling in the endothelium. (A) In the absence of Wnt, β -catenin associates with a multiprotein destruction complex that consists of Axin, APC and GSK3b. β -catenin is phosphorylated by GSK3b. This phosphorylation leads to the ubiquitination of β -catenin and its degradation by the proteasome. Members of the TCF (T-cell factor)/ LEF (lymphocyte-enhancer-binding factor) family are inactive. **(B)** Wnt proteins bind their receptors, frizzled proteins, which results in the recruitment of Dishevelled (Dvl) and consequent inactivation of GSK3b. β -catenin is stabilised in the cytoplasm and translocates to the nucleus, where it binds TCF to activate target genes. β -catenin also binds to VE-cadherin at adherens junctions.

3.1.3 Wnt/ β -catenin signalling in the vasculature

Previous work using a β -catenin-activated transgenic (BAT-Gal) mouse has shown that canonical Wnt-signalling is active in EC (Maretto et al., 2003). Various *in vitro* and *in vivo* studies have shown that EC can express a wide range of Wnt ligands, receptors and signalling modulators. Also, Wnts expressed from a variety of cellular sources (including endothelial, mural, or epithelial cells) could act in an autocrine and/or paracrine manner to regulate EC function. It has been reported that Wnt-related gene expression profiles differ between HUVEC and human dermal microvascular EC (Goodwin et al., 2006), suggesting that Wnt signalling could be regulating different aspects of EC biology, depending on which ligand and receptors are expressed in a particular endothelial subset.

Recent evidence implicates β -catenin in aspects of vascular development and angiogenesis. Endothelial specific deletion of β -catenin results in a defective embryonic vasculature and results in early lethality in utero at E12.5 (Cattelino et al., 2003). Within these embryos, the vasculature presents defects in vascular remodelling; diffuse vascular haemorrhages and the β -catenin mutant mice have pale and less perfused yolk sacs. Since β -catenin functions in stabilising endothelial adherens junctions, without it, these altered cell-cell contacts may contribute to vascular vulnerability.

Interestingly, angiogenic defects are also reported in the postnatal retinas from endothelial-specific β -catenin knockout mice (Phng et al., 2009; Corada et al., 2010), which display significant reduction in vascular progression and density. Endothelial deletion of β -catenin or LEF1 leads to excessive vessel regression during retinal angiogenesis (Phng et al., 2009), supporting a role for canonical Wnt signalling in regulating vessel stability. During sprouting retinal angiogenesis, stalk cells avidly proliferate to support nascent vessel growth and analysis of the developing retinal vasculature in BAT-gal reporter mice showed high Wnt/ β -catenin signalling activity in stalk cells. Several studies show that *in vitro* stimulation of EC with Wnt ligands, including Wnt1, Wnt3a and Wnt5a, induce EC proliferation (Masckauchan et al., 2006; Masckauchan et al., 2005). Furthermore, lithium chloride (LiCl) treatment, which activates Wnt/ β -catenin signalling by inhibiting GSK-3, the main component of the β -catenin degradation complex, induces EC proliferation. Wnt/ β -catenin signalling can promote EC proliferation (Masckauchan et al., 2005) and induce cell cycle progression

through transcriptional activation of Cyclin D1 (Shtutman et al., 1999). Phng et al. also showed that EC with decreased canonical Wnt signalling showed decreased levels Cyclin D1, and a reduced proliferation rate, supporting an *in vivo* role of Wnt signalling in regulating EC proliferation (Phng et al., 2009).

Genetic evidence for a role of Wnt signalling in vessel development and pathology is provided by the studies of various mouse mutants, where loss of multiple Wnt ligands and receptors have been shown to result in defective vascular phenotypes. Mouse embryos deficient in Wnt-2 display vascular abnormalities including defective placental vasculature (Monkley et al., 1996) and Wnt7b has been shown to control retinal hyaloid vessel regression in the retina (Lobov et al., 2005). Mice deficient for Wnt receptor Frizzled-5 are embryonic lethal by E11.5 due to early defects in yolk sac and placental angiogenesis (Ishikawa et al., 2001).

Important clinical insight into the crucial role of Wnt signalling in vascular morphogenesis has come from studies of the human hereditary ocular disorders, familial exudative vitreoretinopathy (FEVR) and Norrie disease. Both of these diseases are characterised by abnormal retinal and inner ear vascularisation and leaky vessels. Loss of function mutations in the human Wnt receptor Frizzled-4, co-receptor LRP5 and Norrin gene have been linked to FEVR (Toomes et al., 2004; Chen et al., 1993; Robitaille et al., 2002). Norrie disease is also caused by a mutation in the gene encoding for Norrin. Norrin is a ligand that is not related to the Wnt family, but binds to Fzd4 activating canonical Wnt signalling (Ye et al., 2009), illustrating the important role for the pathway in vascular morphogenesis.

During later stages of vascular development, organ-specific vascular differentiation is essential for proper vascular function. Within the central nervous system, EC differentiate to form a crucial permeability barrier termed the blood–brain barrier (BBB), which is key for neural function and homeostasis. An elaborate network of intercellular tight junctions is central to maintaining this barrier. Claudin-3 is predominantly expressed in brain EC and plays a precise role in the establishment and maintenance of BBB tight junctions. Wnt3a-conditioned media has been shown to selectively induce claudin-3 expression in EC via β -catenin activation. Furthermore canonical Wnt signalling has been shown to be required for the molecular and structural properties of these BBB-type tight junctions *in vitro* and *in vivo* (Liebner et al., 2008).

This supports a role for the pathway in regulating the maintenance of the brain microvasculature and blood brain barrier characteristics during embryonic and postnatal development (Liebner et al., 2008).

As mentioned previously, *in vitro* and *in vivo* studies have shown that ERG is essential to maintain the integrity of endothelial junctions, by driving expression of VE-cadherin (Birdsey et al., 2008; Gory et al., 1998) and as mentioned previously VE-cadherin binds β -catenin, protecting it from degradation. Transcription profiling in ERG-deficient HUVEC identified several Wnt-related genes as candidate ERG targets (Birdsey et al., 2012). Moreover, the phenotype of the Erg^{iEC-KO} retina vasculature (Figure 1.12 B; Birdsey, Shah et al., 2015) is similar to that of the β -catenin-deficient mouse models (Corada et al., 2010; Phng et al., 2009), showing decreased vessel density and increased vessel regression. I therefore speculated that ERG might regulate β -catenin and Wnt signalling in EC, since the underlying regulatory pathways of Wnt signalling in the vasculature remain unclear.

The aims of the work described in this chapter are to:

- Determine whether ERG regulates β -catenin expression and localisation in HUVEC and to identify the mechanisms involved.
- Identify molecular targets within the Wnt signalling pathway, which are regulated by ERG.
- Determine whether ERG has a functional role in modulating Wnt signalling *in vitro* and *ex vivo*.

3.2 Results

3.2.1 ERG regulates β -catenin junctional localisation in confluent EC

Since ERG drives expression of VE-cadherin and VE-cadherin tethers β -catenin at the EC junctions (reviewed in Dejana, 2010), I speculated that ERG might regulate β -catenin junctional localisation. To study β -catenin localisation, HUVEC treated with FITC-conjugated siCtrl or siERG (100 nM) and were stained for ERG, VE-cadherin and β -catenin. Cells were stained with DAPI to visualise the nuclei. FITC-siERG-treated HUVEC showed a decrease in nuclear ERG expression compared to control (Figure 3.2 A). Staining of FITC-siCtrl-treated HUVEC showed continuous VE-cadherin staining at the cell membrane, indicative of a well-established mature cell monolayer and stable cell-cell junctions (Figure 3.2 B). Staining of β -catenin showed co-localisation with junctional VE-cadherin, as expected. Conversely, FITC-siERG-treated cells clearly showed downregulation of VE-cadherin, as reported previously (Birdsey et al., 2008), and importantly loss of β -catenin at the cell junctions compared to control (Figure 3.2 B).

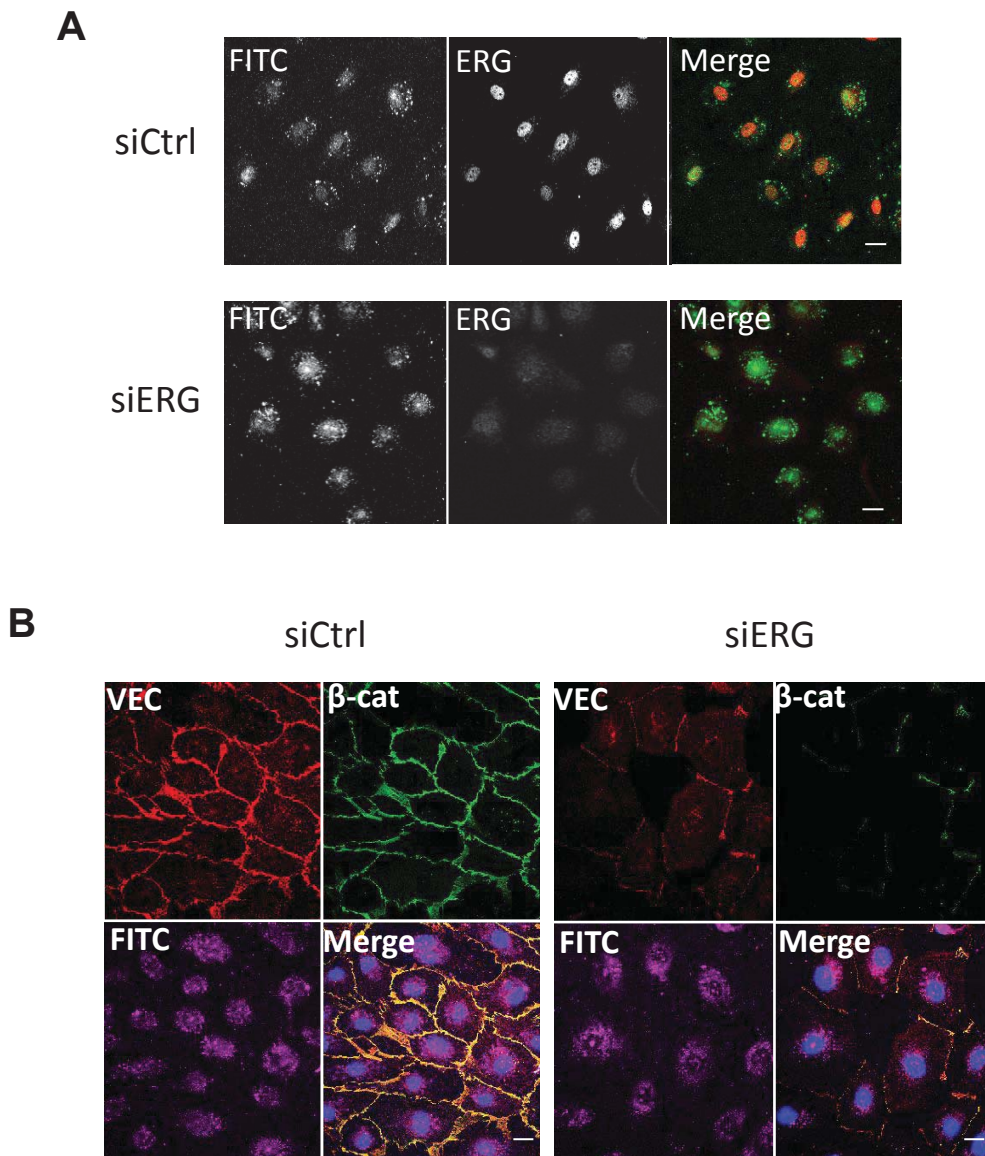


Figure 3.2 ERG is required for β -catenin localisation at endothelial cell junctions. Immunofluorescence analysis of the localisation and expression of β -catenin in confluent FITC-conjugated control GeneBloc (100 nM; siCtrl) and ERG GeneBloc (100nM; siERG)-treated HUVEC grown on gelatin-coated glass coverslips. After 48 hours, cells were labelled and visualised for (A) ERG (red) and FITC tag autofluorescence (green). Scale bar, 20 μ m (n=3). (B) β -catenin (β -cat; green) and VE-cadherin (VEC; red) staining of FITC-conjugated siCtrl and siERG (FITC; purple) treated HUVEC. Merged image includes staining for the nuclear marker DAPI (blue). Scale bar, 20 μ m (n=3).

3.2.2 ERG regulates β -catenin protein expression

Immunoblotting whole-cell lysates of siCtrl and siERG-treated cells was used to determine whether inhibition of ERG expression affects β -catenin protein expression (Figure 3.3). HUVEC were treated with siCtrl or siERG for 24 and 48 h. ERG protein expression was significantly decreased to approximately 20% in HUVEC treated with siERG compared to siCtrl (Figure 3.3 A and B). Moreover, inhibition of ERG expression resulted in an approximate 40% and 30% decrease in β -catenin protein expression after 24 and 48 h ERG inhibition respectively (Figure 3.3 A and C), indicating that ERG is required for β -catenin protein expression in HUVEC.

I investigated whether β -catenin regulation observed at the protein level is a consequence of effects on β -catenin mRNA expression. HUVEC were cultured for 24 and 48 h in the presence of either siCtrl or siERG. Inhibition of ERG expression resulted in approximately 90% downregulation of ERG mRNA levels at 24 and 48 h (Figure 3.4 A). However, as shown in Figure 3.4 B, inhibition of ERG expression resulted in relatively unchanged β -catenin mRNA levels. These results suggest that β -catenin is not a transcriptional ERG target and that an mRNA-independent mechanism of action is regulating β -catenin protein expression.

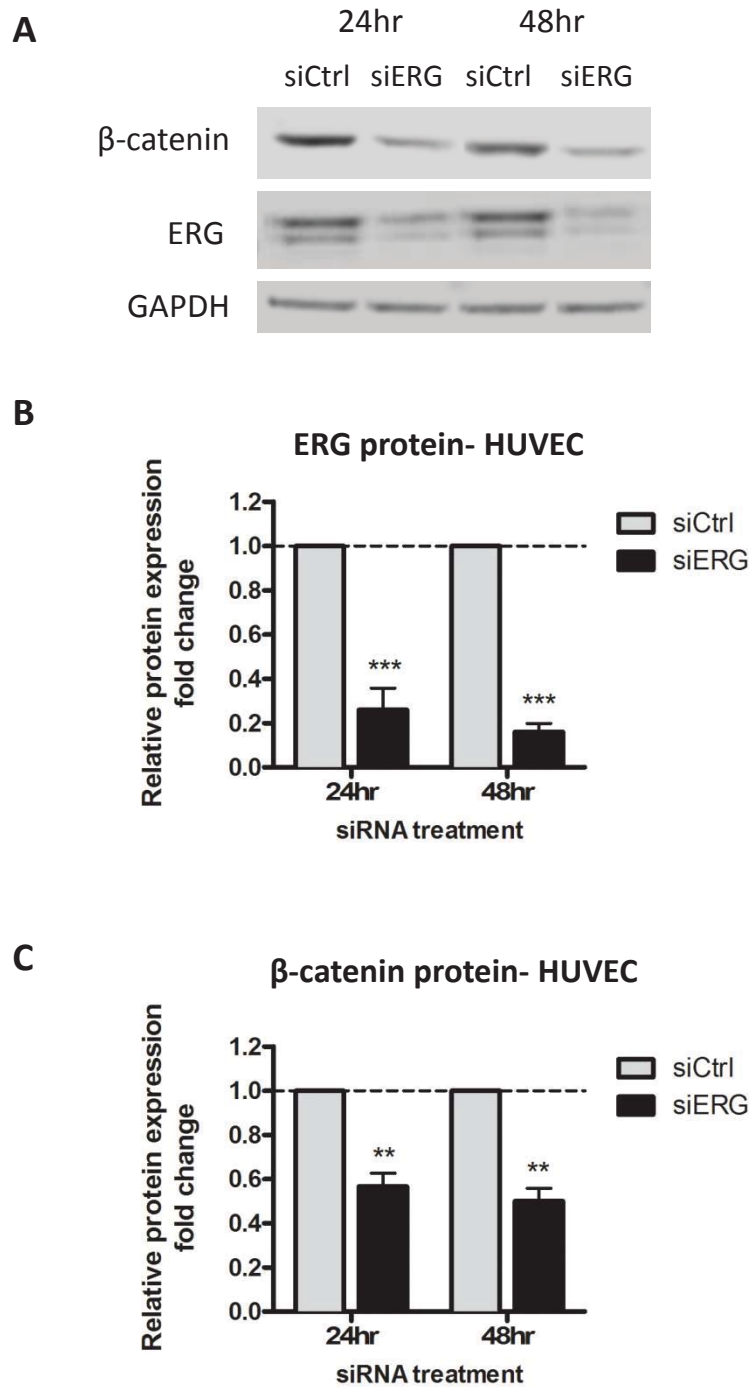
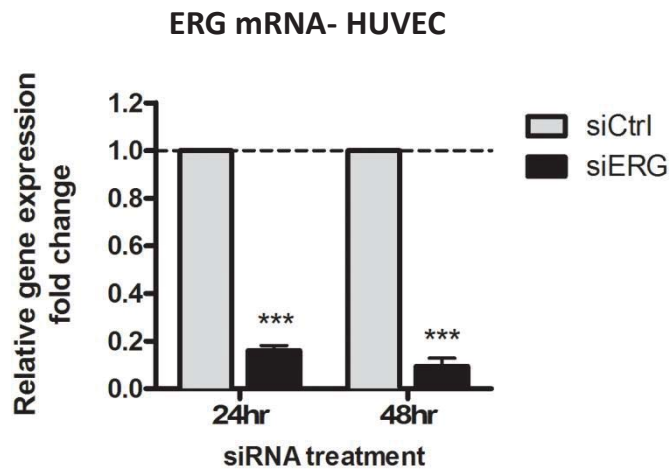


Figure 3.3 ERG regulates β -catenin protein expression. (A) Representative western blot analysis of ERG and β -catenin protein expression in HUVEC treated with siCtrl or siERG (GeneBloc; 100 nM) for 24 and 48 h. (B) Densitometry analysis of ERG and (C) β -catenin total protein levels in siCtrl and siERG-treated cells. Protein levels were normalised to GAPDH and expressed as fold change relative to siCtrl. All graphical data are mean \pm SEM; n=6; asterisks indicate values significantly different from the control (Student t test where ** p < 0.01, *** p < 0.001).

A



B

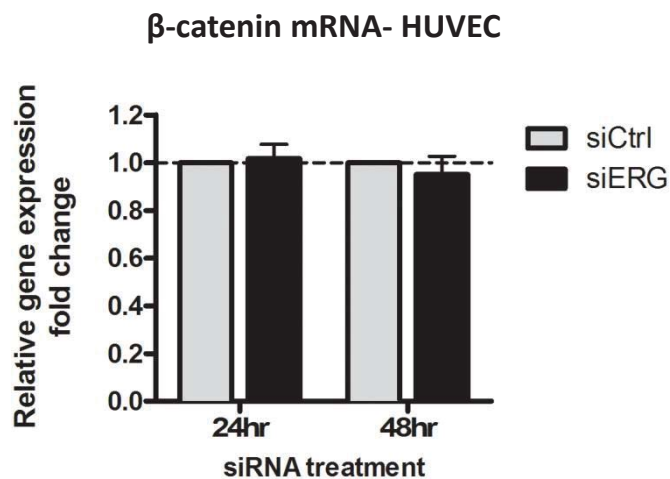


Figure 3.4 β -catenin mRNA expression is unaffected by ERG inhibition.

(A) mRNA levels of ERG in HUVEC treated with siCtrl or siERG (Genebloc; 100 nM) for 24 h and 48 h (n=6). (B) β -catenin mRNA levels measured using RNA extracts from siCtrl and siERG-treated HUVEC. Changes in β -catenin mRNA expression were not observed following ERG inhibition (n=3). All results are normalised to GAPDH and expressed as fold change relative to siCtrl. All graphical data are mean \pm SEM; n=6; asterisks indicate values significantly different from the control (Student t test where * p < 0.05, *** p < 0.001).

3.2.3 Endothelial Wnt/ β -catenin signalling requires ERG

To test whether the decrease in β -catenin expression induced by ERG inhibition correlates with a decrease in canonical Wnt signalling, I measured β -catenin signalling activity in control and ERG-deficient EC using a TOPflash reporter construct (Korinek et al., 1997), which measures the activity of TCF, a transcription factor downstream of β -catenin in the canonical Wnt signalling pathway. Within the TOPflash reporter construct, expression of the firefly luciferase gene is regulated by six tandem TCF binding sites upstream of a minimal TK promoter (Korinek et al., 1997). HUVEC were treated with siERG or siCtrl for 24 h, and then stimulated overnight with either control or conditioned medium (CM) of L cells, producing Wnt3a, which stabilises β -catenin (Willert et al., 2003), or Wnt5a, which does not act through β -catenin in EC (Liebner et al., 2008). Treatment of control cells with Wnt3aCM resulted in a significant 8-fold increase in TCF-luciferase activity. This increase in β -catenin transcriptional activity was lost, however, in ERG-deficient EC (Figure 3.5 A).

Consistently, immunoblotting lysates of control cells treated with Wnt3a-conditioned medium showed increased β -catenin protein levels indicative of its Wnt-induced stabilisation and therefore protection from degradation (Figure 3.5 B). However, ERG-deficient cells showed decreased β -catenin protein levels, and treatment with Wnt3a-conditioned medium had no effect (Figure 3.5 B). Together with the reporter assay data, this indicates that ERG is required for β -catenin-mediated Wnt signalling.

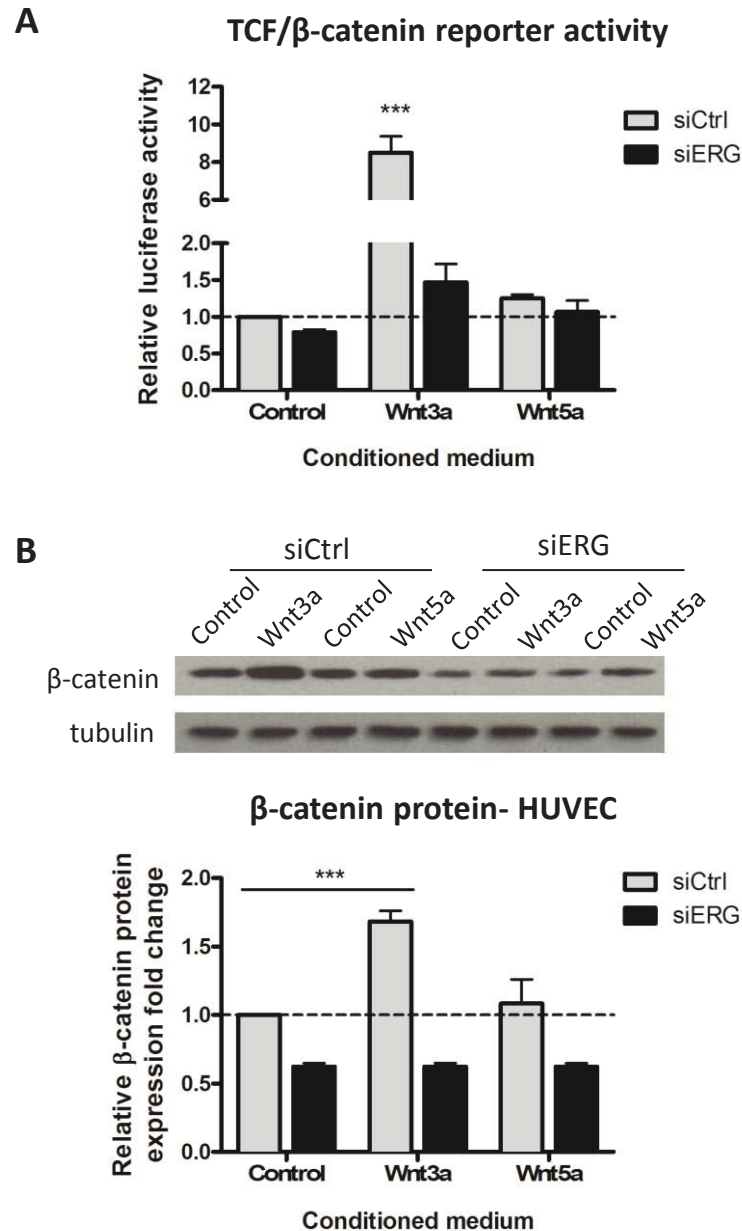


Figure 3.5 β -catenin transcriptional activity is controlled by ERG. (A) ERG is required for TCF- β -catenin transcriptional activity, determined by co-transfecting siCtrl and siERG-treated HUVEC with the TOPFLASH TCF luciferase reporter and pGL4 renilla control vector. Cells were treated for 6 h with control, Wnt3a or Wnt5a conditioned media. Results are presented as dual luciferase ratio of firefly luciferase normalised to pGL4 renilla luciferase and expressed as fold change relative to siCtrl HUVEC treated with control medium. (B) Representative western blot and densitometry analysis of β -catenin protein expression in control and ERG-deficient HUVEC treated with Wnt conditioned medium. Protein levels were normalised to tubulin and expressed as fold change relative to siCtrl. All graphical data are mean \pm SEM; n=3; asterisks indicate significantly different values (ANOVA, followed by Bonferonni's test, where *** p <0.001).

3.2.4 ERG controls downstream β -catenin target gene expression in human and mouse EC

To further confirm ERG regulation of canonical Wnt signalling, I assessed the effect of ERG inhibition on Wnt/ β -catenin target gene expression. Expression levels of Wnt target genes Cyclin D1, Axin2 and TCF1 were decreased in ERG-deficient HUVEC to approximately 60% compared to control HUVEC (Figure 3.6 A). To confirm this *in vivo*, endothelial cells were isolated from lungs of littermate control *Erg^{fl/fl}* and heterozygous Tie2Cre-*Erg^{fl/+}* (*Erg^{cEC-het}*) mice and the gene expression of β -catenin targets was subsequently compared by qPCR. As shown in Figure 3.6 B, primary mouse lung EC from *Erg^{cEC-het}* mice showed an approximate 50% decrease in *Erg* expression as expected. Furthermore, loss of *Erg* in endothelial cells did not result in a significant change in β -catenin mRNA expression when compared to *Erg^{fl/fl}* endothelial cells, in line with the data in ERG-deficient HUVEC. Importantly, primary mouse lung EC from *Erg^{cEC-het}* mice displayed significantly reduced expression levels of Cyclin D1, Axin-2 and TCF1 (Figure 3.6 B). I next examined the level of β -catenin protein in the lung EC lysates from *Erg^{cEC-het}* mice by Western blotting. I observed a trend of reduction in β -catenin protein expression in *Erg^{cEC-het}* when compared to *Erg^{fl/fl}* littermates (Figure 3.6 C), suggesting that ERG also regulates β -catenin protein levels in the mouse. Together, these results indicate that ERG regulates canonical Wnt/ β -catenin signalling in both human and mouse EC.

The adherens junction molecule N-cadherin has also been identified as a β -catenin transcriptional target (Giampietro et al., 2012), where EC expressing a constitutively active β -catenin mutant induced N-cadherin expression. N-cadherin is required for vascular development and in confluent endothelial monolayers, N-cadherin is mostly expressed on the apical and basal membrane, where it plays a crucial role in pericyte attachment during vessel formation (Amsellem et al., 2014; Gerhardt et al., 2000). To test whether a decrease in ERG causes a decrease in N-cadherin expression, I measured N-cadherin mRNA and protein expression in siCtrl and siERG-treated HUVEC. In Figure 3.7 A, inhibition of ERG expression resulted in decreased N-cadherin mRNA levels to 50% compared to control. Immunoblotting whole-cell lysates of siCtrl and siERG-treated cells showed an approximate 60% decrease in N-cadherin protein expression after 48 h ERG inhibition (Figure 3.7 B), indicating that ERG is required for N-cadherin expression in HUVEC.

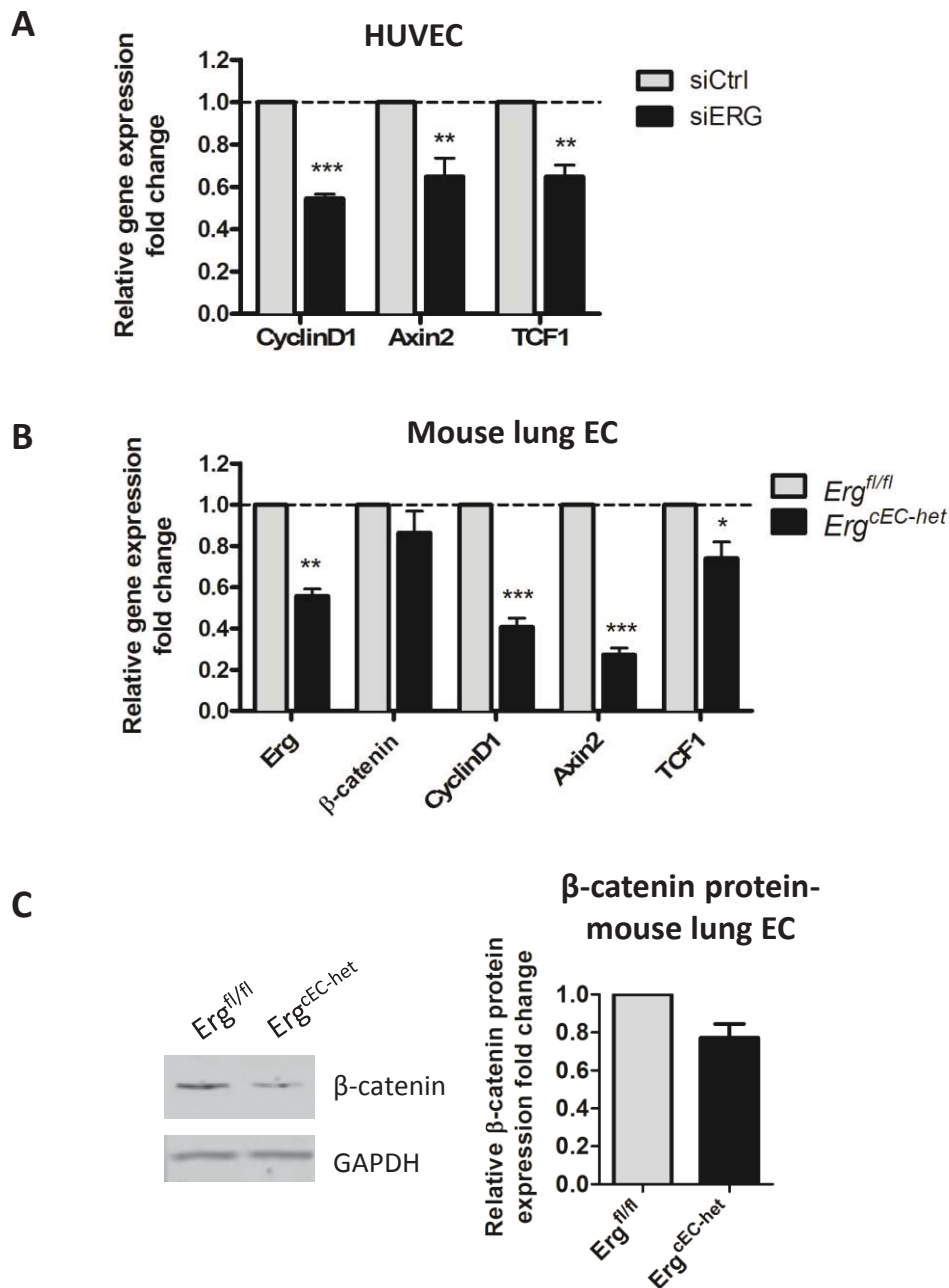


Figure 3.6 ERG regulates β -catenin target gene expression *in vitro* and *in vivo*. (A) mRNA levels of β -catenin downstream target genes CyclinD1, Axin2 and TCF1 were measured in RNA extracts from HUVEC treated with siCtrl or siERG for 48 h. Results are normalised to GAPDH and expressed as fold change relative to siCtrl (n=4). (B) mRNA expression of *Erg*, β -catenin and target genes CyclinD1, Axin2 and TCF1 in primary *Erg*^{cEC-het} mouse lung EC compared to control. Results are normalised to HPRT and expressed as fold change relative to *Erg*^{fl/fl} littermate controls (n=6). (C) Western blot and densitometry analysis of β -catenin protein expression in primary *Erg*^{cEC-het} mouse lung EC compared to control. Results are normalised to GAPDH and expressed as fold change relative to *Erg*^{fl/fl} littermate controls (n=2). All graphical data are mean \pm SEM; asterisks indicate values significantly different from the control (Student t test where * p < 0.05, ** p < 0.01, *** p < 0.001).

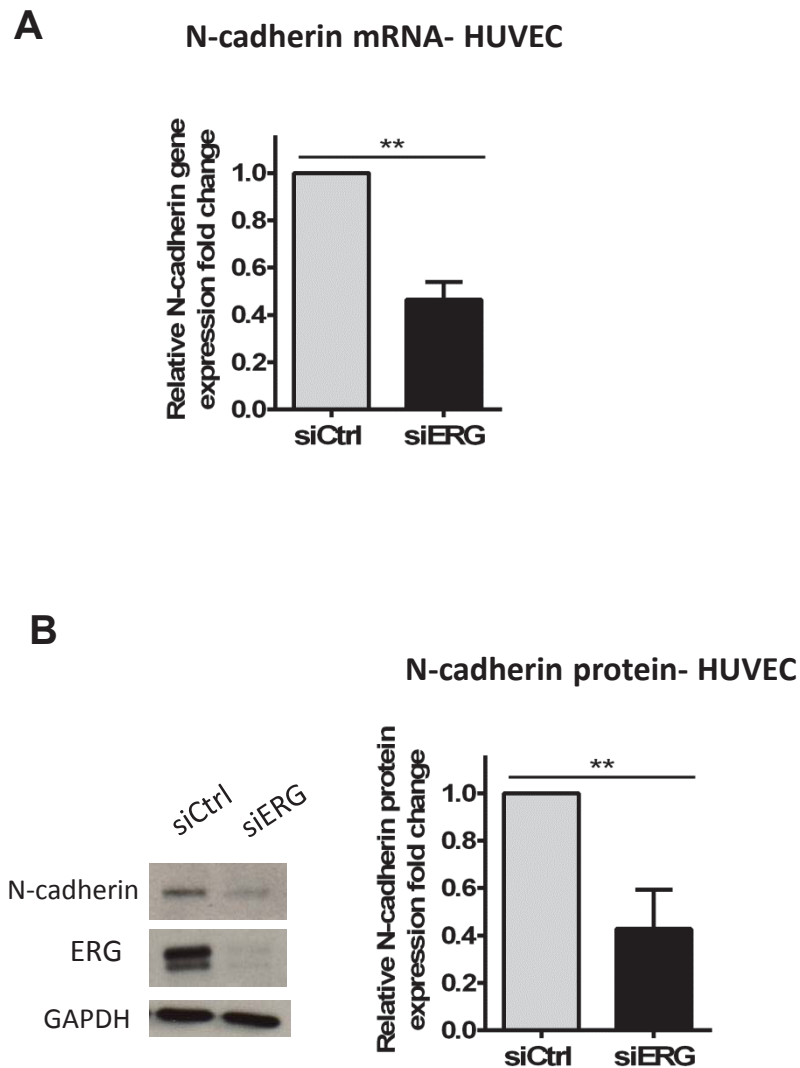


Figure 3.7 ERG is required for N-cadherin mRNA and protein expression. (A) qPCR analysis of N-cadherin expression in HUVEC treated with siCtrl or siERG for 48 h. Results are normalised to GAPDH and expressed as fold change relative to siCtrl (n=3). (B) Left panel: Western blot analysis of N-cadherin protein expression from HUVEC lysates treated with siCtrl or siERG for 48 h. Representative blot shown. Right panel: Densitometry analysis of N-cadherin total protein levels in siCtrl and siERG-treated cells. Protein levels were normalised to GAPDH and expressed as fold change relative to siCtrl (n=3). All graphical data are mean \pm SEM; asterisks indicate values significantly different from the control (Student t test where ** p < 0.01).

To further investigate ERG regulation of canonical Wnt signalling, I assessed the effect of ERG inhibition on expression of endothelial-specific Wnt/ β -catenin target genes. Endothelial β -catenin signalling regulates BBB maintenance through concomitant activation of the tight junction molecule Claudin-3 and repression of the membrane glycoprotein plasmalemma vesicle-associated protein (PLVAP) (Liebner et al., 2008). In line with these findings, qPCR analysis of total brain RNA showed that Claudin-3 expression was significantly downregulated whilst PLVAP was strongly upregulated in brains of *Erg*^{iEC-KO} mice (Figure 3.8 A). Furthermore, brain oedema was estimated by comparing wet to dry weight ratios of brains from *Erg*^{fl/fl} and *Erg*^{iEC-KO} mice. Increased water content was observed in brains of *Erg*^{iEC-KO} (Figure 3.8 B), suggesting impairment of the BBB. ERG may therefore be regulating blood brain barrier integrity through the Wnt signalling pathway.

Since I observed a decrease in expression of β -catenin-target genes following ERG inhibition (Figures 3.6-3.8), we expanded this analysis to the entire ERG dataset to find patterns between the genes down-regulated following ERG inhibition (Birdsey et al., 2012) and the genes down-regulated in human pulmonary artery endothelial cells following β -catenin inhibition (Alastalo et al., 2011) using Gene Set Enrichment Analysis (GSEA; Subramanian et al., 2005). As shown in Figure 3.9 A, GSEA comparison gave a significant normalized enrichment score of 2.46 ($P < 0.001$), indicating a positive correlation between the two datasets. Gene ontology analysis of the enriched genes shared between both datasets, using DAVID bioinformatics resource, suggested a common biological function, as a significant number of genes are involved in endothelial cell functions such as angiogenesis and regulation of cell adhesion (Figure 3.9B), in line with ERG's known role in EC. These results suggest a strong relationship between these two pathways.

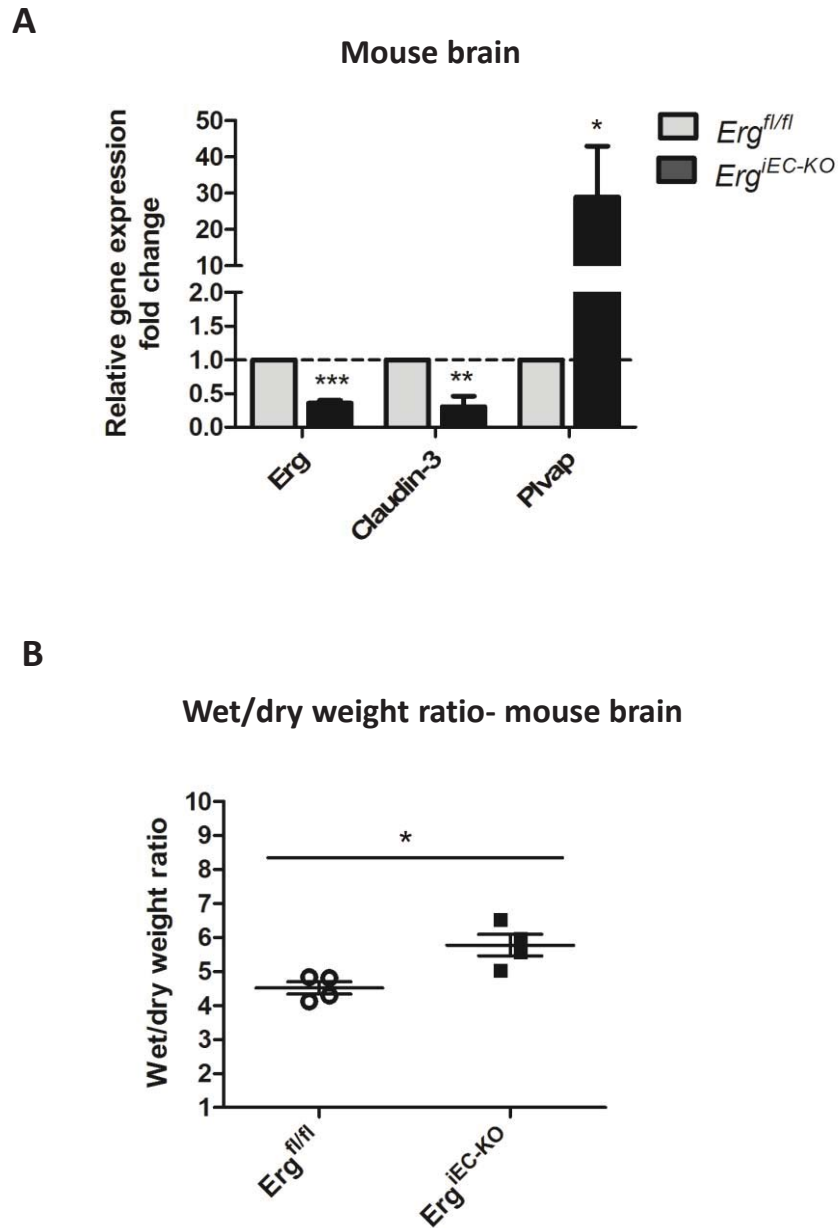


Figure 3.8 ERG regulates blood brain barrier permeability and expression of Claudin-3 and Plvap. (A) qPCR analysis of *Erg*, *Claudin-3* and *Plvap* expression in total brain RNA from control *Erg*^{fl/fl} and *Erg*^{iEC-KO} mice. Results are normalised to *HPRT* and expressed as fold change relative to control *Erg*^{fl/fl} mice (n=4). (B) Water content in the brains of control *Erg*^{fl/fl} and *Erg*^{iEC-KO} mice determined by measuring their wet/dry weight ratios (n=4). All graphical data are mean \pm SEM; asterisks indicate values significantly different from the control (Student t test where * p <0.05, ** p <0.01, *** p <0.001).

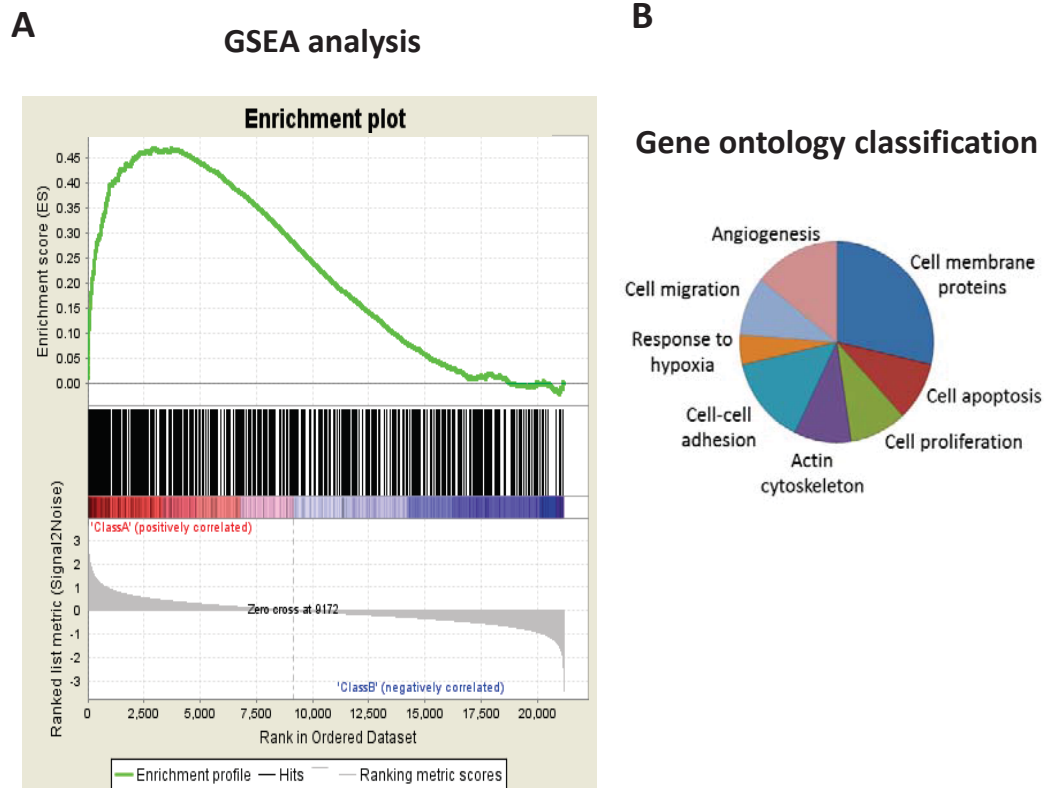


Figure 3.9 Gene set enrichment analysis demonstrates significant correlation between genes regulated by ERG and β -catenin. (A) GSEA was carried out using standard settings. GSEA analysis graphical output shows enrichment (green curve) of genes down-regulated in β -catenin siRNA-treated human pulmonary artery endothelial cells (Alastalo et al., 2011) along a ranked list of genes down-regulated by ERG inhibition in HUVEC (Birdsey et al., 2012). GSEA analysis shows significant correlation (normalized enrichment score: 2.46; $p < 0.001$) between these 2 datasets. The normalised enrichment score reflects the degree to which a gene set is over-represented at the top or bottom of a ranked list, normalized for differences in gene set size and in correlations between gene sets and the expression dataset. Analysis performed by Dr. Graeme Birdsey. (B) Functional classification of the shared genes identified by GSEA was carried out using DAVID analysis (right). The functional categories shown displayed significant enrichment scores ($p < 0.01$).

3.2.5 ERG regulates β -catenin degradation

Regulation of β -catenin activity is thought to occur mainly at the level of protein degradation (Krieghoff et al., 2006). To test whether the decrease in β -catenin protein expression observed in ERG-deficient cells was due to ubiquitin-mediated degradation, siCtrl and siERG-transfected HUVEC were treated with MG132 (10 μ M for 6 h), which is a potent, cell-permeable inhibitor of the proteasome and reduces the degradation of ubiquitin-conjugated proteins. Immunoblotting of whole cell extracts showed, as observed previously, that the levels of total β -catenin decreased following ERG inhibition, MG132 treatment of ERG-depleted HUVEC however, fully restored β -catenin protein expression (Figure 3.10). A smaller increase in β -catenin protein expression was observed in MG132 treated control HUVEC, consistent with the immunofluorescence data in HUVEC (Figure 3.2), which showed β -catenin localisation predominantly at the cell membrane where it is protected from degradation. Taken together this data indicates that ERG controls β -catenin stability.

3.2.6 ERG regulates β -catenin stability partly through VE-cadherin

At the junctions, VE-cadherin binds β -catenin, protecting it from degradation (Dejana, 2010) and this interaction is required for the control of junction stability (Dejana et al., 2008). To investigate whether ERG controls β -catenin stability through VE-cadherin, I tested whether the reduced β -catenin expression induced by ERG inhibition could be reversed by overexpression of a GFP-tagged VE-cadherin adenovirus.

To characterize adenovirus transduction of cells, HUVEC seeded on coverslips were infected with either VE-cadherin–GFP adenovirus (Ad.VEC-GFP) or control GFP (Ad.GFP) adenovirus. Staining of the cells with an antibody to exogenous GFP-tagged VE-cadherin and endogenous VE-cadherin showed that expression levels were proportional to the virus MOI used for the transduction, indicating that the overexpression of the transgene was effective (Figure 3.11). Moreover, in Ad.VEC-GFP-transduced cells, GFP visualisation indicated effective localisation of Ad.VEC-GFP to the junctions unlike the control GFP adenovirus, which was distributed throughout the cell, as shown previously by Birdsey et al., 2008. These results indicate that Ad.VEC-GFP behaves similarly to endogenous VE-cadherin. Thus, I decided to use Ad.VEC-

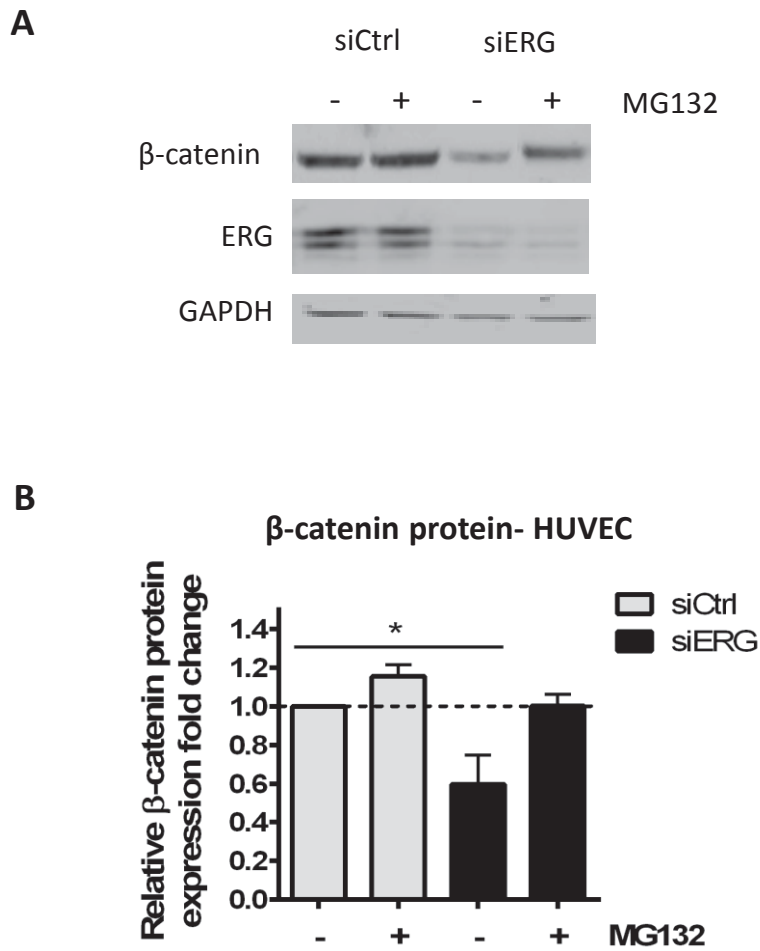


Figure 3.10 MG132 proteosomal degradation inhibitor treatment ablates ERG inhibition-induced β -catenin degradation. (A) Representative western blot analysis and (B) densitometry analysis of β -catenin protein expression in lysates from HUVEC treated with MG132 (10 μ M) for 6 h following transfection with siCtrl or siERG. Protein levels were normalised to GAPDH and expressed as fold change relative to siCtrl. Values are mean \pm SEM; n=3; asterisks indicate significantly different values (ANOVA, followed by Bonferonni's test, where * p <0.05, ** p <0.01).

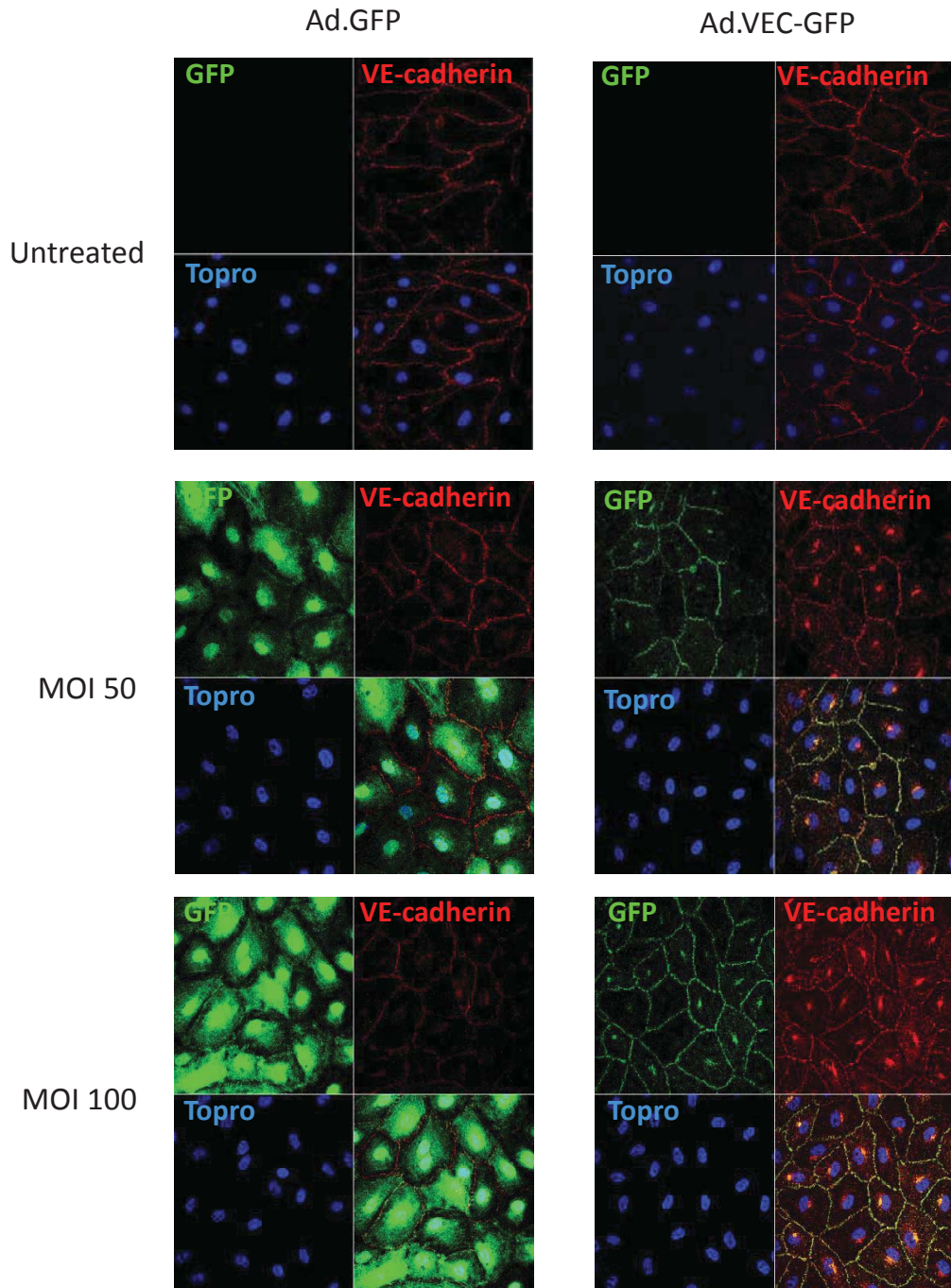


Figure 3.11 Control GFP and VE-cadherin-GFP adenovirus transduction of HUVEC. HUVEC were transduced with adenoviruses coding for Ad.GFP and Ad.VEC-GFP at the indicated multiplicities of infection (MOI) and grown on gelatin-coated glass coverslips. After 4 days, cells were labelled and visualised for GFP (green), VE-cadherin (red), and nuclear marker Topro (blue). Scale bar, 20 μ m. Total VE-cadherin protein level is enhanced by Ad.VEC-GFP adenovirus infection. Ad.VEC-GFP, but not Ad.GFP, expressed in confluent HUVEC localized at the cell-cell contacts, as does endogenous VE-cadherin.

GFP as a tool to analyse the role of VE-cadherin in ERG regulation of β -catenin stability.

Ad.VEC-GFP or Ad.GFP adenovirus-transduced HUVEC (MOI: 70) were treated with siERG or siCtrl for 48 h. Immunofluorescence of the cells showed levels of ERG expression were significantly reduced in siERG-treated HUVEC (Figure 3.12), and this resulted in a decrease in VE-cadherin and β -catenin junctional staining as shown previously. Over-expression of Ad.VEC-GFP in ERG-depleted HUVEC partly restored β -catenin protein levels acting primarily on the junctional pool of β -catenin (Figure 3.12), suggesting that ERG regulates junctional β -catenin stability by the junctional molecule VE-cadherin.

To further characterize ERG regulation of β -catenin degradation through VE-cadherin, I transduced control or ERG-depleted HUVEC with Ad.VEC-GFP or Ad.GFP adenovirus (MOI: 70) and assessed β -catenin levels in the cytosolic/nuclear fractions of these cells by western blotting. The purity of the fractions was confirmed by western blot, where α -tubulin and HDAC-1 were selectively expressed in the cytoplasmic and nuclear fractions respectively (Figure 3.13). Inhibition of ERG expression decreased ERG nuclear levels. Immunoblotting with an antibody against GFP showed GFP expression in Ad.GFP-transduced cells, with increased levels in the cytoplasm, in line with the immunofluorescence data (Figure 3.12). Immunoblotting with an antibody against VE-cadherin showed two bands: the lower band represented endogenous VE-cadherin expression, with the higher band being expressed in Ad.VEC-GFP-transduced HUVEC and representing the higher molecular weight GFP-tagged form of the protein. In line with the immunofluorescence data (Figure 3.12), quantification of cellular fractionation studies confirmed that in ERG-deficient HUVEC, GFP-tagged VE-cadherin overexpression partially restored junctional β -catenin protein levels (Figure 3.13, lane 6). However, ERG also controls the nuclear pool of β -catenin (Figure 3.13, lane 3), which was not corrected by VE-cadherin over-expression (Figure 3.13, lane 5). This suggests that ERG controls β -catenin also through a Wnt signalling-dependent, VE-cadherin-independent pathway.

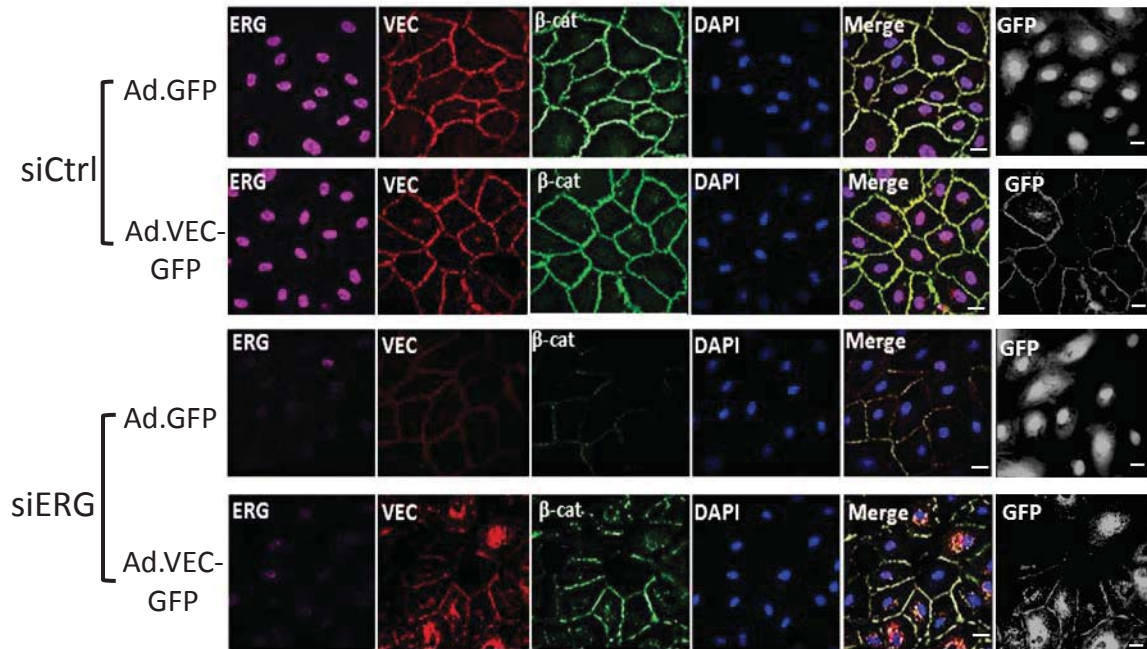


Figure 3.12 ERG controls β -catenin stability partially through VE-cadherin. Immunofluorescence microscopy of control (siCtrl) and ERG-deficient (siERG) HUVEC treated with GFP-tagged control (Ad.GFP) or VE-cadherin (Ad.VEC-GFP) adenovirus. Cells were stained with anti-ERG (magenta), anti-VE-cadherin (VEC; red), anti- β -catenin (β -cat; green) antibodies, and the nuclear marker DAPI (blue). The merged image shows the overlap of ERG, VEC, β -cat and DAPI. Cells were also visualised for GFP autofluorescence (grayscale). Junctional β -catenin was normalised in ERG-deficient cells treated with VE-cadherin-GFP adenovirus. Scale bar, 20 μ m; n=3.

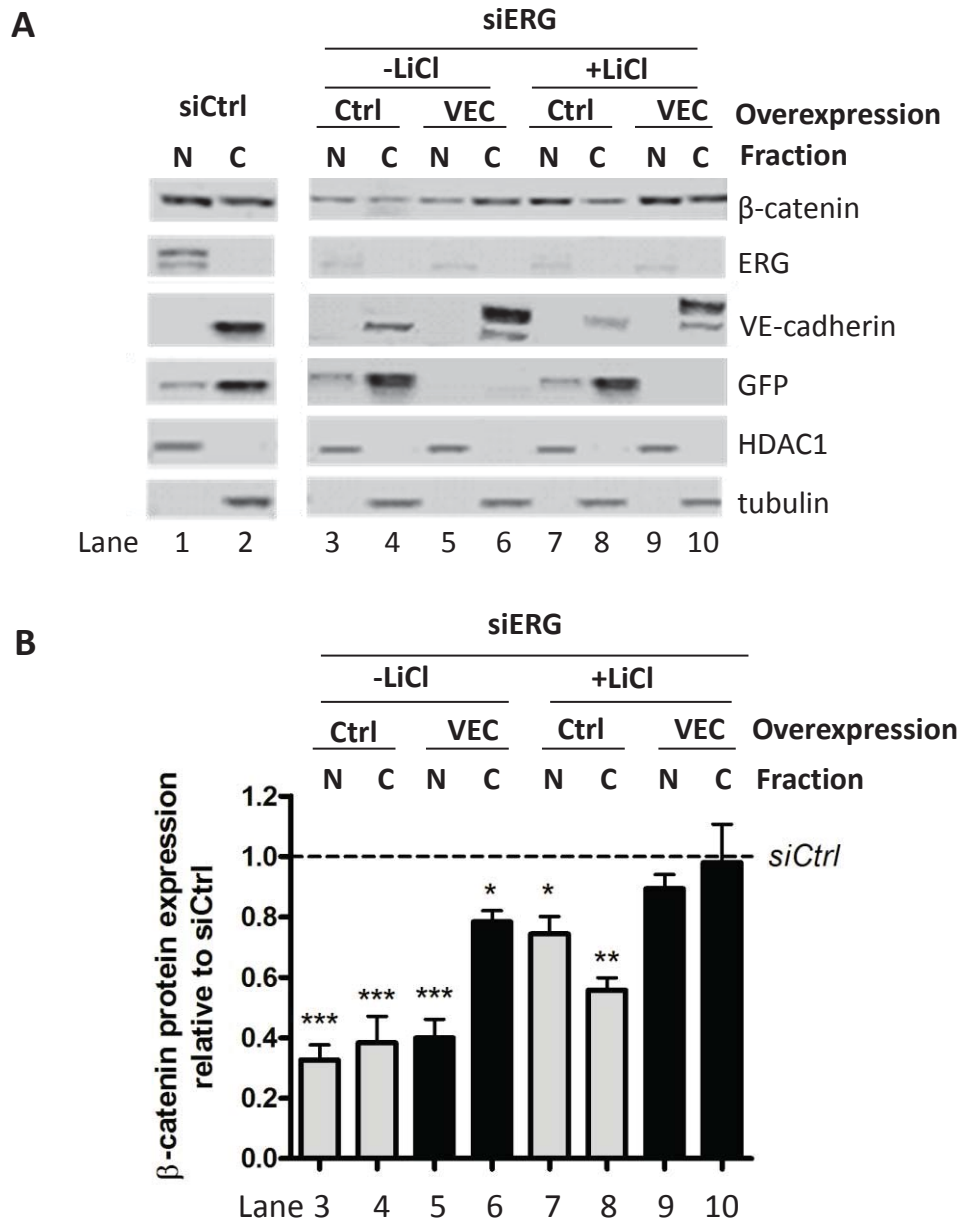


Figure 3.13 ERG controls β-catenin stability through both a VE-cadherin- and Wnt- dependent mechanism. (A) Western blot analysis and (B) quantification of β-catenin expression in nuclear/cytoplasmic fractions of ERG-deficient HUVEC treated with GFP-tagged control (GFP) or VE-cadherin adenovirus (VEC-GFP) and in presence or absence of lithium chloride (LiCl). The nuclear and cytoplasmic localization of β-catenin was rescued in ERG-deficient cells after combined VE-cadherin and lithium chloride treatment. Western blot analysis of VE-cadherin shows a lower and higher band representing the endogenous and GFP-tagged forms of the protein respectively. For normalization, tubulin was used as a cytoplasmic control and HDAC1 as a nuclear marker. Normalised β-catenin protein levels were expressed as fold change relative to siCtrl. Values are mean ± SEM; n=3; asterisks indicate values significantly different from the control (Student t test where * p < 0.05, ** p < 0.01, ***p < 0.001).

3.2.7 ERG regulates β -catenin stability partly through Wnt-dependent mechanisms

To test whether ERG regulates β -catenin stability through the Wnt pathway, control or ERG-depleted HUVEC transduced with Ad.VEC-GFP or Ad.GFP adenovirus were treated with LiCl (10mM) overnight. Activation of Wnt signalling by LiCl inhibits GSK3 β and thus degradation of cytoplasmic β -catenin, allowing its nuclear translocation (Stambolic et al., 1996). LiCl was able to partially normalize β -catenin nuclear levels in ERG-deficient EC (Figure 3.13, lane 7), but did not correct junctional β -catenin protein levels. Finally, combined Wnt signalling activation, through LiCl, and VE-cadherin overexpression were able to rescue both nuclear and junctional β -catenin pools in ERG-deficient EC (Figure 3.13, lanes 9 and 10). These results demonstrate that the balance between VE-cadherin-dependent and Wnt signalling-dependent pathways, which modulates canonical Wnt/ β -catenin signals in EC, is controlled by the transcription factor ERG.

By genome-wide transcriptome profiling of ERG-deficient EC (Birdsey et al., 2012), changes were identified in the expression of genes associated with the Wnt signalling pathway and involved in the regulation of cellular β -catenin levels. Several potential ERG target genes from the microarray, Dapper1 (DACT1), Dishevelled 3 (Dvl3), Frizzled 4 (FZD4) and Glycogen synthase kinase 3 β (GSK3 β), were selected for validation by qPCR (Figure 3.14). Inhibition of ERG for 48 h had no significant effect on expression of Dishevelled or GSK3 β . However, siERG-treated HUVEC showed a significant increase in Dapper1 mRNA levels, which has been shown to negatively modulate Wnt/ β -catenin signalling (Zhang et al., 2006; Gao et al., 2008) Conversely, a decrease in mRNA levels of the Wnt receptor Frizzled 4 was observed following ERG inhibition (Figure 3.14). The changes in expression suggest these candidate targets could be mediating ERG regulation of β -catenin degradation and transcriptional activity.

Wnt ligands bind to receptors of the Frizzled family to inhibit the β -catenin degradation complex and activate Wnt/ β -catenin signalling (Goodwin and D'Amore, 2002). I have shown that LiCl treatment was able to partially stabilize β -catenin nuclear expression in cellular fractions of ERG-deficient EC. This partial rescue of β -catenin expression was confirmed by immunoblotting of whole cell lysates of ERG-deficient

EC treated with LiCl (Figure 3.15). However, treatment of ERG-deficient EC with the upstream ligand Wnt3a was unable to rescue β -catenin expression (Figure 3.15). Wnt3a treatment of control cells, however, significantly stabilized and increased β -catenin protein levels. These data suggest that in ERG-deficient EC, a receptor-mediated defect exists upstream of the degradation complex.

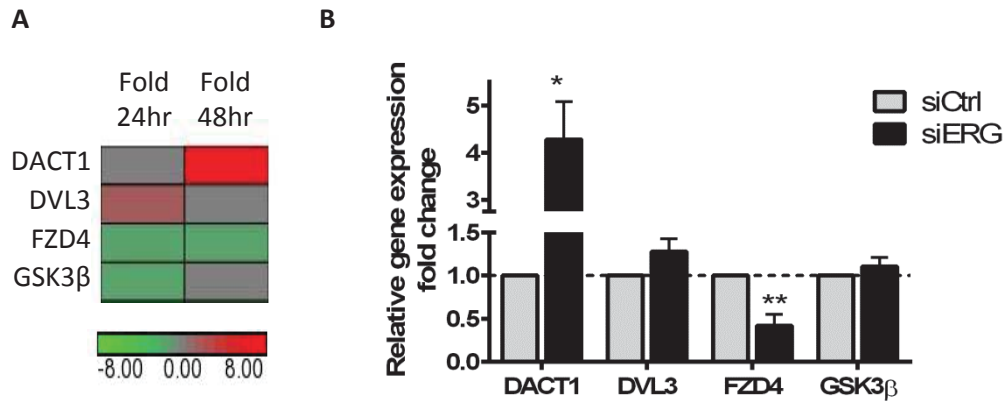


Figure 3.14 ERG regulates genes involved in control of β -catenin degradation. (A) Microarray analysis of differential gene expression in HUVEC was performed at 24 and 48 hours after ERG inhibition (Birdsey et al., 2012), with the fold change in expression of selected genes represented as high (red) and low (green) expression compared to the median (grey). (B) qPCR analysis of mRNA levels of DACT1, DVL3, FZD4 and GSK3 β in 48 hour siCtrl and siERG-treated HUVEC (n=4). Results are normalised to GAPDH and expressed as fold change relative to siCtrl. Values are mean \pm SEM; asterisks indicate values significantly different from the control (Student t test where * p < 0.05, ** p < 0.01).

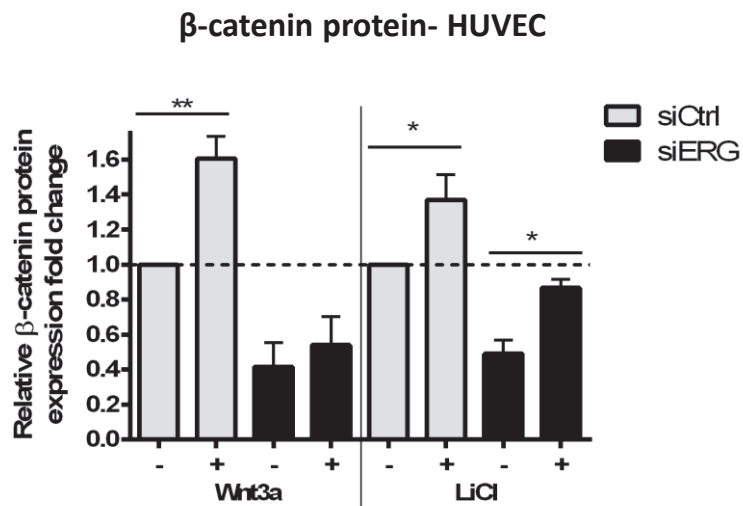
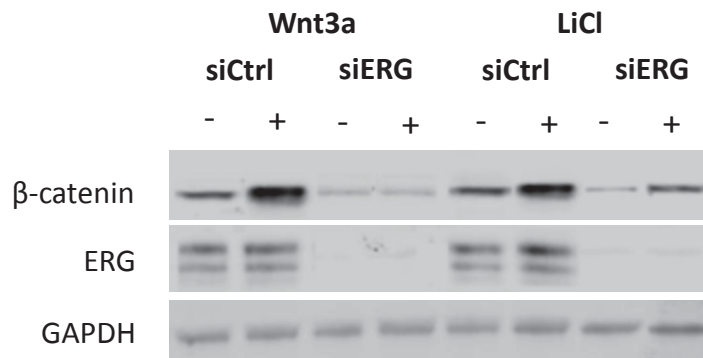


Figure 3.15 Treatment of ERG-deficient EC with the Wnt ligand Wnt3a was unable to rescue β-catenin expression. Western blot analysis of β-catenin expression in extracts of control and ERG-deficient cells treated with β-catenin stabiliser Wnt ligand 3a (Wnt3a) or LiCl. Results are normalised to GAPDH and expressed as fold change relative to siCtrl. Values are mean ±SEM; n=3; asterisks indicate significantly different values (ANOVA, followed by Bonferonni's test, where * p <0.05, ** p <0.01).

3.2.8 ERG drives expression of the Wnt receptor Frizzled-4

3.2.8.1 Endothelial expression of Frizzled-4 is regulated by ERG *in vitro* and *in vivo*

Wnt3a binds to the Frizzled-4 (Fzd4) receptor (Reis and Liebner, 2013), which is highly expressed in cultured EC (Goodwin et al., 2006). Given that Fzd4 was identified as a putative ERG target by transcriptome analysis in HUVEC (Birdsey et al., 2012) and validation by qPCR showed that Frizzled-4 mRNA expression was decreased following siERG inhibition for 48 h (Figure 3.14), I investigated whether ERG regulates Frizzled-4 expression in mouse EC. Consistent with the data in HUVEC, Fzd4 mRNA expression was decreased in mouse EC isolated from *Erg^{cEC-het}* mice (Figure 3.16 A). Frizzled-4 protein levels were also decreased in ERG-depleted HUVEC, indicating ERG is required for endothelial Frizzled-4 expression (Figure 3.16 B).

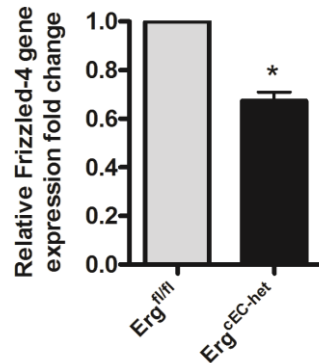
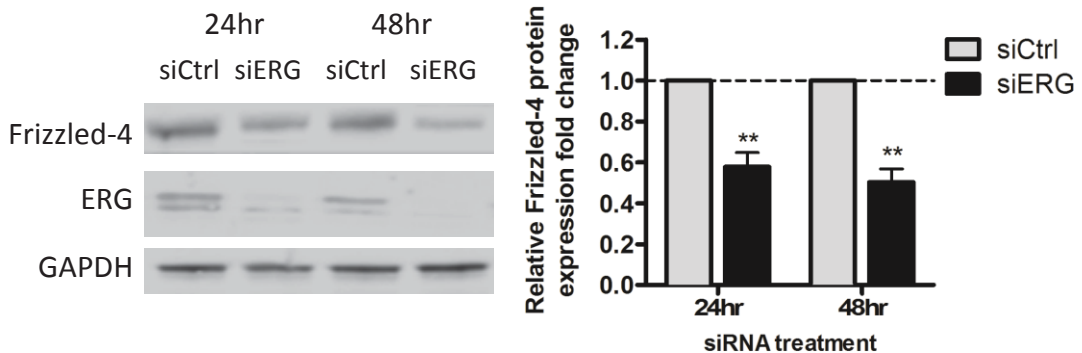
A**Frizzled 4 mRNA- mouse lung EC****B****Frizzled 4 protein- HUVEC**

Figure 3.16 ERG regulates Frizzled4 expression. (A) Frizzled-4 mRNA expression in primary *Erg^{cEC-het}* mouse lung EC compared to control. Results are normalised to HPRT and expressed as fold change relative to *Erg^{fl/fl}* littermate controls (n=6). (B) Western blot and quantification of total Frizzled-4 protein expression from HUVEC lysates treated with siCtrl or siERG for 24 h and 48 h (n=3). Representative blot shown. Protein levels were normalised to GAPDH and expressed as fold change relative to siCtrl. All graphical data are mean \pm SEM; asterisks indicate values significantly different from the control (Student t test where * p <0.05, ** p <0.01, *** p <0.001).

3.2.8.2 ERG binds to the Fzd4 promoter

Chromatin immunoprecipitation followed by parallel sequencing (ChIP-seq) has become an important tool for studying genome-wide protein-DNA interactions and gene regulation. ChIP can be used to analyse DNA-interacting proteins including RNA polymerases, transcription factors, transcriptional co-factors, and histone proteins. The Encyclopaedia of DNA Elements (ENCODE) project consortia (Birney et al., 2007; Myers et al., 2011) has mapped regions of transcription factor association, chromatin structure and histone modification in different cell types, which allow us to identify candidate regulatory elements. Moreover, a number of studies have shown that specific histone modifications can be used to assign functional attributes to genomic regions (Figure 3.17; Table 3.1). To test whether ERG binds to the Frizzled-4 promoter, I analysed ERG chromatin ChIP-seq data (Yang and Randi, unpublished data) and ENCODE datasets for histone marks and RNA polymerase II occupancy from HUVEC. These data showed that ERG-binding peaks were located in the genomic Fzd4 promoter region upstream of the transcription start site (Figure 3.18 A). ENCODE ChIP-seq data for RNA polymerase II occupancy, active methylation mark histone H3, lysine 4, trimethylation (H3K4me3) and active acetylation mark H3K27Ac (Birney et al., 2007; Myers et al., 2011), markers of active promoters, show that the location of these marks correlate with the position of the ERG peak (Figure 3.18 A).

Previous studies suggest that ERG binds a consensus sequence of AGGA(A/t)(G/A) (Wilson et al., 2010) or (C/a/g)(A/C)GGAA(G/A/c) (Wei et al., 2010) and analysis of the ERG-binding peak within the Frizzled-4 promoter indicates that this region contains 3 conserved ERG consensus sequences (Figure 3.18 B). To validate the ERG ChIP-seq data and confirm whether ERG binds to the Frizzled-4 promoter, ChIP was performed using quantitative PCR (qPCR) with primer pairs designed to cover region (R) 1 within the ERG binding ChIP-seq peak as indicated (Figure 3.19). Sheared chromatin from resting HUVEC was immunoprecipitated using an anti-ERG or IgG control antibody, and enriched chromatin was detected by quantitative PCR. Results are expressed as fold change compared to IgG control antibody and normalised for total input levels. Immunoprecipitation with an anti-ERG antibody resulted in greater enrichment of chromatin containing the Fzd4 proximal promoter region compared to immunoprecipitation using an isotype control antibody (Figure 3.19). There was no difference in enrichment for a control region, 3'UTR of

Frizzled-4, using either anti-ERG or IgG control antibodies, indicating no non-specific enrichment. To confirm the specificity for ERG binding at R1 within the Fzd4 promoter, ChIP-qPCR was carried out on chromatin from HUVEC treated with control and ERG siRNA. This showed a decrease in the amount of ERG bound to R1 following ERG inhibition, compared with control siRNA treatment (Figure 3.19).

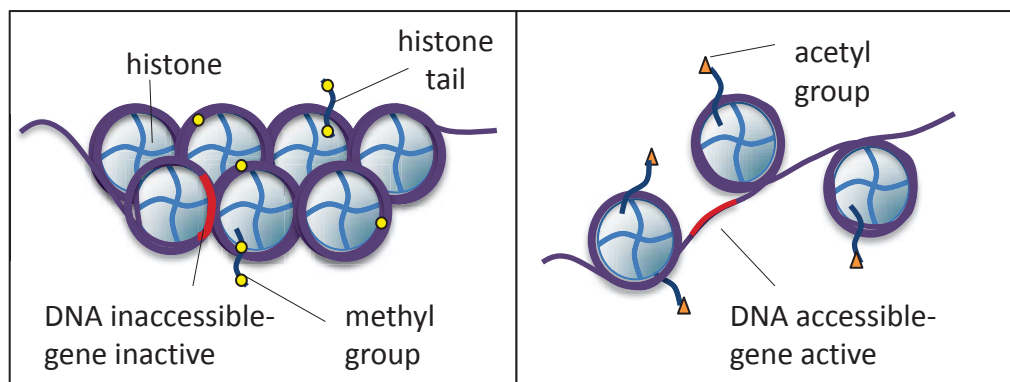


Figure 3.17 Post-translational modifications of the core histones affect DNA accessibility. DNA methylation causes nucleosomes to pack closely together (left), transcription factors cannot bind and gene expression is repressed. Histone acetylation causes histones to be spaced further apart (right), leaving the DNA exposed and accessible. Transcription factors can bind, allowing gene expression to occur.

ChIP-seq mark	Functional association
H3K4me3	Active promoters
H3K4me1	Active enhancers
H3K27Ac	Active promoters and enhancers
H3K27me3	Inactive transcription
RNA pol II	Active transcription

Table 3.1 Table of ChIP-seq histone post-translational modification markers and their functional association. Histone modifications act as markers identifying the putative function of the genomic locus where they are enriched. Active promoters and enhancers are commonly marked by trimethylated and monomethylated histone H3 at lysine 4, denoted by H3K4me3 and 1 respectively, and acetylated histone H3 at lysine 27, H3K27ac. Repressed genes may be located in large domains of H3K27me3. RNA polymerase II occupancy marks active transcription. These various features of chromatin help organize the DNA and distinguish functional elements in the large expanse of the genome.

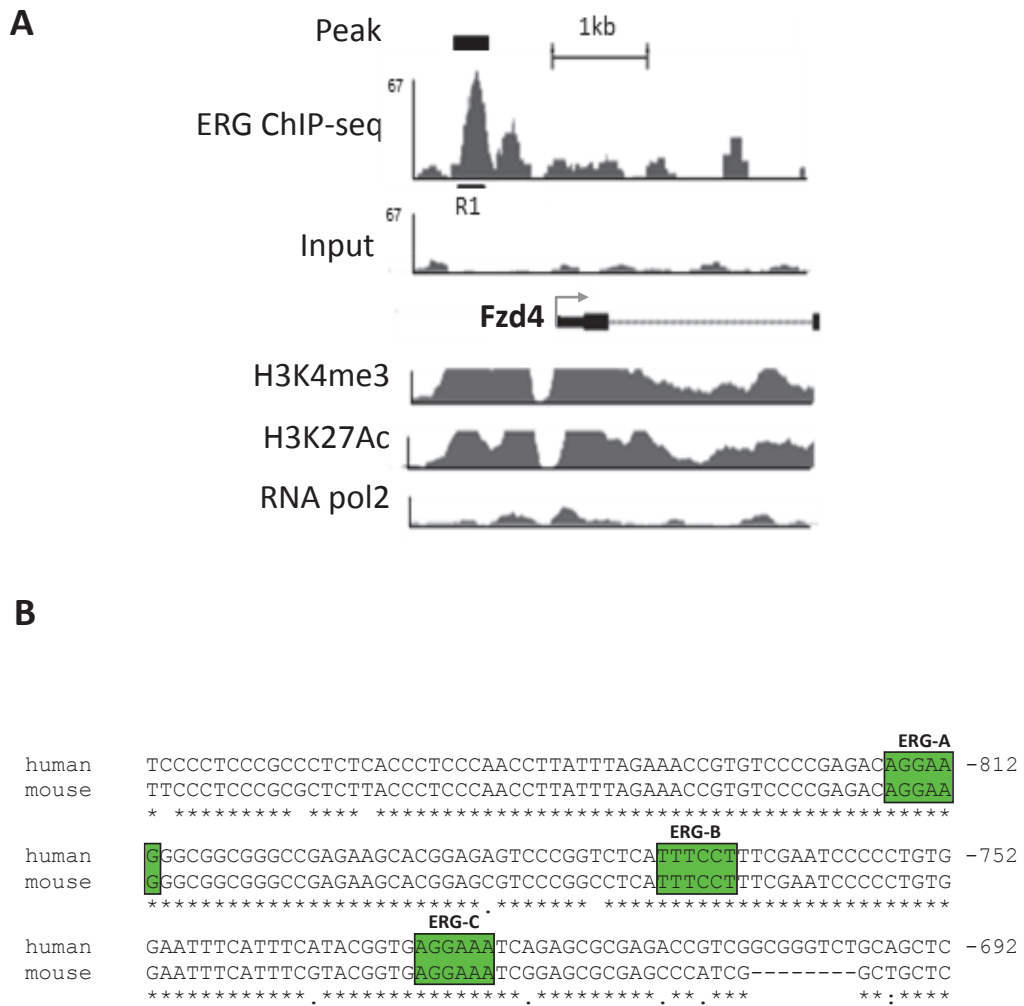


Figure 3.18 ERG binds to the Fzd4 promoter. (A) ERG ChIP-seq analysis in HUVEC (Yang and Randi, unpublished data) shows 1 significant ERG binding peak located within the Fzd4 genomic locus upstream of the transcription start site (arrow); chromatin input profile shows specificity of ERG peaks. ENCODE ChIPseq data peaks for H3K4me3, H3K27Ac and RNAPol2 indicate open chromatin and active transcription. Location of qPCR amplicon covering region R1 is indicated. (B) Sequence comparison of genomic region upstream of the Fzd4 transcription start site in human and mouse. Conserved ERG consensus sequences, (A/C)GGAA(G/A) or AGGA(A/T)(G/A), are shown (ERG A-C). Asterisks denote conserved nucleotides across both species. Nucleotide numbers relative to the Fzd4 transcription start site.

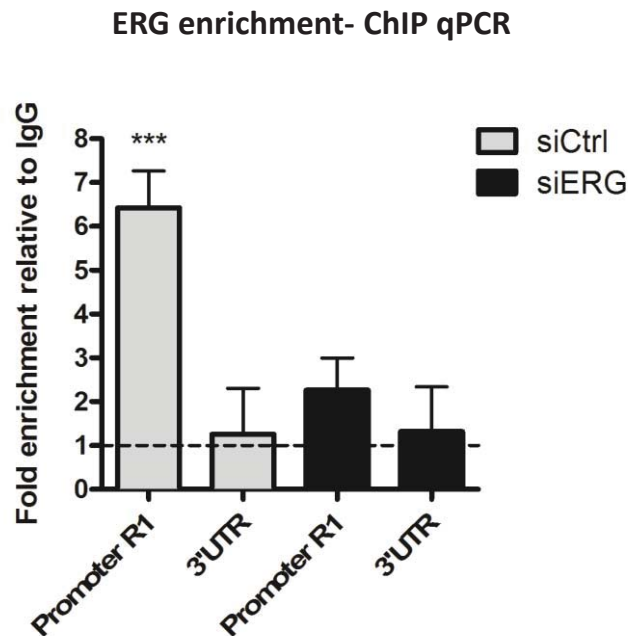


Figure 3.19 ERG binds to the Fzd4 promoter R1 in HUVEC. ChIP was carried out on sheared chromatin from HUVEC treated with Control (siCtrl) or ERG siRNA (siERG; 20 nM) using an anti-ERG or control IgG antibody. Immunoprecipitated DNA was analysed by qPCR with primers covering Fzd4 promoter region 1 and a negative control 3'UTR region to exclude non-specific precipitated DNA. Results are expressed as fold change compared to IgG normalised to input. Values are mean \pm SEM; n=3; asterisks indicate values significantly different from the control (Student t test where *** p <0.001).

3.2.8.3 ERG transactivates the Fzd4 promoter in EC

To determine whether ERG drives Frizzled-4 transcription in EC, a Frizzled-4 promoter luciferase reporter was used in a transactivation assay. In order to generate the Frizzled-4 promoter luciferase reporter, I needed to clone a 1kb region of the Frizzled-4 promoter in the pGL4 firefly luciferase backbone (Promega), which is designed to contain very few responsive elements. I tried to PCR amplify the Frizzled-4 promoter fragment using specific primer pairs which flank the region. However, amplification of the correct sized fragments failed. Instead, amplification products below the expected size and also a heavy smear were typically observed. The Frizzled-4 promoter region I was trying to amplify was characterised to be a GC-rich region and therefore I attempted to adjust the primer annealing temperatures, and used a polymerase specialized for amplifying GC rich region. However, even these changes failed to amplify only the desired fragment (Figure 3.20 A). Interestingly, a positive control region I have previously been able to successfully amplify, gave an amplification product of the correct size, ruling out a problem with the enzyme or machine parameters.

The Fzd4 promoter was therefore subcloned from a purchased Fzd4-pLightswitchprom plasmid into the pGL4 vector, to investigate the response of Fzd4-pGL4. Both plasmids were digested by restriction enzymes SacI and HindIII as the restriction sites were present in the same orientation on both vectors. Restriction digestion of Fzd4-pLightswitchprom resulted in the excision of the 1kb Fzd4 promoter insert (Figure 3.20 B). The digested Fzd4 promoter insert and recipient pGL4 vector were purified from a 1% agarose gel (Figure 3.20 B). The uncut plasmid controls shows a lower band than the linearized DNA as circular plasmid DNA is supercoiled, which migrates faster as it sustains less friction against the agarose matrix. The ligation of the Fzd4 insert and the pGL4 vector were recombined and transformed into competent bacteria. The correct insert was confirmed by sequencing.

To investigate whether ERG transactivates the Fzd4 promoter, HUVEC were co-transfected with an ERG cDNA expression plasmid (pcDNA-ERG) or an empty expression plasmid (pcDNA) and with the Fzd4 promoter (Fzd4-pGL4) or control luciferase construct, and luciferase activity was measured 24 h later. The basal activity of Fzd4-pGL4 was approximately 15-fold higher than pGL4 control, indicating basal

activity of the Fzd4 promoter in HUVEC (Figure 3.21). ERG overexpression resulted in a 4-fold transactivation of the Fzd4 promoter luciferase construct. This result shows that ERG transcriptionally drives the Frizzled-4 promoter.

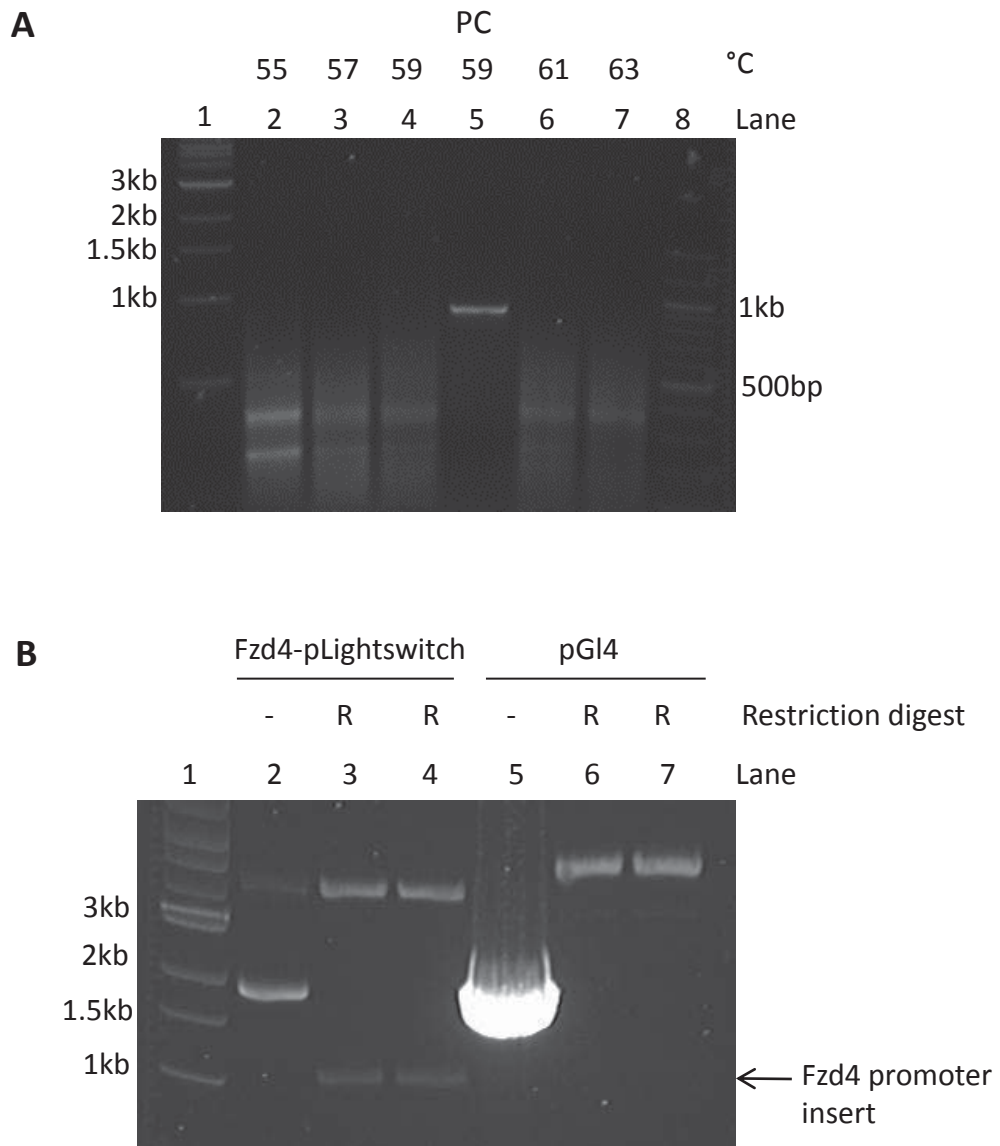


Figure 3.20 Generation of Fzd4-pGI4 luciferase construct (A) Amplification of 1.1 kb Fzd4 promoter fragment was performed using various annealing temperatures. The reaction products were analysed by agarose gel electrophoresis followed by ethidium bromide staining. Lane 1, 1kb DNA ladder; lanes 2, 3, 4 6 and 7, Fzd4 amplification at indicated temperatures; lane 5, amplification of positive control (PC) PCR product; lane 8, 100bp ladder. **(B)** 1% agarose gel electrophoresis of Fzd4-pLightswitch and empty pGI4 vector DNA digested with SacI and HindIII . Lane 2 shows undigested and circular Fzd4-pLightswitch vector DNA. Lanes 3 and 4 show duplicate digestion and linearisation of Fzd4-pLightswitch vector, which causes the liberation of the 1.1kb Fzd4 promoter insert. Lane 5 shows undigested pGI4 vector DNA which is restriction digested using SacI and HindIII in duplicate lanes 6 and 7.

Fzd4 promoter transactivation

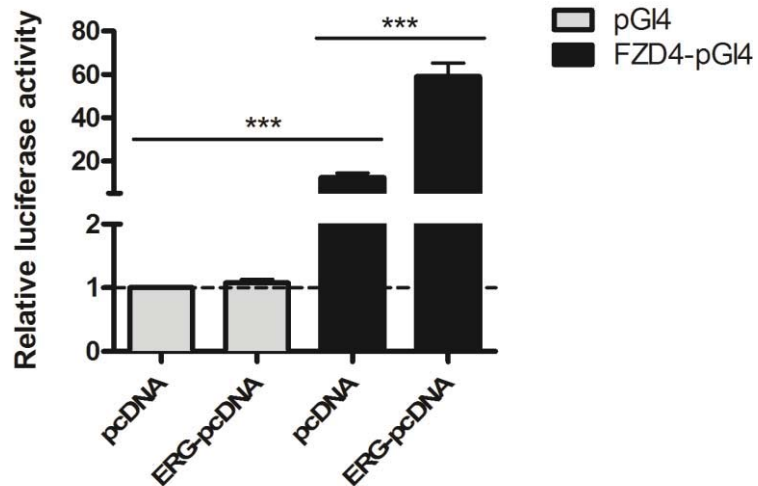


Figure 3.21 ERG transactivates the Frizzled-4 promoter. Luciferase reporter assay, where HUVEC were co-transfected with an ERG cDNA expression plasmid (ERG-pcDNA) or an empty expression plasmid (pcDNA), a control pGI4 luciferase or Fzd4 promoter-luciferase construct (Fzd4-pGI4) and the pGL4 renilla internal control vector in HUVEC, and luciferase activity was measured 24 h later. Values are represented as dual luciferase ratio of firefly luciferase normalised to pGL4 Renilla luciferase and expressed as fold change relative to empty pGL4 vector alone. Values are mean \pm SEM; n=3; asterisks indicate significantly different values (ANOVA, followed by Bonferonni's test, where *** p <0.001).

3.2.8.4 Frizzled-4 overexpression in ERG-deficient EC partially rescues Wnt3a activation of β -catenin transcriptional activity

To examine whether Fzd4 overexpression can rescue β -catenin transcriptional activity in ERG-deficient EC, control and ERG-deficient HUVEC were co-transfected with a control (pCMV6) or Fzd4 expression construct (pCMV6-Fzd4) and TOP TCF reporter and treated with Wnt3a. In line with Figure 3.5 A, Wnt3a activation of β -catenin transcriptional activity was decreased in ERG-deficient HUVEC. However, overexpression of pCMV6-Fzd4 partly rescued β -catenin transcriptional activity in Wnt3a-treated ERG-deficient HUVEC (Figure 3.22). Finally, combined Ad.VEC-GFP transduction and Fzd4 overexpression fully rescued Wnt activation of the reporter in ERG-deficient EC (Figure 3.22). Together, these data demonstrate that ERG controls transcription of the Fzd4 receptor in EC, and point to a molecular mechanism for the VE-cadherin-independent control of Wnt signalling by ERG.

TCF/ β -catenin reporter activity

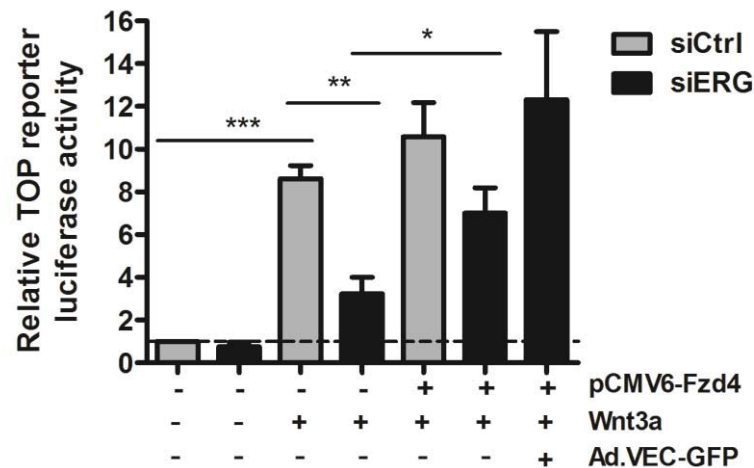


Figure 3.22 Fzd4 overexpression in ERG-deficient EC partly rescues Wnt3a activation of β -catenin transcriptional activity. Control (siCtrl) and ERG siRNA (siERG; 20 nM)-treated HUVEC were transfected with TOPFLASH TCF luciferase reporter construct, with control pCMV6 or pCMV6-Fzd4 plasmids and with the pGL4 renilla control vector. Cells were treated for 6 hr in the presence of absence of rWnt3a and in some conditions were transduced with Ad.VEC-GFP adenovirus (MOI 70). Results are presented as dual luciferase ratio (DLR) of firefly luciferase normalised to pGL4 Renilla luciferase and expressed as fold change relative to control. Values are mean \pm SEM; n=3; asterisks indicate significantly different values (ANOVA, followed by Bonferonni's test, where ** p <0.01, *** p <0.001).

3.2.9 ERG regulates β -catenin nuclear localisation in sparse EC

Since ERG regulates β -catenin levels in confluent EC, a model of mature endothelial monolayers, I examined whether ERG regulates β -catenin in sub-confluent HUVEC, as a model of angiogenic EC. As expected, β -catenin was more clearly localized to the cytoplasm and nucleus in sparse cells (Figure 3.23) compared to in confluent cells (Figure 3.2), where β -catenin was primarily localized to the intercellular junctions. In sparse as in confluent HUVEC, depletion of ERG led to a decrease in β -catenin levels in both the cytoplasm and nucleus (Figure 3.23). Given that Wnt signalling controls the levels of cellular stabilised cytoplasmic and nuclear β -catenin, this supports a role for ERG in controlling Wnt signalling dependent stabilisation of β -catenin. ERG regulates β -catenin protein levels in confluent and sub-confluent EC, suggesting that this control occurs both in stable as well as angiogenic endothelium.

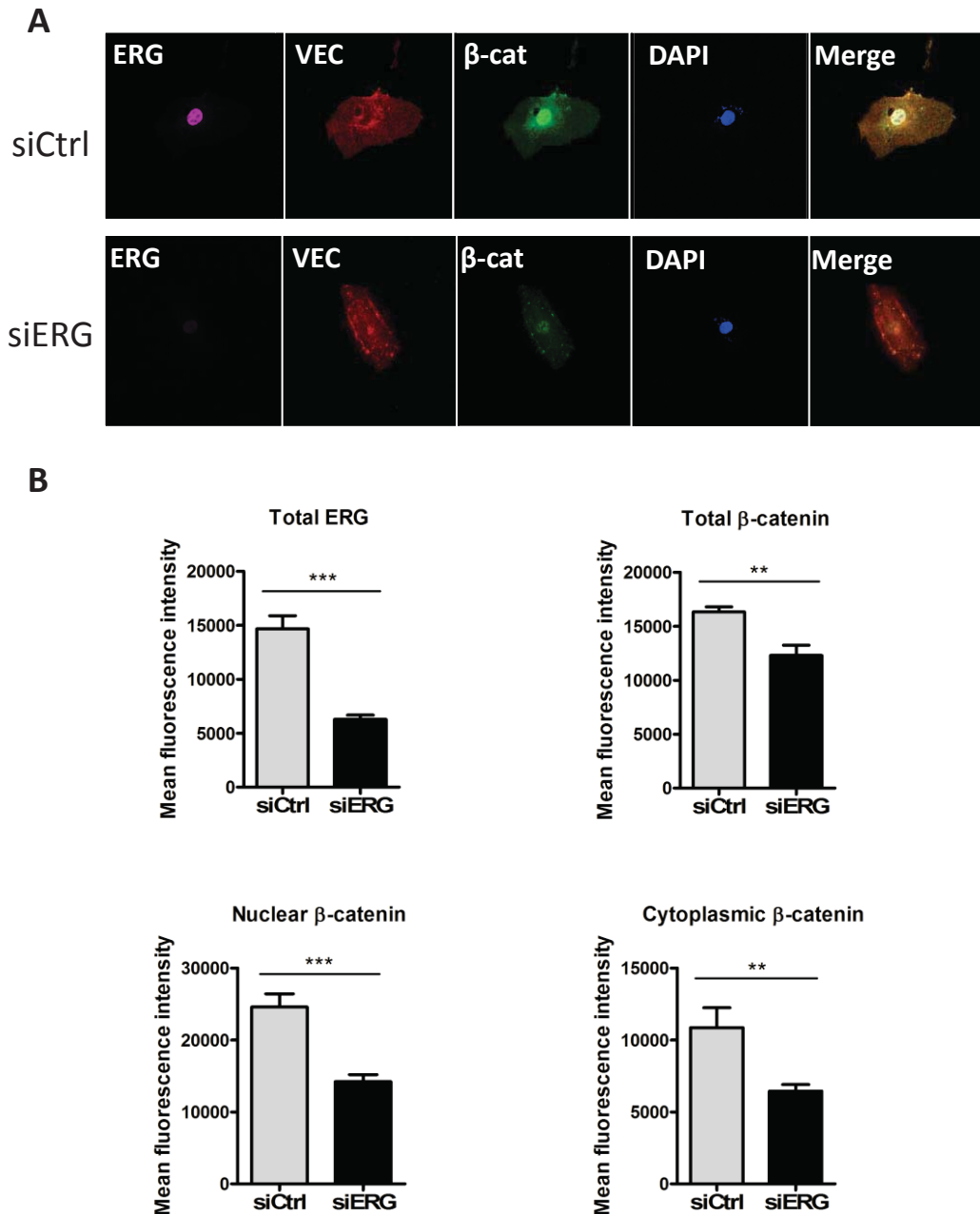


Figure 3.23 ERG is required for β -catenin expression in sparse HUVEC.

(A) ERG (magenta), VE-cadherin (VEC; red), β -catenin (β -cat; green) and DAPI (blue) staining of sparse Control and ERG siRNA (20nM)-treated HUVEC. Scale bar, 20 μ m. (B) Volocity® software quantification of mean ERG and β -catenin fluorescence intensity. Quantification of mean β -catenin fluorescence intensity in the cytoplasm required the exclusion of nuclear areas (objects that touch DAPI), whereas quantification of mean β -catenin intensity in the nucleus required the exclusion of cytoplasmic areas (objects that do not touch or overlap with DAPI) (n=8). Values are mean \pm SEM; n=8; asterisks indicate values significantly different from the control (Student t test where ** p < 0.01, *** p < 0.001).

3.2.10 ERG controls cell proliferation and survival through Wnt signalling

Wnt/ β -catenin signalling can promote EC proliferation (Masckauchan et al., 2005) and induce cell cycle progression through transcriptional activation of Cyclin D1 (Shtutman et al., 1999). To test whether ERG regulates cell proliferation and whether this is mediated via β -catenin, a BrdU incorporation ELISA was used to analyse cell proliferation in sparse control and ERG-depleted HUVEC treated in the presence or absence of LiCl overnight. Western blot analysis showed increased levels of β -catenin in LiCl-treated HUVEC, indicating effective β -catenin stabilisation by LiCl (Figure 3.24 A). ERG inhibition caused a decrease in proliferation of sparse cells compared to control. However, stabilising β -catenin expression using LiCl, normalised the ERG-induced proliferation defect (Figure 3.24 B), suggesting ERG controls endothelial proliferation through the Wnt/ β -catenin pathway.

Previous work shows that both ERG inhibition and increased degradation of β -catenin correlate with increased endothelial apoptosis (Birdsey et al., 2008; Wu et al., 2003). To test whether ERG controls endothelial survival through the Wnt/ β -catenin pathway, cell apoptosis was measured by Caspase 3/9 Glo assay in siCtrl- and siERG-transfected HUVEC treated with LiCl and Ad.VEC-GFP. ERG inhibition induced cell apoptosis and this increase in cell death was partially decreased with VE-cadherin overexpression in ERG-deficient EC, in line with previous data (Birdsey et al., 2008). Cell apoptosis induced by inhibition of ERG, however could be fully reversed by overexpression of VE-cadherin GFP and LiCl treatment (Figure 3.24 C), indicating the functional consequences of ERG regulation of β -catenin stability.

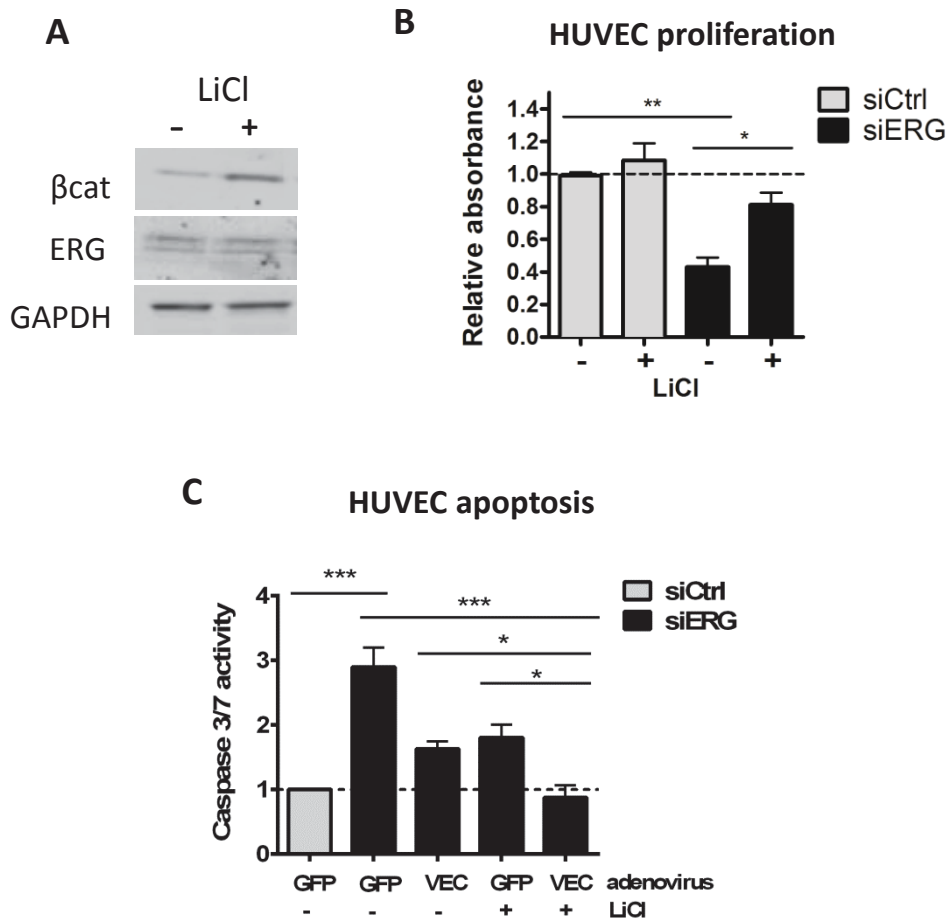


Figure 3.24 ERG regulates cell proliferation and survival through Wnt/β-catenin signalling. (A) HUVEC were treated in the presence or absence of LiCl (30 mM) for 12 h. Cell lysates were immunoblotted with anti-β-catenin, -ERG, or -GAPDH. Representative western blot shown. (B) Cell proliferation of HUVEC treated with siCtrl and siERG for 6 h and replated at a sparse cell density and treated in presence or absence of LiCl (30mM), was quantified by the colorimetric measurement of BrdU incorporation during DNA synthesis in proliferating cells. Results are normalised to cell number and expressed as fold change relative to siCtrl (n=4). (C) HUVEC grown in 96-well microplates were treated with siCtrl and siERG, and transduced with control GFP or Ad.VEC-GFP, and treated in the presence or absence of LiCl. After 48 h, luminescence was measured using the Caspase-3 or -7 Glo Assay. ERG inhibition-induced apoptosis was reversed with combined VEC-GFP overexpression and LiCl treatment. Results are expressed as fold change relative to siCtrl (n=3). All graphical data are mean ±SEM; asterisks indicate significantly different values (ANOVA, followed by Bonferonni's test, where * p <0.05, ** p <0.01, *** p <0.001).

3.2.11 ERG-dependent angiogenesis requires Wnt signalling

To test the functional relevance of Wnt signalling in ERG-dependent angiogenesis, I used an *in vitro* sprouting assay, where HUVEC sprout from the surface of beads embedded in fibrin gels in the presence of co-cultured human skin fibroblast cells (Nakatsu et al., 2007). Fibroblast-derived factors promote sprouting and recapitulate *in vivo* sprouting vessel formation. Quantification of the number and length of sprouts formed at day 3 of the assay showed that ERG-deficient HUVEC formed markedly decreased numbers of sprouts (Figure 3.25 A, panel b; Figure 3.25 B) that were significantly shorter in length (Figure 3.25 C). However, pre-treatment of ERG-deficient cells with LiCl to inhibit β -catenin degradation was sufficient to partially restore normal sprouting behaviour of HUVEC (Figure 3.25 A, panel d). LiCl was able to significantly increase the number (Figure 3.25 B) and length (Figure 3.25 C) of the sprouts formed by ERG-deficient HUVEC, suggesting that ERG controls angiogenesis in a β -catenin-dependent manner.

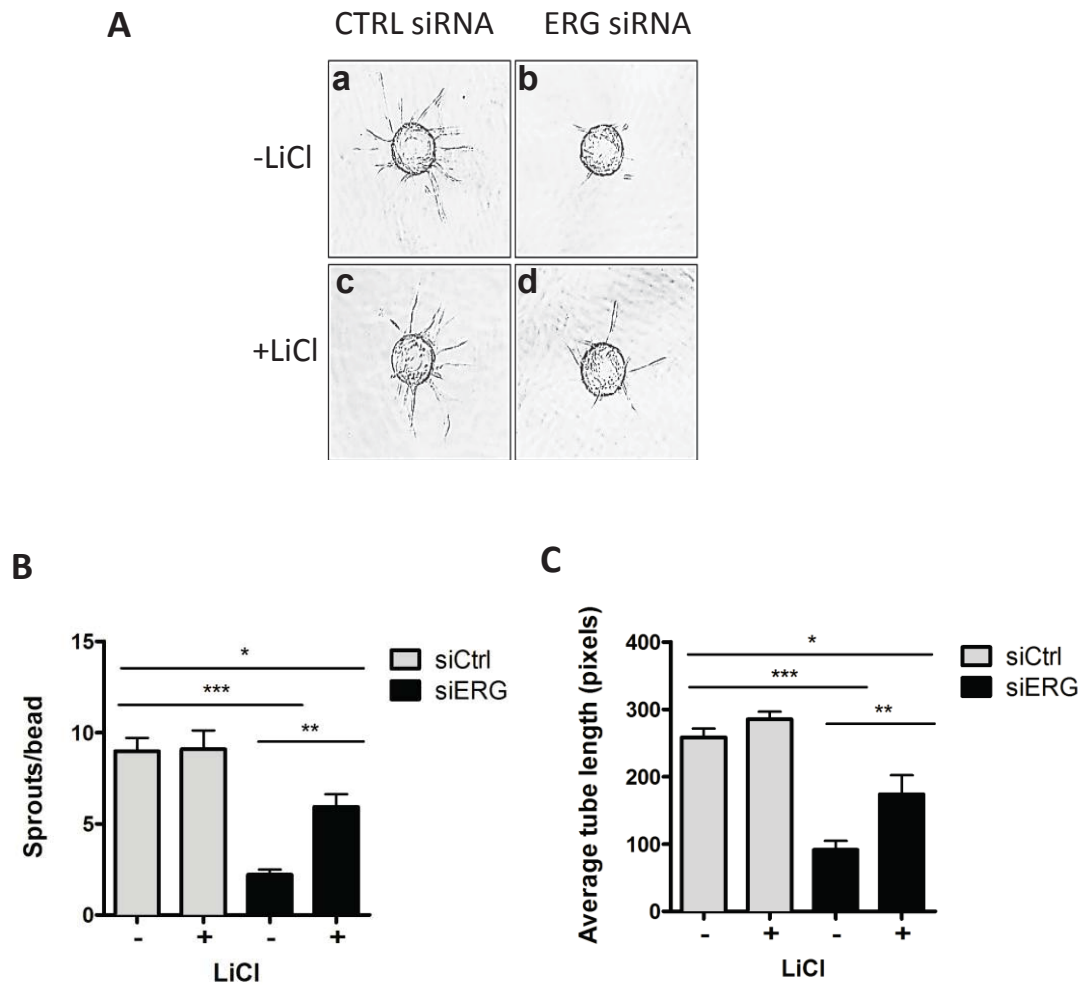


Figure 3.25 ERG regulates angiogenesis through Wnt/ β -catenin signalling. Control and ERG siRNA (20 nM)-transfected HUVEC treated in the presence or absence of LiCl were coated onto beads and embedded in fibrin gels in the presence of fibroblasts. **(A)** Representative images of sprouting fibrin gel beads at day 3. **(B)** Quantification of EC sprouting in the fibrin gel bead assay. Number of sprouts per bead was determined, where a sprout is defined as a vessel of length equal to the diameter of a bead. **(C)** Sprout length was also measured in arbitrary units. 25 beads were assessed and quantified for each condition. Values are mean \pm SEM; n=3; asterisks indicate significantly different values (ANOVA, followed by Bonferonni's test, where * p < 0.05, ** p < 0.01, *** p < 0.001).

3.2.12 Pharmacological stabilisation of β -catenin rescues vascular defects in

Erg^{cEC-KO} mice

To confirm that *in vivo* ERG controls angiogenesis in a Wnt/ β -catenin-dependent manner, a rescue experiment was performed by Dr. Graeme Birdsey, whereby LiCl, a pharmacological stabiliser of Wnt/ β -catenin signalling (Griffin et al., 2011) was administered to pregnant female mice at developmental stages E8.5 and E9.5. Light microscopy examination of the vasculature of the yolk sacs from E10.5 NaCl (control) and LiCl treated embryos revealed a dramatic increase in perfused vessels in the yolk sacs of *Erg*^{cEC-KO} mutants following LiCl treatment (Figure 3.26 A). Endomucin staining revealed disrupted vessel morphology in the yolk sacs from NaCl-treated *Erg*^{cEC-KO} embryos, with reduced vascular branching and decreased diameter of the larger vitelline vessels (Figure 3.26 B). LiCl treatment of *Erg*^{cEC-KO} mutants resulted in significant increase in vitelline vessel diameter, in line with the increase in perfusion. Together, these results demonstrate that endothelial ERG controls embryonic vascular development and angiogenesis through the Wnt/ β -catenin signalling pathway.

qPCR analyses of whole yolk sac tissue showed expression of *Erg* and its transcriptional targets VE-cadherin and Frizzled-4 were decreased in NaCl-treated *Erg*^{cEC-KO} yolk sacs compared to controls (Figure 3.27 A). To investigate whether Wnt signalling is rescued in *Erg*^{cEC-KO} yolk sac vasculature upon LiCl treatment, I studied the expression of the Wnt targets CyclinD1 and Axin2. Transcript levels of Cyclin D1 and Axin2 were shown to be significantly decreased in NaCl-treated *Erg*^{cEC-KO} yolk sacs compared to controls, supporting a role for ERG in regulating Wnt signalling in the yolk sac during vascular development (Figure 3.27 A). LiCl-treatment of *Erg*^{cEC-KO} yolk sacs normalized Cyclin D1 and Axin2 levels to those observed in LiCl-treated control embryos (Figure 3.27 B). Interestingly, ERG targets VE-cadherin and Frizzled-4 were not normalized, in line with the direct transcriptional role of ERG in their regulation.

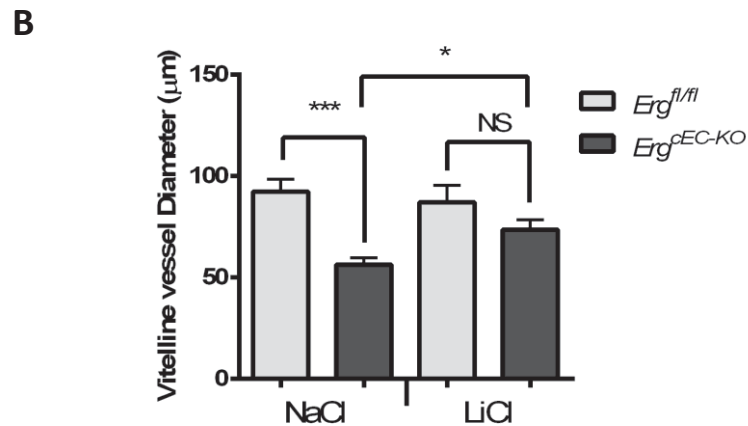
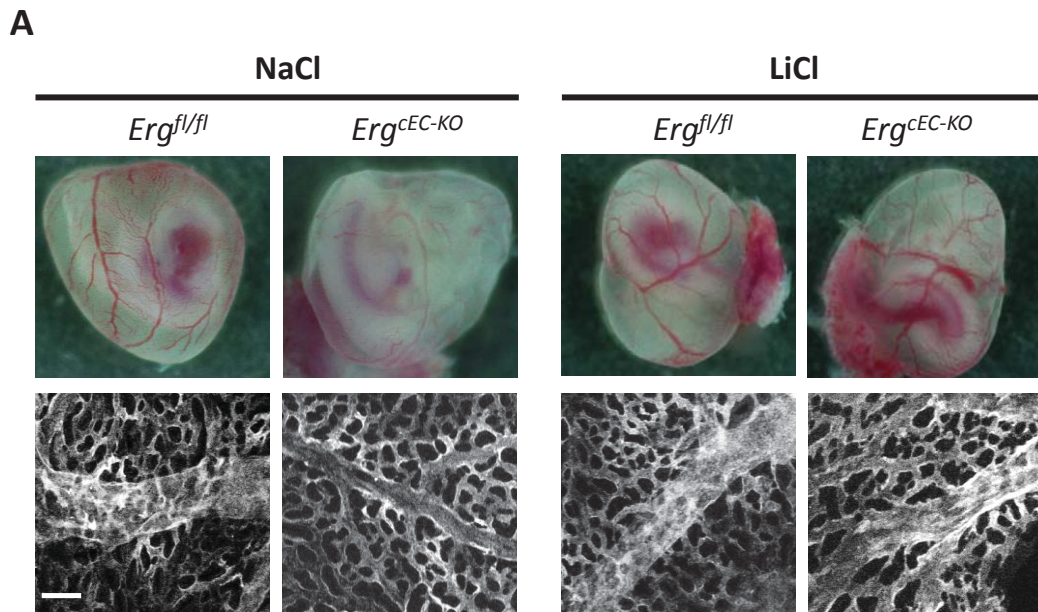


Figure 3.26 Pharmacological inhibition of β -catenin degradation with LiCl rescues vascular defects in *Erg^{cEC-KO}* yolk sacs *in vivo*. (A) (Top panels) Representative whole mount images of E10.5 *Erg^{fl/fl}* and *Erg^{cEC-KO}* embryo yolk sacs from pregnant female mice treated with either NaCl (left) or LiCl (right) at E8.5 and E9.5. Scale bar, 1 mm (n=5). (Bottom panels) Yolk sacs were whole-mount immunostained for endomucin to visualise the yolk sac vasculature; scale bar, 100 μ m. (B) Quantification of diameter of the larger vitelline vessels within the yolk sac. Values are mean \pm SEM; n=4; * p <0.05, ** p <0.01, *** p <0.001. Experiments were carried out by Dr. Graeme Birdsey (figure reproduced from Birdsey, Shah et al., 2015).

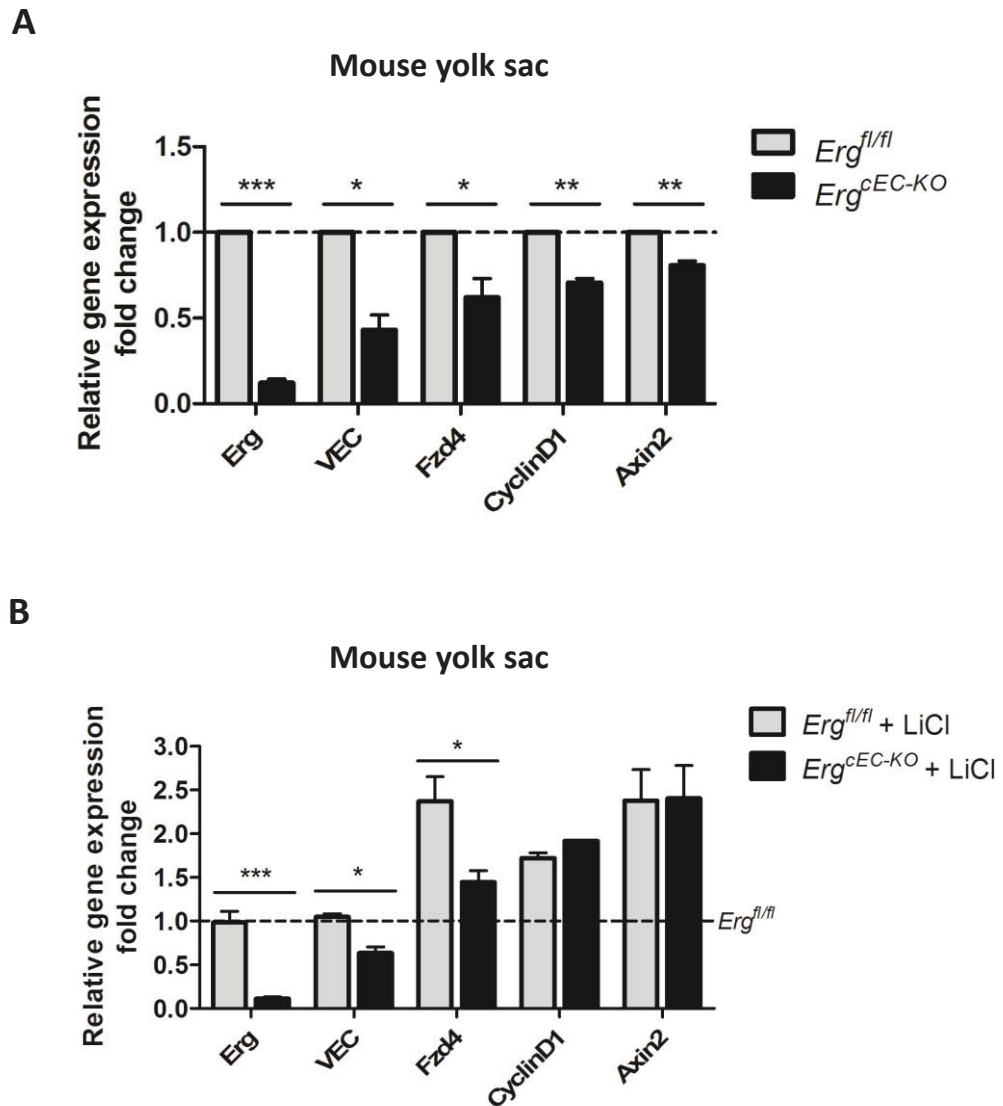


Figure 3.27 Inhibition of β -catenin degradation with LiCl treatment rescues Wnt signalling in *Erg^{cEC-KO}* yolk sacs *in vivo*. (A) qPCR analysis of *Erg*, VE-cadherin, Frizzled-4, CyclinD1 and Axin2 mRNA expression in NaCl-treated *Erg^{fl/fl}* and *Erg^{cEC-KO}* embryo yolk sacs. Data are expressed as fold change versus NaCl-treated *Erg^{fl/fl}* and are \pm SEM from at least three mice per group. (B) qPCR analysis of LiCl-treated *Erg^{fl/fl}* and *Erg^{cEC-KO}* embryo yolk sacs. Data are expressed as fold change versus NaCl-treated *Erg^{fl/fl}* and are \pm SEM from at least three mice per group. Asterisks indicate values significantly different from the control (Student t test where * $p < 0.05$, ** $p < 0.01$, *** $p < 0.001$).

3.2.13 ERG interacts with β -catenin in HUVEC

Combinatorial interactions among transcription factors and co-activators are critical to directing tissue-specific gene expression. Since GSEA indicated a significant correlation between the genes regulated by ERG and genes regulated by β -catenin, I considered the possibility that ERG and β -catenin proteins might cooperate to activate transcription and investigated whether ERG and β -catenin physically associate. To study this potential interaction, HUVEC cell lysates were immunoprecipitated with anti-ERG and rabbit IgG immunoprecipitate was used as a negative control. Western blot analysis was carried out on the immunoprecipitated lysates, using an ERG antibody raised against a different epitope compared to the one used to immunoprecipitate ERG. In HUVEC, endogenous β -catenin protein co-immunoprecipitated with ERG (Figure 3.28 A). This experiment indicates ERG forms a complex with β -catenin, however additional studies are required to determine whether ERG and β -catenin associate through direct protein-protein interactions. Furthermore, stimulation of HUVEC with Wnt3a, which I showed resulted in an increase in Wnt reporter activity (Figure 3.5 A), also induces ERG mRNA expression by 1.3 fold when compared to unstimulated HUVEC (Figure 3.28 B). These data suggest that Wnt signalling may maintain endogenous Wnt activity within the cell through a feedback loop mediated via ERG.

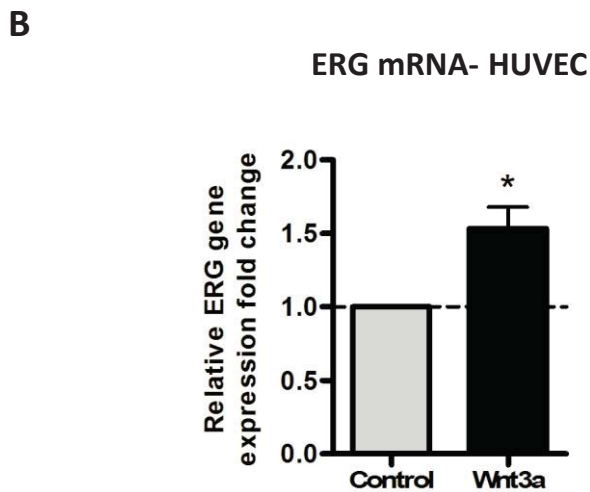
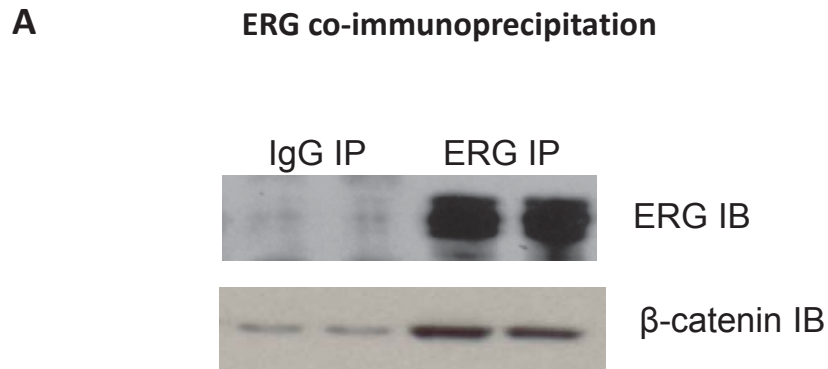


Figure 3.28 ERG interacts with β -catenin and Wnt3a induces ERG expression. (A) Co-immunoprecipitation experiment in HUVEC. 500 μ g of cell lysate from HUVEC was immunoprecipitated with rabbit polyclonal antibodies to ERG, and proteins were separated by SDS-PAGE. Immunoprecipitates (IP), and equal amounts of lysates (TCL) and unbound fractions after immunoprecipitations (Ub) were probed using goat polyclonal antibodies anti-ERG and mouse monoclonal anti- β -catenin. Endogenous β -catenin coimmunoprecipitated with ERG. (B) ERG mRNA expression in HUVEC treated with Wnt 3a conditioned medium. Results are normalised to GAPDH and expressed as fold change relative to siCtrl. Values are mean \pm SEM; n=3; asterisks indicate values significantly different from the control (Student t test where * p <0.05).

3.3 Discussion and Future Work

Canonical Wnt/ β -catenin signalling has been shown to play a role in promoting EC survival, junction stabilization, proliferation and pericyte recruitment and is thus essential for vessel growth and stability (Dejana, 2010; Phng et al., 2009; Franco et al., 2009; Cattelino et al., 2003). By operating as both a component of the junctional cadherin complex and a key mediator of Wnt signalling, β -catenin acts as the lynchpin between cell–cell contact and transcriptional regulation of proliferation, coordinating endothelial homeostasis. In the experiments described above, I establish ERG as a regulator of canonical Wnt/ β -catenin signalling and so identify a relationship between two essential transcriptional regulators of endothelial function. I have shown that ERG controls the Wnt/ β -catenin pathway by promoting β -catenin stability, through signals mediated by VE-cadherin and the Wnt receptor Frizzled-4, the balance of which control β -catenin cellular localization and activity (Figure 3.29). Importantly, I have also shown that ERG's control of cell survival, proliferation and angiogenesis is mediated through β -catenin (Figures 3.24-3.25). It has been proposed that the β -catenin pathway functions to increase cell plasticity and sensitivity to extracellular cues (Franco et al., 2009). Thus my results suggest that in the endothelium ERG is required to maintain homeostatic β -catenin protein expression within the cell, the output of which can be adapted according to the growth or survival signals the cell faces, providing the balance between proliferation and stability required in a sprouting blood vessel (Figure 3.29).

Similar to the endothelial-specific constitutive ERG knockout mice, constitutive endothelial-specific deletion of β -catenin results in early lethality in utero at E12.5 (Cattelino et al., 2003) and both lines displayed diffuse haemorrhages and defects in vascular remodelling. Importantly, experiments carried out in the group showed that the defective yolk sac angiogenesis observed in the *Erg^{EC-KO}* mice and expression of canonical Wnt/ β -catenin targets were normalised by *in vivo* LiCl treatment. While we cannot definitively rule out non-endothelial LiCl effects, these experiments clearly show that ERG controls vascular development through canonical Wnt/ β -catenin signalling. To this end, we could cross the conditional β -catenin GOF line into our conditional ERG knockout background and analyse the vasculature to show cell autonomous effects. To study changes in endothelial gene expression in the yolk sacs we could isolate the endothelial cells specifically to assess target expression. However,

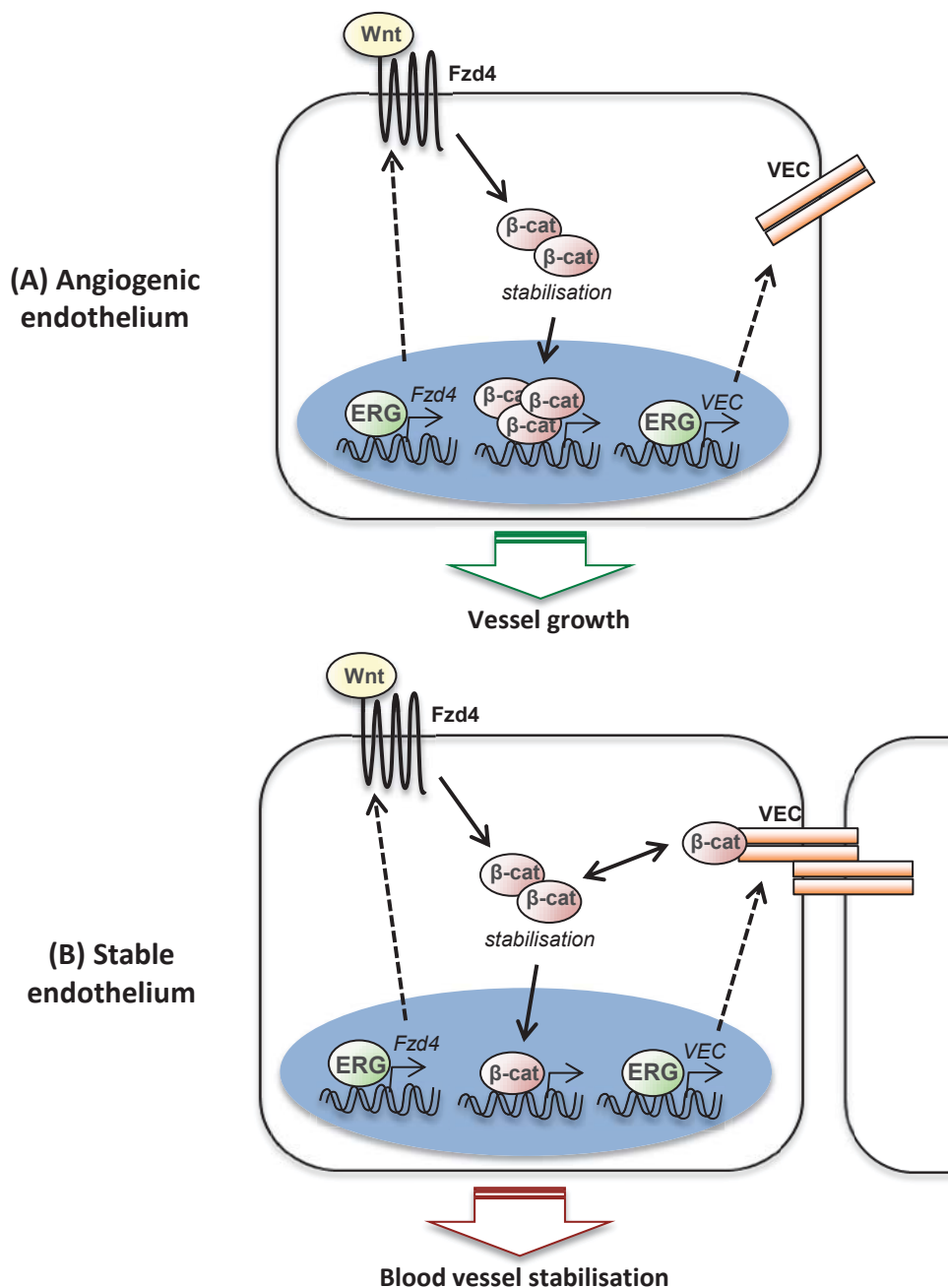


Figure 3.29 Proposed model for ERG regulation of vascular growth and stability through Wnt/β-catenin signalling. ERG drives expression of VE-cadherin (VEC) and the Wnt receptor Frizzled-4 (Fzd4), which both protect β-catenin from degradation. Fzd4-dependent signals stabilize cytoplasmic levels of β-catenin. (A) In angiogenic endothelium, when VE-cadherin is not engaged at the junctions, β-catenin preferentially translocates into the nucleus and regulates transcription of genes involved in cell proliferation. (B) In stable endothelium, VE-cadherin tethers β-catenin at the junctions, reducing proliferative signals and promoting vascular stability. ERG, through both VE-cadherin and the Wnt receptor Fzd4, maintains homeostatic β-catenin levels, which can be functionally modulated by growth and survival signals, thus regulating the balance between vessel growth and stability.

the *in vitro* assays I have used (sprouting, apoptosis and proliferation) provide strong evidence that LiCl rescues the phenotypes associated with ERG-dependent loss in EC.

Interestingly, the *Erg*^{*IEC-KO*} mice display retinal angiogenic defects similar to the endothelial-specific β -catenin and *Fzd4* knockout mice (Xu et al., 2004; Ye et al., 2009; Phng et al., 2009; Corada et al., 2010), where defective angiogenic growth and increased vessel regression are observed. Mutations in either *Fzd4* or its ligand *Norrin* (Xu et al., 2004), which mimics a canonical Wnt ligand, are associated with human ocular diseases, including Norrie disease and familial exudative vitreoretinopathy (FEVR) (Toomes et al., 2004). These diseases are manifested by defective retinal, ear and cerebellum vascularization and leaky vessels. Whether ERG is implicated in these ocular diseases remains to be established. Preliminary evidence in the group shows that, similar to *Norrin* and *Fzd4* deficiency, loss of ERG leads to severe and persistent attenuation of retinal vascularization at postnatal day 15.

Of the 19 Wnt ligands expressed in the mouse, only a few, such as *Wnt3a* and *Wnt7b* are recognized to have effects on angiogenesis. There are, similarly, a large number of Frizzled receptors and coreceptors, whose angiogenic functions are unknown. Therefore, to further understand the function of Wnt signalling *in vivo* during angiogenesis, it is important to analyze the expression pattern of these different Wnt ligands, Frizzled receptors, and co-receptors at different stages of vascular development and whether ERG is involved in their regulation.

Another interesting question that arises and remains unanswered is the mechanisms underlying vessel stability and the role for canonical Wnt signalling in this process. Endothelial-specific *Erg* and β -catenin knockout mouse models (Birdsey, Shah et al., 2015; Phng et al., 2009) display increased retinal vessel regression; a hallmark of decreased vessel stability. However, one study demonstrated that hyaloid vessel regression in the developing eye is mediated by Wnt 7b-dependent signalling through *Fzd4* (Lobov et al., 2005), suggesting ligand-specific responses could occur in different vascular beds. One key mechanism of stabilization is through regulation of endothelial junctions. As mentioned previously, besides being a transcriptional activator, β -catenin is also a key component of adherens junctions; *in vitro* studies show the binding of catenins can act as a plasma-membrane-retention signal for VE-cadherin (Xiao et al., 2005). Therefore, it is possible that besides transcriptional control of VE-cadherin,

ERG may indirectly be involved in preventing VE-cadherin internalisation and degradation through β -catenin. However, the loss of endothelial β -catenin *in vivo* did not affect VE-cadherin immunostaining and junctional organisation in the retina (Phng et al., 2008). Although in a confluent monolayer the majority of β -catenin is tethered to the junctions, a significant pool exists in the nucleus of these cells. Liebner et al. highlighted the importance of the transcriptional regulatory role of β -catenin in maintaining tight junction integrity, by driving expression of tight junction molecules Claudin 3 and Claudin 5 (Liebner et al., 2008). One can therefore question whether β -catenin also stabilizes endothelial junctions of nascent vessels by inducing the expression of “stability genes” to promote vessel homeostasis. Whatever the mechanisms underlying vessel stability, they will likely be transient and dynamic in nature to prevent excessive vessel regression.

It has recently been suggested that LEF1 activity is different between tip and stalk cells (Phng et al., 2009), and that this uneven activity influences blood vessel stability. Therefore, I studied the distribution of β -catenin in sub-confluent HUVEC, as an *in vitro* model of angiogenic EC. ERG regulates β -catenin protein levels in confluent (Figure 3.2) and sub-confluent EC (Figure 3.23), suggesting that this control occurs both in stable as well as angiogenic endothelium. However confocal analysis of β -catenin expression in the retina or fibrin sprouting bead model, for example, would provide a more informative analysis of β -catenin regulation during angiogenesis. Whilst studying ERG in a monoculture of HUVEC allows easy manipulation to identify mechanisms of ERG activity, EC are affected by signals produced by the surrounding cells and environment.

Whilst only the vascular defects in the retina and yolk sacs of *Erg*-deficient mice have been documented (Birdsey, Shah et al., 2015), vascular abnormalities may also occur in other tissues and during physiological processes in which angiogenesis is initiated, such as during pregnancy. Roles for *Fzd4* and *Norrin* have been described in reproductive angiogenesis. Female *Fzd4* null mice are infertile as a result of the failure of embryos to implant (Hsieh et al., 2005), caused by defective vasculature of the corpus luteum and consequent tissue degeneration (Hsieh et al., 2005). In mice deficient for *Norrin*, foetus implantation does occur but bleeding or haemorrhage is observed at the implantation site. Furthermore, the chorioallantois fails to develop, which deprives the embryo of placental support (Luhmann et al., 2005). It would

therefore be interesting to see whether Erg-deficient female mice also display defects in reproductive angiogenesis.

As mentioned previously, endothelial β -catenin signalling regulates blood brain barrier maintenance through concomitant activation of the tight junction molecule Claudin-3 (Liebner et al., 2008). I observed a decrease in Claudin-3 expression and increased water content in brains of Erg^{IEC-KO} mice, suggesting impairment of the BBB (Figure 3.8). This suggests that ERG may be regulating blood brain barrier integrity through both the Wnt signalling pathway and its regulation of multiple junction molecules. To study this hypothesis more comprehensively, one would have to perform vessel perfusion experiments as well as electron microscopy to analyse the ultrastructure of Erg null blood vessels in the brain. Electron microscopy would also allow us to study the integrity and formation of adherens and tight junctions in the mutants, in more detail compared to immunofluorescence studies.

Defective control of Wnt/ β -catenin signalling is commonly observed in many types of cancer. Mutations in β -catenin or genes that control β -catenin stability cause constitutive activation of the Wnt pathway and are associated with aberrant cell proliferation and subsequent cancer progression (reviewed in (Giles et al., 2003; Kypta and Waxman, 2012)). Importantly, Wnt signalling has been shown to be a critical mediator of ERG-induced oncogenesis in several types of cancer. In support of our findings, a recent paper showed that ERG controls Wnt signalling through multiple mechanisms, in prostate cancer cells bearing the TMPRSS-ERG fusion (Wu et al., 2013). I have shown that ERG binds to and transactivates the Fzd4 promoter in EC. A link between Fzd4 and ERG as an oncogene has been observed in prostate cancers, where Fzd4 was co-overexpressed with ERG in prostate cancers and was modulated by ERG manipulation *in vitro* (Gupta et al., 2010).

My results show that in endothelial cells ERG controls β -catenin stability both in confluent, quiescent cells and in sub-confluent cells, where VE-cadherin is not engaged at the junctions. This mechanism could provide the balance between stability and proliferation required in a nascent blood vessel (Figure 3.29). In contrast with the role of ERG in promoting vessel stability through β -catenin, abnormal ERG expression is associated with increased proliferation in several cancers and increasing evidence implicates Wnt signalling as a critical downstream pathway that is important for ERG-

mediated tumorigenesis (Tomlins et al., 2005; Wu et al., 2013, Gupta et al., 2010). The reasons for this cell-specific difference are unknown, and may be due to disrupted cell-cell signalling in malignant cells, thus driving cells to a proliferative fate as a consequence of the dysregulated balance between growth and survival signals. Therefore, strategies to control ERG activity and Wnt signalling in malignant cells through cell-cell adhesion signals may be worth investigating.

Using ChIP analysis, I have shown that ERG binds to the Fzd4 promoter (Figure 3.19); however, this analysis does not allow high enough resolution to identify the specific consensus site/s involved. Sequence comparison identified 3 conserved ERG consensus sequences within the ERG binding region (Figure 3.18 B). I should therefore identify which sites are responsible for ERG activation of Fzd4 by electrophoretic mobility shift assay (EMSA) using nuclear lysate from HUVEC and testing whether ERG is capable of binding to an oligonucleotide containing the ERG binding site of interest. Detailed analysis of the ERG binding sites within the Fzd4 promoter by generating mutants using the luciferase reporter system would also identify the binding sites implicated in this regulation.

Interestingly, Descamps et al. show that Fzd4 represses canonical Wnt signalling in mouse embryonic fibroblasts (Descamps et al., 2012); whereas I have shown that overexpressing Fzd4 in EC (Figure 3.22) activated canonical Wnt signalling, pointing to a cell-specific effect of Fzd4. Whether ERG controls the non-canonical Wnt pathway in EC, however, will require more investigation, as the non-canonical Wnt pathway activates the small GTPases RhoA and Rac and, similar to ERG, modulates cytoskeletal rearrangements. Descamps et al. do however report that loss of Fzd4 expression decreases EC proliferation, migration, and EC tube formation, in line with the roles of ERG in the endothelium (Descamps et al., 2012).

Interestingly, our data shows that ERG inhibition results in an approximate 50 % reduction in Fzd4 protein, but still fully abrogates Wnt3a-induced luciferase reporter activity. This suggests that ERG's control of other nodes of the Wnt pathway may be important. Transcriptome profiling of control versus ERG-deficient HUVEC highlighted additional targets of this pathway (Birdsey et al., 2012). Validation by qPCR confirmed ERG repression of the Wnt inhibitor DACT1 (Gao et al., 2008; Zhang et al., 2006) and activation of TCF4, a Wnt signalling effector transcription factor

(Wang et al., 2002), which could play a role in the phenotypes reported in this study. Moreover, in prostate cancer cell lines, Wu et al. identified LEF1 as a direct target of ERG (Wu et al., 2013)- whether ERG regulates LEF1 expression in the endothelium and whether LEF1 acts as a critical mediator of ERG-induced Wnt signalling remains to be elucidated.

Furthermore, data in this chapter suggests that ERG and Wnt/ β -catenin signalling pathways form a bidirectional positive-feedback loop, which may be key in maintaining cellular β -catenin levels and activity and driving cellular function. I have shown that ERG both promotes and is regulated by Wnt/ β -catenin signalling. I showed that Wnt3a stimulation of HUVEC induced ERG expression (Figure 3.28 B). Interestingly, transcriptome profiling of the genes down-regulated following β -catenin inhibition in human pulmonary artery endothelial cells (Alastalo et al., 2011), identified ERG as a putative β -catenin target. Co-immunoprecipitation studies from nuclear extracts also showed that ERG forms a complex with β -catenin (Figure 3.28 A). Increasing evidence indicates a role for β -catenin in regulating gene transcription through binding partners other than TCF/LEF. Taddei et al. reported that β -catenin formed a repressor complex with TCF and FoxO1 on the claudin-5 promoter and increased FOXO1 repressor activity (Taddei et al., 2008). Besides binding and regulating FOXO, Kaidi et al. show that during hypoxia β -catenin interacts with HIF1 α (Kaidi et al., 2007). β -Catenin and c-jun also interact, albeit indirectly via TCF, creating a β -catenin-mediated positive feedback loop increasing the expression of c-jun (Gan et al., 2008). Whether ERG inhibits TCF-dependent transcription by binding to β -catenin, i.e. whether ERG and TCF compete for the same pool of active β -catenin, or whether ERG can activate TCF and *vice versa* TCF can activate ERG, and therefore act through β -catenin as interdependent positive regulators remains to be investigated, using ChIP studies and analysis of ERG binding to gene loci in response to β -catenin inhibition or overexpression.

Chapter Four

ERG controls multiple pathways required for vessel growth and stability: Notch pathway

4. ERG controls multiple pathways required for vessel growth and stability:

Notch pathway

4.1 Introduction

4.1.1 Notch signalling

The Notch signalling pathway is an evolutionarily conserved cellular signalling system that was originally identified in *Drosophila*, where the first mutant allele gave rise to a wing with a notched defect. Since then, studies of protein members of the Notch pathway in various *in vivo* models have unravelled the various roles of Notch signalling in cell fate specification, tissue patterning, and morphogenesis in many tissues during embryonic and postnatal development through effects on cell differentiation, proliferation, survival, and apoptosis (reviewed in Bray, 2006; Gridley, 1997). In mammals, there are five ligands (Delta-like ligand (Dll)- 1, Dll3, Dll4, Jagged (Jag)-1, and Jag2) (Figure 4.1), which are classified as DSL (Delta, Serrate, LAG-2) ligands and 4 Notch receptors (Notch 1 to 4). Notch ligands and receptors are type 1 transmembrane proteins, and therefore, activation requires cell–cell contact. Generally, interaction between Notch ligands and receptors occurs between homotypic or heterotypic cells, causing trans-signalling events. However, *cis* interactions can also occur. Specificity between the ligands and receptors has not been reported, although recent experimental evidence suggests that not all receptor/ligand conformations lead to downstream signalling and some ligands may actually act as negative modulators of Notch signalling. Nonetheless, the essential contribution of the Notch pathway to vascular morphogenesis has been revealed only recently.

Notch activation requires interaction of a Notch ligand and Notch receptor, which triggers a series of proteolytic events mediated initially by enzymes of the ADAM family (Figure 4.2). The final cleavage within the Notch receptor transmembrane domain catalysed by γ -secretase releases the Notch intracellular domain (NICD) from the cell membrane. The NICD is then able to translocate into the nucleus and directly interact with the transcription factor RBPJ (also known as CSL) (reviewed in Phng and Gerhardt, 2009). This interaction converts RBPJ from a transcriptional repressor to an activator as a result of displacing co-repressors and recruiting co-activators, such as Mastermind-like 1 and p300. This results in transcription of downstream Notch target genes such as the Hairy/Enhancer of Split (Hes), Hes-related

proteins (Hey), and Notch-regulated ankyrin repeat protein (Nrarp) proteins (Figure 4.2). Proteins encoded by the Hes and Hey genes are, in turn, transcriptional repressors of both their own expression and further downstream genes. In this thesis, I will discuss Notch signalling in the context of endothelial cell biology and its role in the vasculature.

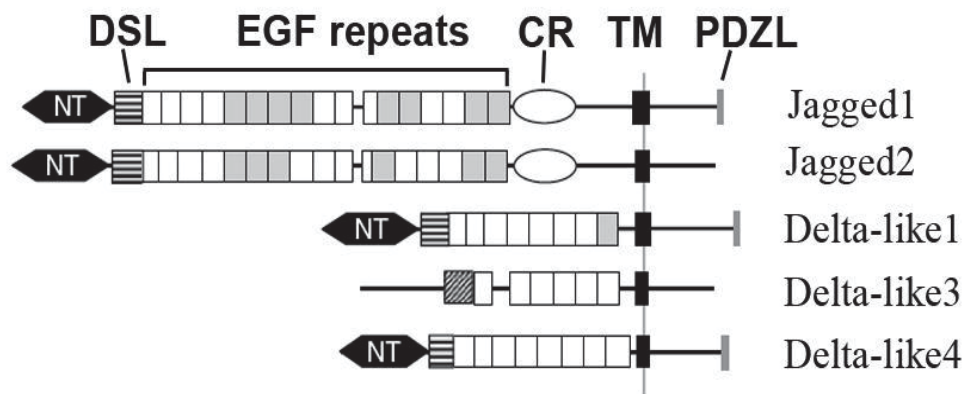


Figure 4.1 Protein structure of the vertebrate DSL family of ligands.

The canonical DSL ligands are type 1 cell-surface proteins that have multiple tandem epidermal growth factor (EGF) repeats in their extracellular domains. The DSL domain, the flanking N-terminal (NT) and the first two EGF repeats are required for DSL ligands to bind Notch (Parks et al., 2006; Shimizu et al., 1999). DSL ligands also contain a transmembrane domain (TM). As well as having almost twice the number of EGF repeats as Delta-like ligands, Jagged-1 and Jagged-2 have an additional cysteine-rich region (CR) (image reproduced from D'Souza et al., 2008, with permission of the rights holder, Nature Publishing Group).

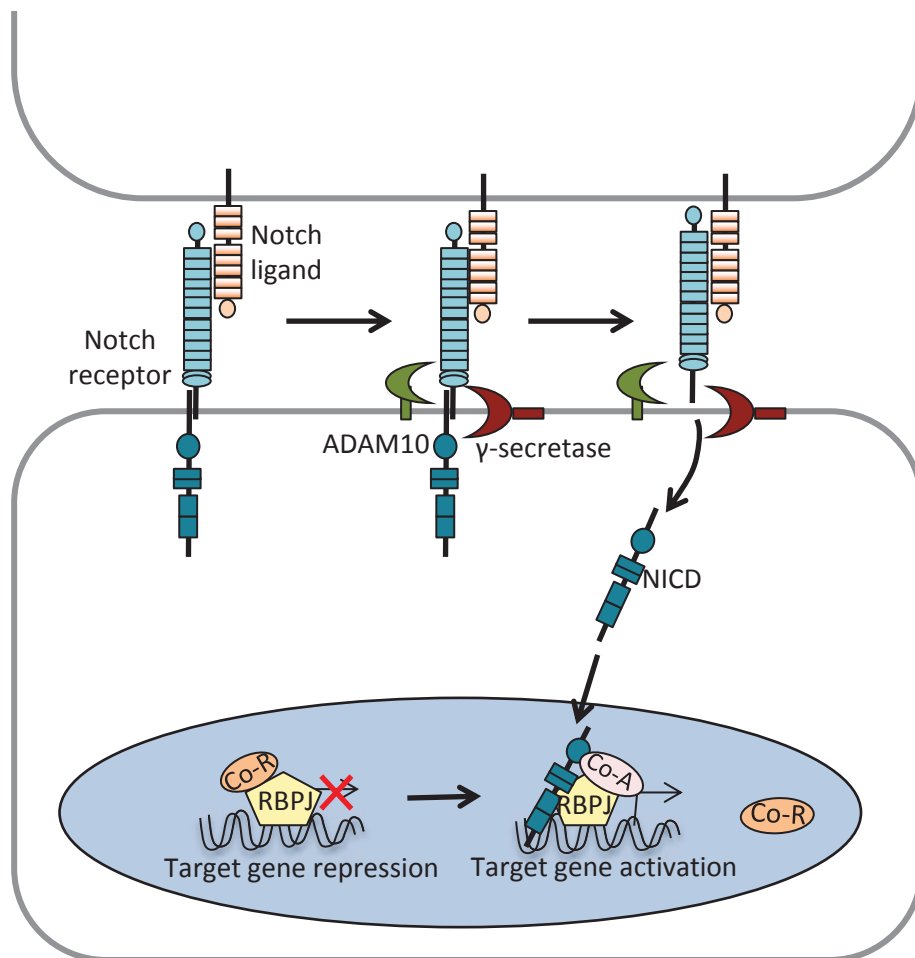


Figure 4.2 Overview of Notch signal transduction. Notch ligands interact with Notch family receptors on an adjacent cell. The receptor-ligand interaction induces two proteolytic cleavages mediated by an ADAM metalloprotease and the γ -secretase complex respectively. Cleavage releases the Notch intracellular domain (NICD) from the cell membrane. NICD translocates to the nucleus, where it associates with the RBPJ transcription factor, displacing a co-repressor (Co-R) complex from the RBPJ protein. Components of an activation complex (Co-A), are recruited to the NICD-RBPJ complex, leading to the transcriptional activation of Notch target genes such as members of the Hes and Hey families and Nrarp (image reproduced from Bray et al., 2006, with permission of the rights holder, Nature Publishing Group).

4.1.2 Notch signalling in the vasculature

Although the Notch signalling pathway is widely known for its role in a myriad of processes during development, its essential role in vascular morphogenesis has been revealed only recently. These roles in the vasculature include the control of arteriovenous specification and differentiation, and regulation of blood vessel sprouting and branching during physiological and pathological angiogenesis (reviewed in Phng and Gerhardt, 2009; Roca and Adams, 2007). It has become increasingly clear that Notch signalling plays a key role in coordinating multiple aspects of endothelial behaviour during vessel patterning and thus in shaping the formation and remodelling of the vascular network. Furthermore, the importance of the pathway is evident from the discovery that certain inherited vascular diseases, such as the degenerative vascular disorder Cerebral Autosomal Dominant Arteriopathy with Subcortical Infarcts and Leukoencephalopathy (CADASIL) and Alagille syndrome are caused by defects in Notch signalling (Louvi et al., 2006).

Deletion of various genes involved in Notch signal transduction, such as receptors, ligands, transcription factors, downstream targets, and molecules that mediate Notch processing, has resulted in embryonic lethality in mice associated with vascular remodelling defects (reviewed in Phng and Gerhardt, 2009). In vertebrates, the receptors Notch1 and Notch4, and ligands Jagged1, Jagged2, Dll1, and Dll4 are expressed in the endothelium (Hofmann and Iruela-Arispe, 2007; Claxton and Fruttiger, 2004; Villa et al., 2001). Targeted Notch 1 and Notch 4 mutations result in vascular defects but in terms of the Notch ligands, only loss of Dll4 or Jagged1 results in vascular defects, suggesting that the other three ligands may not be as crucial in vessel development. Notably, analysis of the phenotypes exhibited by Jag1 (Xue et al., 1999) and Dll4 (Duarte et al., 2004; Gale et al., 2004; Krebs et al., 2004) knockout mice, suggested that these two ligands are not functionally redundant. Recent work has shown that different Notch ligands have distinct roles in angiogenesis; inhibition of angiogenesis by Dll4 was competitively opposed by the pro-angiogenic Jag1 ligand (Benedito et al., 2009). Dynamic and sometimes even oscillating expression of Notch pathway molecules leads to complex spatiotemporal patterns of Notch function during tissue morphogenesis (Claxton and Fruttiger, 2004). The dynamic and partially overlapping expression of multiple ligands (Dll1, Dll4, Jagged1, and Jagged2) and

receptors (Notch1, Notch3, and Notch4) in vascular cells suggest key roles for the Notch pathway in the growth and differentiation of blood vessels.

Dll4 expression is largely restricted to the vascular endothelium, in particular to arteries and capillaries. Genetic deletion of even a single Dll4 allele results in early embryonic death associated with severe vascular abnormalities (Gale et al., 2004). Haploid insufficiency within the vascular system has previously been reported only for VEGF (Carmeliet et al., 1996), suggesting that an appropriate dosage of both of these genes is critical for correct vascular development.

4.1.2.1 Regulation of arteriovenous identity by Notch signalling

Arterial and venous blood vessels are functionally, anatomically and molecularly different. The establishment and maintenance of these distinct endothelial cell fates is critical to the proper function of circulatory networks in the embryo and the mature adult (Marchuk, 1998). It is now increasingly clear that arteriovenous specification is genetically determined and Dll4/Notch signalling has been implicated in its control (Kim et al., 2008; Carlson et al., 2005; Duarte et al., 2004; Lawson et al., 2001).

The spatial expression of specific Notch ligands and receptors differs among blood vessels. Expression of Dll4 and Notch 4, for example, is largely restricted to arterial endothelium in the mouse and zebrafish (Siekman and Lawson, 2007; Leslie et al., 2007; Claxton and Fruttiger, 2004). Dll4 is the first Notch ligand gene expressed in the arterial endothelium, and its expression is induced by VEGF (Lawson et al., 2001). Importantly, Wythe et al. showed a role for ERG in mediating the VEGF-dependent arterial expression of Dll4 during early vascular development (Wythe et al., 2013).

Targeted deletion of Notch ligands, receptors, transcription factors, coactivators and downstream genes in the mouse and zebrafish (Kim et al., 2008; Siekman and Lawson, 2007; Carlson et al., 2005; Duarte et al., 2004; Fischer et al., 2004; Gale et al., 2004; Krebs et al., 2000, 2004; Lawson et al., 2001; reviewed in Phng and Gerhardt, 2009) result in the deregulation of arterial and venous specification of endothelial cells as well as in the deformation of arteries and veins. The decrease in Notch signalling is accompanied by ectopic expression of venous markers such as Ephrin B4 in the zebrafish dorsal aorta (Lawson et al., 2001). Ephrin B2 on the other hand, which marks

arterial identity, is a direct transcriptional target of Notch (Grego-Bessa et al., 2007). Together, the genetic studies in mouse and zebrafish have revealed the requirement of Notch signalling in arterial-venous differentiation.

4.1.2.2 Role of Notch signalling in vessel sprouting

Dll4/Notch signalling is an essential determinant of the specification of endothelial cells into tip and stalk cells and this has been demonstrated in models of the mouse retina, zebrafish intersegmental vessels, tumour angiogenesis, and 3D endothelial sprouting assays (Siekman and Lawson, 2007; Hellstrom et al., 2007; Lobov et al., 2007; Suchting et al., 2007; Leslie et al., 2007; Sainson et al., 2005). VEGFA-induced Dll4 expression in tip cells activates Notch signalling in the neighbouring stalk cell, which is prevented from exhibiting tip cell behaviour. Expression analyses helped first to identify a relationship between Notch signalling and endothelial tip cells, where analysis of developing retinas demonstrated that Dll4 is most prominently expressed in tip cells (Hellstrom et al., 2007; Claxton and Fruttiger, 2004). Whereas the strongest Notch signalling activity and Notch1 receptor expression was regularly observed in the stalk cells, that are in close proximity to the tip cell (Hellstrom et al., 2007; Hofmann and Iruela-Arispe, 2007), suggesting that Dll4 expression in the tip cell signals to Notch in the adjacent stalk cells. Thus many recent studies have demonstrated that the Dll4-Notch signalling axis does indeed coordinate fate specification at angiogenic sprouts.

Genetic and pharmacological inactivation of Dll4-Notch signalling dramatically augments sprouting, branching, and hyperfusion of the capillary network as a result of excessive tip cell formation (Tammela et al., 2008; Hellstrom et al., 2007; Suchting et al., 2007). Nonetheless, the vascular structures formed following Notch inactivation are often not fully lumenized, resulting in non-productive vessels that are inefficient in delivering oxygen to target tissues (Suchting et al., 2007). In zebrafish models, γ -secretase treatment, Dll4 antisense morpholino treatment, or genetic deletion of Dll4 also causes excessive vessel sprouting and branching during the development of intersegmental vessels (Leslie et al., 2007; Siekman and Lawson, 2007). Conversely, ectopic activation of Notch signalling, by injection of the Jag1 peptide in the mouse retina, leads to reduced tip cell formation and decreased vessel density (Hellstrom et al., 2007), and in zebrafish, endothelial cells carrying a constitutive active NICD are

excluded from the tip cell position (Siekman and Lawson, 2007). However, Notch signalling in tip cells is inhibited by stalk cell expression of Jagged1 (Figure 4.3) (Benedito et al., 2009). In particular, Jagged1 blocks Dll4-Notch interaction on tip cells once the extracellular domain of Notch receptor is glycosylated by Fringe family glycosyltransferases. Previous work shows that pro-quiescent Dll4 and pro-angiogenic Jag1 have contrasting functional roles and distinct spatial expression patterns (Figure 4.3 A; Benedito et al., 2009). Combined, the findings indicate that the interplay between both Dll4 and Jagged1 is crucial for tip-stalk cell specification and that both permissive and suppressive signals within the nascent sprout are required for the formation of an effective vascular network.

Microarray analysis comparing ERG-positive and ERG-deficient HUVEC clearly shows that inhibition of ERG expression in EC affects a number of genes involved in the Notch signalling pathway. Therefore, I hypothesised that ERG controls Notch signalling in EC and this chapter investigates the mechanisms involved.

The aims of the work described in this chapter are to:

- Confirm whether ERG controls Notch signalling in primary EC
- Investigate whether ERG regulates the expression of Notch ligands in the endothelium
- Investigate whether ERG binds directly to promoters/enhancers of genes involved in the Notch signalling pathway
- Study whether a ERG-Notch feedback loop exists in the endothelium

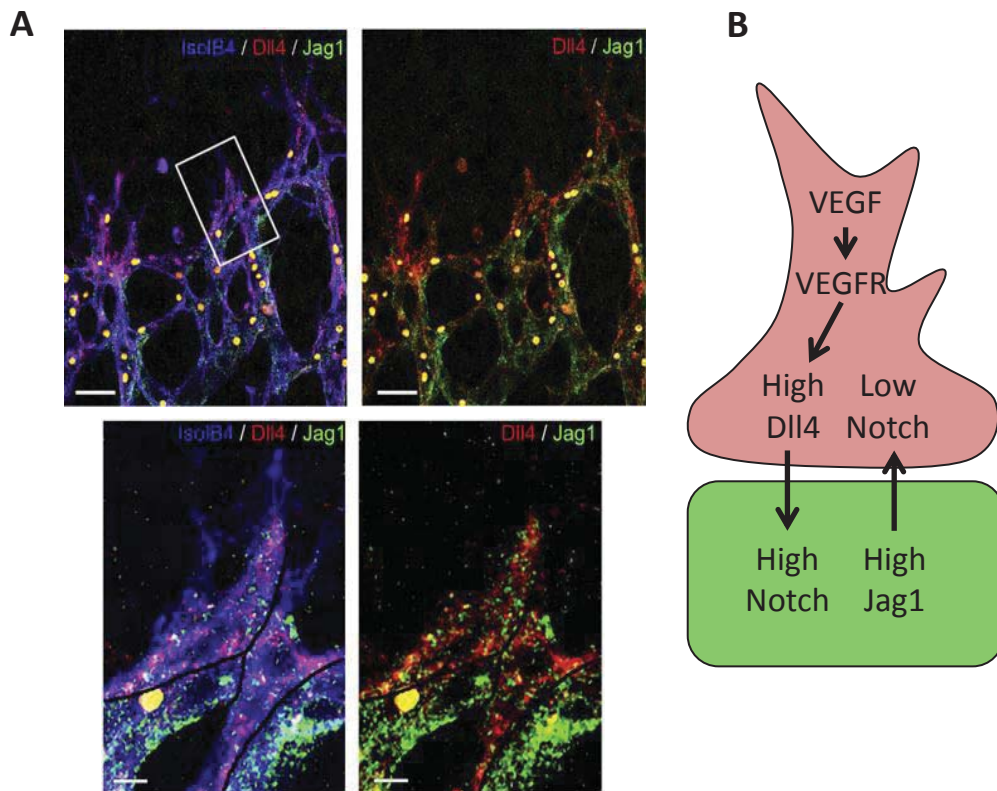


Figure 4.3 Regulation of vessel sprouting by Dll4 and Jagged-1. (A) Top: Triple whole-mount immunofluorescence for Dll4 (red), Jagged-1 (Jag1; green), and isolectin B4 (IsolB4; blue) at the angiogenic front of P6 retinas. Bottom: Higher magnification of the inset in top panel. While Dll4 expression is high in tip cells and also visible in adjacent stalk ECs at the edge of the growing plexus, Jagged-1 expression is low in tips but abundant in adjacent stalk cells and capillaries. Yellow dots are autofluorescent blood cells (image reproduced from Benedito et al., 2009, with permission of the rights holder, Elsevier). (B) VEGF signalling induces Dll4 expression in tip cells, and Dll4, in turn, activates Notch signalling in stalk cells, which reduces stalk-cell sensitivity to VEGF stimulation and, consequently suppresses the tip-cell phenotype. Conversely, Jagged-1 antagonizes Dll4-mediated Notch activation in stalk cells to increase tip cell numbers and enhances vessel sprouting.

4.2 Results

4.2.1 ERG controls Notch signalling in EC

To investigate ERG regulation of endothelial Notch signalling, two approaches were used to examine Notch activity after control or ERG siRNA treatment of HUVEC: i) assessment of Notch receptor cleavage by immunoblotting whole cell lysates using an antibody against Notch1 intracellular domain (NICD1) and ii), transcriptional regulation of downstream endothelial Notch target genes Hey1, Hey2 and Nrarp by qPCR.

Inhibition of ERG expression resulted in significant downregulation of ERG mRNA and protein levels, comparable to levels observed in Figures 3.3 B and 3.4 A (data not shown). ERG inhibition caused a marked decrease in endothelial NICD expression compared to control (Figure 4.4 A) and resulted in a decrease of ~30% in Hey1, Hey2 and Nrarp Notch target gene expression when compared to control HUVEC (Figure 4.4 B). Moreover, Notch activation has been associated with downregulation of p21CIP1 (Nosedá et al., 2004); in line with this, inhibition of ERG results in a decrease in Notch activation and therefore increased levels of p21CIP1 (Figure 4.4 B).

To determine whether there was down-regulation of Notch-induced transcription in ERG-depleted endothelial cells, Notch reporter gene TP1-luciferase activity was measured in HUVEC treated with control and ERG siRNA. Basal RBPJ activity, detected by the TP1-luciferase reporter, was decreased to 50% in ERG-deficient EC (Figure 4.4 C). Dll4 stimulation of control HUVEC increased TP1 luciferase activity compared to the BSA control, however the significant difference in activity between control and ERG-deficient EC was still observed in HUVEC cultured on plates coated with recombinant Dll4 to stimulate Notch signalling (Figure 4.4 C). Together with the NICD immunoblotting data, the Notch target gene expression and reporter activity show that ERG is required for Notch activity in endothelial cells.

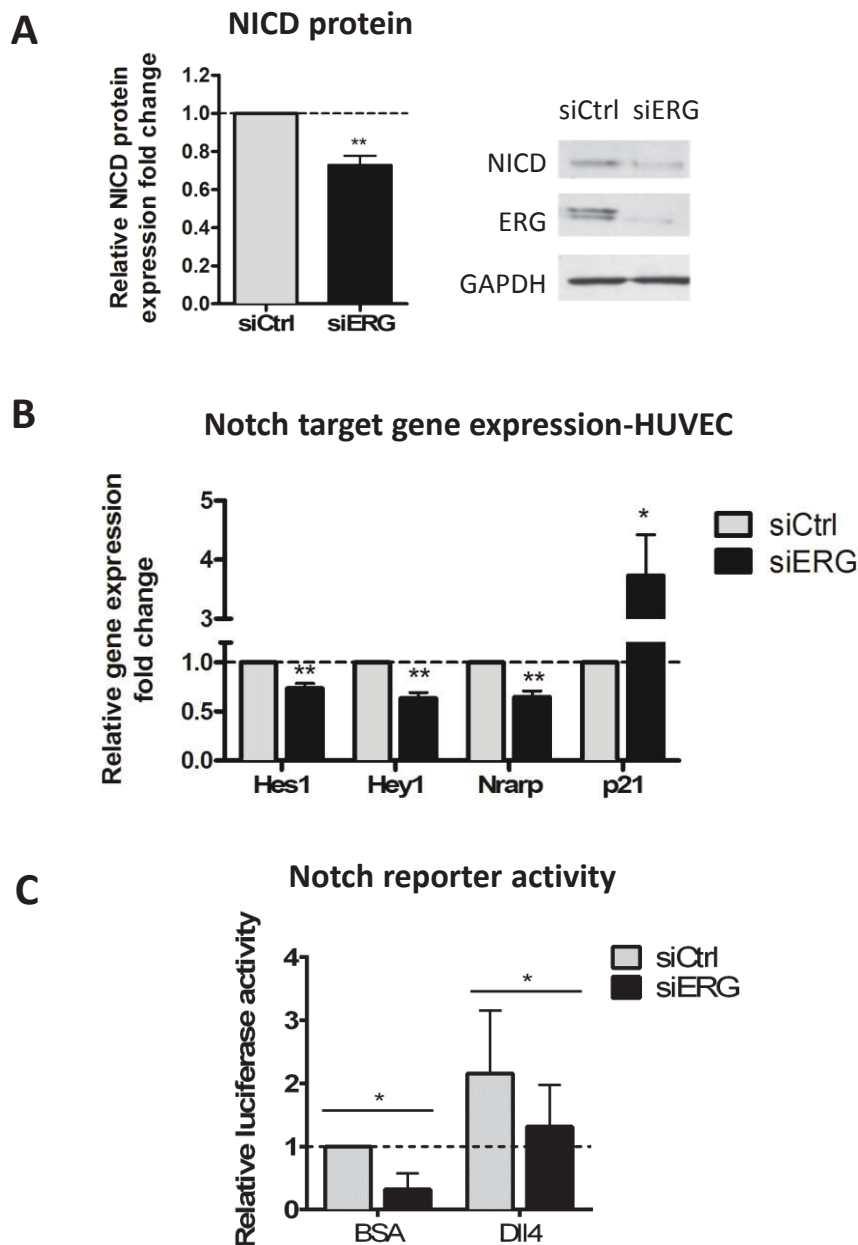


Figure 4.4 ERG regulates endothelial Notch signalling. (A) Western blot analysis and fluorescence quantification of Notch intracellular domain (NICD) expression in extracts of cells treated with siCtrl or siERG for 48 h. (B) qPCR analysis of expression of Notch activated target genes Hes1, Hey1, Nrarp and Notch repressed target gene, p21, in HUVEC treated with siCtrl or siERG for 48 h. (C) RBPJ transcriptional activity was determined by co-transfecting control and ERG-deficient cells plated on BSA or Dll4, with TP-1 Notch reporter construct and pGL4 renilla control vector. Results are presented as dual luciferase ratio of firefly luciferase normalised to pGL4 Renilla luciferase. All graphical data are mean \pm SEM; n=4; asterisks indicate values significantly different from the control (Student t test where * p <0.05, ** p <0.01).

4.2.2 ERG represses expression of Jagged-1 mRNA and protein *in vitro* and *in vivo*

The Notch ligand Jagged1 (Jag1) has been shown to antagonize Notch signalling in mouse endothelial cells. Benedito et al. observed an upregulation of Notch target gene expression in the Jag1^{i#}EC endothelium (Benedito et al., 2009). Jag1 was a candidate repressed target to emerge from the ERG microarray analysis (Birdsey et al., 2012). The ERG microarray analysis indicated a 2.5 fold increase in Jag1 mRNA levels following ERG inhibition at 48 h. To validate the microarray data, Jag1 mRNA and protein levels were analysed in control and ERG-deficient HUVEC. Inhibition of ERG expression resulted in a significant 3-fold increase in Jag1 mRNA levels following 24 and 48 h ERG inhibition (Figure 4.5 A). Jag1 total protein levels were also significantly increased following ERG inhibition (Figure 4.5 B), indicating that ERG represses endothelial Jag1 expression.

To confirm this *in vivo*, gene expression of Jag1 was analysed by qPCR in primary lung EC isolated from *Erg*^{fl/fl} and *Erg*^{cEC-het} mice. As shown in Figure 4.5 C, loss of Erg in endothelial cells resulted in a significant increase in Jag1 expression when compared to *Erg*^{fl/fl} endothelial cells, in line with the regulation observed in ERG-deficient HUVEC.

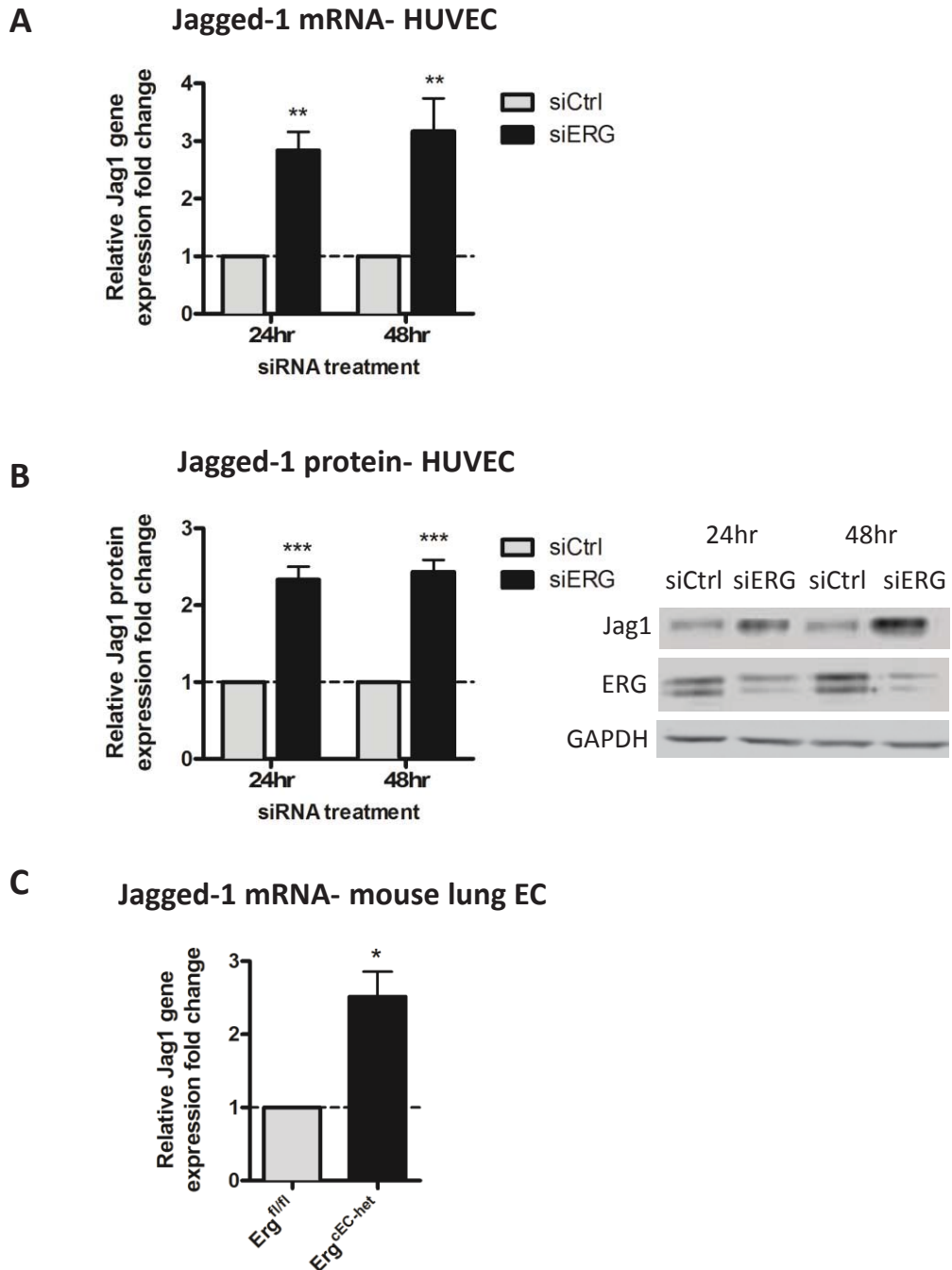


Figure 4.5 ERG represses Jagged-1 expression. (A) mRNA levels of Jagged-1 in HUVEC treated with siCtrl or siERG for 24 h and 48 h. Results are normalised to GAPDH and expressed as fold change relative to siCtrl (n=6). (B) Left panel: Densitometry analysis of Jagged-1 total protein levels in siCtrl and siERG-treated cells. Right panel: Representative blot of Jagged-1 protein expression in siCtrl and siERG-treated HUVEC for 24 and 48 h. Results are normalised to GAPDH and expressed as fold change relative to siCtrl (n=3). (C) mRNA expression of Jagged-1 in primary *Erg^{cEC-het}* mouse lung EC compared to control. Results are normalised to HPRT and expressed as fold change relative to *Erg^{fl/fl}* littermate controls (n=4). All graphical data are mean \pm SEM; asterisks indicate values significantly different from the control (Student t test where * p < 0.05, ** p < 0.01).

4.2.3 ERG binds to the Jagged-1 promoter

ERG-mediated repression of Jagged-1 could occur through either ERG binding directly to the Jag1 promoter, or alternatively through ERG regulating another transcriptional activator or repressor of Jag1. To investigate whether ERG represses Jag1 by binding to the promoter, we carried out ChIP analysis. ERG ChIP-seq analysis in HUVEC (Yang and Randi, unpublished data) showed two regions within the Jag1 promoter were bound by ERG (Figure 4.6 A). These ERG-enriched regions correlated with enrichment of H3K4me3, H3K27Ac and low RNA polymerase II occupancy. ChIP-qPCR was carried out using primer pairs designed to cover regions (R) 1 and 2 as indicated (Figure 4.6 A). Sheared chromatin from resting HUVEC was immunoprecipitated using an anti-ERG or IgG control antibody, and enriched chromatin was detected by quantitative PCR. Results are expressed as fold change compared to IgG control antibody, normalised for total input levels. Immunoprecipitation with an anti-ERG antibody resulted in greater enrichment of chromatin containing the Jag1 proximal promoter regions compared to immunoprecipitation using an isotype control antibody (Figure 4.6 B). There was no difference in enrichment for a control region of Jag1, using either anti-ERG or IgG control antibodies, indicating no non-specific enrichment.

4.2.4 ERG represses Jagged-1 promoter activity

To determine whether ERG represses constitutive Jag1 transcription in EC, I used a Jag1 promoter luciferase reporter. HUVEC were treated with control or ERG siRNA and 24 h later cells transfected with the Jag1 promoter-luciferase construct and luciferase activity was measured 24 h later. Inhibition of ERG expression significantly increased Jag1 promoter activity in HUVEC compared with control (Figure 4.7). Therefore taken together, this data suggests that ERG represses Jag1 promoter activation.

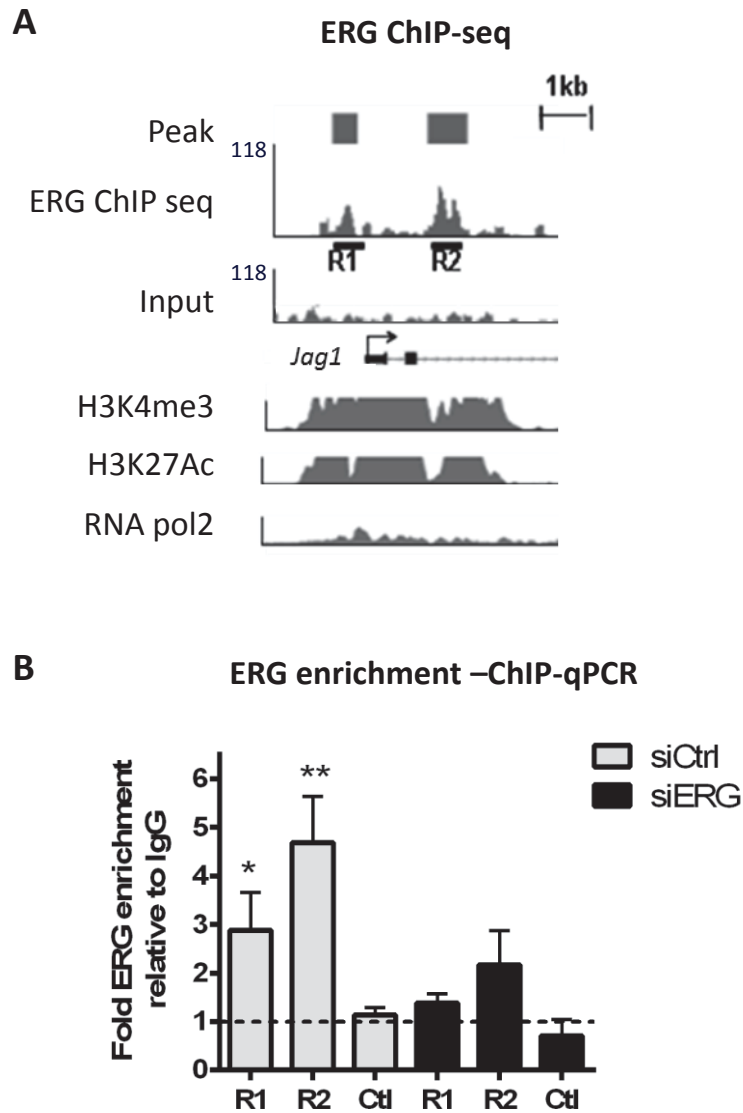


Figure 4.6 ERG binds to the Jagged-1 promoter in EC. (A) ERG ChIP-seq analysis in HUVEC (Yang and Randi, unpublished data) shows two significant ERG binding peaks located within the Jagged-1 promoter; chromatin input profile shows specificity of ERG peaks. ENCODE ChIPseq data peaks for H3K4me3, H3K27Ac and RNAPol2 indicate open chromatin and active transcription. Location of qPCR amplicons covering regions R1 and R2 are indicated. (B) ChIP was carried out on sheared chromatin from HUVEC treated with Control or ERG siRNA (20 nM) using an anti-ERG or control IgG antibody. Immunoprecipitated DNA was analysed by qPCR with primers covering Jagged 1 regions 1 and 2, and a negative control 3'UTR region to exclude non-specific precipitated DNA. Results are expressed as fold change compared to IgG, normalised to input. All graphical data are mean \pm SEM; n=3; asterisks indicate values significantly different from the control (Student t test where * p < 0.05, ** p < 0.01).

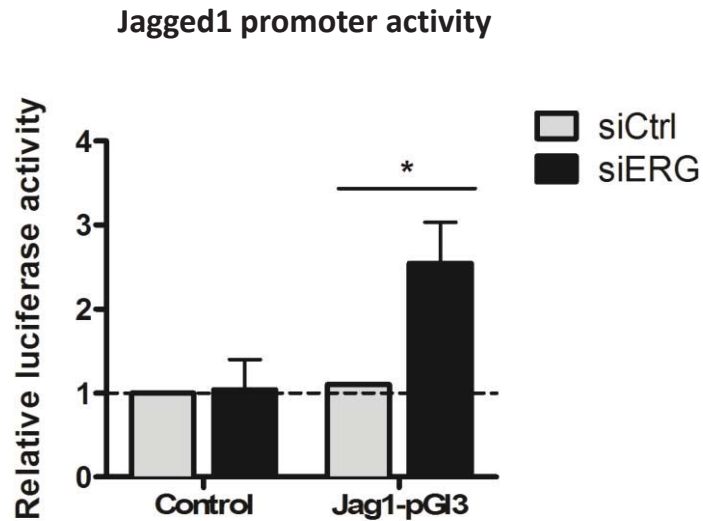


Figure 4.7 ERG represses Jagged-1 promoter activation in resting EC. HUVEC were transfected with either Control or ERG siRNA (20 nM) for 24 h. HUVEC were co-transfected with either Jag1-pGL3 or pGL3 control, and with the renilla control vector. Results are presented as dual luciferase ratio of firefly luciferase normalised to renilla luciferase relative to control plasmid activity in siCtrl HUVEC. All graphical data are mean \pm SEM; n=3; asterisks indicate values significantly different from the control (Student t test where * p <0.05, ** p <0.01).

4.2.5 Jagged-1 induction following ERG inhibition is repressed by NF- κ B inhibitor

TNF- α induces Jag1 expression in EC, through an NF- κ B-dependent mechanism (Sainson et al., 2008). Previous work in our group has shown that both TNF- α -dependent and basal NF- κ B activity are inhibited by ERG overexpression (Sperone et al., 2011), by a direct mechanism of interference where ERG inhibits NF- κ B p65 binding to pro-inflammatory gene promoters (Dryden et al., 2012). I therefore investigated whether NF- κ B is responsible for the upregulation of Jag1 expression after ERG inhibition. NF- κ B activity was inhibited using a BAY-117085 inhibitor compound, which blocks I κ B degradation (Pierce et al., 1997): the up-regulation of Jag1 mRNA levels following ERG inhibition was lost in cells treated with BAY-117085 compared with DMSO (Figure 4.8). The ability of BAY-117085 to repress the NF- κ B pathway was confirmed in TNF- α treated HUVEC (Figure 4.8). Thus, using an inhibitor of NF- κ B, I have demonstrated that the up-regulation of Jagged-1 after ERG inhibition is mediated by the activity of NF- κ B.

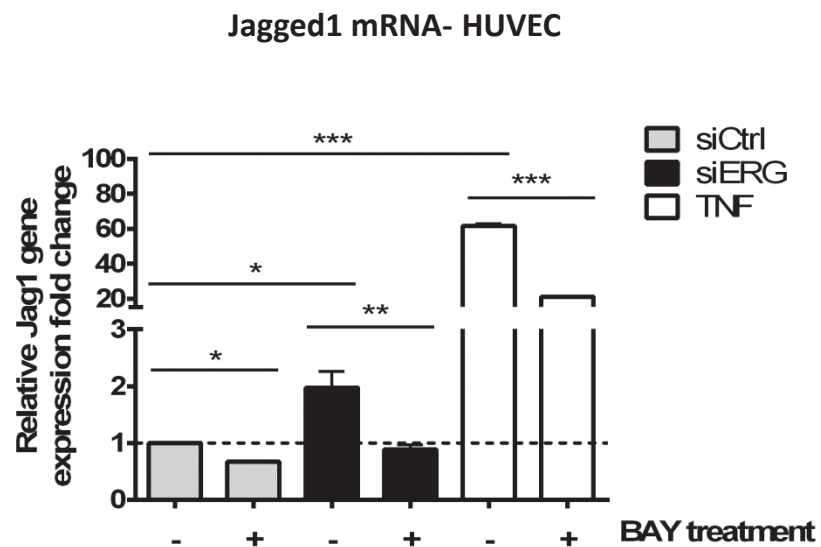


Figure 4.8 Upregulation of Jagged-1 after ERG deletion is repressed by the NF- κ B inhibitor BAY-117085. mRNA expression of Jagged-1 in siCtrl and siERG-treated HUVEC treated with BAY-117085 (5 μ M) or DMSO for 24 hours. For the control experiment HUVEC were pre-treated for 1 hour with BAY-117085 (5 μ M) or DMSO followed by 23 hours incubation with TNF- α (10 ng/ml). Results are normalised to GAPDH and expressed as fold change relative to siCtrl. Values are mean \pm SEM; n=4; asterisks indicate significantly different values (ANOVA, followed by Bonferonni's test, where * p <0.05, ** p <0.01, *** p <0.001).

4.2.6 ERG is required for Dll4 mRNA and protein expression in EC

A recent study has shown a role for ERG in regulating endogenous expression of the Notch ligand Dll4, during vascular development (Wythe et al., 2013). Previous work shows that pro-quiescent Dll4 and pro-angiogenic Jag1 have contrasting functional roles and distinct spatial expression patterns (Figure 4.3), suggesting tight regulation of these ligands is crucial for establishment of stable and mature blood vessels. In certain contexts, Jag1 competes with DLL4 for Notch to decrease DLL4–Notch-mediated signalling. Besides the role for the Dll4/Notch signal in vascular development and tip-stalk cell communication, the Dll4/Notch signal also appears to function in mature blood vessels with tight inter-endothelial cell-cell contacts. I tested whether inhibition of ERG in EC affects Dll4 expression. Indeed, ERG-depleted HUVEC expressed significantly decreased Dll4 mRNA expression (Figure 4.9 A) and protein expression (Figure 4.9 B) following both 24 and 48 h ERG inhibition, indicating that ERG is required for Dll4 expression in HUVEC. ERG regulates Dll4 expression in both human and mouse EC, as Dll4 mRNA expression levels were also decreased in primary mouse EC from *Erg*^{cEC-het} mice compared to *Erg*^{fl/fl} controls (Figure 4.9 C).

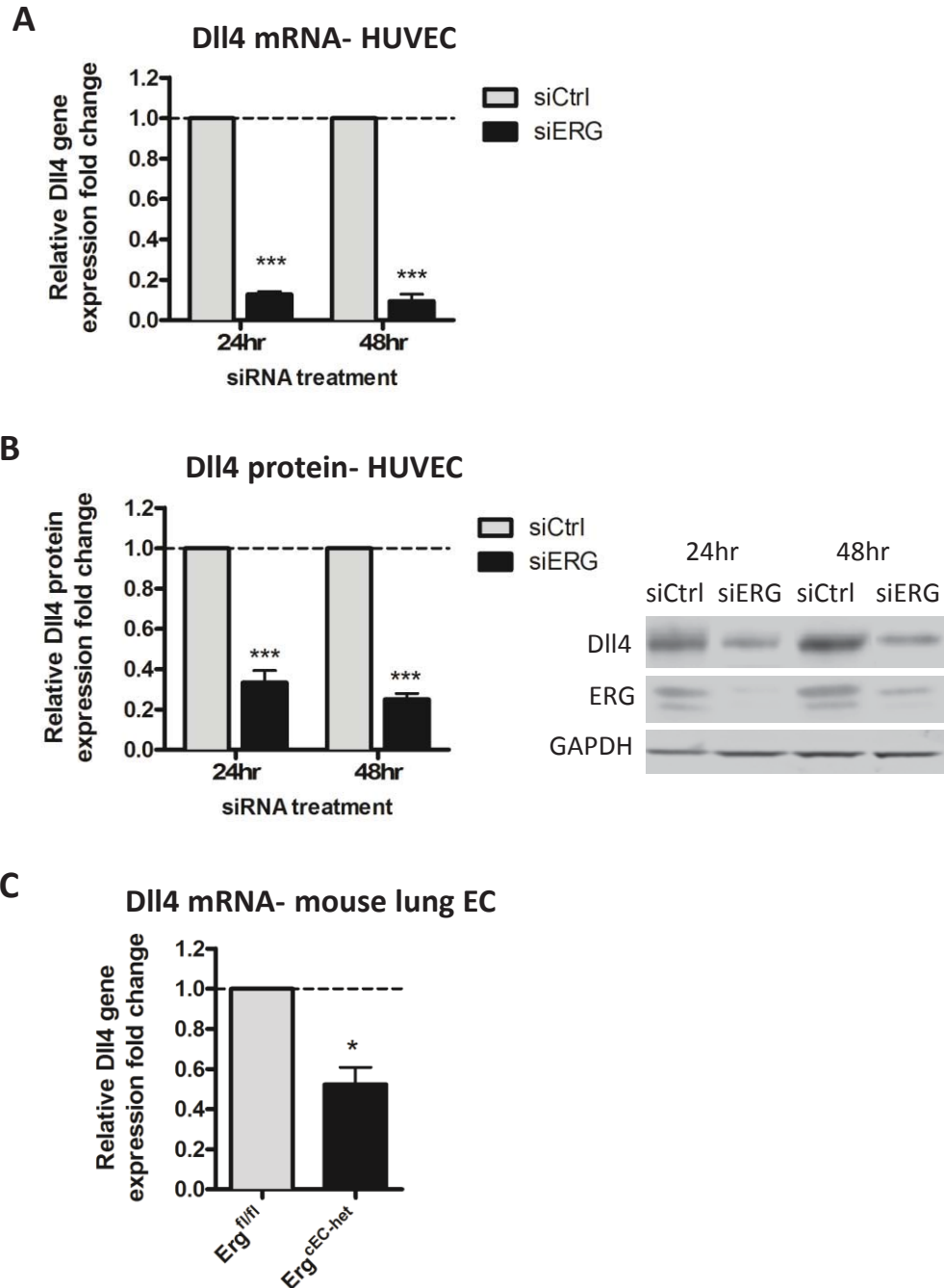


Figure 4.9 ERG is required for Dll4 expression in EC. (A) Dll4 mRNA expression in HUVEC treated with siCtrl or siERG for 24 h and 48 h. Results are normalised to GAPDH and expressed as fold change relative to siCtrl (n=6). (B) Left panel: Densitometry analysis of Dll4 total protein levels in siCtrl and siERG-treated cells. Right panel: Representative blot of Dll4 protein expression in siCtrl and siERG-treated HUVEC for 24 and 48 h. Results are normalised to GAPDH and expressed as fold change relative to siCtrl (n=3). (C) Dll4 mRNA expression in primary *Erg^{cEC-het}* mouse lung EC compared to control. Results are normalised to HPRT and expressed as fold change relative to *Erg^{fl/fl}* littermate controls (n=4). All graphical data are mean \pm SEM; asterisks indicate values significantly different from the control (Student t test where *** p < 0.001).

4.2.7 ERG binds to the Dll4 promoter

Analysis of the human Dll4 promoter identified ERG-specific consensus binding motif sites and ERG ChIP-seq analysis in HUVEC (Yang and Randi, unpublished data) showed an ERG-enriched region within 1kb downstream of the transcription start site. This ERG-bound region co-localised with ENCODE HUVEC ChIP-seq datasets for H3K4me3 and RNA polymerase II enrichment; both markers of active promoters (Figure 4.10 A). To validate whether ERG directly binds to the Dll4 promoter at the region indicated by the ERG ChIP-seq analysis, ChIP-qPCR was carried out using primers for the amplicon region 1 (R1; Figure 4.10 B). Immunoprecipitation with an anti-ERG antibody compared with an isotype control, showed 3.5-fold significant ERG enrichment at R1 compared to a downstream 3' UTR control region (Figure 4.10 B). ChIP-qPCR showed a decrease in the amount of ERG bound to the Dll4 promoter after ERG inhibition, indicating an ERG-specific interaction with the Dll4 promoter. Comparative genomic analysis of the Dll4 promoter revealed the presence of three highly conserved ERG DNA binding motifs in the region downstream of the Dll4 transcription start site (Figure 4.10 C).

4.2.8 ERG transactivates the Dll4 promoter

Next, to show that this interaction is functionally relevant, I tested whether ERG overexpression could enhance Dll4 promoter activity. First, in order to generate the Dll4 luciferase construct, I amplified PCR product derived from HUVEC genomic DNA amplified with primers against the Dll4 promoter. The amplified DNA was processed for agarose gel electrophoresis, and a band with the expected molecular weight was identified (Figure 4.11 A). The amplified Dll4 promoter PCR product was cloned into a pGl4 vector (Promega) and the pGl4-Dll4 vector was checked by sequencing.

HUVEC were co-transfected with the Dll4 promoter-luciferase construct and ERG cDNA in an expression vector and luciferase activity was measured 24 h later. ERG overexpression resulted in 3.5-fold transactivation of Dll4 promoter activity (Figure 4.11 B). Thus, our data indicate that ERG drives constitutive Dll4 expression in human EC.

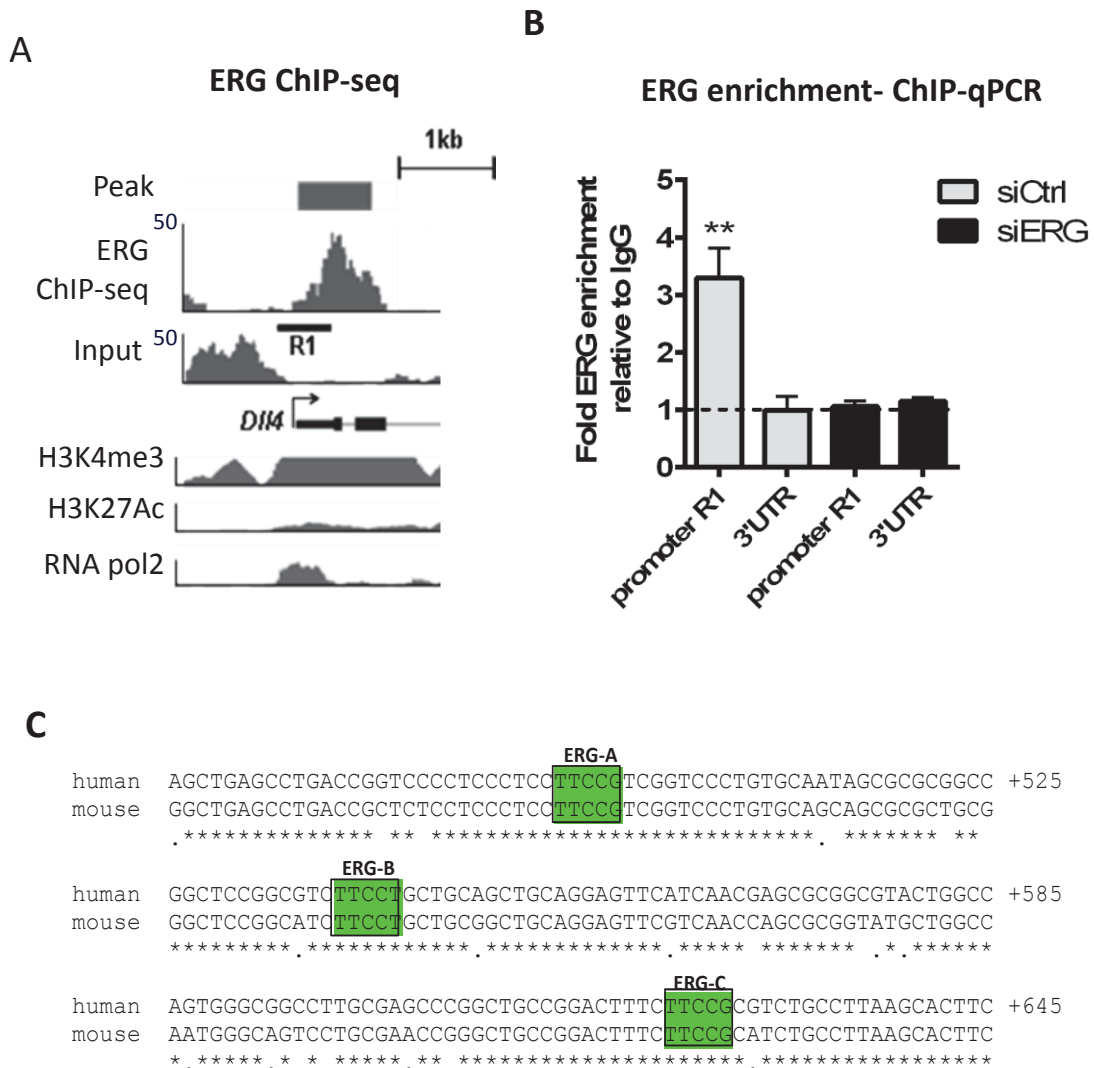


Figure 4.10 ERG binds to the Dll4 promoter. (A) ERG ChIP-seq analysis in HUVEC (Yang and Randi, unpublished data) shows a significant ERG binding peak within the Dll4 promoter, input profile also shown and indicates specificity of the ERG peak. Published ENCODE HUVEC ChIP-seq datasets profiles for H3K4me3, H3K27Ac and RNAPol2 in HUVEC. Location of qPCR amplicon covering region R1 is indicated. (B) Chromatin immunoprecipitation was carried out on Control and ERG siRNA (20 nM)-treated HUVEC using an anti-ERG antibody or IgG control. Enriched chromatin was analysed by quantitative PCR using primers to R1 and control 3'UTR, data is expressed as fold change compared to IgG normalised to input. Values are mean \pm SEM; n=4; asterisks indicate values significantly different from the control (Student t test where ** p < 0.01). (C) Sequence comparison of the significant ERG binding peak on Dll4 locus downstream of the transcription start site in human and mouse. This region contains 3 conserved ERG consensus sequences, (A/C)GGAA(G/A) or AGGA(A/T)(G/A) (ERG A-C). Asterisks denote conserved nucleotides across both species. Nucleotide numbers relative to the Dll4 transcription start site.

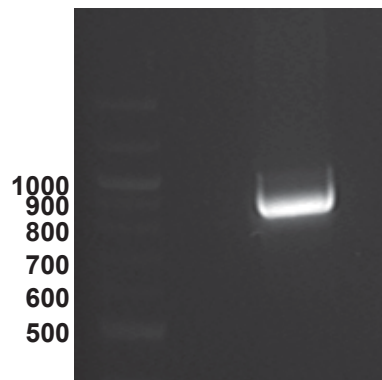
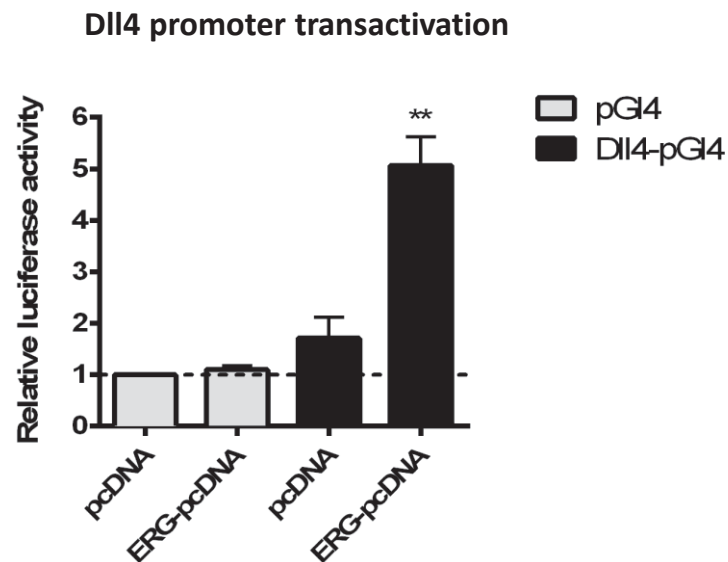
A**B**

Figure 4.11 ERG overexpression transactivates the Dll4 promoter. (A) PCR amplification of 850bp Dll4 promoter from human genomic DNA using primers flanking Dll4 promoter fragment regions. 100bp marker ladder is shown. (B) An ERG cDNA expression plasmid (ERG-pcDNA) or an empty expression plasmid (pcDNA) were co-transfected with empty pGL4 or Dll4-pGL4 luciferase constructs in HUVEC along with internal control pGL4 renilla luciferase. Luciferase activity was measured 24 h later. Values are represented as dual luciferase ratio of firefly luciferase normalised to pGL4 renilla luciferase and expressed as fold change relative to empty pGL4 vector alone. Values are mean \pm SEM; n=6; asterisks indicate values significantly different from the control (Student t test where ** p <0.01).

4.2.9 β -catenin does not cooperate with ERG to regulate Dll4 expression

Prior studies have suggested that β -catenin, the central transcriptional mediator of the canonical Wnt signalling pathway, drives Dll4 promoter activity (Corada et al., 2010). Since we have shown that LiCl treatment *in vitro* and *in vivo* can partially rescue the defective β -catenin signalling observed in ERG deficient cells, I tested whether ERG regulates Dll4 also through a β -catenin dependent mechanism. Initially, to study this, I analysed Dll4 mRNA levels in control and ERG-deficient HUVEC in the presence or absence of LiCl, a pharmacological stabiliser of β -catenin. LiCl-treated control HUVEC did not show an increase in Dll4 mRNA expression (Figure 4.12 A). Furthermore, LiCl treatment of ERG-deficient HUVEC did not have an effect on the decreased Dll4 levels observed in unstimulated ERG-deficient cells (Figure 4.12 A).

qPCR analysis of Dll4 expression was also carried out on yolk sacs from *Erg^{fl/fl}* and *Erg^{EC-KO}* embryos. LiCl treatment of *Erg^{fl/fl}* embryos did not affect transcript levels of Dll4 compared to control NaCl-treated embryos (Figure 4.12 B). Dll4 mRNA expression was shown to be significantly decreased in NaCl-treated *Erg^{EC-KO}* yolk sacs compared to controls, confirming a role for ERG in regulating Dll4 expression in the yolk sac during vascular development, in line with published data (Wythe et al., 2013). Analysis of LiCl-treated *Erg^{EC-KO}* yolk sacs showed that mRNA levels of Dll4 remained downregulated (Figure 4.12 B). Collectively, these results suggest that β -catenin signalling in the endothelium is not crucial for controlling Dll4 expression during both vascular development and in mature EC.

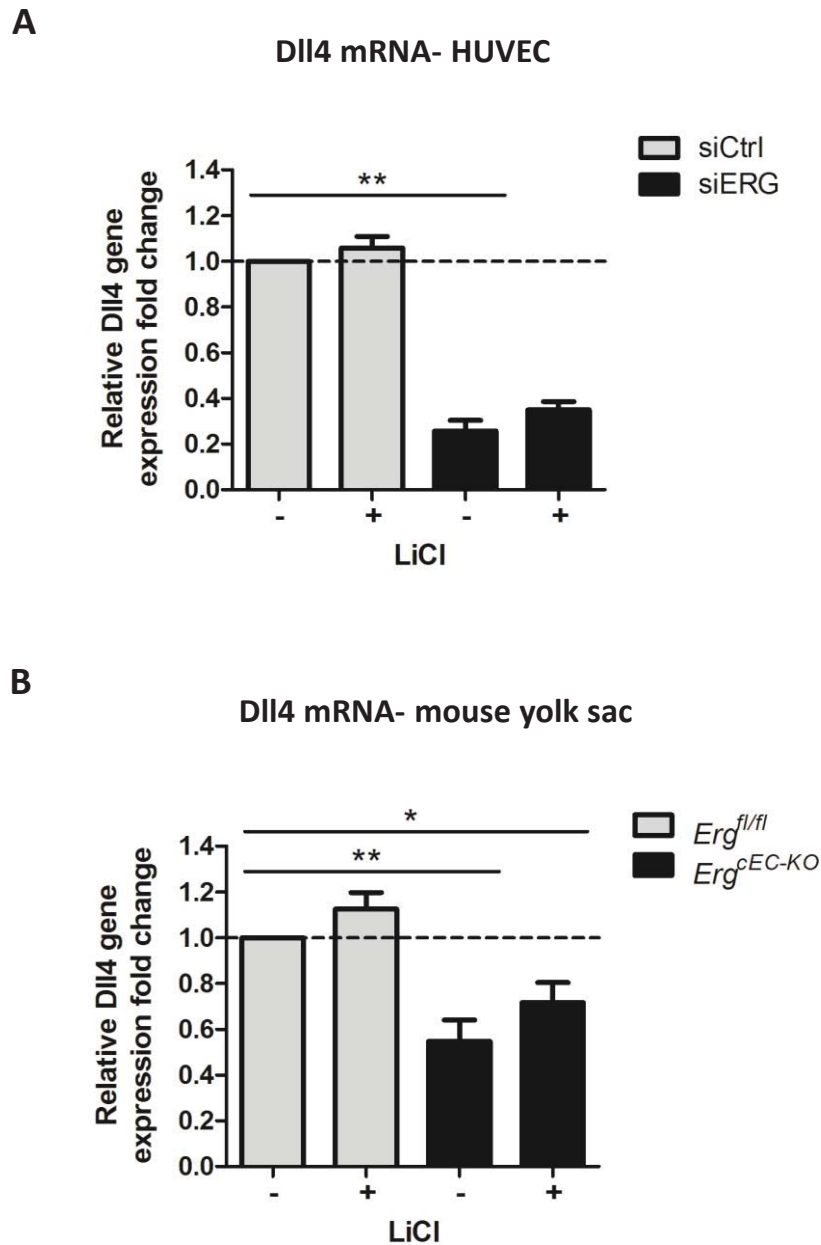


Figure 4.12 β -catenin does not cooperate with ERG to regulate Dll4 expression. (A) Dll4 mRNA expression in siCtrl and siERG-transfected HUVEC treated in the presence or absence of LiCl. Results are normalised to GAPDH and expressed as fold change relative to siCtrl (n=3). (B) qPCR analysis of Dll4 mRNA expression in NaCl- and LiCl-treated *Erg^{fl/fl}* and *Erg^{cEC-KO}* embryo yolk sacs. Data are expressed as fold change versus NaCl-treated *Erg^{fl/fl}* and are \pm SEM from at least three mice per group. All graphical data are mean \pm SEM; asterisks indicate significantly different values (ANOVA, followed by Bonferonni's test, where * p < 0.05, ** p < 0.01, *** p < 0.001).

4.2.10 ERG binds to putative Dll4 enhancer regulatory regions

I have shown that ERG drives the Dll4 promoter; however it has recently become clear that dynamically expressed genes often are regulated by multiple enhancers, which direct patterns of expression in response to physiological stimuli, such as growth factors. Importantly, spatiotemporal regulation of gene transcription during development is primarily accomplished by enhancers, and analysis of mutant animal models, has demonstrated the essential role of ETS transcription factors during endothelial development (De Val and Black, 2009). Sacilotto et al. performed an *in silico* search of the 51-kb Dll4 locus for regions enriched in HUVEC-specific H3K27Ac histone modification, associated with active enhancer regions (Sacilotto et al., 2013). This analysis identified four peaks of HUVEC-specific H3K27Ac at -16 and -12kb proximal to the transcription start site, within the 3rd intron of Dll4 and 14kb downstream of the transcription start site. Both cell-type- and stimulus-specific regulation of Dll4 mRNA expression and DNA binding activity have been previously studied, where the 3rd intron of Dll4 has been identified as a VEGF-responsive arterial enhancer, controlled by ERG (Wythe et al., 2013).

ERG ChIP-seq data from HUVEC (Yang and Randi, unpublished data) showed significant ERG enrichment compared to IgG control at all 4 putative enhancer regions (-16, -12, int3 and +14) identified by epigenetic enhancers marks in addition to the ERG enrichment observed at the Dll4 promoter characterised previously (Figure 4.13 A). ERG enrichment was validated by ChIP-qPCR using primers to the -16, -12, int3 and +14kb regulatory regions within the Dll4 locus. ChIP-qPCR data confirmed ERG binding, as approximately 10-fold ERG enrichment was observed at the putative enhancer regions compared to an isotype control (Figure 4.13 B). ERG enrichment at a downstream control region within exon 11 of the Dll4 locus was comparable to the isotype control.

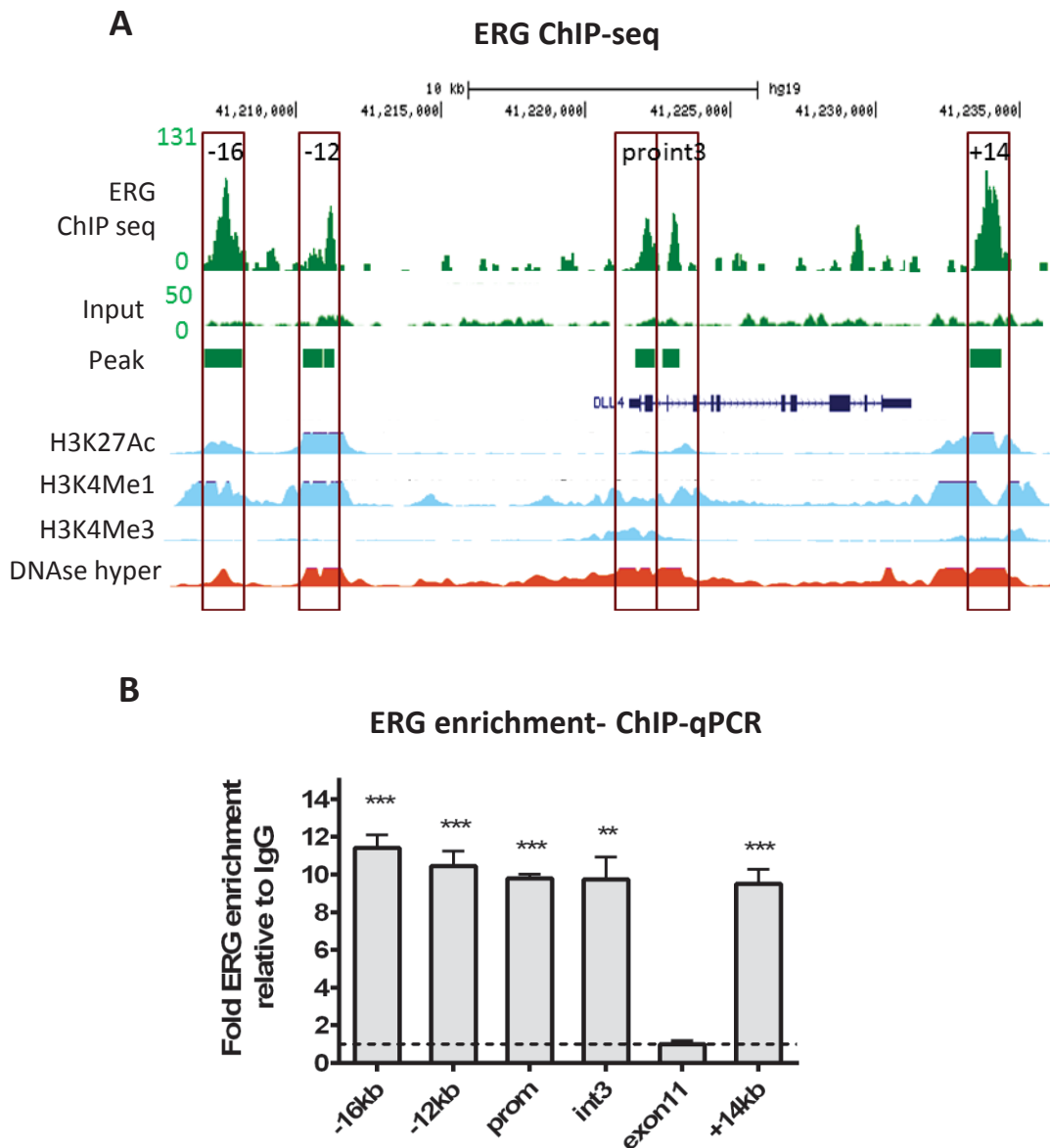


Figure 4.13 ERG binds to putative regulatory enhancer regions of DII4 (A) ERG ChIP-seq analysis in HUVEC (Yang and Randi, unpublished data) shows multiple significant ERG-binding peaks located near the DII4 genomic locus; chromatin input profile shows specificity of ERG peaks. Peaks are located -16kb and -12kb upstream of the TSS, near the TSS (prom), within the 3rd intron of the DII4 locus (int3) and +14kb downstream of the TSS, highlighted by the ENCODE DNase hypersensitivity profile. ENCODE ChIPseq data peaks for H3K27Ac, H3K4me1 and H3K4me3 indicate open chromatin and active transcription. (B) ChIP-qPCR was carried out on sheared HUVEC chromatin using an anti-ERG or control IgG antibody. Immunoprecipitated DNA was analysed by qPCR with primers designed to the DNA sequence within the significant ChIP-seq peaks (green boxes Figure 4.13 A). Primers covering a negative control region (exon 11) were also used. Results are expressed as fold change compared to IgG, normalised to input. Values are mean \pm SEM; n=3; asterisks indicate values significantly different from the control (Student t test where ** $p < 0.01$, *** $p < 0.001$).

4.2.11 ERG and Notch signalling cooperate to control Dll4 expression

Notch signalling itself has been implicated in Dll4 regulation. Treatment of HUVEC with DAPT, a Notch signalling inhibitor, has been shown to reduce basal Dll4 expression (Zhang et al. 2011). Interestingly, Dll4 enhancer activity in the dorsal aorta is greatly reduced in zebrafish models where Notch signalling has been inactivated, suggesting that a Notch-dependent positive feedback loop maintains Dll4 expression (Caolo et al., 2010). Furthermore, Sacilotto et al. implicated Notch signalling in the arterial-specific induction of Dll4 due to direct binding of RBPJ/NICD to the gene enhancers of Dll4 (Sacilotto et al., 2013), which I have now shown are also bound by ERG. Thus based on this evidence, I tested whether ERG could associate with NICD using a co-immunoprecipitation assay in HUVEC cell lysates using the anti-ERG and negative control rabbit IgG antibodies. Western blot analysis was carried out on the immunoprecipitated lysates. In HUVEC, co-immunoprecipitation from nuclear extracts showed that ERG associates with endogenous NICD (Figure 4.14). This experiment indicates that ERG interacts with NICD and places the two proteins in the same complex, suggesting that ERG-mediated activation of Notch signalling could also be through ERG association with NICD.

I also examined the effect of combined depletion of ERG by siRNA and NICD by DAPT, a γ -secretase inhibitor, on Dll4 expression. Treatment of siCtrl-treated confluent HUVEC with DAPT reduced basal Dll4 mRNA expression, in line with the literature (Zhang et al. 2011; Figure 4.15 A). Depletion of ERG decreased Dll4 expression, in line with Figure 4.9. Interestingly, DAPT treatment of siERG-treated HUVEC caused a further decrease in Dll4 expression (Figure 4.15 A), suggesting that Notch signalling contributes to ERG regulation of Dll4 expression and both are required for Dll4 expression. In line with this, Dll4 promoter activity was decreased in HUVEC treated with DAPT and this downregulation remained in cells overexpressing ERG (Figure 4.15 B). Collectively, these findings suggest that ERG binds NICD-RBPJ complexes to co-regulate Dll4 induction.

ERG co-immunoprecipitation

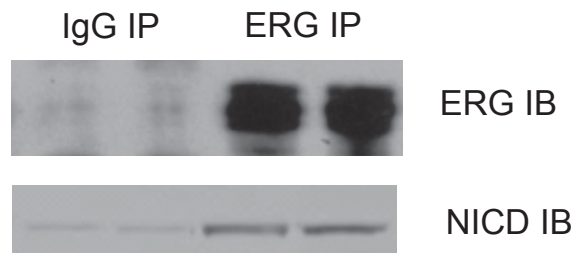


Figure 4.14 ERG interacts with endogenous Notch intracellular domain in HUVEC. Rabbit polyclonal antibody to ERG was used to immunoprecipitate HUVEC lysates and proteins were separated by SDS-PAGE. Immunoprecipitates (IP) were probed using goat polyclonal antibodies anti-ERG and mouse monoclonal anti-NICD. Endogenous NICD co-immunoprecipitated with ERG.

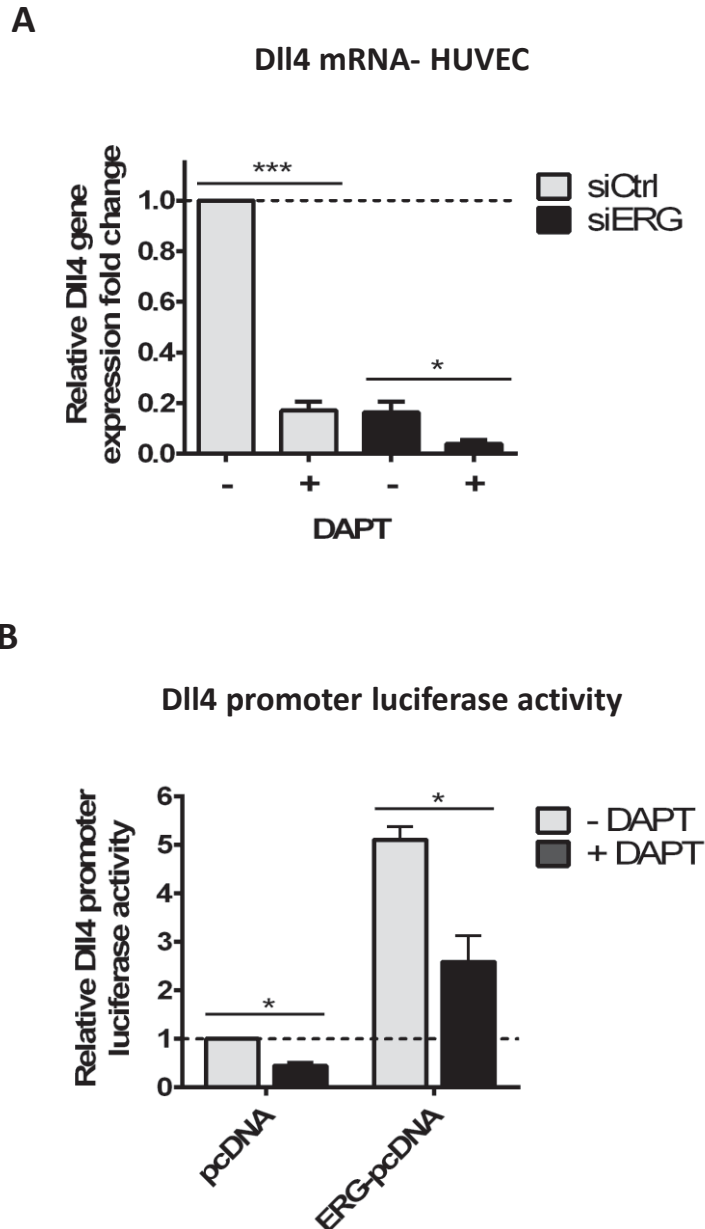


Figure 4.15 Notch signalling contributes to ERG regulation of Dll4. (A) Dll4 mRNA expression in siCtrl and siERG-transfected HUVEC treated in the presence or absence of the γ -secretase inhibitor DAPT. Results are normalised to GAPDH and expressed as fold change relative to siCtrl. (B) ERG cDNA expression plasmid (ERG-pcDNA) or an empty expression plasmid (pcDNA) were co-transfected with the Dll4-pGL4 luciferase construct in HUVEC along with internal control pGL4 renilla luciferase. Cells were treated in the presence or absence of DAPT for 6 h. Luciferase activity was measured 18 h later. Values are represented as dual luciferase ratio of firefly luciferase normalised to pGL4 renilla luciferase and expressed as fold change relative to Dll4-pGL4 vector alone. All graphical data are mean \pm SEM; n=3; asterisks indicate values significantly different from the control (Student t test where * $p < 0.05$, *** $p < 0.001$).

Interestingly, DAPT treatment of HUVEC decreased ERG transcript levels by 50% compared to control (Figure 4.16 A), suggesting Notch signalling regulates ERG expression and that the Notch feedback loop may be mediated by ERG. In support of this hypothesis, Dll4 stimulation of control HUVEC significantly increased ERG mRNA levels compared to the BSA control (Figure 4.16 B). Increased expression of Notch target gene Hey1 indicated effective Notch signalling induction in these cells.

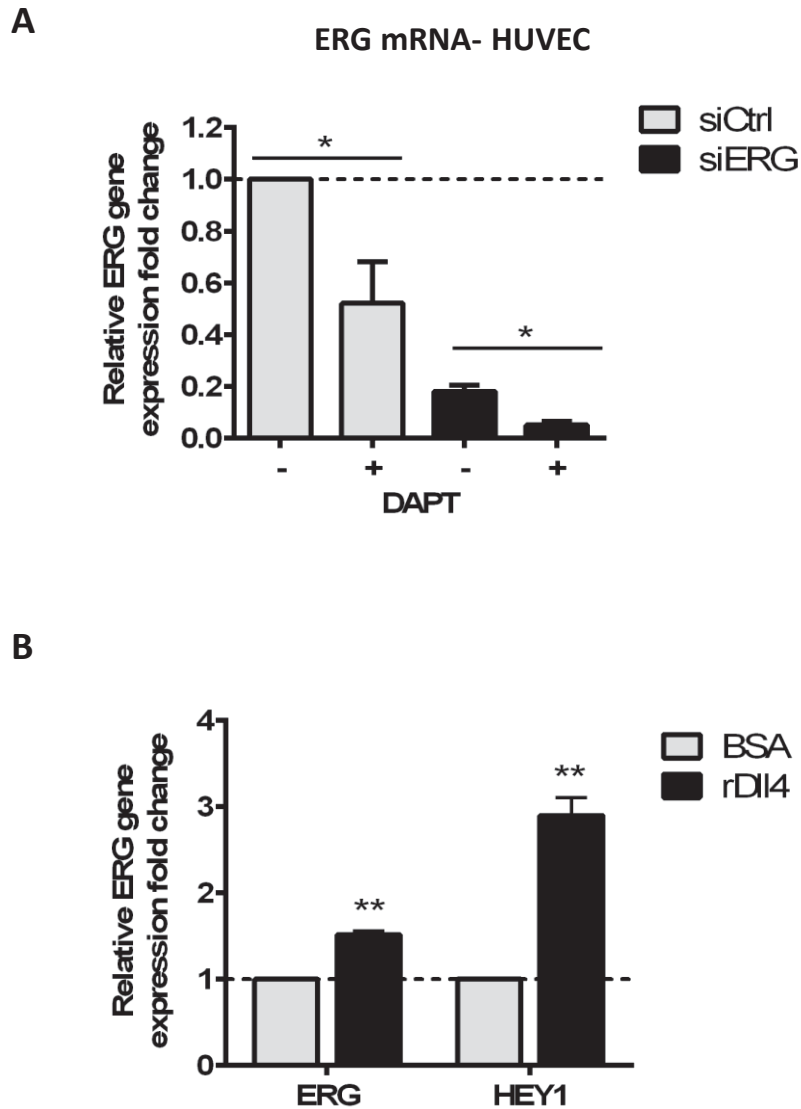


Figure 4.16 Notch signalling regulates ERG levels in EC. (A) ERG mRNA expression in siCtrl and siERG-transfected HUVEC treated in the presence or absence of the γ -secretase inhibitor DAPT. Results are normalised to GAPDH and expressed as fold change relative to siCtrl. Values are mean \pm SEM; n=3; ** p < 0.01. **(B)** mRNA expression of ERG and Notch target gene Hey1 in HUVEC stimulated with BSA as control or rDLL4. Results are normalised to GAPDH and expressed as fold change relative to siCtrl. Values are mean \pm SEM; n=3; asterisks indicate values significantly different from the control (Student t test where ** p < 0.01).

4.2.12 ERG represses expression of Sox17 in EC

The Sox family of transcription factors have also been implicated in Dll4 regulation. Sacilotto et al. showed in zebrafish and mouse models that the arterial-specific induction of Dll4 is due to direct combinatorial binding of RBPJ/NICD and Sox transcription factors to the gene enhancers of Dll4 (Sacilotto et al., 2013). In line with this work, a recent study by Corada et al. reports a combinatorial effect of Sox17 and Notch in increasing Dll4 expression (Corada et al., 2013). Furthermore, using ChIP assays, the authors showed that Sox17 directly interacts with the Dll4 promoter. Importantly, Notch activation by Notch intracellular domain overexpression has been shown to reduce Sox17 expression both in primary endothelial cells and in retinal angiogenesis. Notch inhibition by Dll4 blockade, on the other hand, increases Sox17 (Lee et al., 2014). Therefore, I tested whether inhibition of ERG in EC affects Sox17 expression. ERG-depleted HUVEC and primary lung EC isolated from *Erg*^{cEC-het} mice expressed significantly increased Sox17 mRNA expression (Figure 4.17 A-B). ERG regulates Sox17 protein expression in both human and mouse EC, as Sox17 protein expression levels were also increased in ERG-deficient HUVEC and in retinas from *Erg*^{iEC-KO} mice compared to *Erg*^{fl/fl} controls (Figure 4.18 A-B).

4.2.13 ERG repression of Sox17 is not Notch-dependent

To test whether ERG represses Sox17 expression through a Notch-dependent mechanism, control and ERG-deficient HUVEC were treated with DAPT. DAPT treatment had no further effect on Sox17 expression in siCtrl and siERG-treated HUVEC, suggesting that ERG repression of Sox17 is independent of Notch signalling (Figure 4.19).

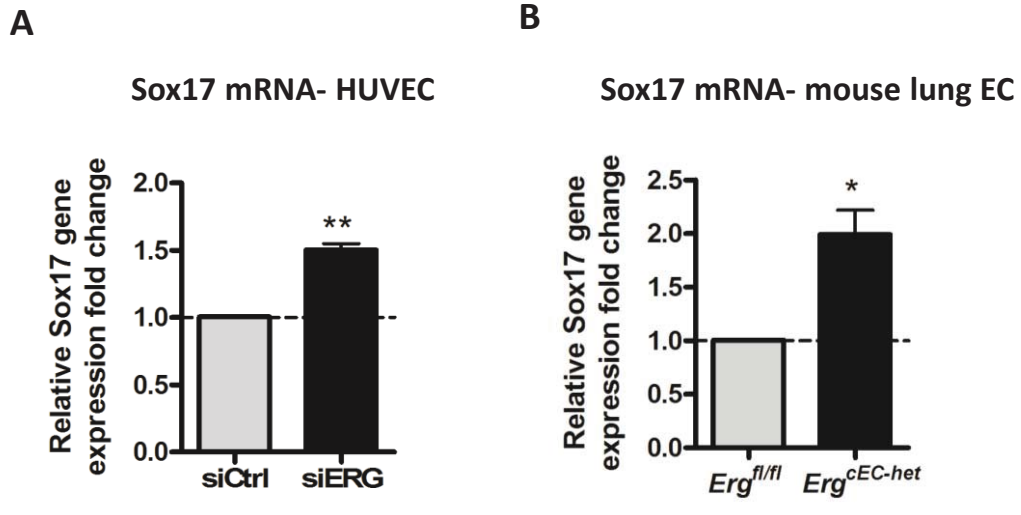


Figure 4.17 ERG represses Sox17 mRNA expression in EC. (A) qPCR analysis of Sox17 mRNA expression in HUVEC treated with siCtrl or siERG for 48 h. Results are normalised to GAPDH and expressed as fold change relative to siCtrl. (B) Sox17 mRNA expression in primary *Erg^{cEC-het}* mouse lung EC compared to control. Results are normalised to HPRT and expressed as fold change relative to *Erg^{fl/fl}* littermate controls. All graphical data are mean \pm SEM; n=4; asterisks indicate values significantly different from the control (Student t test where * p < 0.05, ** p < 0.01).

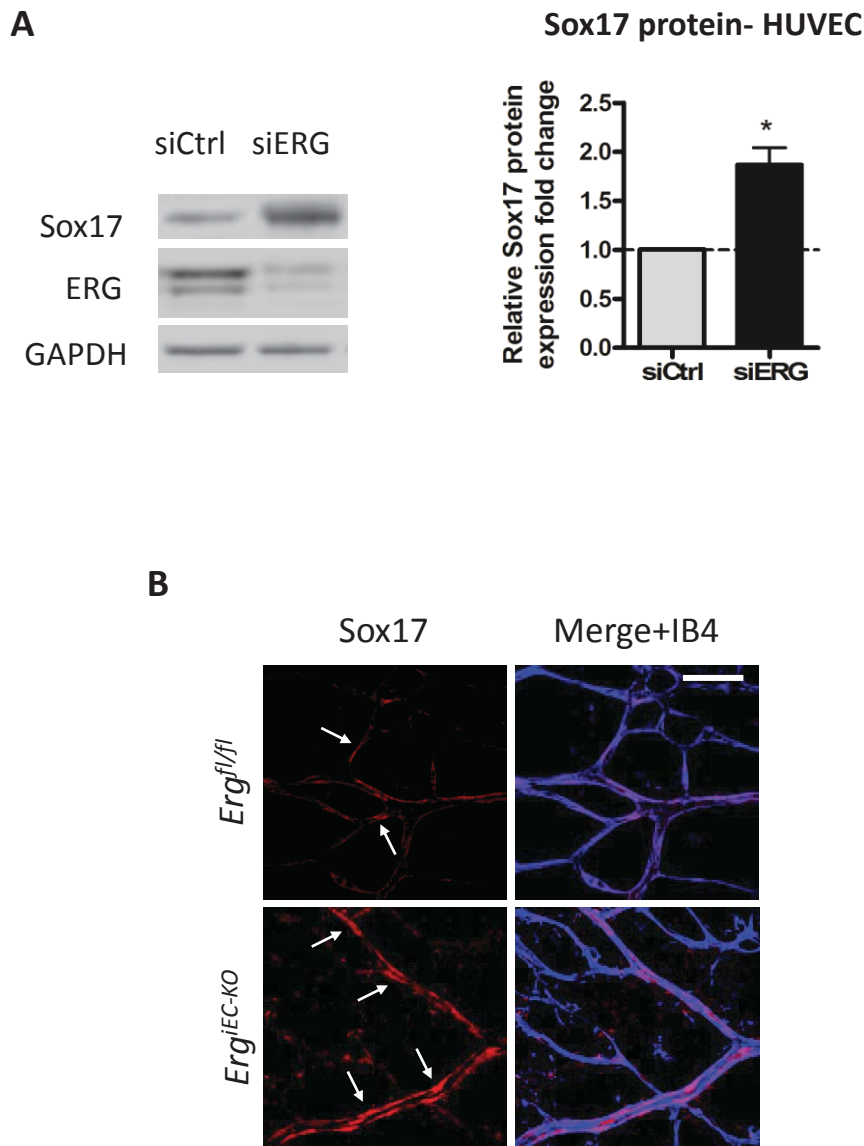


Figure 4.18 *In vitro* and *in vivo* ERG inhibition increases Sox17 protein expression. (A) Left panel: Representative blot of Sox17 protein expression in siCtrl and siERG-treated HUVEC for 48 h. Right panel: Quantification of fluorescence intensity of Sox17 total protein levels in siCtrl and siERG-treated cells. Results are normalised to GAPDH and expressed as fold change relative to siCtrl. Values are mean \pm SEM; n=3; asterisks indicate values significantly different from the control (Student t test where *** p <0.001). (B) Tamoxifen-treated *Erg^{IEC-KO}* and *Erg^{fl/fl}* P6 retinas were immunostained for Sox17 (red) and isolectin B4 (IB4, blue). Arrows show nuclei. Scale bar, 50 μ m; n=2.

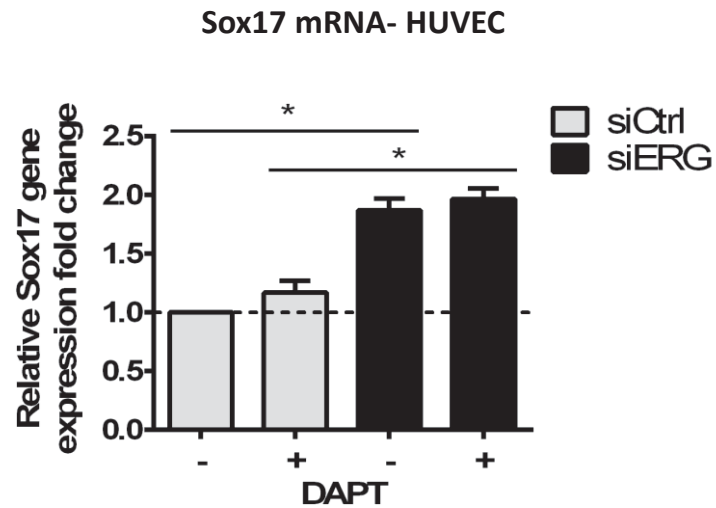


Figure 4.19 ERG repression of Sox17 expression in HUVEC is not Notch-dependent. Sox17 mRNA expression in siCtrl and siERG-transfected HUVEC treated in the presence or absence of the γ -secretase inhibitor DAPT. Results are normalised to GAPDH and expressed as fold change relative to siCtrl. Values are mean \pm SEM; n=3; asterisks indicate significantly different values (ANOVA, followed by Bonferonni's test, where ** p <0.01).

4.3 Discussion and Future Work

During sprouting angiogenesis, the Dll4/Notch signal is well characterized as a tip-stalk cell communication system. VEGF up-regulates Dll4 expression in endothelial tip cells, which in turn leads to Notch activation in adjacent stalk cells. Stalk cells subsequently lose their responsiveness to VEGF through down-regulation of VEGF receptors (Williams et al., 2006), thereby maintaining a quiescent and stabilized phenotype. Notch signalling not only restricts angiogenesis but also maintains vascular quiescence and Dll4/Notch signal appears to function in mature blood vessels with tight interendothelial cell-cell contacts (Fukuhara et al., 2008; Zhang et al., 2011a). It has been reported that conditional deletion of RBP-J, the key transcription factor downstream of the Notch receptor, induces spontaneous angiogenesis in quiescent adult vasculature (Dou et al., 2008). Furthermore, Dll4/Notch signalling promotes recruitment of mural cells to the vessel wall and induces deposition of basement membrane proteins around the vessels, both of which are important for vascular stabilization (Trindade et al., 2008).

The Notch ligand Jagged1, on the other hand, has been shown to antagonize Dll4/Notch signalling in mouse endothelial cells and the opposing effects of Dll4 and Jag1 on sprouting angiogenesis have been clearly illustrated by Benedito et al. (Benedito et al., 2009). They observed an upregulation of Notch target gene expression in the Jag1[#]EC endothelium and demonstrated that reduced angiogenic growth of Jag1[#]EC blood vessels is indeed a consequence of increased Notch signalling. Therefore, pro-quiescent Dll4 and pro-angiogenic Jag1 have contrasting functional roles and distinct spatial expression patterns in the vasculature. My data shows that ERG controls Notch signalling in mature EC, by regulating the activation of Dll4 and repression of Jag1 (Figure 4.20). The balance between these ligands is critical in the processes of tip cell selection and vascular quiescence. In line with this, Jagged1 overexpression in the neonatal retina increases tip cell formation at the angiogenic front, and increases vessel branching, EC density, and proliferation in the mature plexus (Benedito et al., 2009). Thus ERG regulates the balance between Dll4 and Jag1, suggesting that ERG functions to control Notch-mediated endothelial quiescence. To my knowledge, this is the first time that reciprocal transcriptional control of Notch proteins by a single transcription factor has been shown in EC.

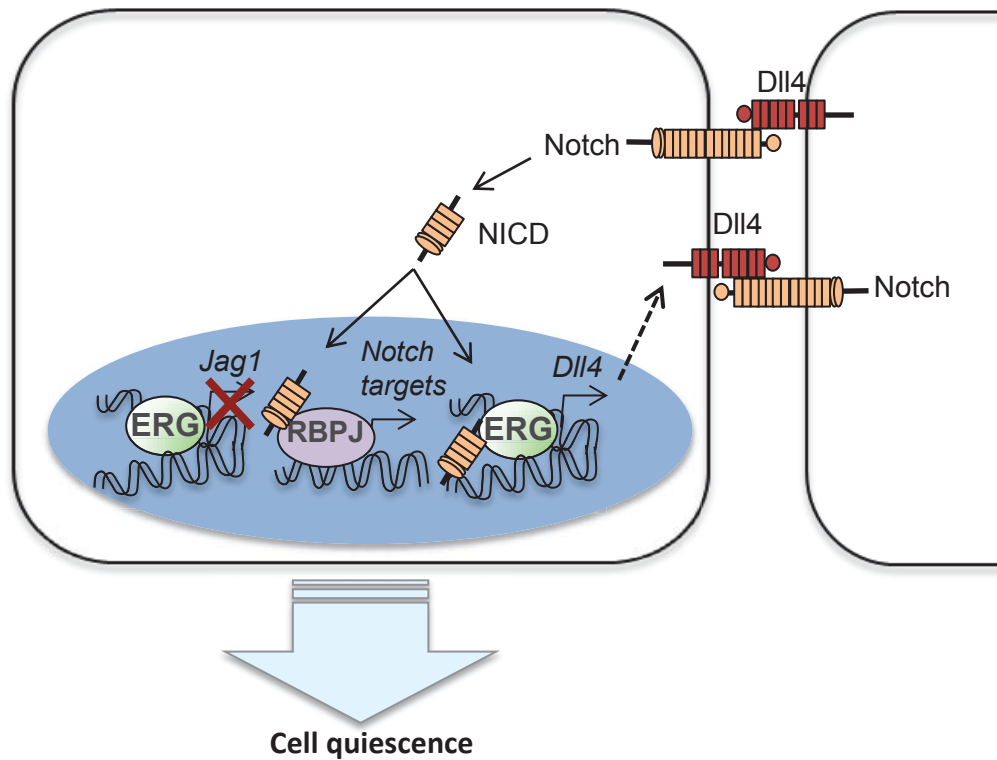


Figure 4.20 Schematic of a model of ERG regulation of Notch signalling in EC. ERG is required for endothelial Notch signalling, critical for maintaining cell quiescence. ERG simultaneously represses expression of the pro-angiogenic ligand Jagged-1 whilst driving expression of the pro-quiescence Notch ligand Dll4. ERG binds to and activates the Dll4 promoter and multiple enhancers. Notch signalling has also been implicated in Dll4 regulation. ERG is induced downstream of Notch signalling, suggesting that continued Notch signalling maintains Dll4 promoter/enhancer activity and expression through ERG.

Given the contrasting roles of Dll4 and Jag1 in angiogenesis, upstream signals controlling the expression of either Dll4 or Jag1 may positively or negatively modulate angiogenesis, by changing the ratio of Dll4 and Jag1 expression. The effects of these signals on ERG would be of great interest and some are discussed in this section. For example, whilst VEGF has been shown to induce endothelial Dll4 expression (Lobov et al., 2007), Jagged1 is absent from tip cells, which are exposed to high levels of VEGF, suggesting that these two ligands are regulated differentially by VEGF (Benedito et al., 2009). Additionally, Notch activation is another positive regulator of Dll4 but does not affect Jagged1 expression, whereas the pro-inflammatory and pro-angiogenic cytokine TNF- α upregulates Jag1 but downregulates Dll4 transcript levels (Sainson et al., 2008). The existence of two Notch ligands with opposing roles and differential regulation could allow the integration of different pro- or anti-angiogenic signals mediated by ERG. Furthermore, Notch signalling pathway components can be expressed in an oscillatory manner (Kageyama et al., 2007), which could provide an appealing explanation for the regulation of dynamic processes such as sprouting angiogenesis.

I have shown that ERG drives the Dll4 promoter; however it has recently become clear that dynamically expressed genes often contain multiple enhancers, which direct patterns of expression. Importantly, lineage-specific and spatiotemporal regulation of gene transcription during development is primarily accomplished by enhancers, and analysis of mutant animal models has demonstrated the essential role of ETS transcription factors during endothelial development (De Val and Black, 2009). Recently, Wythe et al. showed that the Dll4 enhancer within the 3rd intron of the Dll4 gene, which controls Dll4 arterial expression, is bound by ERG in bovine aortic endothelial cells (BAEC) and HUVEC (Wythe et al., 2013). I have shown that ERG, in fact, binds to all 4 putative enhancer regions (-16, -12, int3 and +14; Figure 4.13) identified by Sacilotto et al. (Sacilotto et al., 2013), confirming that ERG plays a crucial role in Dll4 regulation.

Although prior studies suggested that β -catenin, the central transcriptional mediator of the canonical Wnt signalling pathway, drives Dll4 promoter activity (Corada et al., 2010), I have shown that Dll4 expression is unaffected by β -catenin stabilisation in the endothelium *in vitro* and *in vivo* using LiCl (Figure 4.12). This suggests that β -catenin is dispensable for controlling Dll4 expression during both vascular development and in mature EC. Notch signalling has also been implicated in

Dll4 regulation (Zhang et al., 2011b; Caolo et al., 2010), suggesting a Notch-dependent positive feedback loop may maintain Dll4 expression and enhancer activity. Sacilotto et al. implicated Notch signalling in the arterial-specific induction of Dll4 due to direct binding of RBPJ/NICD to the gene enhancers of Dll4 (Sacilotto et al., 2013), which I have now shown are also bound by ERG. Figures 4.14-4.15 in this thesis suggest that ERG binds NICD-RBPJ complexes to co-regulate Dll4 induction. Interestingly, our observation of an increase in ERG mRNA in HUVEC exposed to immobilised rDll4 (Figure 4.16 B), raises the possibility that Notch regulation of Dll4 may be mediated through ERG, and this Notch-mediated positive feedback loop regulating ERG expression may be relevant to its function in maintaining vessel stability (Figure 4.20); whether this is the case *in vivo* remains to be tested.

I have shown that ERG is required for Notch signalling and Dll4 stimulation of ERG-deficient EC is unable to rescue the defective Notch signalling phenotype observed in these cells (Figure 4.4 C). This suggests that other components of the Notch signalling pathway are involved in this regulation. To dissect whether the decrease in Notch signalling observed in ERG-deficient EC and the sprouting defect observed in the *Erg*^{iEC-KO} mice (Figure 1.12 B; Birdsey, Shah et al., 2015) is due to upregulation of the antagonistic Notch ligand Jag1, I would need to inhibit Jagged-1 *in vitro* in ERG-deficient EC and study whether Notch signalling is restored in these cells and performing an *in vivo* rescue experiment with the Jag1LOF model (Benedito et al., 2009) would allow us to analyse whether the sprouting defect in *Erg*^{iEC-KO} mice is normalised following Jagged1 deletion.

A recent paper has reported increased ERG expression in arterial-derived EC *in vitro* (Wythe et al., 2013). However in the mouse retinal vasculature, we observe strong ERG expression in all EC with no detectable difference between arteries and veins. Yet Notch signalling components are restrictively expressed in EC of arteries and capillaries, suggesting that ERG transcriptional activity as well as levels can be modified. Endothelial tip cells selectively express Dll4, but not Jag1 (Hofmann and Luisa Iruela-Arispe, 2007). Endothelial cells located at arterial junctions express Jag1, but not Dll4 (Hofmann and Luisa Iruela-Arispe, 2007). As mentioned previously, some Jagged and Delta-like ligands have been reported to have opposing activities on Notch receptor binding (D'Souza et al., 2008). Endothelial cells may therefore have varying degrees of Notch activity, depending on the number and type of ligands they are

exposed to. Given that blood vessels are composed of multiple cell types and are exposed to basement membrane components, it is likely that Notch signalling in endothelial cells can also be regulated by Notch ligands expressed by non-endothelial vascular cells.

Previous studies have illustrated that the VEGF and Notch signalling pathways are tightly linked. VEGF-A has been shown to induce Dll4 expression in angiogenic vessels and, most prominently, in the tip of endothelial sprouts in the retina (Lobov et al., 2007 and Suchting et al., 2007). DLL4 activates Notch in adjacent cells, which leads to the downregulation of VEGF receptors and thus dampens the VEGF response, thereby suppressing endothelial sprouting and proliferation. VEGF and Notch pathways therefore operate a negative-feedback loop. Therefore it would be interesting to study whether ERG regulates VEGF receptor and/or co-receptor expression and how VEGF affects ERG. In a *Xenopus* model, ERG has been shown to associate in a physical complex with KLF2 and synergistically activate transcription of VEGFR2 (Meadows et al., 2009); whether ERG inhibition affects VEGFR2 expression in the mouse retina remains to be studied. During early vascular development, VEGF signalling specifies arterial fate by inducing the transcription of Dll4. Wythe et al. showed that ERG mediates the VEGF- and MAPK-dependent arterial expression of Dll4 and Notch4 (Wythe et al., 2013). The authors observed an increase in recruitment of ERG to enhancers within the Dll4 and Notch4 loci in response to VEGF. However, this increase in ERG occupancy was not due to changes in ERG levels or localisation, suggesting that VEGF instead increases the DNA binding activity of ERG. Interestingly, several ETS factors are phosphorylated by MAPK signalling (Murakami et al., 2011), and these post-translational modifications affect their binding to DNA and interaction with other transcription factors (Hollenhorst et al., 2011). Therefore, future experiments examining ERG phosphorylation downstream of VEGF signalling and whether this affects functional interactions with other transcription factors and its transcriptional activity would be of interest.

ERG has been previously shown to maintain the endothelium in an anti-inflammatory state, by repressing expression of ICAM-1 and IL-8 due to inhibition of NF-KB p65 binding to the promoter (Sperone et al., 2011; Dryden et al., 2012). Interestingly, ERG expression in EC is inhibited by pro-inflammatory cytokine TNF- α treatment, and TNF- α up-regulates Jag1 expression and down-regulates Dll4 expression

(Sainson et al., 2008), a pattern which we have shown is consistent with ERG regulation of these targets. Moreover, a conserved NF- κ B site exists within R2 of the Jag1 promoter (Johnston et al., 2009) and I demonstrate that the up-regulation of Jagged-1 mRNA levels following ERG inhibition was lost in cells treated with an inhibitor of NF- κ B (Figure 4.8). Thus ERG controls Jag-1 expression in EC through a NF- κ B-dependent mechanism.

While I have identified a potential mechanism for ERG-mediated repression of Jagged-1, it remains unclear what determines ERG's role as a transcriptional activator or repressor, such as promoter binding site motifs, interaction with other transcription factors or regulatory co-factors, or through post-translational modifications of ERG. Co-staining retinas for both Dll4 and Jag1 would allow us to ascertain whether ERG is activating and repressing its targets in the same cell at the same time *in vivo*, since this clearly occurs in EC *in vitro* and *ex vivo*. Composite binding motifs involving ETS factors and other transcription factors which synergise to bind common promoters have been characterised, and analysis of genome wide ERG binding sites using the ChIP-seq data may allow us to identify more of these.

The transcriptional activity of ERG as an activator or repressor may depend on interaction with other transcription factors resulting in activation, inhibition or synergy. ERG could also interact with transcriptional co-factors, which can induce changes in the chromatin profile or mediate post-translational modifications of ERG. Yeast two-hybrid assay analysis has previously shown that ERG interacts with the histone methyltransferase ESET (Yang et al., 2002), which specifically tri-methylates H3K9, a modification that induces a repressive chromatin structure. However, ChIP techniques combined with mass spectrometry analysis of DNA-bound transcriptional protein complexes immunoprecipitated with a tagged-recombinant ERG is another method that could be used to investigate ERG interacting partners and help identify binding complexes on ERG target genes. For example, the majority of ERG binding sites along the Dll4 locus are intergenic or intragenic rather than within promoters, in line with ChIP-seq analysis of ERG binding sites in haematopoietic progenitor cells (Wilson et al., 2010). To investigate this further, a chromosome conformation capture technique could be carried out, which would help identify genomic sites where ERG binds to distal enhancers which then interact or loop with promoters of target genes. Additionally, although ENCODE data is available on histone modifications and co-

factor occupancy in HUVEC, it would be interesting to analyse whether the presence and absence of ERG alters the chromatin profile through effects on patterns of histone modifications and whether ERG is required for epigenetic factor occupancy in endothelial cells.

Chapter Five

ERG controls multiple pathways required for vessel growth and stability: Angiopoietin-1/Tie2 pathway

5. ERG controls multiple pathways required for vascular stability: Angiopoietin-1/Tie2 pathway

5.1 Introduction

5.1.1 Ang1/Tie2 signalling in the vasculature

The receptor tyrosine kinase Tie2 and its activating ligand Angiopoietin-1 (Ang1) are required for vascular development (Davis et al., 1996; Suri et al., 1996; Sato et al., 1995). Mice lacking Ang1 or Tie2 display a lethal phenotype and die between E10.5–E12.5, attributable to defective vascular integrity, reduced pericyte coverage and therefore, compromised vascular function (Suri et al. 1996). In addition to its role in vascular development, the presence of phosphorylated Tie2 in several adult tissues indicates an ongoing role for Ang1 in mature vessels (Wong et al., 1997). Indeed, Ang1/Tie2 signalling is regarded as the prototypic regulator of vessel stability, as overexpression of Ang1 leads to a stabilized, less permeable vasculature (Uemura et al., 2002; Thurston et al., 2000). Ang1 reduces vascular leakage by strengthening VE-cadherin-regulated inter-endothelial adhesion (Figure 5.1; Gamble et al., 2000). In the quiescent adult vasculature, Ang1 secreted from pericytes induces Tie2 activation in endothelial cells to maintain mature blood vessels by enhancing vascular integrity and endothelial survival (Figure 5.1). Furthermore, Ang1/Tie2 signalling promotes recruitment of mural cells to the vessel wall, which are important for vascular stabilization. However, the molecular mechanisms through which Ang1 functions are yet to be fully elucidated and there is limited data regarding the signalling pathways through which Ang1 modulates transcription.

Previous studies have reported that Ang1 assembles distinct Tie2 signalling complexes in the presence or absence of cell-cell junctions, thus regulating both vascular quiescence and angiogenesis (Fukuhara et al., 2008; Saharinen et al., 2008). Tie2 is anchored to the cell-substratum contacts through extracellular matrix-bound Ang1 in sparse cells. In the presence of cell-cell junctions, however, Ang1 induces Tie2 clustering in trans, which causes preferential activation of the Akt kinase pathway (Figure 5.1), which plays essential roles in cell survival (Kim et al., 2000). Thus, microarray analyses carried out by Fukuhara et al. demonstrated a difference in induction of gene expression by Ang1 in the presence or absence of cell–cell contacts, and indicated that Tie2 activation at cell–cell contacts led to induction of expression of

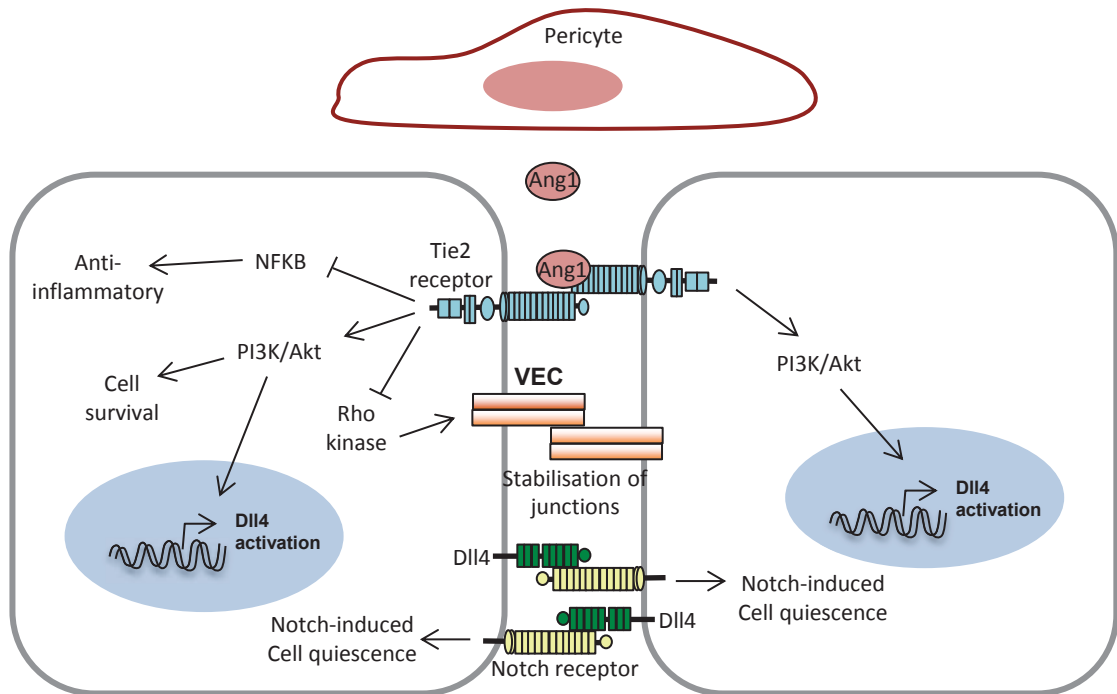


Figure 5.1 Vascular stabilisation by Angiopoietin-1. Ang1 is constitutively expressed by pericytes and vascular smooth muscle cells. In confluent cells, Ang1 bridges Tie2 at cell–cell contacts, resulting in formation of trans-association of Tie2. Trans-associated Tie2 at cell–cell contacts preferentially activates Akt signalling pathways, which may contribute to maintenance of vascular quiescence by enhancing endothelial survival. Ang1/Tie2 signal induces Dll4 expression which signals via Notch receptors on adjacent cells to mediate vascular quiescence. Binding of Ang-1 to Tie2 promotes vessel integrity, inhibits vascular leakage and suppresses inflammatory gene expression.

genes involved in vascular quiescence and stability, including the Notch ligand Dll4 (Fukuhara et al., 2008). The molecular events following Notch activation in the endothelium are well understood, yet the transcriptional cues that function downstream of growth factors to induce the expression of Notch signalling components are less well characterised. Since ERG transcriptionally drives Dll4, I hypothesised that Dll4 up-regulation by Ang1 may be dependent on ERG.

Multiple growth factor signalling pathways are well known for their cell non-autonomous roles in angiogenesis, but how these pathways affect transcription factor function remains largely undefined. In cultured EC, Ang1 inhibits apoptosis and inflammatory responses and promotes differentiation and migration, similar to the roles of ERG within the endothelium, raising the possibility that some of the biological effects of Ang1 on cultured EC may be mediated through ERG

The aims of the work described in this chapter are to:

- Determine whether ERG is required for Ang1-mediated Dll4 induction and Notch signalling.
- Study whether cell confluency affects ERG regulation of Ang1-induced Dll4
- Investigate whether ERG transcriptional activity is regulated by Ang1.

5.2 Results

5.2.1 ERG controls expression of the Angiopoietin receptor Tie2 in human and mouse EC

The Angiopoietin receptor Tie2 is expressed in nearly all EC during development (Augustin et al., 2009). In adult vasculature, Tie2 activation is involved in the maintenance of vascular quiescence (Augustin et al., 2009). Gene expression profiling identified Tie2 as a candidate ERG target and the ERG microarray analysis indicated a 2-fold decrease in Tie2 mRNA expression following ERG inhibition at both 24 and 48 h (Birdsey et al., 2008). To validate the microarray data, Tie2 mRNA and protein levels were analysed in control and ERG-deficient HUVEC. Inhibition of ERG expression resulted in significant downregulation of ERG mRNA and protein levels, comparable to levels observed in Figures 3.3 B and 3.4 A (data not shown). ERG inhibition resulted in a significant 1.6 fold decrease in Tie2 mRNA levels compared to control (Figure 5.2 A). Tie2 total protein levels were also significantly decreased following ERG inhibition (Figure 5.2 B), indicating that ERG is required for endothelial Tie2 expression. ERG regulates Tie2 expression in both human and mouse EC, as Tie2 mRNA expression levels were also decreased in primary mouse EC from *Erg*^{cEC-het} mice compared to *Erg*^{fl/fl} controls (Figure 5.2 C).

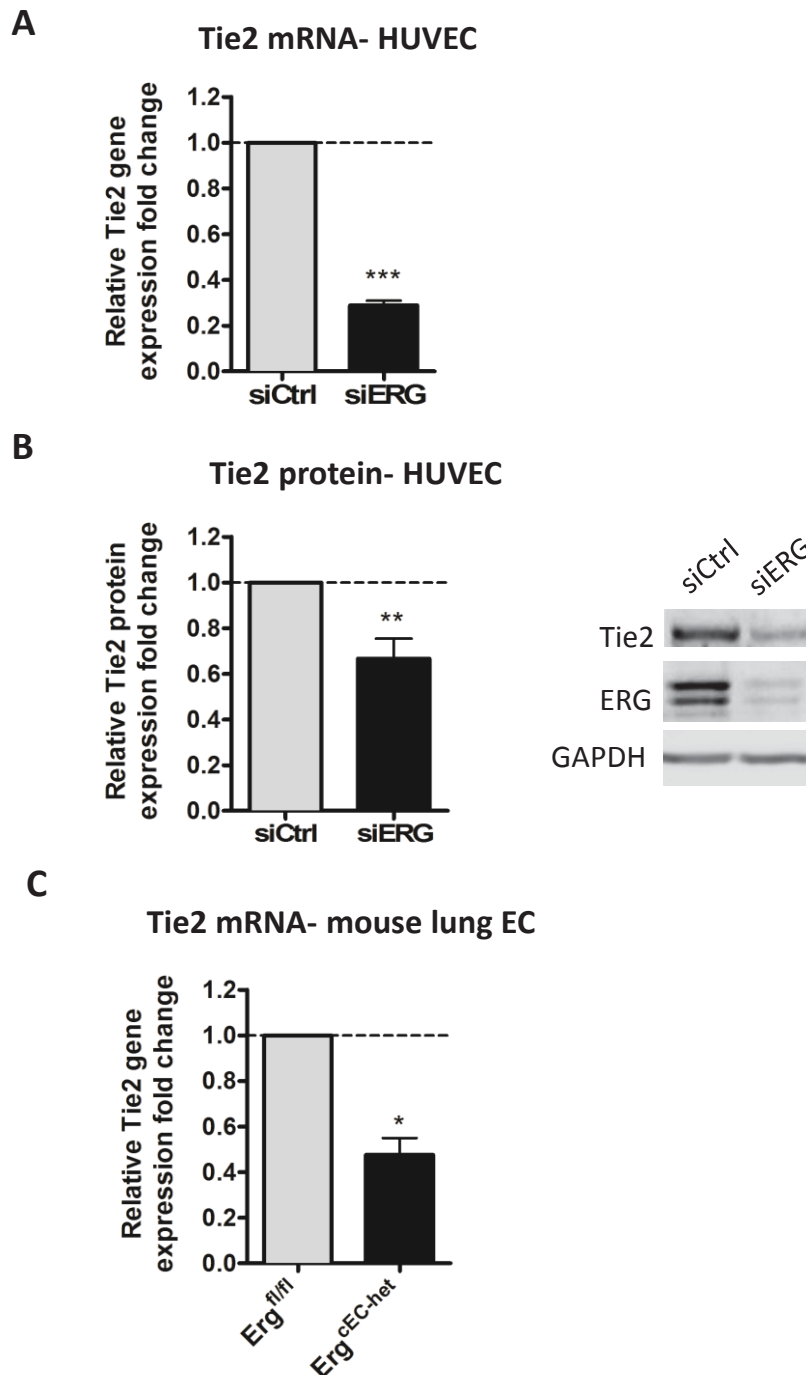
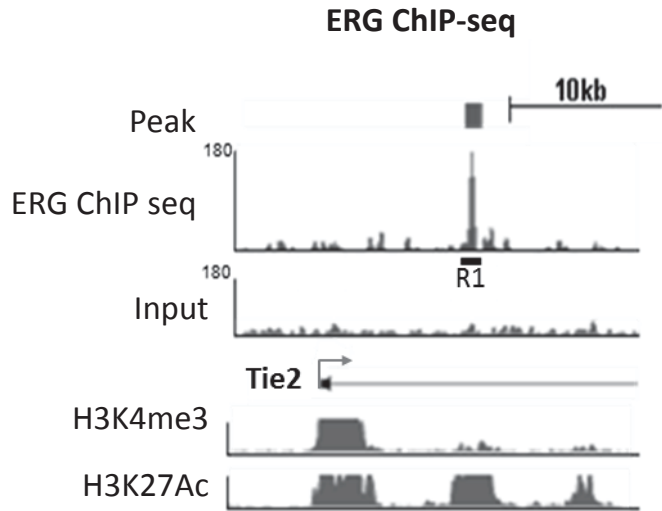


Figure 5.2 ERG regulates Tie2 expression in EC. (A) Tie2 mRNA expression in siCtrl and siERG-treated HUVEC treated. Results are normalised to GAPDH and expressed as fold change relative to siCtrl (n=6). (B) Left panel: Quantification of fluorescence intensity of Tie2 total protein levels in siCtrl and siERG-treated cells. Right panel: Representative blot of Tie2 and ERG protein expression in siCtrl and siERG-treated HUVEC. Results are normalised to GAPDH and expressed as fold change relative to siCtrl (n=3). (C) Tie2 mRNA expression in primary *Erg^{eEC-het}* mouse lung EC compared to control. Results are normalised to HPRT and expressed as fold change relative to *Erg^{fl/fl}* littermate controls (n=4). All graphical data are mean \pm SEM; asterisks indicate values significantly different from the control (Student t test where ** p < 0.01, *** p < 0.001).

5.2.2 Expression of Tie2 is controlled by an ERG-dependent enhancer

ERG ChIP-seq analysis (Yang and Randi, unpublished data) in HUVEC showed a significant ERG-binding peak within the first intron of the Tie2 gene locus (Figure 5.3 A). Alignment with ENCODE ChIP-seq profiles indicates this region as a putative enhancer, characterized by the presence of H3K27Ac and absence of H3K4me3 histone modifications (Creighton et al., 2010). Comparative genomic analysis of R1 revealed the presence of three highly conserved ERG DNA binding motifs (Figure 5.3 B). ChIP-qPCR confirmed that ERG interacts directly with the putative Tie2 enhancer region, as significant enrichment of ERG was observed at region 1 within the first genomic intron compared to a downstream 3'UTR control region (Figure 5.4). To confirm the specificity for ERG binding at R1 within the Tie2 locus, ChIP-qPCR was carried out on chromatin from HUVEC treated with control and ERG siRNA. This showed a decrease in the amount of ERG bound to R1 following ERG inhibition, compared with control siRNA treatment (Figure 5.4).

A**B**

```

human   TCACACCCATCTCAGCAGATCTGTCAGCTTCCCGCTTTTGTAAAGGGTGATATCATGC +8740
mouse   TCACACCCATCTCAGCAGATCTGTCAGCTTCCCGCTTTTGTAGAGGGTGATATCATGC
*****
ERG-A          ERG-B
human   TCCTGGGGGAGCACTGGAAGACAATGCTCGGCCACTTCCTCCAGATACAATAGGCGG +8800
mouse   TCCTGGGGGAGCTCTGGAAGACAATGAGCAGCCACTTCCTCTAGATACAATAGGCGG
*****
ERG-C
human   AGTCAGGAGGCAGTATTGACATTGCTGGGGCTGGGGAGGCACTCACTGCTCTGCGGCCG +8860
mouse   AGTCAGGAGGTAGTATTGACATTGCTGGGGCCTAGGAGCTACTCACTGCTCGGTGGCCG
*****

```

Figure 5.3 ERG binds a putative enhancer region within the 1st intron of the Tie2 locus. (A) ERG ChIP-seq analysis in HUVEC (Yang and Randi, unpublished data) shows a peak located within the Tie2 genomic locus; chromatin input profile shows specificity of ERG peaks. Location of qPCR amplicon covering region (R) 1 is indicated. ENCODE ChIP-seq datasets for H3K4me3, and H3K27Ac in HUVEC are shown. (B) Sequence comparison of R1 within the 1st intron of the Tie2 locus in human and mouse shows 3 conserved ERG consensus sequences (ERG A-C). Asterisks denote conserved nucleotides across both species. Nucleotide numbers relative to the Tie2 transcription start site.

ERG enrichment- CHIP-qPCR

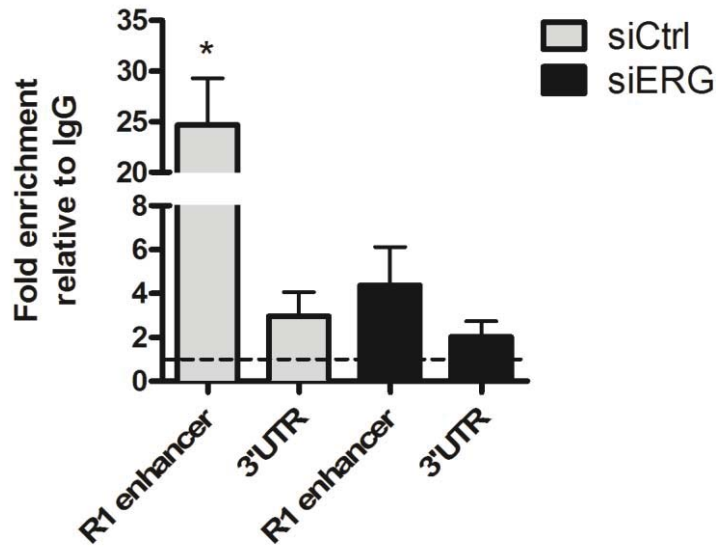


Figure 5.4 ChIP-qPCR validates ERG binding within R1 of the Tie2 locus. ChIP-qPCR on ERG-bound chromatin from Control and ERG siRNA (20 nM) -treated HUVEC was analysed using primers for R1 and control downstream 3'UTR region within the Tie2 genomic locus. Data is expressed as fold change compared to IgG normalised to input. Values are mean \pm SEM; n=4; asterisks indicate values significantly different from the control (Student t test where ** p < 0.01).

5.2.3 Angiotensin-1 promotes canonical Wnt and Notch signalling through ERG

The data presented in previous chapters clearly implicate ERG in the control of endothelial Wnt/ β -catenin and Notch signalling. These pathways are induced by the Ang1/Tie2 signalling system (Zhang et al., 2011); therefore I set out to test whether ERG mediates Ang1 signalling in EC, by treating HUVEC with Ang1*, a potent recombinant Ang1 variant (see section 2.4). To examine Wnt/ β -catenin activity in control or ERG-depleted HUVEC in the presence or absence of Ang1 treatment, cells were transfected with the TCF luciferase reporter construct to detect β -catenin-dependent transcriptional activity. In line with the literature, Ang1 stimulation induced TCF luciferase reporter activity by 1.9-fold in control EC. This induction of TCF luciferase reporter activity in response to Ang1 was lost in ERG-depleted HUVEC (Figure 5.5 A). Consistently, mRNA expression of the Wnt target gene Axin2 was induced by 1.3-fold upon Ang1 stimulation. Ang1 induced expression of Axin2 was dependent on ERG since inhibition of ERG expression by siRNA blocked its induction (Figure 5.5 B). These results suggest that ERG mediates Ang1-dependent activation of the canonical Wnt/ β -catenin pathway.

The essential role of ERG in Ang1-induced activation of Notch signalling was shown by analysing TP luciferase reporter activity and downstream Notch target gene expression in control and ERG-depleted HUVEC following Ang1* treatment. Basal Notch reporter activation was reduced in ERG-deficient EC, in line with Figure 4.4 C. Notch RBPJ transcriptional activity was induced 2.2-fold by Ang1 treatment, as shown previously (Zhang et al., 2011). This increase in luciferase activity was inhibited by depletion of ERG (Figure 5.6 A). In line with this data, both basal expression and induction of Notch target gene Hey1 was decreased in ERG-depleted HUVEC compared to control (Figure 5.6 B), indicating the essential role of ERG in Ang1-induced activation of these signalling pathways.

Since Ang1 induction of Wnt and Notch signalling are ERG-dependent, we examined whether Ang1 induces ERG expression. To test this, HUVEC were treated with two doses of Ang1* for 6 h. Ang1* treatment of HUVEC modestly induced ERG mRNA (Figure 5.7 A) and protein (Figure 5.7 B) expression in a concentration-dependent manner.

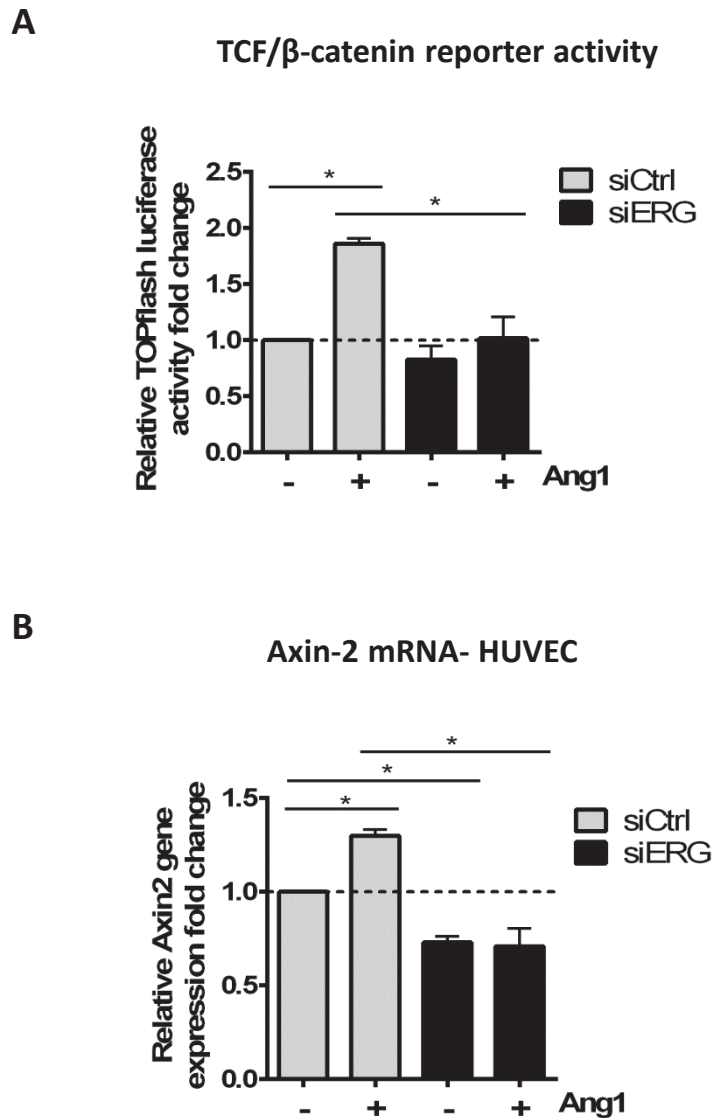


Figure 5.5 ERG is required for Ang1 regulation of Wnt signalling. (A) Ang-1-induced β -catenin transcriptional activity was determined by co-transfecting siCtrl and siERG-treated HUVEC with the TOPflash luciferase reporter and control renilla construct in the presence or absence of rAng-1*. Luciferase activity was measured 24 h later. Values are represented as dual luciferase ratio of firefly luciferase normalised to pGL4 Renilla luciferase and expressed as fold change relative to siCtrl (n=4). (B) β -catenin target gene Axin2 mRNA expression in siCtrl and siERG-transfected HUVEC treated in the presence or absence of Ang1. Results are normalised to GAPDH and expressed as fold change relative to siCtrl (n=3). All graphical data are mean \pm SEM; asterisks indicate significantly different values (ANOVA, followed by Bonferonni's test, where * p <0.05).

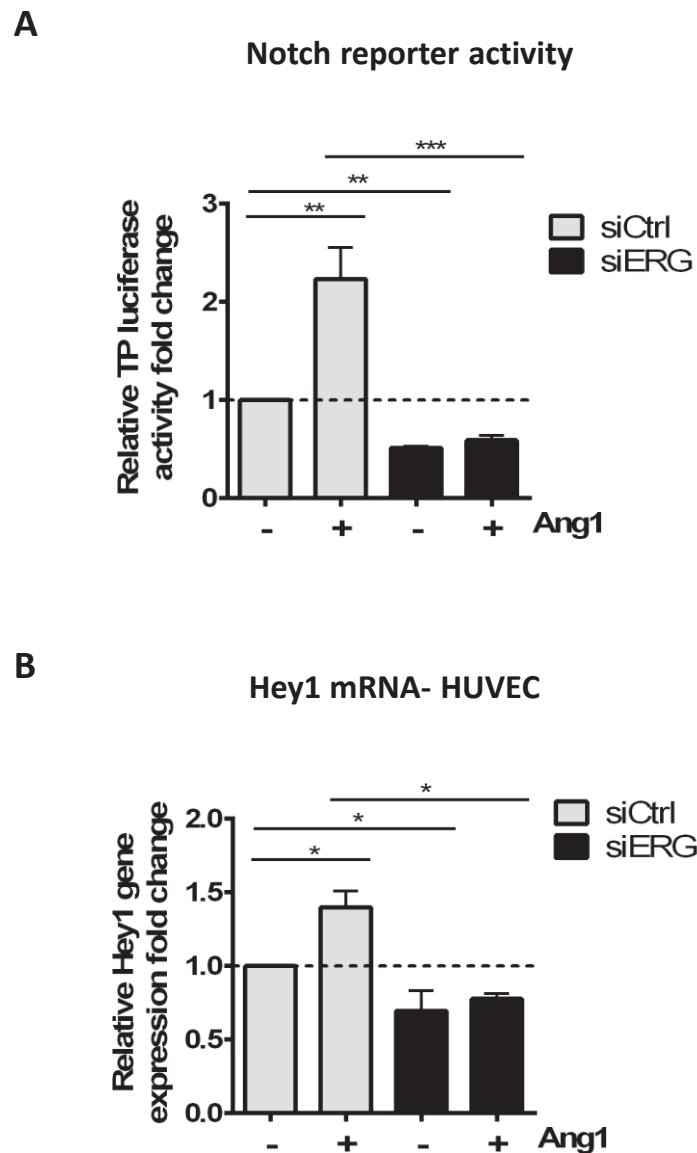


Figure 5.6 ERG is required for Ang1 regulation of Notch signalling. (A) Ang-1-induced Notch transcriptional activity was determined by co-transfecting siCtrl and siERG-treated HUVEC with the TP Notch luciferase reporter and control renilla construct in the presence or absence of rAng-1*. Luciferase activity was measured 24 h later. Values are represented as dual luciferase ratio of firefly luciferase normalised to pGL4 Renilla luciferase and expressed as fold change relative to siCtrl (n=4). (B) Notch target gene Hey1 mRNA expression in siCtrl and siERG-transfected HUVEC treated in the presence or absence of Ang1. Results are normalised to GAPDH and expressed as fold change relative to siCtrl (n=3). All graphical data are mean \pm SEM; asterisks indicate significantly different values (ANOVA, followed by Bonferonni's test, where * p < 0.05, ** p < 0.01, *** p < 0.001)

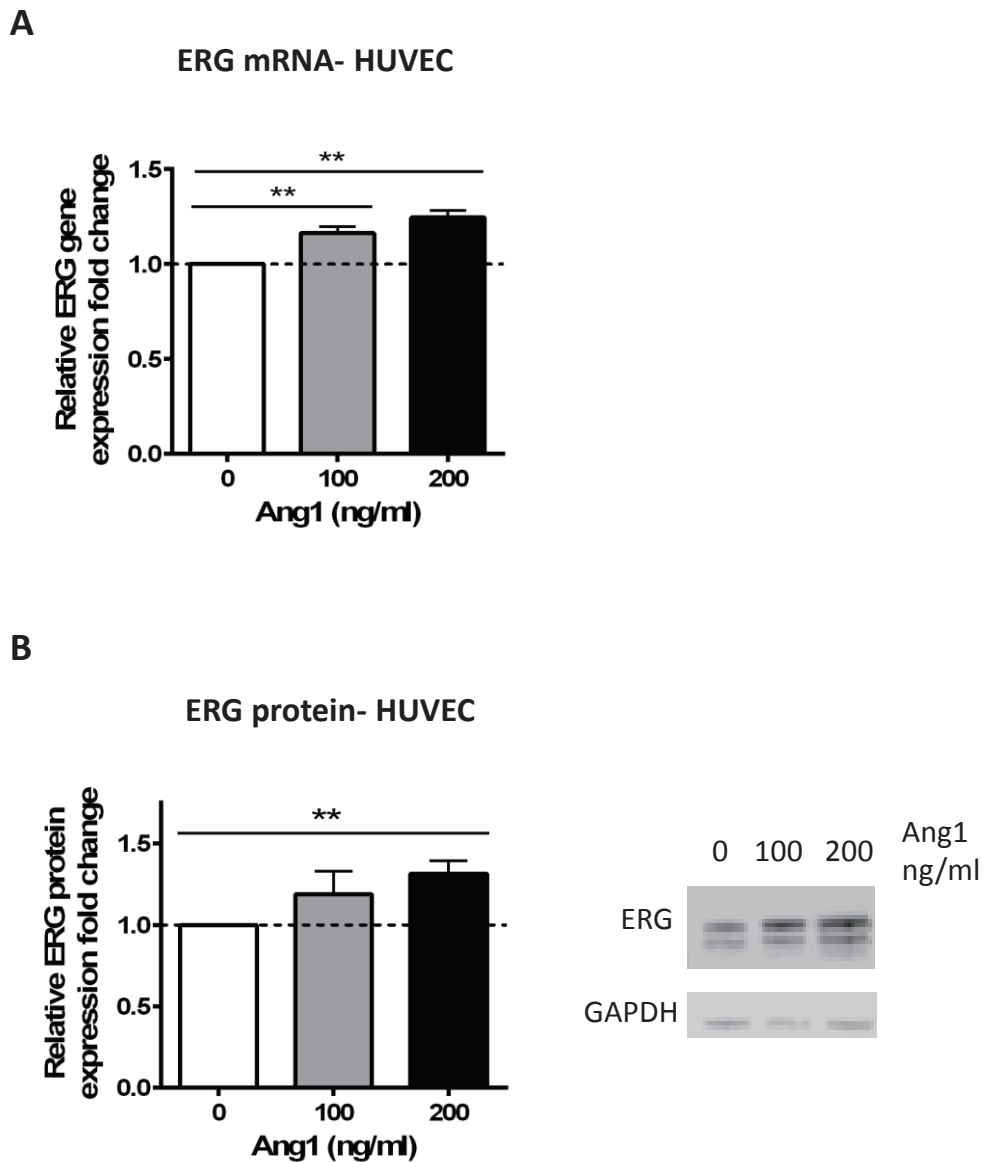


Figure 5.7 Ang1 treatment increases ERG expression in a dose-dependent manner. (A) ERG mRNA expression in HUVEC treated with Ang1 at varying concentrations- 0, 100, 200 ng/ml. Results are normalised to GAPDH and expressed as fold change relative to siCtrl. (B) Western blot analysis of ERG protein expression in extracts of HUVEC treated with rAng1 at 0, 100, 200 ng/ml. Protein levels are normalised to GAPDH and expressed as fold change relative to 0 ng/ml Ang1 treatment. All graphical data are mean \pm SEM; n=3; asterisks indicate significantly different values (ANOVA, followed by Bonferonni's test, where ** p <0.01).

5.2.4 Ang1 induction of Dll4 requires ERG

Studies have shown that Ang1/Tie2 signalling upregulates the Notch ligand Dll4 in confluent cells, promoting vascular stabilization (Fukuhara et al., 2008). Since ERG transcriptionally drives Dll4 expression, I studied whether ERG is required for Ang1-mediated induction of Dll4 expression. Ang1* treatment of HUVEC overnight significantly increased Dll4 mRNA and protein levels in confluent HUVEC by 3 and 1.5 fold respectively, in line with the literature (Figure 5.8). I clarified the requirement of ERG in Ang1-induced Dll4 expression by transfecting HUVEC with siRNA targeting ERG and treating the cells with Ang1. ERG siRNA treatment decreased basal Dll4 mRNA and protein expression to similar levels, as shown previously. Furthermore, depletion of ERG completely abolished Ang1-induction of Dll4 mRNA and protein expression (Figure 5.8). These results suggest that Dll4 up-regulation by Ang1 is dependent on ERG.

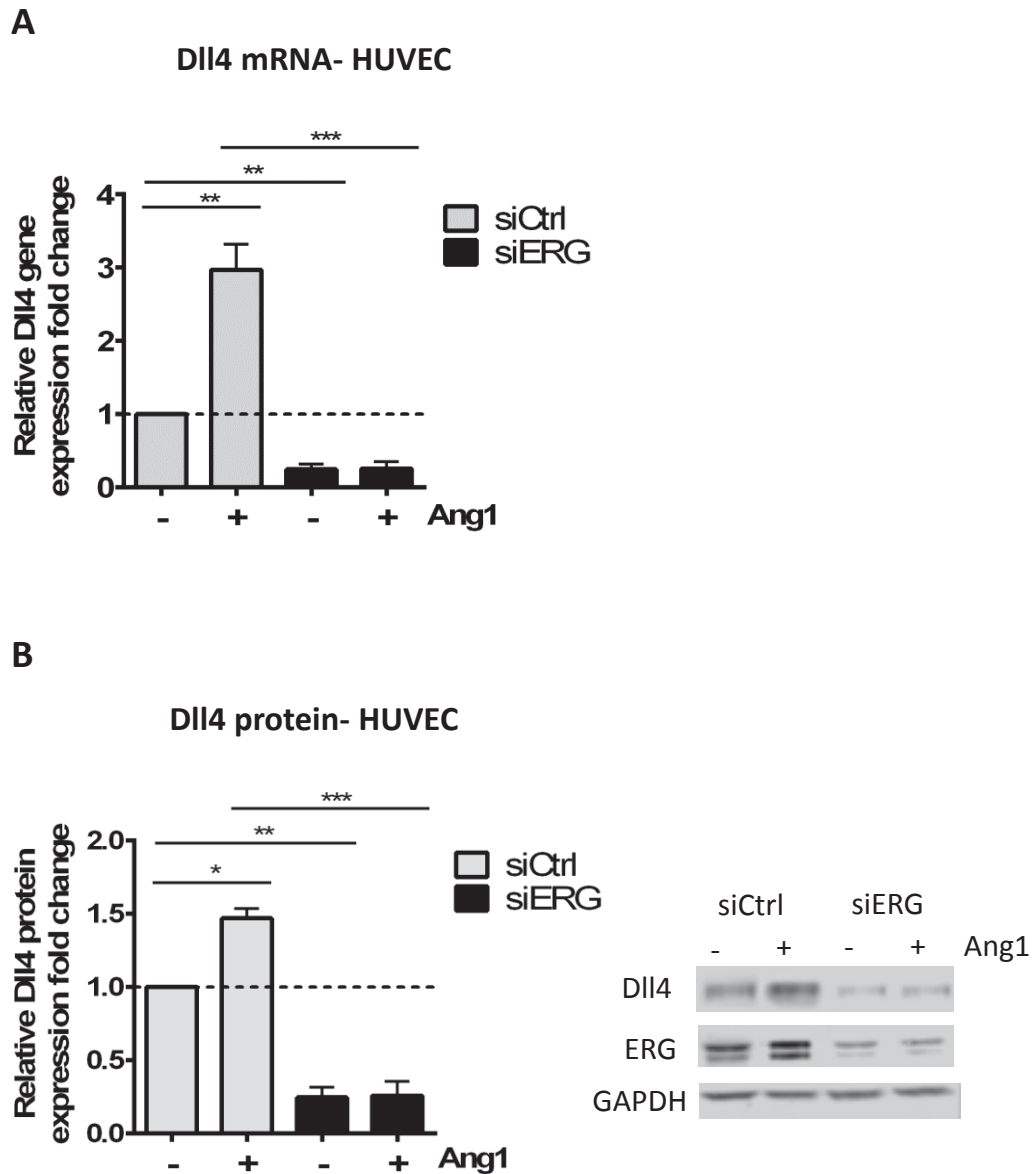


Figure 5.8 ERG is required for Ang1 regulation of Dll4. (A) Dll4 mRNA expression in Control and ERG siRNA (20nM)-transfected HUVEC treated in the presence or absence of Ang1 for 6 hr. Results are normalised to GAPDH and expressed as fold change relative to siCtrl. (B) Left panel: Quantification of fluorescence intensity of Dll4 total protein levels in Control and ERG siRNA-treated cells in the presence or absence of Ang1 for 6 hr. Right panel: Representative blot of Dll4 and ERG protein expression in siCtrl and siERG-treated HUVEC in the presence or absence of Ang1. Results are normalised to GAPDH and expressed as fold change relative to siCtrl. All graphical data are mean \pm SEM; n=3; asterisks indicate significantly different values (ANOVA, followed by Bonferonni's test, where * p < 0.05, ** p < 0.01, *** p < 0.001).

5.2.5 Ang1 increases ERG binding to Dll4 regulatory regions in confluent cells

To investigate whether ERG binding to Dll4 putative regulatory regions is regulated by Ang1 stimulation, ChIP-qPCR was performed on chromatin from HUVEC treated with and without Ang1* for 1 h. Ang1* stimulation increased ERG binding to -16, -12, intron 3, +14 putative enhancer regions and the Dll4 promoter by approximately 2 fold (Figure 5.9). Primers to the negative control region within exon 11 of the Dll4 locus showed no ERG enrichment under control conditions and no further change upon Ang1* stimulation, as expected.

Differential gene expression profiles have been shown in vascular endothelial cells upon Ang1 stimulation in the presence or absence of cell–cell contacts. Since studies have shown that cell-cell contact is required for Ang1 induction of Dll4 expression, I wanted to study whether this effect is mediated through ERG. HUVEC treated with siCtrl or siERG were re-plated at a cell density of 2,000 and 40,000 cells/cm², to model sparse and confluent cultures respectively. Cells were then stimulated with Ang1* under confluent or sparse culture conditions. In line with previous studies, Dll4 mRNA expression was approximately 2 times higher in confluent siCtrl-treated HUVEC than in sparse cells and Ang1* significantly increased Dll4 mRNA levels in confluent, but not sparse, HUVEC (Figure 5.10 A; Zhang et al., 2011; Fukuhara et al., 2008). Depletion of ERG by siRNA decreases basal Dll4 mRNA levels in both sparse and confluent HUVEC and completely abolished Ang1-induced Dll4 expression in confluent HUVEC (Figure 5.10 A).

These findings prompted us to hypothesize that ERG is a cell-cell contact-responsive signal responsible for Ang1-induced Dll4 expression. To address this possibility, the effect of cell confluency and Ang1 on ERG binding to the Dll4 regulatory promoter and enhancer regions was examined by performing a ChIP-qPCR assay. Enrichment of ERG to the DLL4 regulatory regions was detected in sparse HUVEC irrespective of the presence or absence of Ang1* (Figure 5.10 B). In unstimulated confluent cells, I observed a significant increase in ERG binding to Dll4 promoter and enhancers, and Ang1* potently induced additional binding of ERG to the DLL4 regions by approximately 2 fold. Interestingly, this pattern of ERG enrichment in confluent cells following Ang1 treatment mirrors the expression profile of Dll4 in these conditions (Figure 5.10 A).

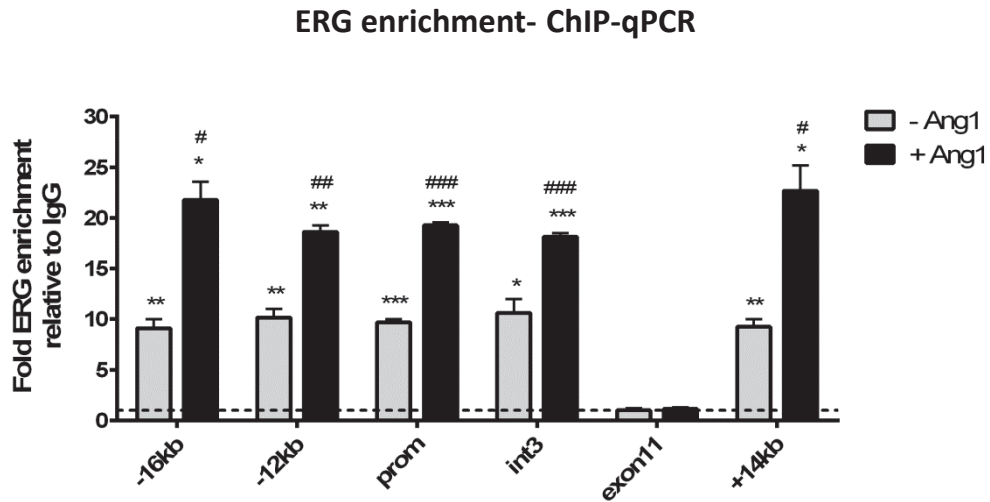


Figure 5.9 Ang1 induces Dll4 expression through increased binding of ERG. ChIP-qPCR analysis of HUVEC treated in the absence or presence of 250 ng/mL Ang1* for 1 hour. Formalin-fixed chromatin was immunoprecipitated with a monoclonal rabbit antibody to ERG or control IgG. Immunoprecipitated DNA was analysed by qPCR with primers to -14kb, -12kb, promoter, intron 3 and +14kb of Dll4 locus. Primers covering a negative control region within exon 11 were also used. Results are expressed as fold change compared to IgG, normalised to input. Values are mean \pm SEM; n=3; (ANOVA, followed by Bonferonni's test, where * p <0.05, ** p <0.01, * p <0.001 indicate significantly different values comparing ERG enrichment to IgG control; where # p <0.05, ## p <0.01, ### p <0.001 indicate significantly different values comparing ERG enrichment in cells in the presence of Ang1 compared to ERG enrichment in cells in the absence of Ang1).

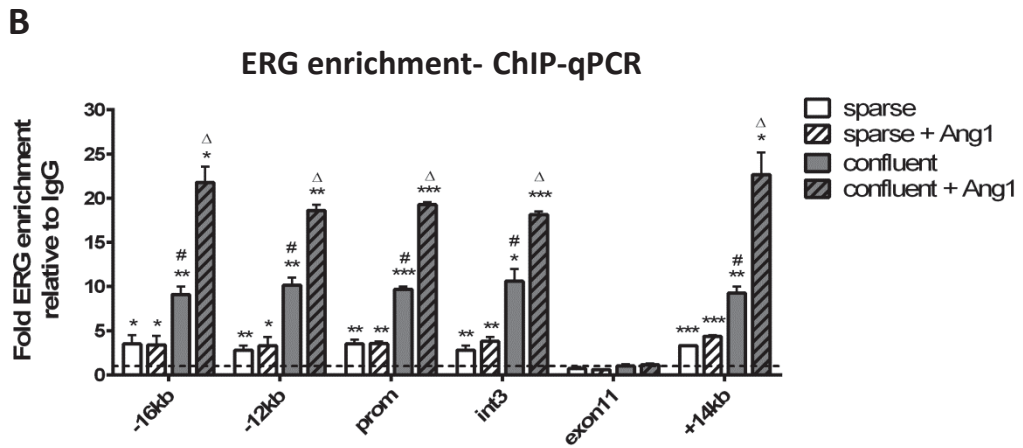
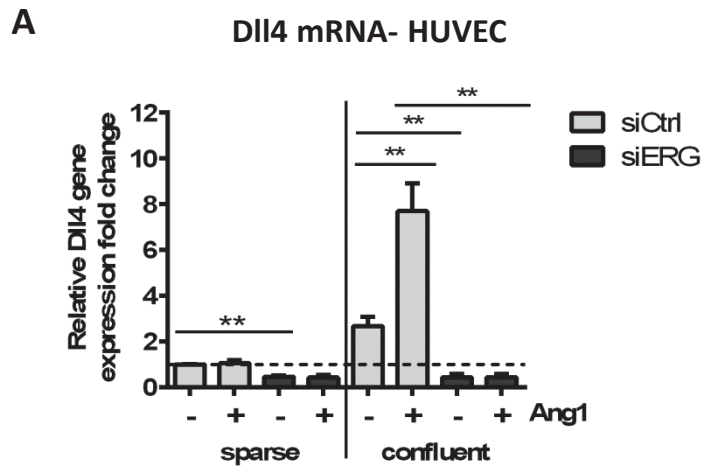


Figure 5.10 Ang1 induction of DII4 in confluent HUVEC is mediated by ERG. (A) Sparse and confluent siCtrl and siERG HUVEC were starved and stimulated with Ang1*. RNA extracts were analysed for DII4 mRNA expression. Results are normalised to GAPDH and expressed as fold change relative to sparse siCtrl HUVEC. Values are mean \pm SEM; n=3; ANOVA, followed by Bonferonni's test, where ** p < 0.01. (B) ChIP assays of sparse and confluent HUVEC treated with Ang1* for 1 hour. Sheared chromatin was immunoprecipitated with an antibody to ERG or control IgG. Immunoprecipitated DNA was analysed by qPCR with primers to -14kb, -12kb, promoter, intron 3 and +14kb of DII4 locus and negative control region exon 11. Results are expressed as fold change compared to IgG, normalised to input. Values are mean \pm SEM; n=3; (ANOVA, followed by Bonferonni's test, where * p < 0.05, ** p < 0.01, *** p < 0.001 indicate significantly different values comparing ERG enrichment to IgG control; where # p < 0.05 indicates significantly different values comparing ERG enrichment in confluent cells to sparse cells; where Δ p < 0.05 indicates significantly different values comparing ERG enrichment in confluent cells treated with Ang1 compared to ERG enrichment in confluent cells in the absence of Ang1).

5.2.6 Ang1 induces Dll4 through a PI3K–Akt–ERG signal axis

It has been proposed that Ang1 stimulation of confluent and sparse cells, recapitulating vascular quiescence and angiogenesis, results in preferential activation of Akt and Erk kinase pathways respectively (Fukuhara et al., 2008; Saharinen et al., 2008). Western blotting analysis of Akt phosphorylation in lysates of sparse and confluent HUVEC treated in the presence or absence of Ang1 confirmed baseline Akt phosphorylation was higher in confluent cells compared to sparse cells (Figure 5.11 A) and Ang1 treatment in confluent cells further increased Akt phosphorylation. This indicates that endothelial cell–cell adhesions positively regulate the Tie2-mediated Akt pathway. Thus, I investigated whether a PI3K–Akt–ERG signal axis is involved in ERG-induced Dll4 expression by using specific inhibitors for PI3K and Akt. HUVEC were transfected with the Dll4 promoter luciferase construct and treated with the PI3K inhibitor LY294002 or Akt inhibitor IV. ERG transactivated the Dll4 promoter by 3.5-fold, as shown previously. Either inhibitor prevented ERG transactivation of the Dll4 promoter construct (Figure 5.11 B), indicating the requirement of the PI3K/Akt pathway for ERG-induced Dll4 expression.

ChIP-qPCR experiments were performed to examine whether the PI3K/Akt pathway could influence the binding of ERG to Dll4 regulatory regions in response to Ang1. ChIP analysis was performed on confluent Ang1*-treated HUVEC that were pre-treated with LY294002 or Akt inhibitor IV. As in Figures 5.9 and 5.10 B, Ang1 induced ERG enrichment to Dll4 regulatory regions (Figure 5.12 A). Interestingly, Ang1-induced ERG enrichment at these loci was ablated in the presence of PI3K or Akt inhibitors (Figure 5.12 A), implicating the PI3K–Akt–ERG signal axis in Ang1-induced Dll4 expression.

Western blot analysis of Ang1*-treated HUVEC that were pre-treated with Akt inhibitor IV showed that Akt inhibitor treatment did not affect ERG protein expression, (Figure 5.12 B). These data provide further evidence for the role of the Ang1-PI3K/Akt axis in regulating ERG function, possibly through indirectly or directly regulating ERG phosphorylation, rather than levels.

Since both β -catenin and NICD have been implicated in Dll4 regulation, I wanted to understand whether β -catenin and NICD potentiate Ang1/ERG signal-mediated Dll4 expression. Therefore I examined the complex formation of β -catenin,

NICD, and ERG on the Dll4 enhancer regions by performing ChIP-qPCR analyses in confluent Ang1*-treated siCtrl and siERG HUVEC. NICD enrichment was examined by ChIP-qPCR using primers to the Dll4 regulatory regions and negative control region (exon 11). Significant binding of NICD to the DLL4 promoter and enhancer regions was detected in confluent HUVEC. This enrichment was unaffected, however, by Ang1 treatment and inhibition of ERG (Figure 5.13 A).

ChIP-qPCR analysis for β -catenin occupancy at Dll4 regulatory regions showed that β -catenin was not enriched at the Dll4 promoter and enhancers in the unstimulated confluent HUVEC. However, Ang1 potently induced binding of β -catenin to the DLL4 promoter and enhancers and importantly this binding required ERG as siERG-treated HUVEC showed no induction of β -catenin occupancy upon Ang1 treatment (Figure 5.13 B). These findings suggest that the Ang1 signal recruits β -catenin to the Dll4 enhancers and this recruitment is ERG-dependent.

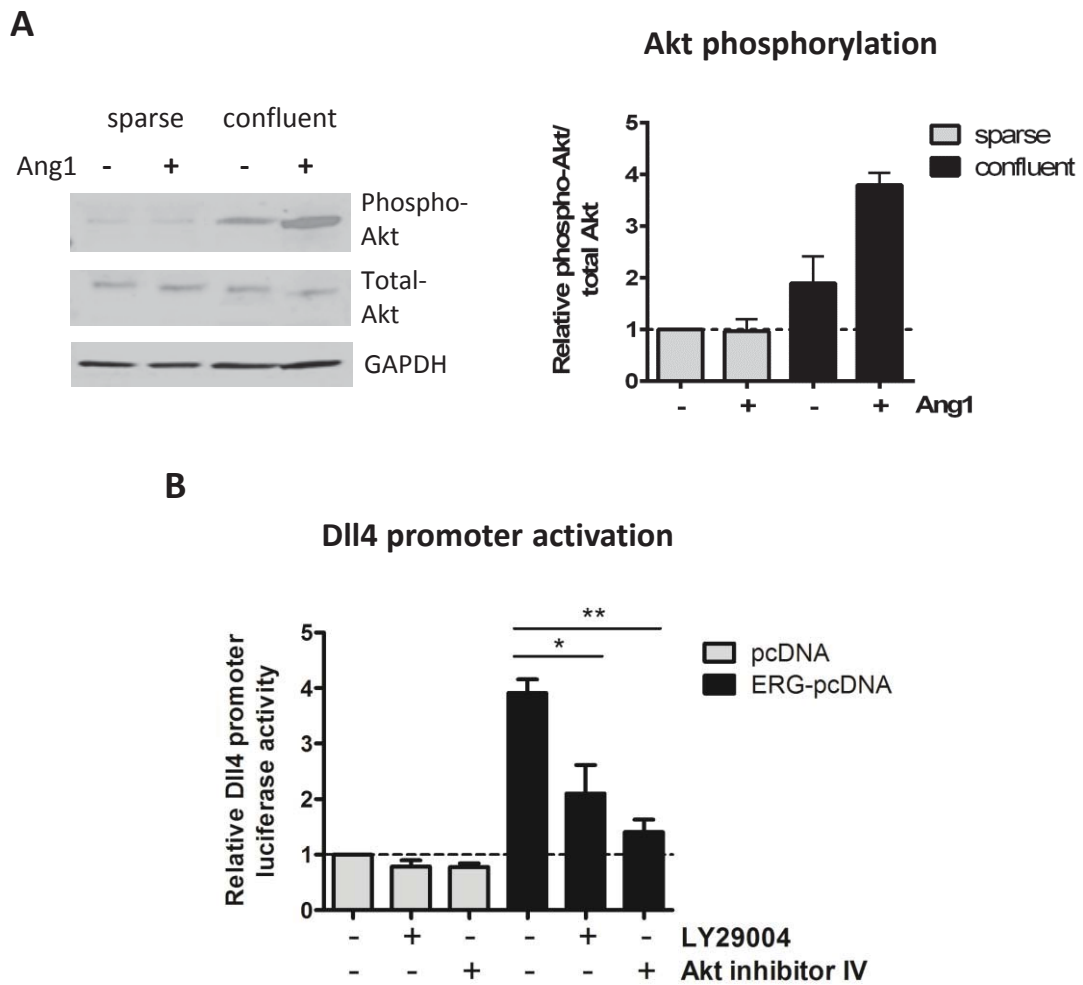


Figure 5.11 ERG induces Dll4 transactivation through the PI3K/AKT pathway. (A) Sparse and confluent HUVEC were starved for 6 h and stimulated with Ang1* for 30 min. Cell lysates were analysed for phosphorylation of Akt and total Akt. Ang1 stimulation of confluent cells preferentially activates Akt phosphorylation. Quantification of Akt phosphorylation represents the ratio of phosphorylated Akt to total Akt protein relative to the ratio in the confluent cells stimulated with Ang1. Values are mean \pm SEM; n=2. (B) ERG cDNA expression plasmid (ERG-pcDNA) or an empty expression plasmid (pcDNA) were cotransfected with the Dll4-pGL4 luciferase construct in HUVEC along with internal control pGL4 renilla luciferase. Cells were treated in the presence or absence of LY294002 or Akt inhibitor IV. Luciferase activity was measured 18 h later. Values are represented as dual luciferase ratio of firefly luciferase normalised to pGL4 renilla luciferase and expressed as fold change relative to Dll4-pGL4 vector alone. Values are mean \pm SEM; n=3; asterisks indicate significantly different values (ANOVA, followed by Bonferonni's test, where * p < 0.05, ** p < 0.01).

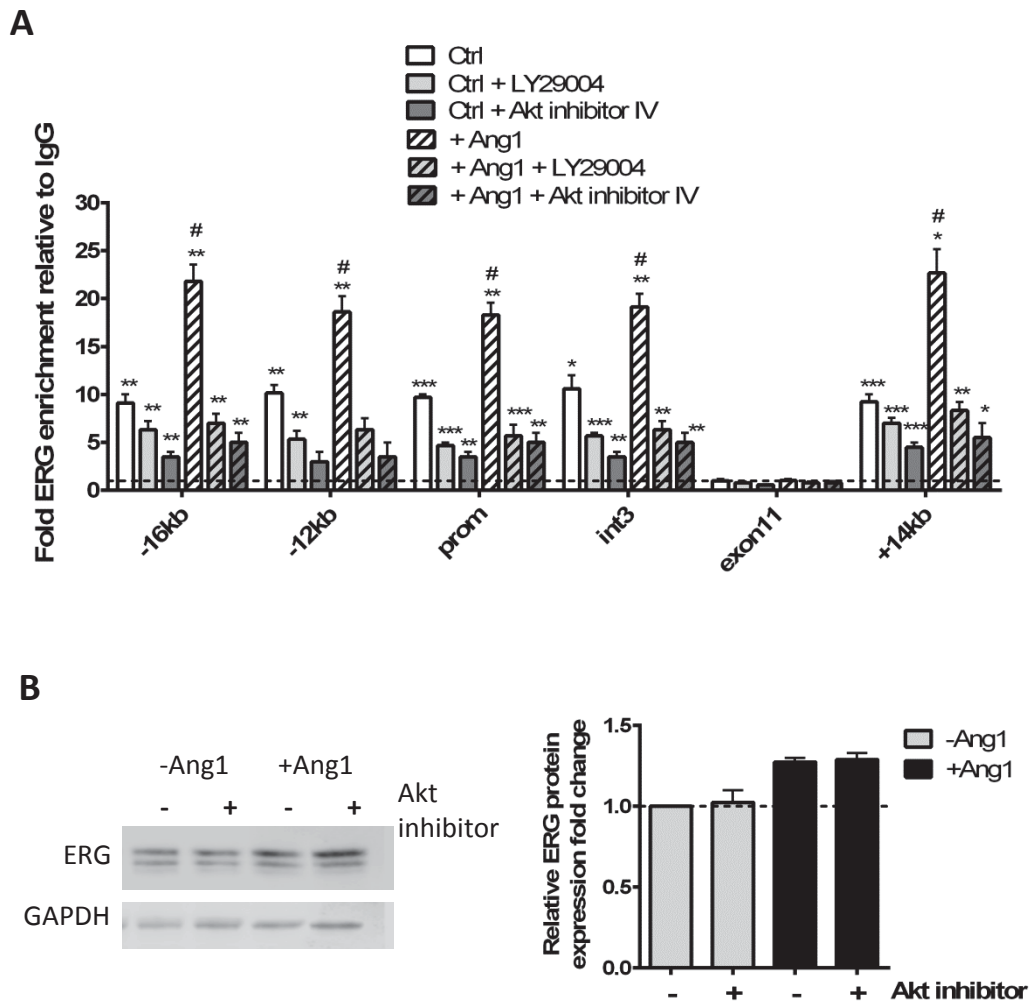


Figure 5.12 Ang1 induces increased binding of ERG to the Dll4 locus through the PI3K/AKT pathway. (A) ChIP assays of HUVEC treated with Ang1 and LY294002 or Akt inhibitor IV. Sheared chromatin was immunoprecipitated with an antibody to ERG or control IgG. Immunoprecipitated DNA was analysed by qPCR with primers to -14kb, -12kb, promoter, intron 3 and +14kb of Dll4 locus and negative control region exon 11. Results are expressed as fold change compared to IgG, normalised to input. Values are mean \pm SEM; n=3; (ANOVA, followed by Bonferonni's test, where * p <0.05, ** p <0.01, *** p <0.001 indicate significantly different values comparing ERG enrichment to IgG control; where # p <0.05 indicates significantly different values comparing ERG enrichment in cells in the presence of Ang1 compared to ERG enrichment in cells in the absence of Ang1). (B) HUVEC were stimulated with Ang1* for 1 h and treated in the presence or absence of Akt inhibitor IV. Cell lysates were analysed for total ERG protein levels. Representative blot shown. Protein levels were normalised to GAPDH and expressed as fold change relative to control treatment. Values are mean \pm SEM; n=2.

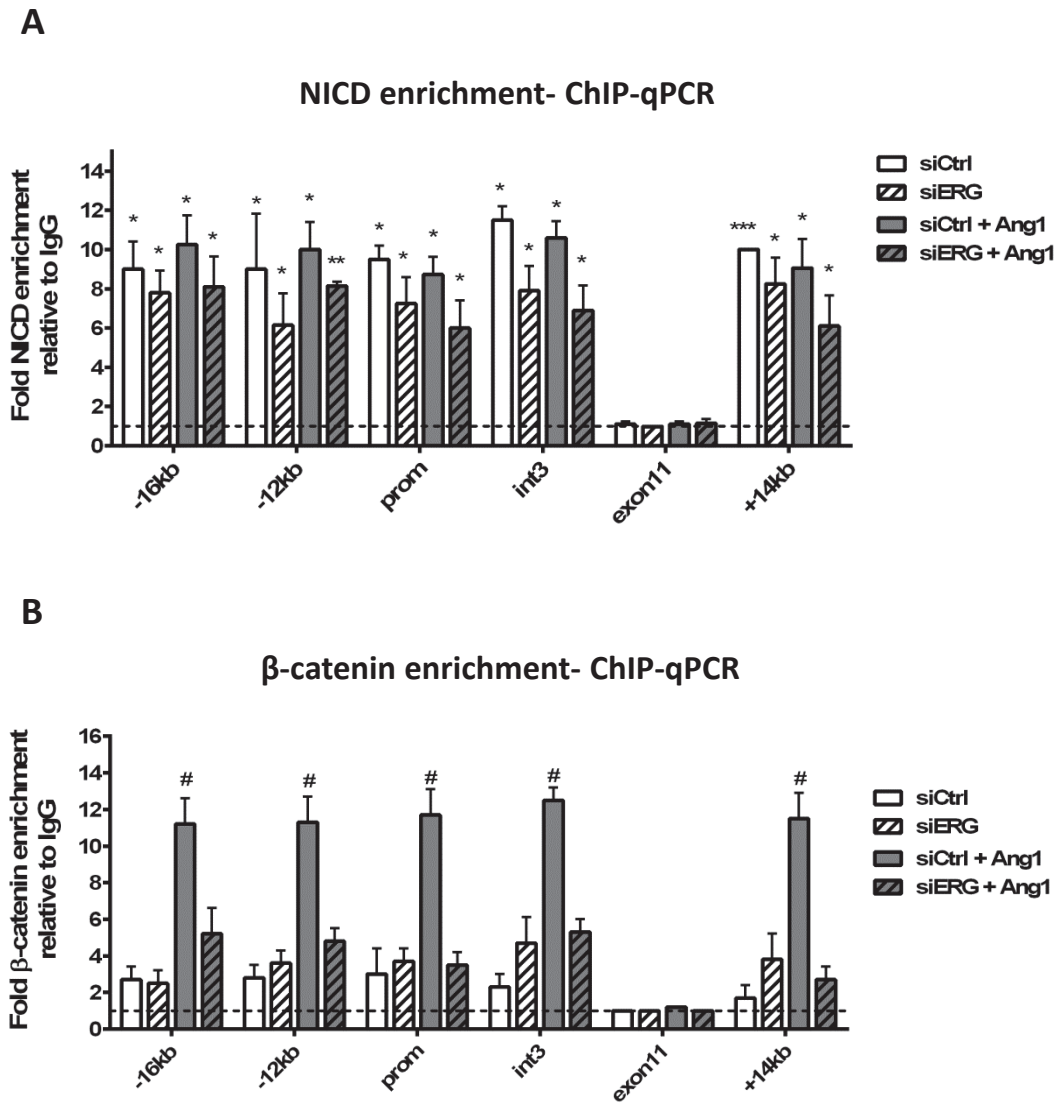


Figure 5.13 Ang1 induces β -catenin occupancy at Dll4 enhancers. ChIP assays of Control and ERG siRNA (20 nM)-treated HUVEC treated in the presence or absence of Ang1*. Sheared chromatin was immunoprecipitated with (A) anti-NICD and (B) anti- β -catenin antibodies or control IgG. Immunoprecipitated DNA was analysed by qPCR with primers to -14kb, -12kb, promoter, intron 3 and +14kb of Dll4 locus. Primers covering a negative control region within exon 11 were also used. Results are expressed as fold change compared to IgG, normalised to input. Values are mean \pm SEM; n=3; (ANOVA, followed by Bonferonni's test, where * p < 0.05, ** p < 0.01, *** p < 0.001 indicate significantly different values comparing NICD or β -catenin enrichment to IgG control; where # p < 0.05 indicates significantly different values comparing NICD or β -catenin enrichment in cells in the presence of Ang1 compared to enrichment in cells in the absence of Ang1).

5.3 Discussion and Future work

Ang1 regulates both vascular quiescence and angiogenesis through the receptor tyrosine kinase Tie2. Previous work has shown that Ang1 and Tie2 form distinct signalling complexes at cell-cell and cell-matrix contacts and that Ang1 upregulates the Notch ligand Dll4 only in the presence of cell-cell contacts (Fukuhara et al., 2008). Dll4/Notch signals restrict sprouting angiogenesis and promote vascular stabilization (reviewed in Phng and Gerhardt, 2009). To clarify the role of the Dll4/Notch signal in Ang1/Tie2 signal-mediated vascular quiescence I investigated the mechanism of how the Ang1/Tie2 signal induces Dll4 expression. My results show that Ang1 induces Dll4 expression through ERG and explore ERG's contribution to Ang1-regulated vascular quiescence (Figure 5.14).

I found that the Ang1/Tie2 signal induces activation of ERG through an Akt-mediated pathway and that ERG combines with β -catenin and Notch to form transcriptional complexes on all putative Dll4 regulatory regions, thereby potentiating the Dll4/Notch signal leading to vascular quiescence (Figure 5.14). Basal Dll4 expression and NICD are higher in confluent cells than in the sparse cells (Zhang et al., 2011), consistent with the previous reports showing that cell-cell contact-dependent Notch signalling induces Dll4 expression. Importantly, Ang1-induced Dll4 expression requires endothelial cell-cell contacts, and is sensitive to DAPT (Zhang et al., 2011), suggesting that Notch signalling is a prerequisite for ERG-mediated Dll4 expression (Figure 5.14).

Augmentation of Dll4 expression by Ang1 is dependent on ERG. It has previously been shown that the Ang1/Tie2 signal preferentially activates PI3K/Akt signalling (Fukuhara et al., 2008). Dll4 expression by Ang1 was inhibited by depletion of ERG and inhibition of either PI3K or Akt, indicating the essential role of ERG for Ang1-induced Dll4 expression.

Ang1 induces recruitment of β -catenin to regulatory regions, also bound by ERG and NICD (Figure 5.14). Thus, Ang1/Tie2 upstream growth factor signals could converge into ERG- β -catenin-NICD transcriptional complexes on the Dll4 promoter and enhancers to cooperatively induce Dll4 expression. Consistently, functional interaction between NICD and β -catenin has recently been reported. Zhang et al. showed that β -catenin enhances Notch signal-mediated Dll4 expression by forming a

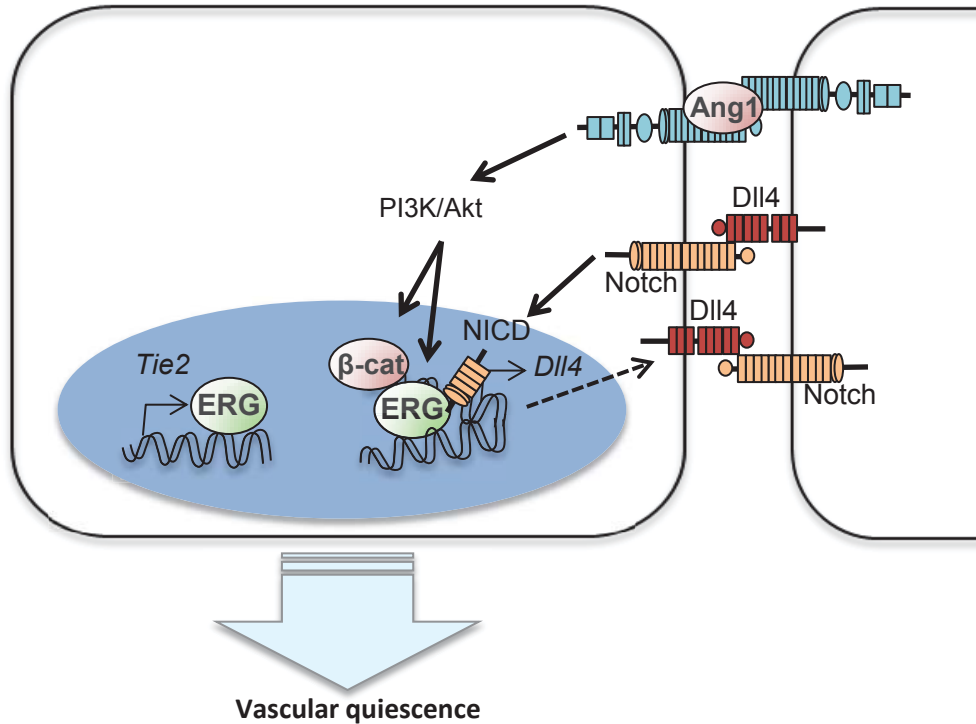


Figure 5.14 Model for how Ang1/Tie2 signal induces Dll4 expression through ERG. In confluent cells, the Ang1/Tie2 signal stimulates the DNA-binding activity of ERG through the PI3K/AKT pathway. Ang1/Tie2 induces Dll4 expression through increased binding of ERG to the Dll4 promoter and multiple enhancer regions. ERG is required for Ang1 induced recruitment of β -catenin to Dll4 regulatory regions. In confluent endothelial cells, cell-cell contact-dependent Notch signalling induces production of NICD, which is also bound to Dll4 regulatory regions but its binding is not effected by Ang1. ERG may be forming a complex with NICD and β -catenin on Dll4 regulatory regions, which potentiates the Notch signal. Additionally, ERG controls expression of the receptor Tie2 in human and mouse EC through a putative enhancer region downstream of the transcription start site (arrow).

complex with NICD/RBP-J on the RBP-J binding site in Dll4 intron 3 (Zhang et al., 2011). In arterial, but not venous, endothelial cells, β -catenin-NICD-RBP-J complexes are formed on the RBP-J binding sites of arterial genes, thereby regulating their expression leading to arterial fate specification (Yamamizu et al., 2010). Here, I show that ERG binds to endogenous NICD and β -catenin in HUVEC, however further investigation is required to elucidate whether stimulus- or cell confluence-specific assembly of transcriptional complexes occur.

Sacilotto et al. have shown that Dll4 expression during embryogenesis requires the direct binding of NICD to the intron 3 and -12kb enhancer (Sacilotto et al., 2013). The authors of this study hypothesized that Notch signalling acquires specificity through the formation of transcriptional complexes with other, more specific factors. This hypothesis is in line with my data, where I showed that NICD occupancy at Dll4 regulatory regions was unaffected by ERG inhibition or Ang1 treatment. Together, this suggests that the Notch signal could, in fact, act upstream of ERG in the transcriptional network and be required for ERG occupancy at these regions; this requires testing.

Interestingly, Ang1 induction of β -catenin occupancy to Dll4 regions could be attributable to Ang1/Akt phosphorylation of GSK3 β (Frame and Cohen, 2001). AKT phosphorylation of GSK3 β on Ser9 renders it inactive and a recent study has shown that GSK3 β inactivation is sufficient to induce Dll4 expression in confluent HUVEC (Zhang et al., 2011). β -catenin undergoes degradation through GSK3 β -mediated phosphorylation, suggesting that Ang1 could stimulate β -catenin-dependent enrichment through AKT-mediated inhibition of GSK3 β .

It is known that EC are extraordinarily diverse in their function and gene-expression profile (Aird, 2007). EC heterogeneity is regulated, in part, by distinct transcriptional mechanisms, which will result in differences in transcription factor binding between cells at any one time. Hence, to further define whether ERG, β -catenin and NICD are binding in the same cell, to the same region, at the same time, requires ChIP re-ChIP analysis, where ERG immunoprecipitated chromatin is probed for the presence of co-factors or transcription factors. ChIP and expression analyses at a single cell level would facilitate the unravelling of critical transcription factor patterns and interactions, especially useful for studying EC dynamically competing for tip and stalk cell positions during angiogenic sprouting.

Confluent cells exhibit preferential PI3K/Akt activation, as cadherin engagement at the junctions induces this kinase pathway (reviewed in Dejana, 2004). In the presence of cell-cell junctions, Ang1 preferentially induces Akt-dependent phosphorylation (Fukuhara et al., 2008; Saharinen et al., 2008). Our data suggests that ERG is a cell-cell contact-responsive signal responsible for Ang1-induced Dll4 expression. Interestingly, the pattern of relative ERG occupancy at Dll4 regulatory regions in confluent cells following Ang1 treatment mirrors the expression profile of Dll4 in these conditions. It would be interesting to test whether a differential gene expression profile is observed in vascular endothelial cells upon ERG inhibition in the presence or absence of cell–cell contacts. This would also help elucidate whether the mechanisms that control Dll4 expression are a more general mechanism regulating ERG function and therefore a panel of transcriptional target genes or instead specific to Dll4. Importantly, Ang1-induced ERG enrichment at Dll4 loci was ablated in the presence of PI3K or Akt inhibitors, without affecting ERG protein expression, providing evidence for the role of the Ang1-PI3K/Akt axis in regulating ERG function, possibly through regulating ERG phosphorylation. Therefore it is crucial to test in future experiments whether PI3K–Akt mediates phosphorylation of ERG and whether this is preferentially induced by Ang1 stimulation in the presence of cell contacts.

As discussed in the introduction, the activity of ETS factors can be altered by modifications such as phosphorylation. Little is known about the post-translational modifications of ERG in endothelial cells. In myeloblast cells ERG is phosphorylated on a serine residue by an activator of the protein kinase C pathway (Murakami et al., 1993); and in TMPRSS2-ERG fusion positive VCaP cells ERG is phosphorylated at Serine-81 and -215, by both IKK and Akt kinases (Singareddy et al., 2013). The phosphorylation of ERG in EC may alter the activity of ERG by affecting its DNA binding, or affecting its interaction with other transcription factors or epigenetic co-factors. There is a lack of tools to investigate ERG phosphorylation directly; however, identification of residues within ERG involved in post-translational modifications and interactions with modifying enzymes would allow us to dissect the roles for these interactions in the transcriptional activity of ERG.

The Akt–FOXO1 pathway is known to be involved in Ang1-induced endothelial cell survival and blood vessel stability. In the presence of cell-cell junctions, Akt-dependent phosphorylation negatively regulates transcriptional activity of FOXO1 by

promoting its nuclear exclusion. This is in line with a prior study where inhibition of FOXO1 activity in mature endothelial cells was shown to be an important mechanism through which Ang1 modulates endothelial function (Daly et al., 2004). The observation that a large subset of genes, including Dll4, that are repressed by FOXO1 are in fact activated by ERG, and vice versa, raise the possibility that FOXO1 and ERG play opposite roles in the endothelium. It is likely that Ang1 signalling influences the post-translational modifications of numerous other transcription factors in the endothelium. An attractive possibility is that Ang1, in the presence of cell-cell contacts, may be phosphorylating both FOXO1 and ERG through Akt, causing inhibition of FOXO1 activity whilst activating ERG transcriptional activity. It is important to determine how ERG is regulated by phosphorylation and whether this influences protein-DNA or protein-protein interactions.

Ang1 binds to and activates Tie2 and recent studies have demonstrated the different signals mediated by Tie2 in the presence or absence of endothelial cell-cell contacts (Fukuhara et al., 2008; Saharinen et al., 2008). I showed that ERG binds within the first intron of the Tie2 gene locus (Figure 5.3A), which previously has been shown *in vivo* to contain endothelial-specific transcriptional enhancer sequences (Schlaeger et al., 1997). Conserved ETS-binding sites have been identified in the Tie2 promoter and members of the ETS gene family, such as NERF2 and ELF-1, have been shown to transcriptionally activate the Tie2 promoter (Dube et al., 1999). These results suggest that multiple ETS factors, including ERG, may cooperate to regulate Tie2 expression through both promoter and enhancer regions. However, regulation of Tie2 is complex, since it has been reported that in the retina Tie2 is expressed in stalk cells, but not in tip cells (Felcht et al., 2012). ERG is expressed in both tip and stalk cells, thus further investigation is required to resolve this mechanism. Immunofluorescence analysis of Tie2 expression in the retinas of *Erg*^{iEC-KO} mice and studying whether ERG regulates Tie2 localisation in the presence of cell-cell contacts would be of interest.

6 Final Summary and Discussion

6.1 ERG regulation of Wnt, Notch and Ang1/Tie2 angiogenesis pathways

The ultimate goal of the complex morphogenetic process of angiogenesis is to produce a functional network of vessels, where cells actively maintain homeostasis and exist mostly in a quiescent state. Whilst this is achieved in physiological angiogenesis, during pathological processes such as tumours and chronic inflammation, new vessels fail to achieve stability and quiescence and remain in a dynamic state of growth, remodelling and regression. Therefore the molecular and cellular mechanisms regulating vessel growth and stability represent promising targets to modulate angiogenesis in disease.

In this study, I focus on the transcription factor ERG as a regulator of angiogenesis. Transcriptome analysis has previously shown that ERG controls a wide network of genes and functions that are essential to vessel growth and stability (Birdsey et al., 2012). These data identify a novel and important level of regulation of angiogenesis mediated by the cross talk between three inter-connected pathways, namely Wnt, Notch and Ang1/Tie2, that are crucial to angiogenesis and show that ERG controls them through multiple, complex mechanisms. Many cellular processes need to be integrated for an organised blood vessel network to form and these three pathways serve as regulators of vessel patterning.

In Chapter 3 of this thesis, I show that ERG controls the Wnt/ β -catenin pathway by promoting β -catenin stability, through signals mediated by VE-cadherin and the Wnt receptor Frizzled-4, the balance of which control β -catenin cellular localization and activity. Importantly, I also show that ERG control of cell survival, proliferation and angiogenesis is mediated through β -catenin. I also show in Chapter 4 that ERG controls Notch signalling in mature EC, by regulating the activation of pro-quiescent Dll4 and repression of pro-angiogenic Jag1, and therefore the balance between these two Notch ligands, suggesting that ERG functions to control Notch-mediated endothelial quiescence.

By controlling both Wnt and Notch pathways, ERG provides a previously undisclosed connection between these essential players in the processes that determine angiogenesis and vascular stability. The Ang1/Tie-2 pathway, also connected to the

Wnt and Notch pathways, is a regulatory molecular system essential for vessel remodelling, maturation and quiescence. Its multiple effects on vascular homeostasis and stability overlap with the functions controlled by ERG. Ang1 also induces β -catenin activation and Dll4 expression, leading to vascular quiescence (Zhang et al., 2011). In Chapter 5, I show that ERG is a cell-cell contact-responsive signal responsible for Ang1-induced Notch and Wnt signalling and explore ERG contribution to Ang1-regulated vascular quiescence. Interestingly, Ang1 itself increases ERG levels in resting cells, in a positive loop to maintain quiescence.

Wnt and Notch signalling pathways act in concert during embryo development in patterning processes and in cell fate decisions (Clevers, 2006; Phng and Gerhardt, 2009). Although the relevance of these two signalling systems is undoubted, the molecular mechanisms that mediate their reciprocal regulation are still not understood completely. In a previous study, Phng et al. reported that Notch can upregulate β -catenin signalling through induction of Nrarp. ERG regulates the Notch target gene Nrarp and this factor acts as a feedback mechanism by limiting Notch on one side while upregulating Wnt signalling on the other. The phenotype of loss of Nrarp *in vivo* is vascular regression. Therefore, Wnt and Notch pathways can reciprocally modulate each other by induction of activators or repressors.

6.2 Control of ERG transcriptional activity

How signalling pathways influence the array of transcription factors involved in the endothelial gene expression program remains an important question in vascular biology. Data in this thesis suggests that ERG and Wnt, Notch and Ang1/Tie2 signalling axes form positive-feedback loops, which may be key in maintaining signalling activity and driving homeostasis. I show that ERG both promotes and is regulated by Wnt, Notch and Ang1/Tie2 signalling as Wnt3a, rDll4 and Ang1 stimulation of HUVEC induced ERG expression. ERG levels are maintained in mature EC from all vascular beds investigated so far, and the pathways to its regulation are still to be investigated. Thus, this is the first report of pathways that physiologically up-regulate ERG expression in EC. Further investigation is required to elucidate whether endothelial ERG expression is regulated by these upstream signals *in vivo* and whether these signals directly drive ERG promoter or enhancer activity. Furthermore, co-immunoprecipitation studies from nuclear extracts also showed that ERG associates

with endogenous β -catenin and NICD. Interestingly, our data suggested that Ang1/Tie2 could converge into ERG- β -catenin-NICD complexes on the Dll4 promoter and enhancers to cooperatively induce Dll4 expression. Consistently, functional interaction between NICD and β -catenin has recently been reported (Yamamizu et al., 2010). Whether ERG- β -catenin-NICD-RBPJ complexes form on gene loci and whether ERG acts to stabilise, mediate or repress their interaction remains to be elucidated. Investigating whether the ERG binding sites identified by ChIP-seq are enriched for β -catenin or NICD/RBPJ motifs and mass spectrometry analysis combined with ChIP techniques, would help elucidate transcriptional protein complexes on ERG target genes. To further define whether ERG, β -catenin and NICD are binding in the same cell, to the same region, at the same time, requires ChIP re-ChIP analysis. Furthermore, ChIP and co-immunoprecipitation studies on control and ERG-deficient HUVEC would help investigate whether the formation of these complexes requires ERG.

As discussed in the introduction, post-translational modifications of ETS factors such as phosphorylation, glycosylation, ubiquitylation, and sumoylation have been shown to affect their activity. Little is known about the post-translational modifications of ERG in endothelial cells, however ERG has been shown to be phosphorylated in other cell types (Singareddy et al., 2013; Murakami et al., 1993). Our data shows that Ang1-induced ERG enrichment at Dll4 loci was ablated in the presence of PI3K or Akt inhibitors, without affecting ERG protein expression, providing evidence for the role of the Ang1-PI3K/Akt axis in regulating ERG function, possibly through regulating ERG phosphorylation. Post-translational modifications of ERG may alter its activity by affecting its DNA binding, or affecting its interaction with other transcription factors or epigenetic co-factors. Identification of residues within ERG involved in mediating post-translational modifications and interactions with modifying enzymes by mass spectrometry analysis, would allow us to dissect the roles for these interactions in the transcriptional activity and function of ERG.

As discussed in previous chapters, the activity of ERG as a transcriptional activator or repressor may depend on interaction with other protein partners. ERG may associate with other transcription factors resulting in activation, inhibition or synergistic regulation of target genes. Likewise, ERG may bind to co-factors, which may cause changes in the chromatin state or post-translationally modify ERG itself. A yeast two-hybrid assay has previously been used to study proteins that bind ERG, and identified

the interaction between ERG and ESET. In addition to providing evidence of direct regulation by ERG proximity to individual genes, the ERG ChIP-seq data provide a resource for exploring the cofactor TFs that bind DNA in complex or nearby, and for discovering the identities of these cofactors. Therefore combining this data with motif discovery software would allow us to probe the ERG ChIP-seq data and identify potential stand-alone or composite motifs located within the ERG-binding sites. Mass spectrometry analysis of would allow analysis of ERG-interacting partners, and combined with CHIP techniques, would help elucidate transcriptional protein complexes on ERG target genes.

We used bioinformatics analysis (GSEA) to investigate whether there was a correlation between genes regulated by ERG and genes regulated by β -catenin. Similar comparison between our ERG microarray data and microarray or ChIP-seq analysis of NICD or β -catenin binding sites would help indicate whether there were a pattern of genes co-regulated by these factors and therefore a potential functional relationship between these pathways. Data from the ENCODE project includes analysis of a number of genetic/epigenetic regulatory features in HUVEC. This allowed *in silico* analysis of the target gene promoters/enhancers to complement our work. Validating whether ERG directly affects the presence of activating modifications on the dynamically regulated genes compared to target genes that are constitutively active in resting EC and assessing DNaseI hypersensitivity sites and RNA polymerase enrichment could help elucidate whether ERG directly confers an activated or repressed chromatin state though the recruitment of activating/repressive epigenetic co-factors.

6.3 ERG as an integrating hub for interconnected pathways

Interestingly, the pathways that control vascular stability can also control destabilising signals, which are required to promote growth; this has been clearly shown for Notch, Wnt and the Ang1/Tie2 system. Equally, ERG deficiency is associated with a decrease in tip cell formation, whilst ERG over-expression results in increased angiogenesis. In a nascent sprout, proliferation and quiescence need to be tightly coordinated with EC junction formation in order to allow stalk cell proliferation whilst maintaining cell-cell contact and sealed vessels. Thus a coordinated balance between these signals must be achieved in order to produce a functional vessel. At the centre of many of these pathways are cell-cell junctions. Ang1 regulates a different set

of genes in sparse versus confluent cells (Fukuhara et al., 2008) and Ang1 up-regulates Dll4 expression only in the presence of cell-cell contacts. In the case of Wnt signalling, cell confluence is clearly at the centre of the control of β -catenin activity. As for Notch signalling, this is also controlled by cell confluence, where cell-cell contact-dependent Notch signalling has been shown to induce Dll4 expression (Benedito et al., 2009). The Notch pathway itself is a cell-cell communication system, mediated by ligands and receptor on neighbouring cells. Thus the ability of ERG to control the expression of multiple endothelial adhesion molecules, namely VE-cadherin, Claudin-5 and ICAM-2, and of other cell surface systems such as Notch and Ang1/Tie2, provides a cell communication network, which orchestrates the signals controlling angiogenesis and vascular quiescence.

The Wnt, Notch and Ang1/Tie2 pathways play pleiotropic roles during tissue and organ development. How these sole pathways produce such morphological complexity at different stages of development is an interesting question. The key to this may lie in the ability of the pathways to integrate with each other and with other signalling pathways to form a more complex signalling system termed a hyper-network (Hurlbut et al., 2007), mediated by an orchestrating core transcriptional network, including ERG. Maybe it is through such an interconnected system that a single pathway generates such a diverse output. In the past few years, we have begun to understand that different endothelial cells have specialized properties and functions. As illustrated in this thesis, ERG is able to integrate with three distinct signalling pathways, potentially to regulate blood vessel patterning during angiogenesis through different mechanisms. It remains to be seen whether ERG signals can integrate with additional pathways in the temporal and spatial regulation of angiogenesis.

References

- Aberle,H., Bauer,A., Stappert,J., Kispert,A., and Kemler,R. (1997). beta-catenin is a target for the ubiquitin-proteasome pathway. *EMBO J.* 16, 3797-3804.
- Aird,W.C. (2007). Phenotypic heterogeneity of the endothelium: I. Structure, function, and mechanisms. *Circ. Res.* 100, 158-173.
- Alastalo,T.P., Li,M., Perez,V.J., Pham,D., Sawada,H., Wang,J.K., Koskenvuo,M., Wang,L., Freeman,B.A., Chang,H.Y., and Rabinovitch,M. (2011). Disruption of PPARgamma/beta-catenin-mediated regulation of apelin impairs BMP-induced mouse and human pulmonary arterial EC survival. *J. Clin. Invest* 121, 3735-3746.
- Alva,J.A. and Iruela-Arispe,M.L. (2004). Notch signaling in vascular morphogenesis. *Curr. Opin. Hematol.* 11, 278-283.
- Amsellem,V., Dryden,N.H., Martinelli,R., Gavins,F., Almagro,L.O., Birdsey,G.M., Haskard,D.O., Mason,J.C., Turowski,P., and Randi,A.M. (2014). ICAM-2 regulates vascular permeability and N-cadherin localization through ezrin-radixin-moesin (ERM) proteins and Rac-1 signalling. *Cell Commun. Signal.* 12, 12.
- Anderson,M.K., Hernandez-Hoyos,G., Diamond,R.A., and Rothenberg,E.V. (1999). Precise developmental regulation of Ets family transcription factors during specification and commitment to the T cell lineage. *Development* 126, 3131-3148.
- Armulik,A., Abramsson,A., and Betsholtz,C. (2005). Endothelial/pericyte interactions. *Circ. Res.* 97, 512-523.
- Armulik,A., Genove,G., Mae,M., Nisancioglu,M.H., Wallgard,E., Niaudet,C., He,L., Norlin,J., Lindblom,P., Strittmatter,K., Johansson,B.R., and Betsholtz,C. (2010). Pericytes regulate the blood-brain barrier. *Nature* 468, 557-561.
- Baltzinger,M., Mager-Heckel,A.M., and Remy,P. (1999). Xl erg: expression pattern and overexpression during development plead for a role in endothelial cell differentiation. *Dev. Dyn.* 216, 420-433.
- Barr,F.G. and Meyer,W.H. (2010). Role of fusion subtype in Ewing sarcoma. *J. Clin. Oncol.* 28, 1973-1974.
- Bazzoni,G. and Dejana,E. (2004). Endothelial cell-to-cell junctions: molecular organization and role in vascular homeostasis. *Physiol Rev.* 84, 869-901.
- Benedito,R., Roca,C., Sorensen,I., Adams,S., Gossler,A., Fruttiger,M., and Adams,R.H. (2009). The notch ligands Dll4 and Jagged1 have opposing effects on angiogenesis. *Cell* 137, 1124-1135.
- Bhanot,P., Brink,M., Samos,C.H., Hsieh,J.C., Wang,Y., Macke,J.P., Andrew,D., Nathans,J., and Nusse,R. (1996). A new member of the frizzled family from Drosophila functions as a Wingless receptor. *Nature* 382, 225-230.
- Birdsey,G.M., Dryden,N.H., Amsellem,V., Gebhardt,F., Sahnan,K., Haskard,D.O., Dejana,E., Mason,J.C., and Randi,A.M. (2008). Transcription factor Erg regulates angiogenesis and endothelial apoptosis through VE-cadherin. *Blood* 111, 3498-3506.

- Birdsey,G.M., Dryden,N.H., Shah,A.V., Hannah,R., Hall,M.D., Haskard,D.O., Parsons,M., Mason,J.C., Zvelebil,M., Gottgens,B., Ridley,A.J., and Randi,A.M. (2012). The transcription factor Erg regulates expression of histone deacetylase 6 and multiple pathways involved in endothelial cell migration and angiogenesis. *Blood* 119, 894-903.
- Birdsey, G.M., Shah, A.V., Dufton, N., Reynolds, L.E., Osuna Almagro, L., Yang, Y., Aspalter, I.M., Khan, S.T., Mason, J.C., Dejana, E., Gttgens, B., Hodivala-Dilke, K., Gerhardt, H., Adams, R.H. and Randi, A.M. (2015). The endothelial transcription factor ERG promotes vascular stability and growth through Wnt/ β -catenin signaling. *Dev Cell*, *in press*
- Birney,E., Stamatoyannopoulos,J.A., Dutta,A., Guigo,R., Gingeras,T.R., Margulies,E.H., Weng,Z., Snyder,M., Dermitzakis,E.T., Thurman,R.E., et al. (2007). Identification and analysis of functional elements in 1% of the human genome by the ENCODE pilot project. *Nature* 447, 799-816.
- Bovolenta,P., Esteve,P., Ruiz,J.M., Cisneros,E., and Lopez-Rios,J. (2008). Beyond Wnt inhibition: new functions of secreted Frizzled-related proteins in development and disease. *J. Cell Sci.* 121, 737-746.
- Bray,S.J. (2006). Notch signalling: a simple pathway becomes complex. *Nat. Rev. Mol. Cell Biol.* 7, 678-689.
- Camuzeaux,B., Spriet,C., Heliot,L., Coll,J., and Duterque-Coquillaud,M. (2005). Imaging Erg and Jun transcription factor interaction in living cells using fluorescence resonance energy transfer analyses. *Biochem. Biophys. Res. Commun.* 332, 1107-1114.
- Caolo,V., van den Akker,N.M., Verbruggen,S., Donners,M.M., Swennen,G., Schulten,H., Waltenberger,J., Post,M.J., and Molin,D.G. (2010). Feed-forward signaling by membrane-bound ligand receptor circuit: the case of NOTCH DELTA-like 4 ligand in endothelial cells. *J. Biol. Chem.* 285, 40681-40689.
- Carlson,T.R., Yan,Y., Wu,X., Lam,M.T., Tang,G.L., Beverly,L.J., Messina,L.M., Capobianco,A.J., Werb,Z., and Wang,R. (2005). Endothelial expression of constitutively active Notch4 elicits reversible arteriovenous malformations in adult mice. *Proc. Natl. Acad. Sci. U. S. A* 102, 9884-9889.
- Carmeliet,P. (2003). Angiogenesis in health and disease. *Nat. Med.* 9, 653-660.
- Carmeliet,P., Ferreira,V., Breier,G., Pollefeyt,S., Kieckens,L., Gertsenstein,M., Fahrig,M., Vandenhoek,A., Harpal,K., Eberhardt,C., Declercq,C., Pawling,J., Moons,L., Collen,D., Risau,W., and Nagy,A. (1996). Abnormal blood vessel development and lethality in embryos lacking a single VEGF allele. *Nature* 380, 435-439.
- Carmeliet,P. and Jain,R.K. (2011). Molecular mechanisms and clinical applications of angiogenesis. *Nature* 473, 298-307.
- Carmeliet,P., Lampugnani,M.G., Moons,L., Breviario,F., Compernelle,V., Bono,F., Balconi,G., Spagnuolo,R., Oosthuysen,B., Dewerchin,M., Zanetti,A., Angellilo,A., Mattot,V., Nuyens,D., Lutgens,E., Clotman,F., de Ruiter,M.C., Gittenberger-de,G.A., Poelmann,R., Lupu,F., Herbert,J.M., Collen,D., and Dejana,E. (1999). Targeted deficiency or cytosolic truncation of the VE-cadherin gene in mice impairs VEGF-mediated endothelial survival and angiogenesis. *Cell* 98, 147-157.

- Carrere,S., Verger,A., Flourens,A., Stehelin,D., and Duterque-Coquillaud,M. (1998). Erg proteins, transcription factors of the Ets family, form homo, heterodimers and ternary complexes via two distinct domains. *Oncogene* 16, 3261-3268.
- Cattelino,A., Liebner,S., Gallini,R., Zanetti,A., Balconi,G., Corsi,A., Bianco,P., Wolburg,H., Moore,R., Oreda,B., Kemler,R., and Dejana,E. (2003). The conditional inactivation of the beta-catenin gene in endothelial cells causes a defective vascular pattern and increased vascular fragility. *J. Cell Biol.* 162, 1111-1122.
- Caveda,L., Martin-Padura,I., Navarro,P., Breviario,F., Corada,M., Gulino,D., Lampugnani,M.G., and Dejana,E. (1996). Inhibition of cultured cell growth by vascular endothelial cadherin (cadherin-5/VE-cadherin). *J. Clin. Invest* 98, 886-893.
- Chen,Z.Y., Battinelli,E.M., Fielder,A., Bunday,S., Sims,K., Breakefield,X.O., and Craig,I.W. (1993). A mutation in the Norrie disease gene (NDP) associated with X-linked familial exudative vitreoretinopathy. *Nat. Genet.* 5, 180-183.
- Claxton,S. and Fruttiger,M. (2004). Periodic Delta-like 4 expression in developing retinal arteries. *Gene Expr. Patterns.* 5, 123-127.
- Clevers,H. (2006). Wnt/beta-catenin signaling in development and disease. *Cell* 127, 469-480.
- Clevers,H. and Nusse,R. (2012). Wnt/beta-catenin signaling and disease. *Cell* 149, 1192-1205.
- Corada,M., Mariotti,M., Thurston,G., Smith,K., Kunkel,R., Brockhaus,M., Lampugnani,M.G., Martin-Padura,I., Stoppacciaro,A., Ruco,L., McDonald,D.M., Ward,P.A., and Dejana,E. (1999). Vascular endothelial-cadherin is an important determinant of microvascular integrity in vivo. *Proc. Natl. Acad. Sci. U. S. A* 96, 9815-9820.
- Corada,M., Nyqvist,D., Orsenigo,F., Caprini,A., Giampietro,C., Taketo,M.M., Iruela-Arispe,M.L., Adams,R.H., and Dejana,E. (2010). The Wnt/beta-catenin pathway modulates vascular remodeling and specification by upregulating Dll4/Notch signaling. *Dev. Cell* 18, 938-949.
- Corada,M., Orsenigo,F., Morini,M.F., Pitulescu,M.E., Bhat,G., Nyqvist,D., Breviario,F., Conti,V., Briot,A., Iruela-Arispe,M.L., Adams,R.H., and Dejana,E. (2013). Sox17 is indispensable for acquisition and maintenance of arterial identity. *Nat. Commun.* 4, 2609.
- Creyghton,M.P., Cheng,A.W., Welstead,G.G., Kooistra,T., Carey,B.W., Steine,E.J., Hanna,J., Lodato,M.A., Frampton,G.M., Sharp,P.A., Boyer,L.A., Young,R.A., and Jaenisch,R. (2010). Histone H3K27ac separates active from poised enhancers and predicts developmental state. *Proc. Natl. Acad. Sci. U. S. A* 107, 21931-21936.
- Crosby,C.V., Fleming,P.A., Argraves,W.S., Corada,M., Zanetta,L., Dejana,E., and Drake,C.J. (2005). VE-cadherin is not required for the formation of nascent blood vessels but acts to prevent their disassembly. *Blood* 105, 2771-2776.
- D'Souza,B., Miyamoto,A., and Weinmaster,G. (2008). The many facets of Notch ligands. *Oncogene* 27, 5148-5167.
- Daly,C., Wong,V., Burova,E., Wei,Y., Zabski,S., Griffiths,J., Lai,K.M., Lin,H.C., Ioffe,E., Yancopoulos,G.D., and Rudge,J.S. (2004). Angiopoietin-1 modulates endothelial cell function and gene expression via the transcription factor FKHR (FOXO1). *Genes Dev.* 18, 1060-1071.

- Daneman,R., Zhou,L., Kebede,A.A., and Barres,B.A. (2010). Pericytes are required for blood-brain barrier integrity during embryogenesis. *Nature* 468, 562-566.
- Davis,G.E. and Senger,D.R. (2005). Endothelial extracellular matrix: biosynthesis, remodeling, and functions during vascular morphogenesis and neovessel stabilization. *Circ. Res.* 97, 1093-1107.
- Davis,S., Aldrich,T.H., Jones,P.F., Acheson,A., Compton,D.L., Jain,V., Ryan,T.E., Bruno,J., Radziejewski,C., Maisonpierre,P.C., and Yancopoulos,G.D. (1996). Isolation of angiopoietin-1, a ligand for the TIE2 receptor, by secretion-trap expression cloning. *Cell* 87, 1161-1169.
- De Val,S. and Black,B.L. (2009). Transcriptional control of endothelial cell development. *Dev. Cell* 16, 180-195.
- De,V.S., Chi,N.C., Meadows,S.M., Minovitsky,S., Anderson,J.P., Harris,I.S., Ehlers,M.L., Agarwal,P., Visel,A., Xu,S.M., Pennacchio,L.A., Dubchak,I., Krieg,P.A., Stainier,D.Y., and Black,B.L. (2008). Combinatorial regulation of endothelial gene expression by ets and forkhead transcription factors. *Cell* 135, 1053-1064.
- Dejana,E. (2004). Endothelial cell-cell junctions: happy together. *Nat. Rev. Mol. Cell Biol.* 5, 261-270.
- Dejana,E. (2010). The role of wnt signaling in physiological and pathological angiogenesis. *Circ. Res.* 107, 943-952.
- Dejana,E., Orsenigo,F., and Lampugnani,M.G. (2008). The role of adherens junctions and VE-cadherin in the control of vascular permeability. *J. Cell Sci.* 121, 2115-2122.
- Dejana,E., Taddei,A., and Randi,A.M. (2007). Foxs and Ets in the transcriptional regulation of endothelial cell differentiation and angiogenesis. *Biochim. Biophys. Acta* 1775, 298-312.
- Delattre,O., Zucman,J., Plougastel,B., Desmaze,C., Melot,T., Peter,M., Kovar,H., Joubert,I., de,J.P., Rouleau,G., and . (1992). Gene fusion with an ETS DNA-binding domain caused by chromosome translocation in human tumours. *Nature* 359, 162-165.
- Deramaudt,B.M., Remy,P., and Abraham,N.G. (1999). Upregulation of human heme oxygenase gene expression by Ets-family proteins. *J. Cell Biochem.* 72, 311-321.
- Descamps,B., Sewduth,R., Ferreira,T.N., Jaspard,B., Reynaud,A., Sohet,F., Lacolley,P., Allieres,C., Lamaziere,J.M., Moreau,C., Dufourcq,P., Couffignal,T., and Duplaa,C. (2012). Frizzled 4 regulates arterial network organization through noncanonical Wnt/planar cell polarity signaling. *Circ. Res.* 110, 47-58.
- Dou,G.R., Wang,Y.C., Hu,X.B., Hou,L.H., Wang,C.M., Xu,J.F., Wang,Y.S., Liang,Y.M., Yao,L.B., Yang,A.G., and Han,H. (2008). RBP-J, the transcription factor downstream of Notch receptors, is essential for the maintenance of vascular homeostasis in adult mice. *FASEB J.* 22, 1606-1617.
- Dryden,N.H., Sperone,A., Martin-Almedina,S., Hannah,R.L., Birdsey,G.M., Khan,S.T., Layhadi,J.A., Mason,J.C., Haskard,D.O., Gottgens,B., and Randi,A.M. (2012). The transcription factor Erg controls endothelial cell quiescence by repressing activity of nuclear factor (NF)-kappaB p65. *J. Biol. Chem.* 287, 12331-12342.

- Duarte,A., Hirashima,M., Benedito,R., Trindade,A., Diniz,P., Bekman,E., Costa,L., Henrique,D., and Rossant,J. (2004). Dosage-sensitive requirement for mouse Dll4 in artery development. *Genes Dev.* 18, 2474-2478.
- Dube,A., Akbarali,Y., Sato,T.N., Libermann,T.A., and Oettgen,P. (1999). Role of the Ets transcription factors in the regulation of the vascular-specific Tie2 gene. *Circ. Res.* 84, 1177-1185.
- Dumont,D.J., Gradwohl,G., Fong,G.H., Puri,M.C., Gertsenstein,M., Auerbach,A., and Breitman,M.L. (1994). Dominant-negative and targeted null mutations in the endothelial receptor tyrosine kinase, tek, reveal a critical role in vasculogenesis of the embryo. *Genes Dev.* 8, 1897-1909.
- Duterque-Coquillaud,M., Niel,C., Plaza,S., and Stehelin,D. (1993). New human erg isoforms generated by alternative splicing are transcriptional activators. *Oncogene* 8, 1865-1873.
- Eilken,H.M. and Adams,R.H. (2010). Dynamics of endothelial cell behavior in sprouting angiogenesis. *Curr. Opin. Cell Biol.* 22, 617-625.
- Felcht,M., Luck,R., Schering,A., Seidel,P., Srivastava,K., Hu,J., Bartol,A., Kienast,Y., Vettel,C., Loos,E.K., Kutschera,S., Bartels,S., Appak,S., Besemfelder,E., Terhardt,D., Chavakis,E., Wieland,T., Klein,C., Thomas,M., Uemura,A., Goerdts,S., and Augustin,H.G. (2012). Angiopoietin-2 differentially regulates angiogenesis through TIE2 and integrin signaling. *J. Clin. Invest* 122, 1991-2005.
- Feng,J., Liu,T., Qin,B., Zhang,Y., and Liu,X.S. (2012). Identifying ChIP-seq enrichment using MACS. *Nat. Protoc.* 7, 1728-1740.
- Ferrara,N. (2004). Vascular endothelial growth factor: basic science and clinical progress. *Endocr. Rev.* 25, 581-611.
- Ferrara,N., Carver-Moore,K., Chen,H., Dowd,M., Lu,L., O'Shea,K.S., Powell-Braxton,L., Hillan,K.J., and Moore,M.W. (1996). Heterozygous embryonic lethality induced by targeted inactivation of the VEGF gene. *Nature* 380, 439-442.
- Fischer,A., Schumacher,N., Maier,M., Sendtner,M., and Gessler,M. (2004). The Notch target genes Hey1 and Hey2 are required for embryonic vascular development. *Genes Dev.* 18, 901-911.
- Frame,S., and Cohen,P. (2001). GSK3 takes centre stage more than 20 years after its discovery. *Biochem. J.* 359, 1-16.
- Franco,C.A., Liebner,S., and Gerhardt,H. (2009). Vascular morphogenesis: a Wnt for every vessel? *Curr. Opin. Genet. Dev.* 19, 476-483.
- Fukuhara,S., Sako,K., Minami,T., Noda,K., Kim,H.Z., Kodama,T., Shibuya,M., Takakura,N., Koh,G.Y., and Mochizuki,N. (2008). Differential function of Tie2 at cell-cell contacts and cell-substratum contacts regulated by angiopoietin-1. *Nat. Cell Biol.* 10, 513-526.
- Gale,N.W., Dominguez,M.G., Noguera,I., Pan,L., Hughes,V., Valenzuela,D.M., Murphy,A.J., Adams,N.C., Lin,H.C., Holash,J., Thurston,G., and Yancopoulos,G.D. (2004). Haploinsufficiency of delta-like 4 ligand results in embryonic lethality due to major defects in arterial and vascular development. *Proc. Natl. Acad. Sci. U. S. A* 101, 15949-15954.

- Gamble, J.R., Drew, J., Trezise, L., Underwood, A., Parsons, M., Kasminkas, L., Rudge, J., Yancopoulos, G., and Vadas, M.A. (2000). Angiopoietin-1 is an antipermeability and anti-inflammatory agent in vitro and targets cell junctions. *Circ. Res.* 87, 603-607.
- Gan, X.Q., Wang, J.Y., Xi, Y., Wu, Z.L., Li, Y.P., and Li, L. (2008). Nuclear Dvl, c-Jun, beta-catenin, and TCF form a complex leading to stabilization of beta-catenin-TCF interaction. *J. Cell Biol.* 180, 1087-1100.
- Gao, X., Wen, J., Zhang, L., Li, X., Ning, Y., Meng, A., and Chen, Y.G. (2008). Dapper1 is a nucleocytoplasmic shuttling protein that negatively modulates Wnt signaling in the nucleus. *J. Biol. Chem.* 283, 35679-35688.
- Gerhardt, H., Golding, M., Fruttiger, M., Ruhrberg, C., Lundkvist, A., Abramsson, A., Jeltsch, M., Mitchell, C., Alitalo, K., Shima, D., and Betsholtz, C. (2003). VEGF guides angiogenic sprouting utilizing endothelial tip cell filopodia. *J. Cell Biol.* 161, 1163-1177.
- Gerhardt, H., Wolburg, H., and Redies, C. (2000). N-cadherin mediates pericytic-endothelial interaction during brain angiogenesis in the chicken. *Dev. Dyn.* 218, 472-479.
- Giampietro, C., Taddei, A., Corada, M., Sarra-Ferraris, G.M., Alcalay, M., Cavallaro, U., Orsenigo, F., Lampugnani, M.G., and Dejana, E. (2012). Overlapping and divergent signaling pathways of N-cadherin and VE-cadherin in endothelial cells. *Blood* 119, 2159-2170.
- Giles, R.H., van Es, J.H., and Clevers, H. (2003). Caught up in a Wnt storm: Wnt signaling in cancer. *Biochim. Biophys. Acta* 1653, 1-24.
- Ginsberg, M., James, D., Ding, B.S., Nolan, D., Geng, F., Butler, J.M., Schachterle, W., Pulijaal, V.R., Mathew, S., Chasen, S.T., Xiang, J., Rosenwaks, Z., Shido, K., Elemento, O., Rabbany, S.Y., and Rafii, S. (2012). Efficient direct reprogramming of mature amniotic cells into endothelial cells by ETS factors and TGFbeta suppression. *Cell* 151, 559-575.
- Glinka, A., Wu, W., Delius, H., Monaghan, A.P., Blumenstock, C., and Niehrs, C. (1998). Dickkopf-1 is a member of a new family of secreted proteins and functions in head induction. *Nature* 391, 357-362.
- Goodwin, A.M. and D'Amore, P.A. (2002). Wnt signaling in the vasculature. *Angiogenesis*. 5, 1-9.
- Goodwin, A.M., Sullivan, K.M., and D'Amore, P.A. (2006). Cultured endothelial cells display endogenous activation of the canonical Wnt signaling pathway and express multiple ligands, receptors, and secreted modulators of Wnt signaling. *Dev. Dyn.* 235, 3110-3120.
- Gory, S., Dalmon, J., Prandini, M.H., Kortulewski, T., de, L.Y., and Huber, P. (1998). Requirement of a GT box (Sp1 site) and two Ets binding sites for vascular endothelial cadherin gene transcription. *J. Biol. Chem.* 273, 6750-6755.
- Goujon, M., McWilliam, H., Li, W., Valentin, F., Squizzato, S., Paern, J., and Lopez, R. (2010). A new bioinformatics analysis tools framework at EMBL-EBI. *Nucleic Acids Res.* 38, W695-W699.
- Green, S.M., Coyne, H.J., III, McIntosh, L.P., and Graves, B.J. (2010). DNA binding by the ETS protein TEL (ETV6) is regulated by autoinhibition and self-association. *J. Biol. Chem.* 285, 18496-18504.

Grego-Bessa,J., Luna-Zurita,L., del,M.G., Bolos,V., Melgar,P., Arandilla,A., Garratt,A.N., Zang,H., Mukoyama,Y.S., Chen,H., Shou,W., Ballestar,E., Esteller,M., Rojas,A., Perez-Pomares,J.M., and de la Pompa,J.L. (2007). Notch signaling is essential for ventricular chamber development. *Dev. Cell* 12, 415-429.

Gridley,T. (1997). Notch signaling in vertebrate development and disease. *Mol. Cell Neurosci.* 9, 103-108.

Griffin,C.T., Curtis,C.D., Davis,R.B., Muthukumar,V., and Magnuson,T. (2011). The chromatin-remodeling enzyme BRG1 modulates vascular Wnt signaling at two levels. *Proc. Natl. Acad. Sci. U. S. A* 108, 2282-2287.

Gupta,S., Iljin,K., Sara,H., Mpindi,J.P., Mirtti,T., Vainio,P., Rantala,J., Alanen,K., Nees,M., and Kallioniemi,O. (2010). FZD4 as a mediator of ERG oncogene-induced WNT signaling and epithelial-to-mesenchymal transition in human prostate cancer cells. *Cancer Res.* 70, 6735-6745.

Hellstrom,M., Phng,L.K., Hofmann,J.J., Wallgard,E., Coultas,L., Lindblom,P., Alva,J., Nilsson,A.K., Karlsson,L., Gaiano,N., Yoon,K., Rossant,J., Iruela-Arispe,M.L., Kalen,M., Gerhardt,H., and Betsholtz,C. (2007). Dll4 signalling through Notch1 regulates formation of tip cells during angiogenesis. *Nature* 445, 776-780.

Hewett,P.W., Nishi,K., Daft,E.L., and Clifford,M.J. (2001). Selective expression of erg isoforms in human endothelial cells. *Int. J. Biochem. Cell Biol.* 33, 347-355.

Hofmann,J.J. and Iruela-Arispe,M.L. (2007). Notch signaling in blood vessels: who is talking to whom about what? *Circ. Res.* 100, 1556-1568.

Hollenhorst,P.C., Jones,D.A., and Graves,B.J. (2004). Expression profiles frame the promoter specificity dilemma of the ETS family of transcription factors. *Nucleic Acids Res.* 32, 5693-5702.

Hollenhorst,P.C., Shah,A.A., Hopkins,C., and Graves,B.J. (2007). Genome-wide analyses reveal properties of redundant and specific promoter occupancy within the ETS gene family. *Genes Dev.* 21, 1882–1894.

Hollenhorst,P.C., McIntosh,L.P., and Graves,B.J. (2011). Genomic and biochemical insights into the specificity of ETS transcription factors. *Annu. Rev. Biochem.* 80, 437-471.

Hurlbut,G.D., Kankel,M.W., Lake,R.J., and Artavanis-Tsakonas,S. (2007). Crossing paths with Notch in the hyper-network. *Curr. Opin. Cell Biol.* 19, 166-175.

Ishikawa,T., Tamai,Y., Zorn,A.M., Yoshida,H., Seldin,M.F., Nishikawa,S., and Taketo,M.M. (2001). Mouse Wnt receptor gene *Fzd5* is essential for yolk sac and placental angiogenesis. *Development* 128, 25-33.

Isogai,S., Lawson,N.D., Torrealday,S., Horiguchi,M., and Weinstein,B.M. (2003). Angiogenic network formation in the developing vertebrate trunk. *Development* 130, 5281-5290.

Iwamoto,M., Higuchi,Y., Koyama,E., Enomoto-Iwamoto,M., Kurisu,K., Yeh,H., Abrams,W.R., Rosenbloom,J., and Pacifici,M. (2000). Transcription factor ERG variants and functional diversification of chondrocytes during limb long bone development. *J. Cell Biol.* 150, 27-40.

Johnston,D.A., Dong,B., and Hughes,C.C. (2009). TNF induction of jagged-1 in endothelial cells is NFkappaB-dependent. *Gene* 435, 36-44.

- Kageyama,R., Masamizu,Y., and Niwa,Y. (2007). Oscillator mechanism of Notch pathway in the segmentation clock. *Dev. Dyn.* 236, 1403-1409.
- Kaidi,A., Williams,A.C., and Paraskeva,C. (2007). Interaction between beta-catenin and HIF-1 promotes cellular adaptation to hypoxia. *Nat. Cell Biol.* 9, 210-217.
- Kim,I., Kim,H.G., So,J.N., Kim,J.H., Kwak,H.J., and Koh,G.Y. (2000). Angiopoietin-1 regulates endothelial cell survival through the phosphatidylinositol 3'-Kinase/Akt signal transduction pathway. *Circ. Res.* 86, 24-29.
- Kim,Y.H., Hu,H., Guevara-Gallardo,S., Lam,M.T., Fong,S.Y., and Wang,R.A. (2008). Artery and vein size is balanced by Notch and ephrin B2/EphB4 during angiogenesis. *Development* 135, 3755-3764.
- Kisanuki,Y.Y., Hammer,R.E., Miyazaki,J., Williams,S.C., Richardson,J.A., and Yanagisawa,M. (2001). Tie2-Cre transgenic mice: a new model for endothelial cell-lineage analysis in vivo. *Dev. Biol.* 230, 230-242.
- Korinek,V., Barker,N., Morin,P.J., van Wichen D., de Weger R., Kinzler,K.W., Vogelstein,B., and Clevers,H. (1997). Constitutive transcriptional activation by a beta-catenin-Tcf complex in APC-/- colon carcinoma. *Science* 275, 1784-1787.
- Krebs,L.T., Shutter,J.R., Tanigaki,K., Honjo,T., Stark,K.L., and Gridley,T. (2004). Haploinsufficient lethality and formation of arteriovenous malformations in Notch pathway mutants. *Genes Dev.* 18, 2469-2473.
- Krebs,L.T., Xue,Y., Norton,C.R., Shutter,J.R., Maguire,M., Sundberg,J.P., Gallahan,D., Closson,V., Kitajewski,J., Callahan,R., Smith,G.H., Stark,K.L., and Gridley,T. (2000). Notch signaling is essential for vascular morphogenesis in mice. *Genes Dev.* 14, 1343-1352.
- Krieghoff,E., Behrens,J., and Mayr,B. (2006). Nucleo-cytoplasmic distribution of beta-catenin is regulated by retention. *J. Cell Sci.* 119, 1453-1463.
- Kypta,R.M. and Waxman,J. (2012). Wnt/beta-catenin signalling in prostate cancer. *Nat. Rev. Urol.* 9, 418-428.
- Lacronique,V., Boureux,A., Valle,V.D., Poirel,H., Quang,C.T., Mauchauffe,M., Berthou,C., Lessard,M., Berger,R., Ghysdael,J., and Bernard,O.A. (1997). A TEL-JAK2 fusion protein with constitutive kinase activity in human leukemia. *Science* 278, 1309-1312.
- Larkin,M.A., Blackshields,G., Brown,N.P., Chenna,R., McGettigan,P.A., McWilliam,H., Valentin,F., Wallace,I.M., Wilm,A., Lopez,R., Thompson,J.D., Gibson,T.J., and Higgins,D.G. (2007). Clustal W and Clustal X version 2.0. *Bioinformatics.* 23, 2947-2948.
- Lawson,N.D., Scheer,N., Pham,V.N., Kim,C.H., Chitnis,A.B., Campos-Ortega,J.A., and Weinstein,B.M. (2001). Notch signaling is required for arterial-venous differentiation during embryonic vascular development. *Development* 128, 3675-3683.
- Lee,S.H., Lee,S., Yang,H., Song,S., Kim,K., Saunders,T.L., Yoon,J.K., Koh,G.Y., and Kim,I. (2014). Notch pathway targets proangiogenic regulator Sox17 to restrict angiogenesis. *Circ. Res.* 115, 215-226.
- Leslie,J.D., Ariza-McNaughton,L., Bermange,A.L., McAdow,R., Johnson,S.L., and Lewis,J. (2007). Endothelial signalling by the Notch ligand Delta-like 4 restricts angiogenesis. *Development* 134, 839-844.

- Liebner,S., Corada,M., Bangsow,T., Babbage,J., Taddei,A., Czupalla,C.J., Reis,M., Felici,A., Wolburg,H., Fruttiger,M., Taketo,M.M., von,M.H., Plate,K.H., Gerhardt,H., and Dejana,E. (2008). Wnt/beta-catenin signaling controls development of the blood-brain barrier. *J. Cell Biol.* 183, 409-417.
- Liu,F. and Patient,R. (2008). Genome-wide analysis of the zebrafish ETS family identifies three genes required for hemangioblast differentiation or angiogenesis. *Circ. Res.* 103, 1147-1154.
- Lobov,I.B., Rao,S., Carroll,T.J., Vallance,J.E., Ito,M., Ondr,J.K., Kurup,S., Glass,D.A., Patel,M.S., Shu,W., Morrisey,E.E., McMahon,A.P., Karsenty,G., and Lang,R.A. (2005). WNT7b mediates macrophage-induced programmed cell death in patterning of the vasculature. *Nature* 437, 417-421.
- Lobov,I.B., Renard,R.A., Papadopoulos,N., Gale,N.W., Thurston,G., Yancopoulos,G.D., and Wiegand,S.J. (2007). Delta-like ligand 4 (Dll4) is induced by VEGF as a negative regulator of angiogenic sprouting. *Proc. Natl. Acad. Sci. U. S. A* 104, 3219-3224.
- Loughran,S.J., Kruse,E.A., Hacking,D.F., de Graaf,C.A., Hyland,C.D., Willson,T.A., Henley,K.J., Ellis,S., Voss,A.K., Metcalf,D., Hilton,D.J., Alexander,W.S., and Kile,B.T. (2008). The transcription factor Erg is essential for definitive hematopoiesis and the function of adult hematopoietic stem cells. *Nat. Immunol.* 9, 810-819.
- Louvi,A., Arboleda-Velasquez,J.F., and Artavanis-Tsakonas,S. (2006). CADASIL: a critical look at a Notch disease. *Dev. Neurosci.* 28, 5-12.
- Lu,X., Le,N.F., Yuan,L., Jiang,Q., De,L.B., Sugiyama,D., Breant,C., Claes,F., De,S.F., Thomas,J.L., Autiero,M., Carmeliet,P., Tessier-Lavigne,M., and Eichmann,A. (2004). The netrin receptor UNC5B mediates guidance events controlling morphogenesis of the vascular system. *Nature* 432, 179-186.
- Marchuk,D.A. (1998). Genetic abnormalities in hereditary hemorrhagic telangiectasia. *Curr. Opin. Hematol.* 5, 332-338.
- Maretto,S., Cordenonsi,M., Dupont,S., Braghetta,P., Broccoli,V., Hassan,A.B., Volpin,D., Bressan,G.M., and Piccolo,S. (2003). Mapping Wnt/beta-catenin signaling during mouse development and in colorectal tumors. *Proc. Natl. Acad. Sci. U. S. A* 100, 3299-3304.
- Masckauchan,T.N., Agalliu,D., Vorontchikhina,M., Ahn,A., Parmalee,N.L., Li,C.M., Khoo,A., Tycko,B., Brown,A.M., and Kitajewski,J. (2006). Wnt5a signaling induces proliferation and survival of endothelial cells in vitro and expression of MMP-1 and Tie-2. *Mol. Biol. Cell* 17, 5163-5172.
- Masckauchan,T.N., Shawber,C.J., Funahashi,Y., Li,C.M., and Kitajewski,J. (2005). Wnt/beta-catenin signaling induces proliferation, survival and interleukin-8 in human endothelial cells. *Angiogenesis.* 8, 43-51.
- McLaughlin,F., Ludbrook,V.J., Cox,J., von Carlowitz,I., Brown,S., and Randi,A.M. (2001). Combined genomic and antisense analysis reveals that the transcription factor Erg is implicated in endothelial cell differentiation. *Blood* 98, 3332-3339.
- McLaughlin,F., Ludbrook,V.J., Kola,I., Campbell,C.J., and Randi,A.M. (1999). Characterisation of the tumour necrosis factor (TNF)-(alpha) response elements in the human ICAM-2 promoter. *J. Cell Sci.* 112 (Pt 24), 4695-4703.

- Meadows,S.M., Salanga,M.C., and Krieg,P.A. (2009). Kruppel-like factor 2 cooperates with the ETS family protein ERG to activate Flk1 expression during vascular development. *Development* 136, 1115-1125.
- Mohamed,A.A., Tan,S.H., Mikhailkevich,N., Ponniah,S., Vasioukhin,V., Bieberich,C.J., Sesterhenn,I.A., Dobi,A., Srivastava,S., and Sreenath,T.L. (2010). Ets family protein, erg expression in developing and adult mouse tissues by a highly specific monoclonal antibody. *J. Cancer* 1, 197-208.
- Monkley,S.J., Delaney,S.J., Pennisi,D.J., Christiansen,J.H., and Wainwright,B.J. (1996). Targeted disruption of the Wnt2 gene results in placentation defects. *Development* 122, 3343-3353.
- Moulton,K.S., Semple,K., Wu,H., and Glass,C.K. (1994). Cell-specific expression of the macrophage scavenger receptor gene is dependent on PU.1 and a composite AP-1/ets motif. *Mol. Cell Biol.* 14, 4408-4418.
- Murakami,K., Mavrothalassitis,G., Bhat,N.K., Fisher,R.J., and Papas,T.S. (1993). Human ERG-2 protein is a phosphorylated DNA-binding protein--a distinct member of the ets family. *Oncogene* 8, 1559-1566.
- Myers,R.M., Stamatoyannopoulos,J., Snyder,M., Dunham,I., Hardison,R.C., Bernstein,B.E., Gingeras,T.R., Kent,W.J., Birney,E., Wold,B., and Crawford,G.E. (2011). A user's guide to the encyclopedia of DNA elements (ENCODE). *PLoS. Biol.* 9, e1001046.
- Nakatsu,M.N., Davis,J., and Hughes,C.C. (2007). Optimized fibrin gel bead assay for the study of angiogenesis. *J. Vis. Exp.* 186.
- Navarro,P., Caveda,L., Breviario,F., Mandoteanu,I., Lampugnani,M.G., and Dejana,E. (1995). Catenin-dependent and -independent functions of vascular endothelial cadherin. *J. Biol. Chem.* 270, 30965-30972.
- Nikolova-Krstevski,V., Yuan,L., Le,B.A., Vijayaraj,P., Kondo,M., Gebauer,I., Bhasin,M., Carman,C.V., and Oettgen,P. (2009). ERG is required for the differentiation of embryonic stem cells along the endothelial lineage. *BMC. Dev. Biol.* 9, 72.
- Nosedá,M., Chang,L., McLean,G., Grim,J.E., Clurman,B.E., Smith,L.L., and Karsan,A. (2004). Notch activation induces endothelial cell cycle arrest and participates in contact inhibition: role of p21Cip1 repression. *Mol. Cell Biol.* 24, 8813-8822.
- Oellerich,M.F. and Potente,M. (2012). FOXOs and sirtuins in vascular growth, maintenance, and aging. *Circ. Res.* 110, 1238-1251.
- Oikawa,T. and Yamada,T. (2003). Molecular biology of the Ets family of transcription factors. *Gene* 303, 11-34.
- Owczarek,C.M., Portbury,K.J., Hardy,M.P., O'Leary,D.A., Kudoh,J., Shibuya,K., Shimizu,N., Kola,I., and Hertzog,P.J. (2004). Detailed mapping of the ERG-ETS2 interval of human chromosome 21 and comparison with the region of conserved synteny on mouse chromosome 16. *Gene* 324, 65-77.
- Paik,J.H., Skoura,A., Chae,S.S., Cowan,A.E., Han,D.K., Proia,R.L., and Hla,T. (2004). Sphingosine 1-phosphate receptor regulation of N-cadherin mediates vascular stabilization. *Genes Dev.* 18, 2392-2403.

- Peter,M., Mugneret,F., Aurias,A., Thomas,G., Magdelenat,H., and Delattre,O. (1996). An EWS/ERG fusion with a truncated N-terminal domain of EWS in a Ewing's tumor. *Int. J. Cancer* 67, 339-342.
- Phng,L.K. and Gerhardt,H. (2009). Angiogenesis: a team effort coordinated by notch. *Dev. Cell* 16, 196-208.
- Phng,L.K., Potente,M., Leslie,J.D., Babbage,J., Nyqvist,D., Lobov,I., Ondr,J.K., Rao,S., Lang,R.A., Thurston,G., and Gerhardt,H. (2009). Nrarp coordinates endothelial Notch and Wnt signaling to control vessel density in angiogenesis. *Dev. Cell* 16, 70-82.
- Pierce,J.W., Schoenleber,R., Jesmok,G., Best,J., Moore,S.A., Collins,T., and Gerritsen,M.E. (1997). Novel inhibitors of cytokine-induced IkappaBalpha phosphorylation and endothelial cell adhesion molecule expression show anti-inflammatory effects in vivo. *J. Biol. Chem.* 272, 21096-21103.
- Pimanda,J.E., Chan,W.Y., Donaldson,I.J., Bowen,M., Green,A.R., and Gottgens,B. (2006). Endoglin expression in the endothelium is regulated by Fli-1, Erg, and Elf-1 acting on the promoter and a -8-kb enhancer. *Blood* 107, 4737-4745.
- Prasad,D.D., Rao,V.N., Lee,L., and Reddy,E.S. (1994). Differentially spliced erg-3 product functions as a transcriptional activator. *Oncogene* 9, 669-673.
- Rainis,L., Toki,T., Pimanda,J.E., Rosenthal,E., Machol,K., Strehl,S., Gottgens,B., Ito,E., and Izraeli,S. (2005). The proto-oncogene ERG in megakaryoblastic leukemias. *Cancer Res.* 65, 7596-7602.
- Randi,A.M., Sperone,A., Dryden,N.H., and Birdsey,G.M. (2009). Regulation of angiogenesis by ETS transcription factors. *Biochem. Soc. Trans.* 37, 1248-1253.
- Rao,V.N., Papas,T.S., and Reddy,E.S. (1987). erg, a human ets-related gene on chromosome 21: alternative splicing, polyadenylation, and translation. *Science* 237, 635-639.
- Reddy,E.S. and Rao,V.N. (1991). erg, an ets-related gene, codes for sequence-specific transcriptional activators. *Oncogene* 6, 2285-2289.
- Regan,M.C., Horanyi,P.S., Pryor,E.E., Jr., Sarver,J.L., Cafiso,D.S., and Bushweller,J.H. (2013). Structural and dynamic studies of the transcription factor ERG reveal DNA binding is allosterically autoinhibited. *Proc. Natl. Acad. Sci. U. S. A* 110, 13374-13379.
- Reginato,S., Gianni-Barrera,R., and Banfi,A. (2011). Taming of the wild vessel: promoting vessel stabilization for safe therapeutic angiogenesis. *Biochem. Soc. Trans.* 39, 1654-1658.
- Reis,M. and Liebner,S. (2013). Wnt signaling in the vasculature. *Exp. Cell Res.* 319, 1317-1323.
- Robitaille,J., MacDonald,M.L., Kaykas,A., Sheldahl,L.C., Zeisler,J., Dube,M.P., Zhang,L.H., Singaraja,R.R., Guernsey,D.L., Zheng,B., Siebert,L.F., Hoskin-Mott,A., Trese,M.T., Pimstone,S.N., Shastry,B.S., Moon,R.T., Hayden,M.R., Goldberg,Y.P., and Samuels,M.E. (2002). Mutant frizzled-4 disrupts retinal angiogenesis in familial exudative vitreoretinopathy. *Nat. Genet.* 32, 326-330.
- Roca,C. and Adams,R.H. (2007). Regulation of vascular morphogenesis by Notch signaling. *Genes Dev.* 21, 2511-2524.

Sacilotto,N., Monteiro,R., Fritzsche,M., Becker,P.W., Sanchez-Del-Campo,L., Liu,K., Pinheiro,P., Ratnayaka,I., Davies,B., Goding,C.R., Patient,R., Bou-Gharios,G., and De,V.S. (2013). Analysis of Dll4 regulation reveals a combinatorial role for Sox and Notch in arterial development. *Proc. Natl. Acad. Sci. U. S. A* 110, 11893-11898.

Saharinen,P., Eklund,L., Miettinen,J., Wirkkala,R., Anisimov,A., Winderlich,M., Nottebaum,A., Vestweber,D., Deutsch,U., Koh,G.Y., Olsen,B.R., and Alitalo,K. (2008). Angiopoietins assemble distinct Tie2 signalling complexes in endothelial cell-cell and cell-matrix contacts. *Nat. Cell Biol.* 10, 527-537.

Sainson,R.C., Aoto,J., Nakatsu,M.N., Holderfield,M., Conn,E., Koller,E., and Hughes,C.C. (2005). Cell-autonomous notch signaling regulates endothelial cell branching and proliferation during vascular tubulogenesis. *FASEB J.* 19, 1027-1029.

Sainson,R.C., Johnston,D.A., Chu,H.C., Holderfield,M.T., Nakatsu,M.N., Crampton,S.P., Davis,J., Conn,E., and Hughes,C.C. (2008). TNF primes endothelial cells for angiogenic sprouting by inducing a tip cell phenotype. *Blood* 111, 4997-5007.

Sato,T.N., Tozawa,Y., Deutsch,U., Wolburg-Buchholz,K., Fujiwara,Y., Gendron-Maguire,M., Gridley,T., Wolburg,H., Risau,W., and Qin,Y. (1995). Distinct roles of the receptor tyrosine kinases Tie-1 and Tie-2 in blood vessel formation. *Nature* 376, 70-74.

Schachterle,W., Rojas,A., Xu,S.M., and Black,B.L. (2012). ETS-dependent regulation of a distal Gata4 cardiac enhancer. *Dev. Biol.* 361, 439-449.

Schlaeger,T.M., Bartunkova,S., Lawitts,J.A., Teichmann,G., Risau,W., Deutsch,U., and Sato,T.N. (1997). Uniform vascular-endothelial-cell-specific gene expression in both embryonic and adult transgenic mice. *Proc. Natl. Acad. Sci. U. S. A* 94, 3058-3063.

Schwachtgen,J.L., Janel,N., Berek,L., Duterque-Coquillaud,M., Ghysdael,J., Meyer,D., and Kerbiriou-Nabias,D. (1997). Ets transcription factors bind and transactivate the core promoter of the von Willebrand factor gene. *Oncogene* 15, 3091-3102.

Seidel,J.J. and Graves,B.J. (2002). An ERK2 docking site in the Pointed domain distinguishes a subset of ETS transcription factors. *Genes Dev.* 16, 127-137.

Seth,A. and Watson,D.K. (2005). ETS transcription factors and their emerging roles in human cancer. *Eur. J. Cancer* 41, 2462-2478.

Sharrocks,A.D. (2001). The ETS-domain transcription factor family. *Nat. Rev. Mol. Cell Biol.* 2, 827-837.

Shing,D.C., McMullan,D.J., Roberts,P., Smith,K., Chin,S.F., Nicholson,J., Tillman,R.M., Ramani,P., Cullinane,C., and Coleman,N. (2003). FUS/ERG gene fusions in Ewing's tumors. *Cancer Res.* 63, 4568-4576.

Shtutman,M., Zhurinsky,J., Simcha,I., Albanese,C., D'Amico,M., Pestell,R., and Ben-Ze'ev,A. (1999). The cyclin D1 gene is a target of the beta-catenin/LEF-1 pathway. *Proc. Natl. Acad. Sci. U. S. A* 96, 5522-5527.

Siddique,H.R., Rao,V.N., Lee,L., and Reddy,E.S. (1993). Characterization of the DNA binding and transcriptional activation domains of the erg protein. *Oncogene* 8, 1751-1755.

Siekman,A.F. and Lawson,N.D. (2007). Notch signalling limits angiogenic cell behaviour in developing zebrafish arteries. *Nature* 445, 781-784.

- Singareddy,R., Semaan,L., Conley-Lacomb,M.K., St,J.J., Powell,K., Iyer,M., Smith,D., Heilbrun,L.K., Shi,D., Sakr,W., Cher,M.L., and Chinni,S.R. (2013). Transcriptional regulation of CXCR4 in prostate cancer: significance of TMPRSS2-ERG fusions. *Mol. Cancer Res.* 11, 1349-1361.
- Sorensen,P.H., Lessnick,S.L., Lopez-Terrada,D., Liu,X.F., Triche,T.J., and Denny,C.T. (1994). A second Ewing's sarcoma translocation, t(21;22), fuses the EWS gene to another ETS-family transcription factor, ERG. *Nat. Genet.* 6, 146-151.
- Sperone,A., Dryden,N.H., Birdsey,G.M., Madden,L., Johns,M., Evans,P.C., Mason,J.C., Haskard,D.O., Boyle,J.J., Paleolog,E.M., and Randi,A.M. (2011). The transcription factor Erg inhibits vascular inflammation by repressing NF-kappaB activation and proinflammatory gene expression in endothelial cells. *Arterioscler. Thromb. Vasc. Biol.* 31, 142-150.
- Stambolic,V., Ruel,L., and Woodgett,J.R. (1996). Lithium inhibits glycogen synthase kinase-3 activity and mimics wingless signalling in intact cells. *Curr. Biol.* 6, 1664-1668.
- Subramanian,A., Tamayo,P., Mootha,V.K., Mukherjee,S., Ebert,B.L., Gillette,M.A., Paulovich,A., Pomeroy,S.L., Golub,T.R., Lander,E.S., and Mesirov,J.P. (2005). Gene set enrichment analysis: a knowledge-based approach for interpreting genome-wide expression profiles. *Proc. Natl. Acad. Sci. U. S. A* 102, 15545-15550.
- Suchting,S., Freitas,C., Le,N.F., Benedito,R., Breant,C., Duarte,A., and Eichmann,A. (2007). The Notch ligand Delta-like 4 negatively regulates endothelial tip cell formation and vessel branching. *Proc. Natl. Acad. Sci. U. S. A* 104, 3225-3230.
- Suri,C., Jones,P.F., Patan,S., Bartunkova,S., Maisonpierre,P.C., Davis,S., Sato,T.N., and Yancopoulos,G.D. (1996). Requisite role of angiopoietin-1, a ligand for the TIE2 receptor, during embryonic angiogenesis. *Cell* 87, 1171-1180.
- Taddei,A., Giampietro,C., Conti,A., Orsenigo,F., Breviario,F., Pirazzoli,V., Potente,M., Daly,C., Dimmeler,S., and Dejana,E. (2008). Endothelial adherens junctions control tight junctions by VE-cadherin-mediated upregulation of claudin-5. *Nat. Cell Biol.* 10, 923-934.
- Tamai,K., Semenov,M., Kato,Y., Spokony,R., Liu,C., Katsuyama,Y., Hess,F., Saint-Jeannet,J.P., and He,X. (2000). LDL-receptor-related proteins in Wnt signal transduction. *Nature* 407, 530-535.
- Tammela,T., Zarkada,G., Wallgard,E., Murtomaki,A., Suchting,S., Wirzenius,M., Waltari,M., Hellstrom,M., Schomber,T., Peltonen,R., Freitas,C., Duarte,A., Isoniemi,H., Laakkonen,P., Christofori,G., Yla-Herttuala,S., Shibuya,M., Pytowski,B., Eichmann,A., Betsholtz,C., and Alitalo,K. (2008). Blocking VEGFR-3 suppresses angiogenic sprouting and vascular network formation. *Nature* 454, 656-660.
- Taoudi,S., Bee,T., Hilton,A., Knezevic,K., Scott,J., Willson,T.A., Collin,C., Thomas,T., Voss,A.K., Kile,B.T., Alexander,W.S., Pimanda,J.E., and Hilton,D.J. (2011). ERG dependence distinguishes developmental control of hematopoietic stem cell maintenance from hematopoietic specification. *Genes Dev.* 25, 251-262.
- Thoms,J.A., Birger,Y., Foster,S., Knezevic,K., Kirschenbaum,Y., Chandrakanthan,V., Jonquieres,G., Spensberger,D., Wong,J.W., Oram,S.H., Kinston,S.J., Groner,Y., Lock,R., MacKenzie,K.L., Gottgens,B., Izraeli,S., and Pimanda,J.E. (2011). ERG promotes T-acute lymphoblastic leukemia and is transcriptionally regulated in leukemic cells by a stem cell enhancer. *Blood* 117, 7079-7089.

- Thurston,G., Rudge,J.S., Ioffe,E., Zhou,H., Ross,L., Croll,S.D., Glazer,N., Holash,J., McDonald,D.M., and Yancopoulos,G.D. (2000). Angiopoietin-1 protects the adult vasculature against plasma leakage. *Nat. Med.* 6, 460-463.
- Tomlins,S.A., Laxman,B., Varambally,S., Cao,X., Yu,J., Helgeson,B.E., Cao,Q., Prensner,J.R., Rubin,M.A., Shah,R.B., Mehra,R., and Chinnaiyan,A.M. (2008). Role of the TMPRSS2-ERG gene fusion in prostate cancer. *Neoplasia*. 10, 177-188.
- Tomlins,S.A., Rhodes,D.R., Perner,S., Dhanasekaran,S.M., Mehra,R., Sun,X.W., Varambally,S., Cao,X., Tchinda,J., Kuefer,R., Lee,C., Montie,J.E., Shah,R.B., Pienta,K.J., Rubin,M.A., and Chinnaiyan,A.M. (2005). Recurrent fusion of TMPRSS2 and ETS transcription factor genes in prostate cancer. *Science* 310, 644-648.
- Toomes,C., Bottomley,H.M., Jackson,R.M., Towns,K.V., Scott,S., Mackey,D.A., Craig,J.E., Jiang,L., Yang,Z., Trembath,R., Woodruff,G., Gregory-Evans,C.Y., Gregory-Evans,K., Parker,M.J., Black,G.C., Downey,L.M., Zhang,K., and Inglehearn,C.F. (2004). Mutations in LRP5 or FZD4 underlie the common familial exudative vitreoretinopathy locus on chromosome 11q. *Am. J. Hum. Genet.* 74, 721-730.
- Trindade,A., Kumar,S.R., Sehnet,J.S., Lopes-da-Costa,L., Becker,J., Jiang,W., Liu,R., Gill,P.S., and Duarte,A. (2008). Overexpression of delta-like 4 induces arterialization and attenuates vessel formation in developing mouse embryos. *Blood* 112, 1720-1729.
- Uemura,A., Ogawa,M., Hirashima,M., Fujiwara,T., Koyama,S., Takagi,H., Honda,Y., Wiegand,S.J., Yancopoulos,G.D., and Nishikawa,S. (2002). Recombinant angiopoietin-1 restores higher-order architecture of growing blood vessels in mice in the absence of mural cells. *J. Clin. Invest* 110, 1619-1628.
- Verger,A., Buisine,E., Carrere,S., Wintjens,R., Flourens,A., Coll,J., Stehelin,D., and Duterque-Coquillaud,M. (2001). Identification of amino acid residues in the ETS transcription factor Erg that mediate Erg-Jun/Fos-DNA ternary complex formation. *J. Biol. Chem.* 276, 17181-17189.
- Vijayaraj,P., Le,B.A., Mitchell,N., Kondo,M., Juliao,S., Wasserman,M., Beeler,D., Spokes,K., Aird,W.C., Baldwin,H.S., and Oettgen,P. (2012). Erg is a crucial regulator of endocardial-mesenchymal transformation during cardiac valve morphogenesis. *Development* 139, 3973-3985.
- Villa,N., Walker,L., Lindsell,C.E., Gasson,J., Iruela-Arispe,M.L., and Weinmaster,G. (2001). Vascular expression of Notch pathway receptors and ligands is restricted to arterial vessels. *Mech. Dev.* 108, 161-164.
- Vincent,P.A., Xiao,K., Buckley,K.M., and Kowalczyk,A.P. (2004). VE-cadherin: adhesion at arm's length. *Am. J. Physiol Cell Physiol* 286, C987-C997.
- Vlaeminck-Guillem,V., Carrere,S., Dewitte,F., Stehelin,D., Desbiens,X., and Duterque-Coquillaud,M. (2000). The Ets family member Erg gene is expressed in mesodermal tissues and neural crests at fundamental steps during mouse embryogenesis. *Mech. Dev.* 91, 331-335.
- Wakiya,K., Begue,A., Stehelin,D., and Shibuya,M. (1996). A cAMP response element and an Ets motif are involved in the transcriptional regulation of flt-1 tyrosine kinase (vascular endothelial growth factor receptor 1) gene. *J. Biol. Chem.* 271, 30823-30828.
- Wallez,Y. and Huber,P. (2008). Endothelial adherens and tight junctions in vascular homeostasis, inflammation and angiogenesis. *Biochim. Biophys. Acta* 1778, 794-809.

- Wang,X., Xiao,Y., Mou,Y., Zhao,Y., Blankesteyn,W.M., and Hall,J.L. (2002). A role for the beta-catenin/T-cell factor signaling cascade in vascular remodeling. *Circ. Res.* 90, 340-347.
- Wang,Y., Nakayama,M., Pitulescu,M.E., Schmidt,T.S., Bochenek,M.L., Sakakibara,A., Adams,S., Davy,A., Deutsch,U., Luthi,U., Barberis,A., Benjamin,L.E., Makinen,T., Nobes,C.D., and Adams,R.H. (2010). Ephrin-B2 controls VEGF-induced angiogenesis and lymphangiogenesis. *Nature* 465, 483-486.
- Wei,G.H., Badis,G., Berger,M.F., Kivioja,T., Palin,K., Enge,M., Bonke,M., Jolma,A., Varjosalo,M., Gehrke,A.R., Yan,J., Talukder,S., Turunen,M., Taipale,M., Stunnenberg,H.G., Ukkonen,E., Hughes,T.R., Bulyk,M.L., and Taipale,J. (2010). Genome-wide analysis of ETS-family DNA-binding in vitro and in vivo. *EMBO J.* 29, 2147-2160.
- Willert,K., Brown,J.D., Danenberg,E., Duncan,A.W., Weissman,I.L., Reya,T., Yates,J.R., III, and Nusse,R. (2003). Wnt proteins are lipid-modified and can act as stem cell growth factors. *Nature* 423, 448-452.
- Williams,C.K., Li,J.L., Murga,M., Harris,A.L., and Tosato,G. (2006). Up-regulation of the Notch ligand Delta-like 4 inhibits VEGF-induced endothelial cell function. *Blood* 107, 931-939.
- Wilson,N.K., Foster,S.D., Wang,X., Knezevic,K., Schutte,J., Kaimakis,P., Chilarska,P.M., Kinston,S., Ouwehand,W.H., Dzierzak,E., Pimanda,J.E., de Bruijn,M.F., and Gottgens,B. (2010). Combinatorial transcriptional control in blood stem/progenitor cells: genome-wide analysis of ten major transcriptional regulators. *Cell Stem Cell* 7, 532-544.
- Wong,A.L., Haroon,Z.A., Werner,S., Dewhirst,M.W., Greenberg,C.S., and Peters,K.G. (1997). Tie2 expression and phosphorylation in angiogenic and quiescent adult tissues. *Circ. Res.* 81, 567-574.
- Wu,G., Xu,G., Schulman,B.A., Jeffrey,P.D., Harper,J.W., and Pavletich,N.P. (2003). Structure of a beta-TrCP1-Skp1-beta-catenin complex: destruction motif binding and lysine specificity of the SCF(beta-TrCP1) ubiquitin ligase. *Mol. Cell* 11, 1445-1456.
- Wu,L., Zhao,J.C., Kim,J., Jin,H.J., Wang,C.Y., and Yu,J. (2013). ERG is a critical regulator of Wnt/LEF1 signaling in prostate cancer. *Cancer Res.* 73, 6068-6079.
- Wythe,J.D., Dang,L.T., Devine,W.P., Boudreau,E., Artap,S.T., He,D., Schachterle,W., Stainier,D.Y., Oettgen,P., Black,B.L., Bruneau,B.G., and Fish,J.E. (2013). ETS factors regulate Vegf-dependent arterial specification. *Dev. Cell* 26, 45-58.
- Xiao,K., Garner,J., Buckley,K.M., Vincent,P.A., Chiasson,C.M., Dejana,E., Faundez,V., and Kowalczyk,A.P. (2005). p120-Catenin regulates clathrin-dependent endocytosis of VE-cadherin. *Mol. Biol. Cell* 16, 5141-5151.
- Xu,Q., Wang,Y., Dabdoub,A., Smallwood,P.M., Williams,J., Woods,C., Kelley,M.W., Jiang,L., Tasman,W., Zhang,K., and Nathans,J. (2004). Vascular development in the retina and inner ear: control by Norrin and Frizzled-4, a high-affinity ligand-receptor pair. *Cell* 116, 883-895.
- Xue,Y., Gao,X., Lindsell,C.E., Norton,C.R., Chang,B., Hicks,C., Gendron-Maguire,M., Rand,E.B., Weinmaster,G., and Gridley,T. (1999). Embryonic lethality and vascular defects in mice lacking the Notch ligand Jagged1. *Hum. Mol. Genet.* 8, 723-730.

- Yamamizu,K., Matsunaga,T., Uosaki,H., Fukushima,H., Katayama,S., Hiraoka-Kanie,M., Mitani,K., and Yamashita,J.K. (2010). Convergence of Notch and beta-catenin signaling induces arterial fate in vascular progenitors. *J. Cell Biol.* 189, 325-338.
- Yang,L., Xia,L., Wu,D.Y., Wang,H., Chansky,H.A., Schubach,W.H., Hickstein,D.D., and Zhang,Y. (2002). Molecular cloning of ESET, a novel histone H3-specific methyltransferase that interacts with ERG transcription factor. *Oncogene* 21, 148-152.
- Ye,X., Wang,Y., Cahill,H., Yu,M., Badea,T.C., Smallwood,P.M., Peachey,N.S., and Nathans,J. (2009). Norrin, frizzled-4, and Lrp5 signaling in endothelial cells controls a genetic program for retinal vascularization. *Cell* 139, 285-298.
- Yu,J., Yu,J., Mani,R.S., Cao,Q., Brenner,C.J., Cao,X., Wang,X., Wu,L., Li,J., Hu,M., Gong,Y., Cheng,H., Laxman,B., Vellaichamy,A., Shankar,S., Li,Y., Dhanasekaran,S.M., Morey,R., Barrette,T., Lonigro,R.J., Tomlins,S.A., Varambally,S., Qin,Z.S., and Chinnaiyan,A.M. (2010). An integrated network of androgen receptor, polycomb, and TMPRSS2-ERG gene fusions in prostate cancer progression. *Cancer Cell* 17, 443-454.
- Yuan,L., Le,B.A., Sacharidou,A., Itagaki,K., Zhan,Y., Kondo,M., Carman,C.V., Davis,G.E., Aird,W.C., and Oettgen,P. (2012). ETS-related gene (ERG) controls endothelial cell permeability via transcriptional regulation of the claudin 5 (CLDN5) gene. *J. Biol. Chem.* 287, 6582-6591.
- Yuan,L., Nikolova-Krstevski,V., Zhan,Y., Kondo,M., Bhasin,M., Varghese,L., Yano,K., Carman,C.V., Aird,W.C., and Oettgen,P. (2009). Antiinflammatory effects of the ETS factor ERG in endothelial cells are mediated through transcriptional repression of the interleukin-8 gene. *Circ. Res.* 104, 1049-1057.
- Yuan,L., Sacharidou,A., Stratman,A.N., Le,B.A., Zwiers,P.J., Spokes,K., Bhasin,M., Shih,S.C., Nagy,J.A., Molema,G., Aird,W.C., Davis,G.E., and Oettgen,P. (2011). RhoJ is an endothelial cell-restricted Rho GTPase that mediates vascular morphogenesis and is regulated by the transcription factor ERG. *Blood* 118, 1145-1153.
- Zhang,J., Fukuhara,S., Sako,K., Takenouchi,T., Kitani,H., Kume,T., Koh,G.Y., and Mochizuki,N. (2011a). Angiopoietin-1/Tie2 signal augments basal Notch signal controlling vascular quiescence by inducing delta-like 4 expression through AKT-mediated activation of beta-catenin. *J. Biol. Chem.* 286, 8055-8066.
- Zhang,J., Fukuhara,S., Sako,K., Takenouchi,T., Kitani,H., Kume,T., Koh,G.Y., and Mochizuki,N. (2011b). Angiopoietin-1/Tie2 signal augments basal Notch signal controlling vascular quiescence by inducing delta-like 4 expression through AKT-mediated activation of beta-catenin. *J. Biol. Chem.* 286, 8055-8066.
- Zhang,L., Gao,X., Wen,J., Ning,Y., and Chen,Y.G. (2006). Dapper 1 antagonizes Wnt signaling by promoting dishevelled degradation. *J. Biol. Chem.* 281, 8607-8612.

Appendix 1:

Birdsey, Shah, et al. (2015). The endothelial transcription factor ERG promotes vascular stability and growth through Wnt/ β -catenin signaling. *Dev Cell*
(*in press*)

The Endothelial Transcription Factor ERG Promotes Vascular Stability and Growth through Wnt/ β -Catenin Signaling

Graeme M. Birdsey,^{1,7} Aarti V. Shah,^{1,7} Neil Dufton,¹ Louise E. Reynolds,² Lourdes Osuna Almagro,¹ Youwen Yang,¹ Irene M. Aspalter,³ Samia T. Khan,¹ Justin C. Mason,¹ Elisabetta Dejana,⁴ Berthold Göttgens,⁵ Kairbaan Hodivala-Dilke,² Holger Gerhardt,³ Ralf H. Adams,⁶ and Anna M. Randi^{1,*}

¹National Heart and Lung Institute (NHLI) Vascular Sciences, Hammersmith Hospital, Imperial College London, London W12 0NN, UK

²Centre for Tumour Biology, Barts Cancer Institute – a CR-UK Centre of Excellence, John Vane Science Centre, Queen Mary University of London, Charterhouse Square, London EC1M 6BQ, UK

³Vascular Biology Laboratory, London Research Institute, Cancer Research UK, London WC2A 3PX, UK

⁴FIRC Institute of Molecular Oncology Foundation, IFOM, 20139 Milan, Italy

⁵Department of Haematology, Wellcome Trust and MRC Cambridge Stem Cell Institute and Cambridge Institute for Medical Research, University of Cambridge, Cambridge CB2 0XY, UK

⁶Department of Tissue Morphogenesis, Max Planck Institute for Molecular Biomedicine and Faculty of Medicine, University of Münster, 48149 Münster, Germany

⁷Co-first author

*Correspondence: a.randi@imperial.ac.uk

<http://dx.doi.org/10.1016/j.devcel.2014.11.016>

This is an open access article under the CC BY license (<http://creativecommons.org/licenses/by/3.0/>).

SUMMARY

Blood vessel stability is essential for embryonic development; in the adult, many diseases are associated with loss of vascular integrity. The ETS transcription factor ERG drives expression of VE-cadherin and controls junctional integrity. We show that constitutive endothelial deletion of ERG (*Erg*^{cEC-KO}) in mice causes embryonic lethality with vascular defects. Inducible endothelial deletion of ERG (*Erg*^{iEC-KO}) results in defective physiological and pathological angiogenesis in the postnatal retina and tumors, with decreased vascular stability. ERG controls the Wnt/ β -catenin pathway by promoting β -catenin stability, through signals mediated by VE-cadherin and the Wnt receptor Frizzled-4. Wnt signaling is decreased in ERG-deficient endothelial cells; activation of Wnt signaling with lithium chloride, which stabilizes β -catenin levels, corrects vascular defects in *Erg*^{cEC-KO} embryos. Finally, overexpression of ERG in vivo reduces permeability and increases stability of VEGF-induced blood vessels. These data demonstrate that ERG is an essential regulator of angiogenesis and vascular stability through Wnt signaling.

INTRODUCTION

Angiogenesis is essential during embryogenesis and is a critical component of many diseases. Coordination of growth and stability signals is required for effective angiogenesis (Jain, 2003). Diseases such as cancer, diabetic retinopathy, and vascular mal-

formations are associated with vascular instability, which causes increased permeability and edema, excessive and/or dysfunctional angiogenesis, and hemorrhage. New strategies that target the maturation of blood vessels and restore vascular integrity could therefore have important therapeutic implications.

Multiple interactions at endothelial cell-cell junctions control vascular integrity. Crucial among these are the adhesion molecule vascular endothelial (VE)-cadherin and its intracellular partner β -catenin, an essential component of the canonical Wnt pathway (reviewed in Dejana, 2010). β -catenin is a multifunctional protein that can act as a scaffold between VE- and N-cadherins and the actin cytoskeleton, and as a coregulator for the T cell factor (TCF)/lymphoid enhancer-binding factor transcription factor complex. β -catenin levels are controlled by phosphorylation through a cytoplasmic degradation complex (reviewed in Reis and Liebner, 2013; Dejana, 2010). In the presence of Wnt ligands, which bind to a receptor complex containing members of the Frizzled (Fzd) family, the degradation complex is inactivated; β -catenin is stabilized and translocates to the nucleus to promote transcription. In the vasculature, the Wnt/ β -catenin pathway controls vascular stability through remodeling, junction assembly, and pericyte recruitment (reviewed in Reis and Liebner, 2013; Dejana, 2010; Franco et al., 2009).

The ETS transcription factor family is implicated in vascular development and angiogenesis (reviewed in Randi et al., 2009). The ETS related gene (ERG), expressed throughout the life of the endothelium, regulates multiple pathways involved in vascular homeostasis and angiogenesis, such as monolayer integrity, endothelial permeability, and survival (Birdsey et al., 2008, 2012; Yuan et al., 2012). Previous studies have indicated a role for ERG in vascular development and angiogenesis (Baltzinger et al., 1999; Birdsey et al., 2008; Liu and Patient, 2008). Vijayaraj et al. reported that global deletion of a subset of endothelial ERG isoforms in mice results in defects in vascular and cardiac morphogenesis, causing embryonic lethality (Vijayaraj et al., 2012).

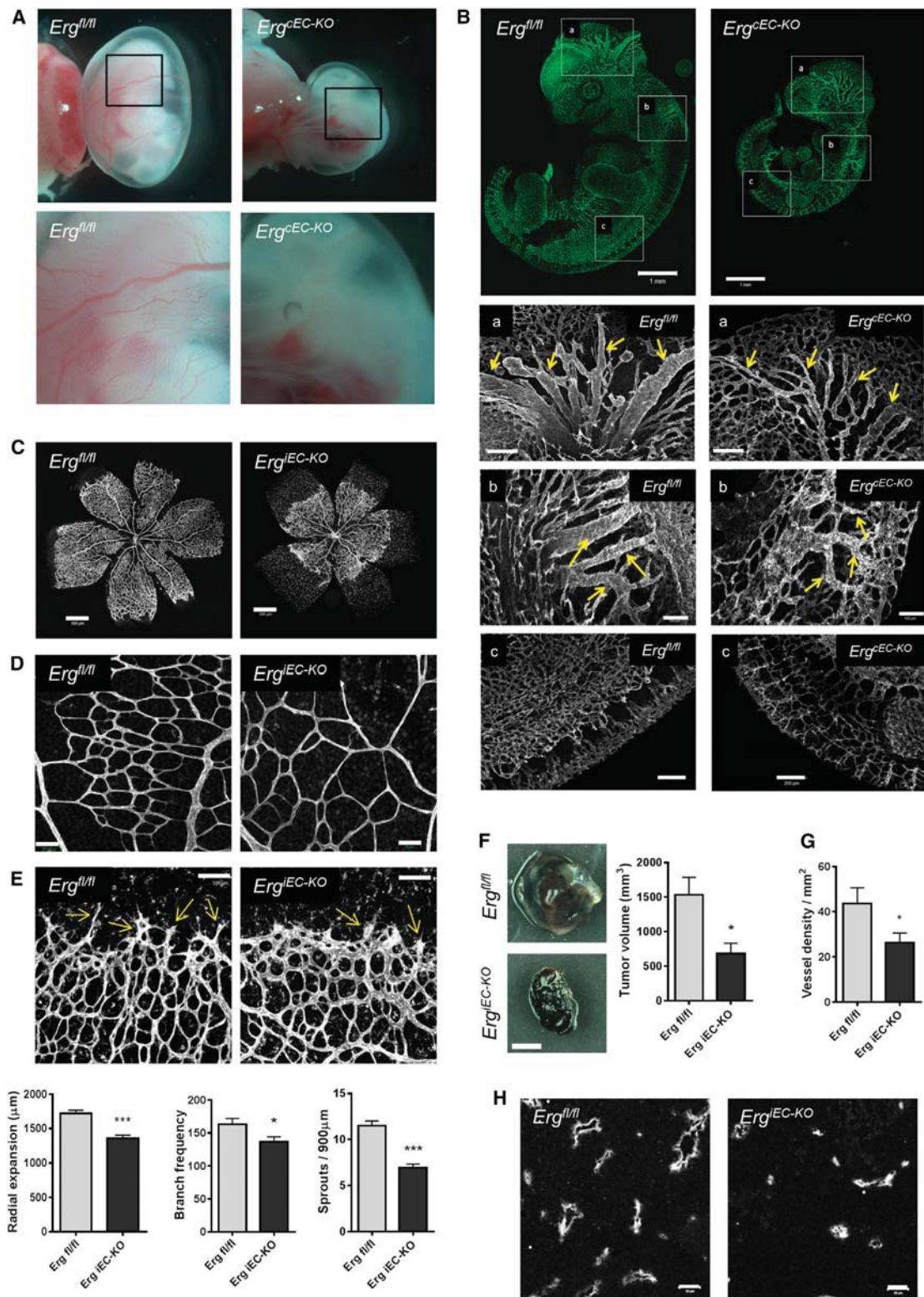


Figure 1. ERG Is Required for Vascular Development, Physiological Postnatal Angiogenesis, and Pathological Tumor Angiogenesis
 (A) Representative whole mount images of E10.5 *Erg^{fl/fl}* and *Erg^{cEC-KO}* embryo yolk sacs (magnification $\times 0.7$). Bottom panel shows higher magnification of yolk sacs (magnification $\times 2$).

(legend continued on next page)

et al., 2012). The mechanisms through which ERG controls blood vessel formation are still unclear, and its therapeutic potential is unexplored.

In this study, we use genetic lineage-specific mouse models and multiple in vitro models to show that ERG promotes vascular growth and stability, through control of the canonical Wnt/ β -catenin pathway. Crucially, we demonstrate that overexpression of ERG in vivo enhances VE growth factor (VEGF)-dependent angiogenesis and promotes stability of VEGF-induced new blood vessels.

RESULTS

Endothelial ERG Is Required for Vascular Development, Angiogenesis, and Tumor Growth

To investigate the role of endothelial ERG in vivo, we used a *Cre/loxP* strategy. The floxed allele of ERG was obtained by inserting two loxP sites flanking exon 6 (Figure S1A available online). Constitutive endothelial-specific deletion of *Erg* was achieved by breeding floxed *Erg* mice with mice expressing the *Cre* transgene under the control of the *Tie2* promoter and enhancer (Kisanuki et al., 2001). Homozygous deletion of endothelial *Erg* (*Tie2Cre-Erg^{fl/fl}*; henceforth referred to as *Erg^{cEC-KO}*) resulted in embryonic lethality between embryonic day (E)10.5 and E11.5, with no live offspring (Figure S1B). Analysis of the yolk sacs from *Erg^{cEC-KO}* embryos at E10.5 showed a significant reduction in perfused large vessels, consistent with defects in yolk sac vascular remodeling (Figures 1A, 5E, and 5F). Between E10.5 and E11.5, some mutant embryos appeared pale with no evidence of vessel blood flow, whereas others displayed hemorrhages and an enlarged pericardial cavity, suggesting defective heart function (Figures S1C and S1D). *Erg^{cEC-KO}* embryos were reduced in size compared to littermate controls (Figure 1B), with growth retardation clearly visible at E9.5 (Figure S1E). These results are in agreement with the phenotypes caused by global deletion of endothelial ERG isoforms (Vijayaraj et al., 2012). Endomucin staining of blood vessels in *Erg^{cEC-KO}* embryos at E10.5 revealed an immature disorganized vascular plexus, with significant disruption of the large vessels in the cranial vasculature (Figure 1B, panels a and b), altered development of the hyaloid vessels of the eye (Figure S1F), and irregular blind ending vessels in the head microvasculature (Figure S1G). Mutant embryos also exhibited disorganization of the intersomitic vessels in the trunk (Figure 1B, panel c). These data confirm that ERG is required for vascular development in mice.

To investigate the role of ERG in physiological and pathological postnatal angiogenesis, floxed *Erg* mice were bred with mice carrying tamoxifen-inducible Cre recombinase under the control of the *Cdh5* promoter (*Cdh5(PAC)-iCreERT2*) (Wang

et al., 2010). Following tamoxifen administration, efficient Cre-recombinase deletion of *Erg* was confirmed by PCR in *Erg^{fl/fl}/Cdh5(PAC)-iCreERT2* mice (henceforth referred to as *Erg^{iEC-KO}*) (Figure S1H). The reduction in ERG protein levels was demonstrated by western blotting and immunofluorescence microscopy (Figures S1I and S1J). In the retinal vasculature of littermate controls (*Erg^{fl/fl}*), ERG was strongly expressed in endothelial cells (EC) from all regions of the vascular plexus, including tip and stalk cells, arteries, veins, and capillaries (Figure S1K), in line with previous studies (Korn et al., 2014). Deletion of endothelial *Erg* resulted in significant reduction of vascular coverage (Figure 1C) and density (Figure 1D) in the retinal plexus, and reduction in the numbers of vascular sprouts at the front (Figure 1E). Next, we investigated whether ERG is involved in pathological angiogenesis, using the B16F0 melanoma tumor model, which depends on angiogenesis for growth (Reynolds et al., 2002). At day 14, tumor size and microvessel density were significantly reduced in adult *Erg^{iEC-KO}* mice compared to controls (Figures 1F–1H). These studies confirm that ERG is required for postnatal angiogenesis and show that endothelial ERG is involved in tumor angiogenesis and tumor growth.

ERG Controls Vascular Stability and Pericyte Coverage

Costaining for isolectin B4 and the basement matrix component collagen IV showed a greater number of empty collagen IV sleeves in the capillary plexus (Figure 2A) and at the angiogenic front (Figure S2A) in retinas from *Erg^{iEC-KO}* mice compared to controls, indicating increased vessel regression. Pericyte recruitment, measured by staining with neuron-glial antigen 2 (NG2) and desmin, was significantly decreased along all vessels in the vascular plexus, including veins and arteries in *Erg^{iEC-KO}* mice (Figures 2B, S2B, and S2C). Similar signs of decreased vessel stability were observed in tumors grown in *Erg^{iEC-KO}* mice, with a marked increase in the number of empty collagen IV sleeves (Figure 2C) and a reduction in pericyte coverage of blood vessels (Figure 2D). These data suggest that ERG controls both physiological and pathological angiogenesis through pathways that promote vascular stability.

ERG Controls β -Catenin Stability and Signaling through VE-Cadherin- and Wnt-Dependent Mechanisms

In vitro studies have shown that ERG is essential to maintain the integrity of endothelial junctions, by driving expression of VE-cadherin (Gory et al., 1998; Birdsey et al., 2008). A marked reduction in VE-cadherin expression and junctional localization was also observed in the retinal vasculature of *Erg^{iEC-KO}* mice (Figure 3A), demonstrating that loss of endothelial ERG leads to a disruption of cell-cell junctions in vivo. Isolated primary mouse lung EC from heterozygous *Tie2Cre-Erg^{fl/+}* mice

(B) Endomucin staining of blood vessels in E10.5 *Erg^{fl/fl}* and *Erg^{cEC-KO}* embryos; scale bars, 1 mm. Higher magnification of embryos shows vessel detail in the head region (panels a and b; scale bars, a, 200 μ m and scale bars, b, 100 μ m) and the trunk (panel c, scale bar, 200 μ m).

(C) Isolectin B4 staining of postnatal day 6 retinas from *Erg^{fl/fl}* and *Erg^{iEC-KO}* mice, showing vascular progression, scale bar, 500 μ m; quantification (n = 6).

(D) Vascular density of isolectin B4 stained branches in the central plexus, scale bar, 50 μ m; quantification (n = 6).

(E) EC sprouts at the angiogenic front (arrows), scale bar, 100 μ m; quantification (n = 6).

(F) Representative images of B16F0 tumors which were grown for 14 days on adult *Erg^{iEC-KO}* and *Erg^{fl/fl}* mice, scale bar, 2 mm; tumor volume was quantified (n = 6).

(G and H) Panels show endomucin staining of blood vessels in B16F0 tumors and the quantification of the number of endomucin-positive vessels, (n = 6), scale bar, 50 μ m. All graphical data are \pm SEM, *p < 0.05, and ***p < 0.001. See also Figure S1.

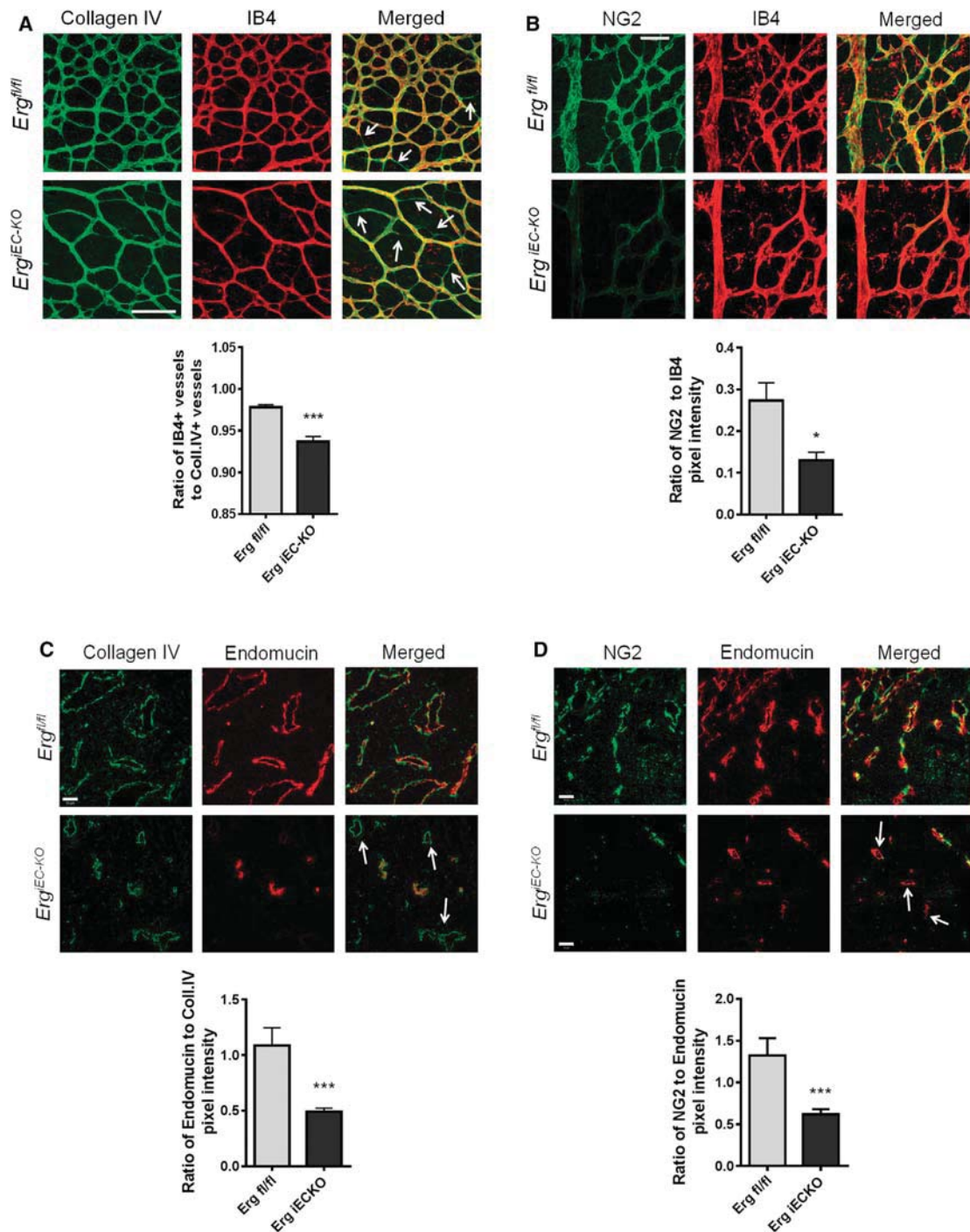


Figure 2. ERG Controls Vascular Remodeling

(A) Collagen IV (green) and isolectin B4 (IB4, red) staining of *Erg^{IEC-KO}* and *Erg^{fl/fl}* P6 retinal vessels. Arrows show empty collagen IV sleeves, quantification of number of vessels, (n = 4).

(B) NG2-positive pericytes (green) associated with isolectin B4 labeled retinal vessels (red) from *Erg^{IEC-KO}* and *Erg^{fl/fl}* mice; quantification of pixel intensity, (n = 4).

(C) Sections from B16F0 tumors grown on adult *Erg^{IEC-KO}* and *Erg^{fl/fl}* mice were stained for collagen IV (green) and endomucin (red); quantification of pixel intensity, (n = 3). Arrows show empty collagen IV sleeves.

(D) Tumor sections from *Erg^{IEC-KO}* and *Erg^{fl/fl}* mice were stained for NG2 (green) and endomucin (red); quantification of pixel intensity, (n = 3). Arrows show NG2-negative, endomucin-positive vessels. Scale bars, 100 μ m (A), scale bars, 50 μ m (B-D). All graphical data are \pm SEM, *p < 0.05, and ***p < 0.001. See also Figure S2.

(*Erg*^{cEC-het}) (Figure S3A) showed an approximate 50% decrease in VE-cadherin expression (Figure 3B), as expected.

At the junctions, VE-cadherin binds β -catenin, protecting it from degradation; this interaction is required for the control of junction stabilization (Dejana, 2010). β -catenin plays a pivotal role in Wnt signaling (Goodwin and D'Amore, 2002); interestingly, transcription profiling in ERG-deficient human umbilical vein EC (HUVEC) identified several Wnt-related genes as candidate ERG targets (Birdsey et al., 2012) (Figure S3B). We therefore speculated that ERG might regulate β -catenin and Wnt signaling in EC.

Inhibition of ERG expression in HUVEC (Figures S3C and S3D) significantly reduced β -catenin junctional staining and protein expression (Figures 3C and 3D). ERG regulates β -catenin protein levels in confluent (Figure 3C) and subconfluent (Figure S3E) EC, suggesting that this pathway functions both in quiescent and angiogenic endothelium. However, β -catenin mRNA levels were unaffected by ERG inhibition in HUVEC (Figures 3E and S3F) or in primary mouse EC from *Erg*^{cEC-het} mice (Figure 3H). The decrease in β -catenin protein expression correlated with a decrease in canonical Wnt signaling: Wnt3a stimulation of β -catenin transcriptional activity was lost in ERG-deficient EC (Figure 3F). Moreover, expression levels of the Wnt target genes Cyclin D1, Axin-2, and TCF-1 (Shtutman et al., 1999; Roose et al., 1999; Jho et al., 2002) were decreased in ERG-deficient HUVEC (Figure 3G) and primary mouse EC from *Erg*^{cEC-het} mice (Figure 3H). Endothelial β -catenin signaling regulates blood brain barrier maintenance through concomitant activation of the tight junction molecule Claudin-3 and repression of plasmalemma vesicle-associated protein (PLVAP) (Liebner et al., 2008). In line with these findings, Claudin-3 expression was significantly downregulated, while PLVAP was strongly upregulated in *Erg*^{IEC-KO} mouse brains (Figure 3I). Together, these results indicate that ERG regulates canonical Wnt/ β -catenin signaling in both human and mouse EC.

To confirm the relationship between ERG and β -catenin pathways, we used gene set enrichment analysis (GSEA) to compare the data set from transcriptome profiling of ERG-deficient HUVEC (Birdsey et al., 2012) with the data set from transcriptome analysis of human pulmonary artery EC (HPAEC) following β -catenin inhibition (Alastalo et al., 2011). GSEA showed a significant positive correlation between the genes regulated by ERG and β -catenin (Figure 3J, left). Interestingly, gene ontology analysis of shared genes identified a significant number of regulators of angiogenesis, cell adhesion, migration, and apoptosis (Figure 3J, right). These results suggest a strong relationship between these two pathways.

Since ERG inhibition decreases β -catenin protein, but not mRNA levels, we tested whether ERG regulates β -catenin degradation. β -catenin protein expression was restored in ERG-deficient EC in the presence of the proteasomal degradation inhibitor MG132 (Figure 4A). We investigated whether ERG controls β -catenin stability through VE-cadherin. In ERG-deficient HUVEC, GFP-tagged VE-cadherin overexpression (Figure S4A) partially restored junctional β -catenin protein levels (Figures 4B and 4C, lane 6). However, cellular fractionation studies showed that ERG also controls the nuclear pool of β -catenin (Figure 4C, lane 3), which was not corrected by VE-cadherin overexpression (Figure 4C, lane 5). This suggests that ERG controls β -catenin

also through a Wnt signaling-dependent, VE-cadherin-independent pathway. Activation of Wnt signaling by lithium chloride (LiCl) inhibits GSK3 β , and thus degradation of cytoplasmic β -catenin, allowing its nuclear translocation (Stambolic et al., 1996). LiCl was able to partially normalize β -catenin nuclear levels in ERG-deficient EC (Figure 4C, lane 7). Finally, combined Wnt signaling activation (through LiCl) and VE-cadherin overexpression were able to rescue both nuclear and junctional β -catenin pools in ERG-deficient EC (Figure 4C, lanes 9 and 10). These results demonstrate that the balance between VE-cadherin-dependent and Wnt signaling-dependent pathways, which modulates canonical Wnt/ β -catenin signals in EC, is controlled by the transcription factor ERG.

Expression of the Wnt Receptor Fzd-4 Is Regulated by ERG

Wnt ligands bind to receptors of the Fzd family to inhibit the β -catenin degradation complex and activate Wnt signaling (Goodwin and D'Amore, 2002). LiCl treatment was able to partially stabilize β -catenin expression in ERG-deficient EC (Figure 4C, lanes 7 and 8). However, the upstream ligand Wnt3a was unable to do so (Figure S4B), suggesting a receptor-mediated defect upstream of the degradation complex. Wnt3a interacts with the Fzd-4 (Fzd4) receptor (Reis and Liebner, 2013), which is highly expressed in cultured EC (Goodwin et al., 2006). Fzd4 was identified as a putative ERG target by transcriptome analysis in HUVEC (Birdsey et al., 2012). We confirmed that Fzd4 mRNA (Figure 4D) and protein levels (Figure 4E) were significantly decreased in ERG-deficient HUVEC. Consistently, Fzd4 expression was decreased in mouse EC isolated from *Erg*^{cEC-het} mice (Figure S4C).

Comparative genomic analysis of the Fzd4 promoter revealed the presence of three highly conserved ERG DNA binding motifs in the 800 base pair (bp) region upstream of the Fzd4 transcription start site (Figures 4F and S4D). Analysis of the Encyclopedia of DNA Elements (ENCODE) chromatin immunoprecipitation sequencing (ChIP-seq) data (Birney et al., 2007) for histone marks H3K4me1 and H3K27Ac and RNA polymerase II occupancy, markers of active promoters, show that the location of these marks correlates with the position of the ERG binding motifs (Figure 4F). ChIP-quantitative (q)PCR demonstrated that ERG interacts directly with the human Fzd4 promoter (Figure 4G); specificity of the interaction was confirmed in ERG-deficient EC (Figure 4G). ERG overexpression resulted in a 6-fold transactivation of a Fzd4 promoter luciferase construct in HUVEC (Figure 4H). Finally, Fzd4 overexpression in ERG-deficient EC was able to partially rescue Wnt3a activation of β -catenin transcriptional activity (Figure 4I). These data demonstrate that ERG controls transcription of the Fzd4 receptor in EC and point to a molecular mechanism for the VE-cadherin-independent control of Wnt signaling by ERG.

ERG Controls Angiogenesis through Wnt Signaling

Wnt/ β -catenin signaling can promote EC proliferation (Masckauhan et al., 2005) and induce cell cycle progression through transcriptional activation of Cyclin D1 (Shtutman et al., 1999). Therefore, we tested whether ERG may also control EC proliferation through Wnt signaling. As shown in Figure 5A, inhibition of ERG expression by siRNA decreased HUVEC proliferation; LiCl

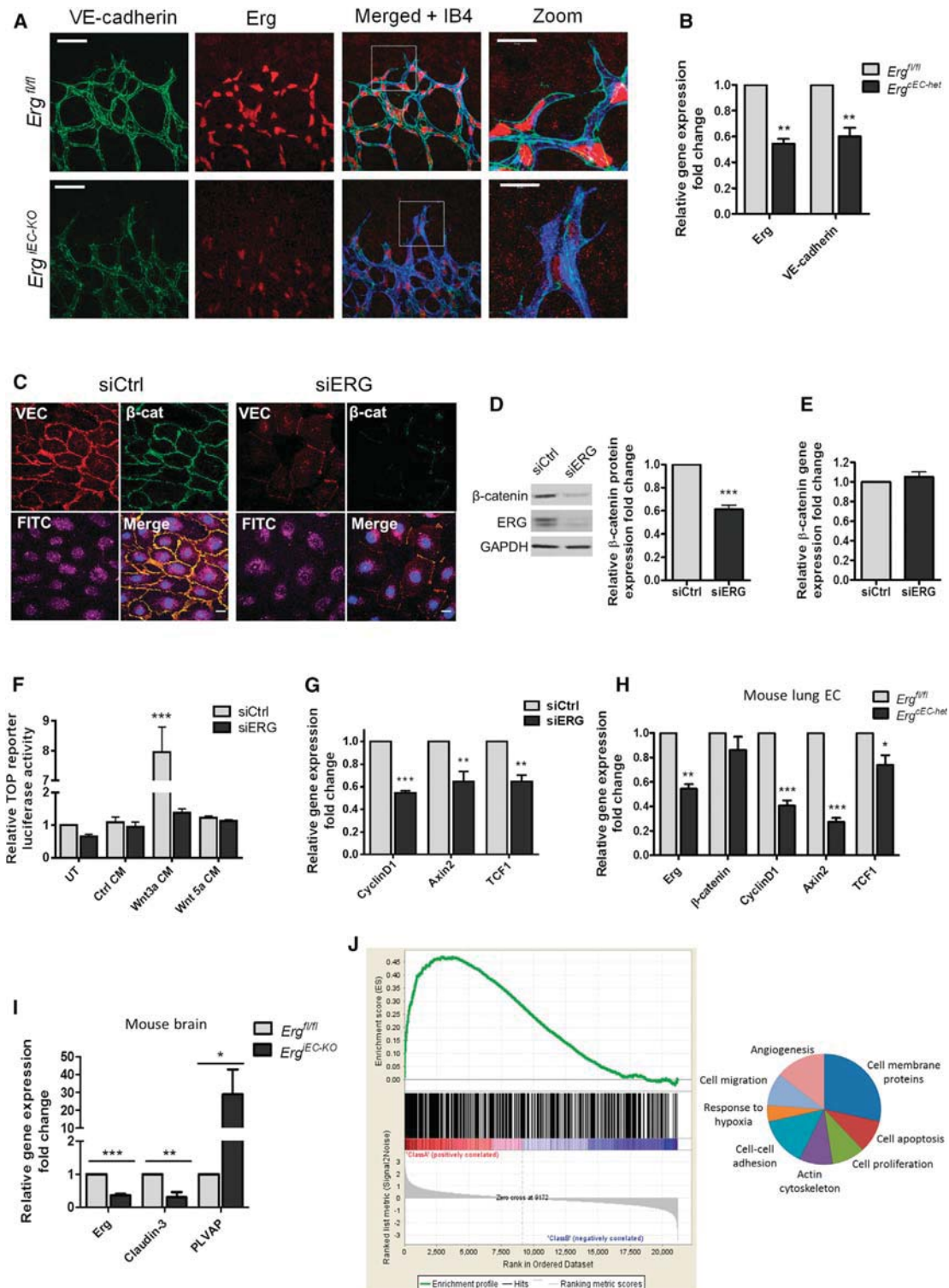


Figure 3. Endothelial Canonical Wnt Signaling and β -Catenin Stability Are Regulated by ERG

(A) Staining for VE-cadherin (green), ERG (red), and isolectin B4 (IB4, blue) in *Erg^{IEC-KO}* and *Erg^{fl/fl}* P6 retinas. Scale bar, 50 μ m; zoom, 20 μ m.
 (B) Relative mRNA expression of Erg and VE-cadherin in primary *Erg^{IEC-het}* mouse lung EC compared to control (n = 6).
 (C) β -catenin (β -cat; green) and VE-cadherin (VEC; red) staining of FITC-conjugated siCtrl and siERG (FITC; purple) treated HUVEC (n = 3). Scale bar, 20 μ m.
 (D and E) (D) Western blot and (E) qPCR analysis of β -catenin expression in control (siCtrl) and ERG-deficient (siERG) HUVEC (n = 4).
 (F) TCF reporter activity (TOP) in control and ERG-deficient cells treated with control (Ctrl), Wnt3a, or Wnt5a conditioned medium (CM); (n = 3).
 (G) Relative gene expression of CyclinD1, Axin2, and TCF1 in control (siCtrl) and ERG-deficient (siERG) HUVEC (n = 4).
 (H) Relative gene expression of Erg, β -catenin, CyclinD1, Axin2, and TCF1 in mouse lung EC of *Erg^{fl/fl}* and *Erg^{IEC-het}* mice (n = 3).
 (I) Relative gene expression of Erg, Claudin-3, and PLVAP in mouse brain of *Erg^{fl/fl}* and *Erg^{IEC-KO}* mice (n = 3).
 (J) GSEA plot showing enrichment of HITS genes in mouse lung EC. The pie chart shows the biological processes enriched in the HITS genes.

which prevents β -catenin degradation, rescued proliferation of ERG-deficient HUVEC. These results indicate that ERG controls endothelial proliferation through the Wnt/ β -catenin pathway. We have previously shown that ERG deficiency causes increased EC apoptosis (Birdsey et al., 2008). Combination of VE-cadherin overexpression and LiCl treatment could completely prevent cell death in ERG-deficient cells, indicating that ERG controls EC survival through Wnt/ β -catenin signaling (Figure S5A).

To test the functional relevance of Wnt signaling in ERG-dependent angiogenesis, we used an in vitro sprouting assay (Nakatsu et al., 2007). ERG-deficient HUVEC formed markedly decreased numbers of significantly shorter sprouts (Figures 5B, panel b, 5C, and 5D). However, pretreatment of ERG-deficient cells with LiCl to inhibit β -catenin degradation was able to partially restore normal sprouting behavior of HUVEC (Figure 5B, panel d), by rescuing the number (Figure 5C) and length (Figure 5D) of the sprouts. These results suggest that Wnt/ β -catenin signaling is required for ERG to control sprout formation during angiogenesis.

To confirm that ERG controls angiogenesis and vascular development in a Wnt/ β -catenin-dependent manner in vivo, we carried out a rescue experiment by pharmacological stabilization of Wnt/ β -catenin signaling (Griffin et al., 2011). Light microscopy examination of the yolk sacs from NaCl (control) and LiCl treated mice revealed a dramatic increase in perfused vessels in the yolk sacs of *Erg*^{EC-KO} mutants following LiCl treatment (Figure 5E). Endomucin staining revealed disrupted vessel morphology in the yolk sacs from NaCl-treated *Erg*^{EC-KO} embryos, with reduced microvasculature branching and decreased diameter of the larger vitelline vessels (Figures 5E and 5F). LiCl treatment of *Erg*^{EC-KO} mutants resulted in significant increase in vitelline vessel diameter and in the remodeling of the microvascular plexus (Figures 5E and 5F), in line with the increase in perfusion.

Wnt targets CyclinD1 and Axin2, previously shown to be decreased in ERG-deficient endothelium (see Figures 3G and 3H), were significantly decreased in NaCl-treated *Erg*^{EC-KO} yolk sacs compared to controls (Figure S5B). LiCl-treatment of *Erg*^{EC-KO} yolk sacs normalized Cyclin D1 and Axin2 levels to those observed in LiCl-treated control embryos (Figure 5G). Interestingly, ERG targets VE-cadherin and Fzd4 were not normalized, in line with the direct transcriptional role of ERG in their regulation.

These results demonstrate that endothelial ERG controls embryonic vascular development and angiogenesis through the Wnt/ β -catenin signaling pathway.

ERG Overexpression Stabilizes VEGF-Induced Blood Vessels and Promotes Angiogenesis In Vivo

The data presented so far show that the transcription factor ERG controls angiogenesis through pathways mediating vascular stability and growth. The importance of the coordinated regulation

of these pathways is highlighted by the variable and disappointing results of clinical trials for therapeutic angiogenesis in ischemic diseases, using the proangiogenic growth factor VEGF. VEGF has been shown to induce the formation of unstable and highly permeable vessels in vivo (Reginato et al., 2011), giving rise to local edema and inefficient tissue perfusion. Therefore, we investigated the ability of ERG to stabilize new vessels induced by VEGF in vivo. C57BL/6 mice received a subcutaneous injection of Matrigel supplemented with VEGF-A₁₆₅ and ERG (Ad.ERG) or Lacz (Ad.Lacz) adenovirus; basic fibroblast growth factor (bFGF), which can induce stable new vessels in this model (Bussolati et al., 2004), was used as control. Immunofluorescence staining for the adenovirus hexon coat protein showed localization of the adenovirus to endomucin-positive neovessels in the Matrigel plugs (Figure S6A). In addition, qPCR analysis confirmed significant expression of V5-tagged ERG in Matrigel samples treated with Ad.ERG compared to Ad.Lacz control (Figure S6B).

To evaluate the stability of the new vessels, vascular permeability was measured using two different sized dextran tracers. In the presence of bFGF (Figure 6A, top panel), the lower molecular weight tetramethylrhodamine (TRITC)-dextran was fully contained within the vascular structures and colocalized with the larger molecular weight Fluorescein isothiocyanate (FITC)-tracer, confirming that bFGF induces the formation of stable, nonleaky vessels. Plugs containing VEGF-A₁₆₅ and Ad.Lacz revealed a less organized vascular network with the smaller molecular weight dextran dispersed both inside and outside of the vessels (Figure 6A, middle panel, and Movie S1A). Interestingly, overexpression of ERG in the presence of VEGF-A₁₆₅ resulted in reduced diffusion of the smaller molecular weight dextran (Figure 6A, bottom panel, and Movie S1B), indicating a more stable, less permeable vasculature. Quantification of the net amount of extravasated TRITC-dextran tracer shows that Ad.ERG caused an approximate 4-fold reduction in tracer extravasation in VEGF-A₁₆₅-induced new vessels compared to Ad.Lacz control (Figure 6B). Consistently, quantification of FITC-dextran area showed that ERG overexpression in the presence of VEGF-A₁₆₅ resulted in an increase in perfused vessels within the Matrigel plug after 7 and 10 days, compared to control (Figures 6C and S6C). ERG overexpression also resulted in a significant increase in the number of new vessels within the Matrigel plug; however this difference was observed only at the later time point (Figure 6D), suggesting that the increase in blood vessel number is secondary mainly to stabilization of VEGF-induced angiogenesis. These results confirm that ERG promotes stabilization of VEGF-induced angiogenesis in vivo.

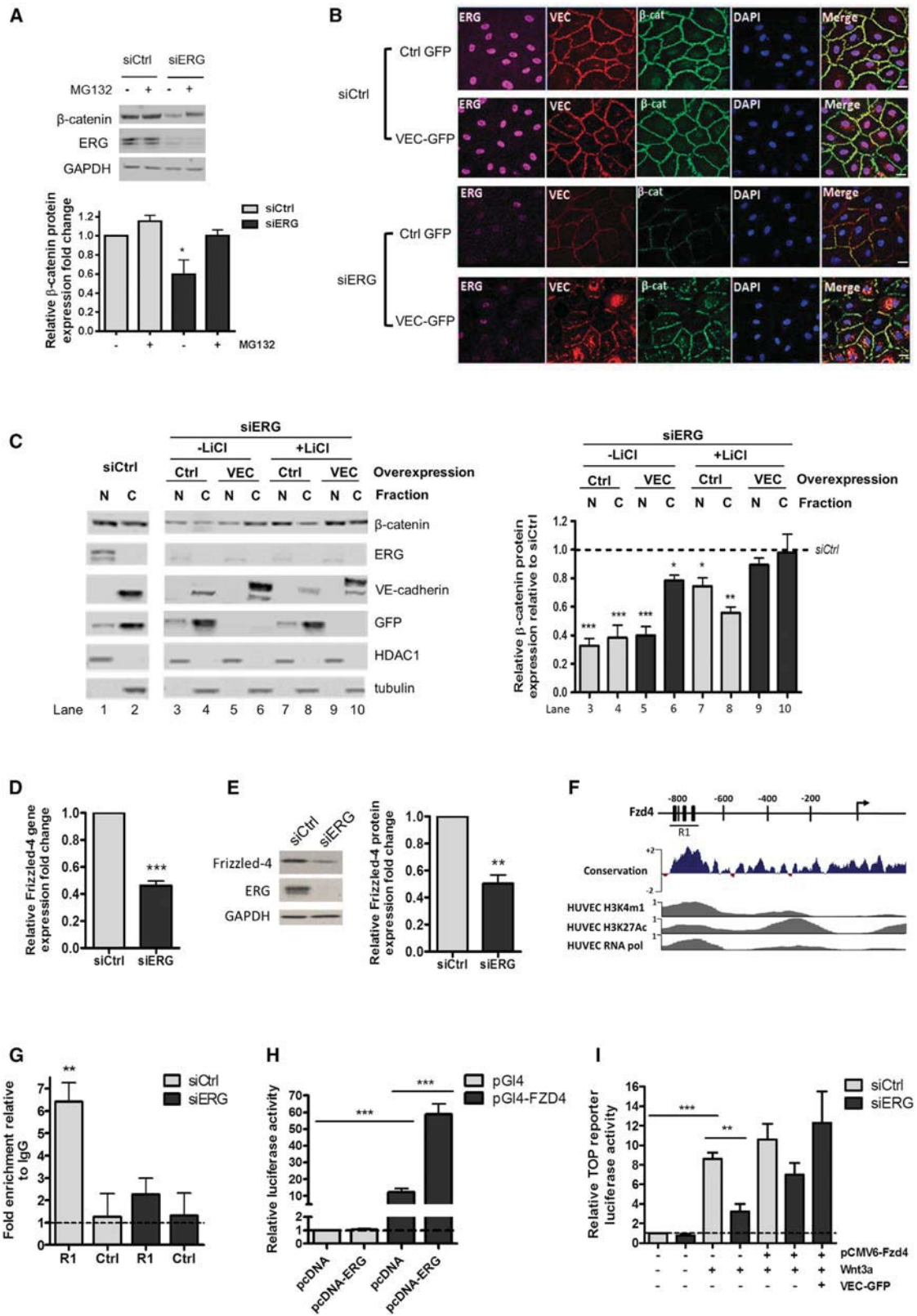
Pericyte recruitment is a critical step in vascular stability and maturation, and lack of pericytes has been shown to cause increased permeability (Hellström et al., 2001). Since pericyte recruitment was decreased in two models of angiogenesis in

(G) qPCR of downstream β -catenin target gene expression in control and ERG-deficient HUVEC: Cyclin D1, Axin-2, and TCF-1 (n = 4).

(H) mRNA expression of *Erg*, β -catenin, and its target genes Cyclin D1, Axin-2, and TCF-1 in primary *Erg*^{EC-het} mouse lung EC compared to control (n = 6).

(I) qPCR analysis of total brain mRNA from control and *Erg*^{EC-KO} mice for *Erg*, Claudin-3, and PLVAP.

(J) GSEA shows enrichment and significant correlation (normalized enrichment score, 2.46; p < 0.001) between genes downregulated in β -catenin siRNA-treated HPAEC (green curve) (Alastalo et al., 2011) and the ranked list of genes downregulated by ERG inhibition in HUVEC (Birdsey et al., 2012). Functional classification of the shared genes identified by GSEA was carried out using DAVID analysis (right). The functional categories shown displayed significant enrichment scores (p < 0.01). All graphical data are \pm SEM, *p < 0.05, **p < 0.01, and ***p < 0.001. See also Figure S3.



(legend on next page)

the *Erg*^{IEC-KO} mice (see Figure 2), we investigated whether ERG overexpression could increase the recruitment of vascular pericytes in the in vivo Matrigel plug model. Indeed, pericyte recruitment as measured by desmin staining was increased in the Ad.ERG-treated plugs compared to controls (Figures 6E and 6F). These results suggest that ERG may promote stabilization of angiogenesis also through control of pericyte recruitment.

DISCUSSION

Over the last decade, major progress has been made in understanding the molecular mechanisms that regulate angiogenesis. However, the pathways that control vessel stability are less well characterized. In this study, we identify a transcriptional program regulated by ERG that controls vascular stability and growth through the Wnt/ β -catenin pathway, in both a physiological and pathological context.

We show that constitutive deletion of endothelial ERG in the mouse embryo causes embryonic lethality with severe vascular disruption. These observations are in line with a previous report where global deletion of a subset of endothelial ERG isoforms resulted in vascular defects and lethality between E10.5 and E11.5 (Vijayaraj et al., 2012). Instead of a strategy based on a posteriori knowledge of ERG isoform expression, the *Cre/LoxP* system allowed us to delete all endothelial isoforms of *Erg*, by targeting exon 6, which encodes a region of the protein present in all isoforms. A previous transgenic model, where ERG's function was disrupted by a mutation in the DNA binding ETS domain (*Erg*^{Mld2/Mld2}), caused embryonic lethality at a later stage (E13.5) (Loughran et al., 2008) and did not appear to display early vascular defects, suggesting that ERG's functions in the vasculature are not exclusively mediated by its DNA binding activity.

Using the inducible endothelial specific *Cdh5*(PAC)-iCreERT2 line, we show that ERG is required for angiogenesis in the developing retina of newborn mice and for tumor blood vessel growth in adult mice. ERG deficiency results in vessel regression and reduced pericyte recruitment, demonstrating that ERG controls vascular stability. Interestingly, ERG overexpression in the in vivo Matrigel plug model resulted in increased pericyte recruitment to vessels. This suggests that ERG may promote stabilization of angiogenesis in part through control of pericyte recruitment. A recent paper has described a role for ETS factors (including

ERG) in arterial specification and reported increased ERG expression in arterial-derived EC in vitro (Wythe et al., 2013). However, in the mouse retinal vasculature, ERG was strongly expressed in all EC with no detectable difference between arteries and veins.

The in vivo developmental vascular defects in the *Erg*^{IEC-KO} embryos are reminiscent of those associated with deletion of endothelial β -catenin. Endothelial deletion of ERG causes embryonic lethality earlier than the E12.5 reported for endothelial deletion of β -catenin (Cattellino et al., 2003). This study proposed that EC might not require β -catenin for early vascular development, but rather for maintenance of vascular integrity and vascular patterning at later stages. ERG's regulation of other genes involved in earlier stages of vascular development, such as VE-cadherin, may be partly accountable for this difference in phenotypes. Constitutive endothelial deletion of ERG also causes diffuse hemorrhages and defects in vascular remodeling, similar to those observed in the β -catenin deficient embryos. In both lines, vitelline vessels of the yolk sac are significantly smaller in diameter; however, unlike *Erg*^{IEC-KO} embryos, endothelial-specific loss of β -catenin does not affect vessel formation in the head, but causes hyperbranching of intersomitic vessels (Corada et al., 2010). Thus, embryonic mouse phenotypes of ERG versus β -catenin endothelial deletion show similarities, but not complete overlap, as expected, given the complex role of ERG as a transcriptional regulator of multiple vascular pathways. Crucially, the yolk sac vascular defects in the *Erg*^{IEC-KO} and expression of Wnt targets were rescued by in vivo treatment with LiCl. Although we cannot completely rule out non-EC effects of LiCl, these experiments clearly demonstrate that ERG controls vascular development through Wnt signaling.

Interestingly, similar angiogenic defects are observed in the retinas from *Erg*^{IEC-KO} and from the reported endothelial-specific β -catenin and *Fzd4* knockout mice (Xu et al., 2004; Ye et al., 2009; Phng et al., 2009; Corada et al., 2010). Whether ERG is implicated in human ocular diseases, including Norrie disease and familial exudative vitreoretinopathy, which are associated with *Fzd4* and its ligand Norrin (Xu et al., 2004), remains to be established. In line with our data, a link between *Fzd4* and ERG has been previously observed in prostate cancer (Gupta et al., 2010). Interestingly, our results show that ERG deficiency results in about 50% reduction in *Fzd4* protein, but completely abrogates

Figure 4. ERG Controls β -Catenin Stability through VE-Cadherin- and Wnt-Dependent Mechanisms

(A) Western blot of β -catenin expression in control and ERG-deficient cells treated in presence or absence of MG132 (n = 4).

(B) ERG (magenta), VEC (red), β -cat (green), and DAPI (blue) staining of control and ERG-deficient HUVEC transduced with GFP-tagged control (Ctrl-GFP) or VE-cadherin (VEC-GFP) adenovirus. Scale bar, 20 μ m.

(C) Western blot (left) and quantification (right) of β -catenin expression in nuclear/cytoplasmic fractions of ERG-deficient HUVEC transduced with GFP or VEC-GFP adenovirus in presence or absence of LiCl. For normalization, tubulin was used as a cytoplasmic control and HDAC1 as a nuclear marker (n = 3).

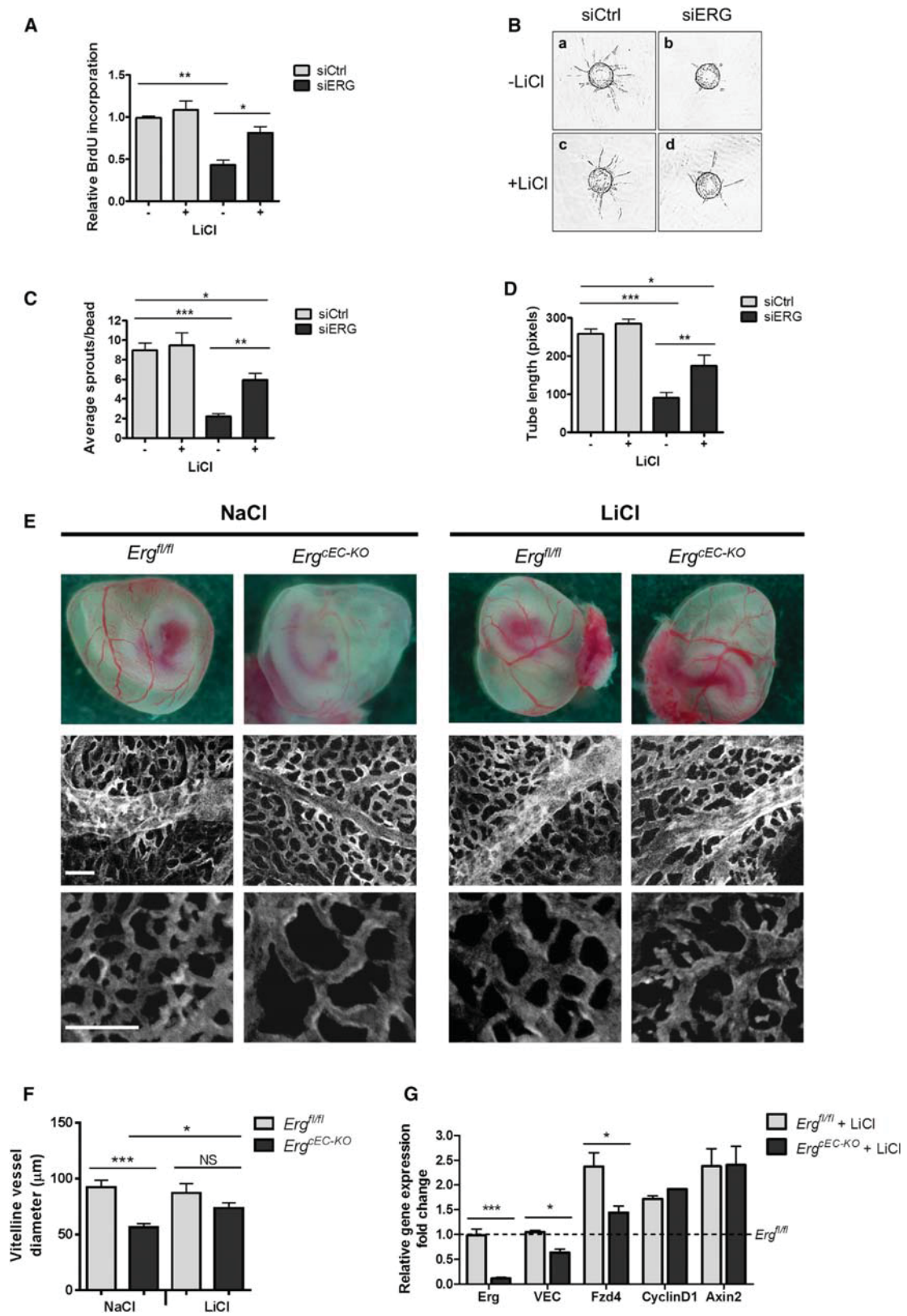
(D and E) (D) qPCR and (E) western blot analysis of *Fzd4* expression in control and ERG-deficient cells (n = 3).

(F) There are three putative ERG binding sites (black bars) located within the *Fzd4* locus upstream of the transcription start site (arrow); sequence conservation between 100 vertebrates is shown across this region. ENCODE ChIP-seq data profiles for H3K4me1, H3K27Ac, and RNA polymerase II indicate open chromatin and active transcription. Location of qPCR amplicon covering region R1 is indicated.

(G) ChIP-qPCR using primers to region R1 on ERG-bound chromatin from HUVEC treated with siCtrl or siERG. Primers for a downstream region within the *Fzd4* gene were used as a negative control. Data are shown as fold change over IgG (n = 3).

(H) Luciferase reporter assay, an ERG cDNA expression plasmid (pcDNA-ERG), or an empty expression plasmid (pcDNA) were cotransfected with a *Fzd4* promoter-luciferase construct (pGL4-*Fzd4*) in HUVEC and luciferase activity was measured. Values are represented as the fold change in relative luciferase activity over the empty pGL4 vector alone.

(I) TCF reporter (TOP) activity in control and ERG-deficient HUVEC treated with rWnt3a. Cells were transfected with control pCMV6 or pCMV6-*Fzd4* plasmids and transduced with VEC-GFP adenovirus (n = 3). All graphical data are \pm SEM, *p < 0.05, **p < 0.01, and ***p < 0.001. See also Figure S4.



Wnt luciferase reporter activity in response to Wnt3a. This suggests that ERG's control of other nodes in this pathway, including repression of the Wnt inhibitor DACT1 (Zhang et al., 2006) and activation of the transcription factor TCF4 (Wang et al., 2002), may be important.

Canonical Wnt signaling promotes EC survival, junction stabilization, proliferation, and pericyte recruitment and is essential for vessel stability (Cattellino et al., 2003; Phng et al., 2009; reviewed in Franco et al., 2009; Dejana, 2010). In this study, we establish ERG as a regulator of canonical Wnt/ β -catenin signaling, and therefore identify a connection between two key transcriptional regulators essential for EC function. We show that ERG controls cell survival, proliferation, angiogenesis, and vessel stability through β -catenin. Whether ERG controls pericyte recruitment via Wnt signaling remains to be elucidated; preliminary evidence suggests that ERG regulates expression of the junction molecule and β -catenin transcriptional target, N-cadherin (data not shown), which plays a crucial role in pericyte attachment during vessel formation (Giampietro et al., 2012; Gerhardt et al., 2000). Our data show that ERG controls Wnt/ β -catenin levels and signaling through VE-cadherin-dependent and -independent pathways both in confluent, quiescent monolayers and in subconfluent, proliferating cells. The balance between VE-cadherin and Wnt-dependent signals controls β -catenin cellular localization and activity. It has been suggested that β -catenin could function to increase cell plasticity and sensitivity to extracellular signals (Franco et al., 2009). Transcriptional activity of ERG itself has been shown to be modulated by extracellular signals (Wythe et al., 2013). Thus, we propose that in EC, ERG is required to maintain homeostatic levels of β -catenin protein, the output of which can be modulated according to the growth and survival signals it encounters, providing the balance between proliferation and stability required in a nascent blood vessel.

Dysregulation of the Wnt/ β -catenin signaling pathway is frequently observed in many types of cancer. Constitutive Wnt signaling activation caused by mutations in β -catenin or genes that control β -catenin stability has been associated with aberrant cell proliferation and subsequent cancer progression (reviewed in Giles et al., 2003). Wnt signaling has been shown to be a critical mediator of ERG-induced oncogenesis in several types of cancer, where aberrant ERG overexpression is a marker of aggressive malignancy and associated with increased proliferation (Gupta et al., 2010; Wu et al., 2013; Li et al., 2011; Mochmann et al., 2011). This is in contrast with its role in healthy endothelium, where ERG promotes homeostasis and stability. The reasons for this discrepancy are unknown and may be linked to the lack of balance between growth and survival signals, due to disrupted cell-cell signaling in malignant cells, thus driving

the cells to a proliferative fate. Thus, strategies to control ERG's activity in malignant cells through cell-cell adhesion signals might be worthy of investigation.

Finally, in this study, we explore the potential for ERG in promoting vascular stability during VEGF-induced angiogenesis. Numerous studies have shown that the new vasculature induced by VEGF in vivo, to promote revascularization in ischemic diseases (Zachary and Morgan, 2011), can be dysfunctional due to vascular instability and increased permeability (Reginato et al., 2011). Here, we show that overexpression of ERG can reduce permeability and promote VEGF-induced angiogenesis in vivo. Combined with the homeostatic and anti-inflammatory role of ERG (Sperone et al., 2011; Yuan et al., 2009), these results establish the ERG pathway as a potential target to promote vascular quiescence and stability.

EXPERIMENTAL PROCEDURES

Detailed methods are available in the [Supplemental Experimental Procedures](#).

Mice and Breeding

Generation of *Erg* floxed mice was carried out by genOway. LoxP sequences were inserted around exon 6. Deletion of this exon leads to a frameshift mutation resulting in a premature stop codon in exon 7. *Erg*^{fl/fl} mice were crossed with the following *Cre* transgenic deleter lines: *Cdh5(PAC)-CreERT2* (Wang et al., 2010) and *Tie2-Cre* (Kisanuki et al., 2001). All experiments were conducted in accordance with the Animals (Scientific Procedures) Act of 1986.

Postnatal Retinal Angiogenesis

Mice were administered Tamoxifen (50 μ g per mouse; Sigma) by intraperitoneal injection (IP) at postnatal (P) day 1, P2 and P3. Retinas were collected at P6 and processed as described (Pitulescu et al., 2010).

Syngeneic Tumor Experiments

Mouse melanoma B16F0 tumors were grown in tamoxifen-treated adult *Erg*^{fl/fl} and *Erg*^{IEC-KO} mice as described (Reynolds et al., 2002).

In Vivo LiCl Treatment

LiCl or NaCl (400 mg/kg, dissolved in water) was injected IP into pregnant female mice at E8.5 and E9.5. Embryos were harvested at E10.5 and yolk sac vasculature was analyzed by light microscopy and immunostaining.

In Vivo Matrigel Angiogenesis Assay

C57BL/6 mice received a subcutaneous injection of Matrigel (BD Biosciences), as described (Birdsey et al., 2008). Matrigel was supplemented with 80 nanogram (ng)/ml bFGF (R&D Systems), or with 100 ng/ml murine VEGF-A₁₆₅ (Peprotech) containing 10⁹ plaque-forming unit adenovirus expressing either Lacz or ERG. After 3, 7, or 10 days, 100 μ l of a 1:1 mixture of 10 mg/ml Dextran:FITC (2 \times 10⁶ MW) and Dextran:TRITC (4.4 \times 10⁴ MW) was injected intravenously 15 min prior to harvesting plugs. Plugs were imaged whole-mount using confocal microscopy. Volocity software (Perkin Elmer) was used to reconstruct 3D images of the vessels from serial Z-sections. The extent of TRITC-dextran tracer extravasation was quantified by subtracting the signal corresponding to

Figure 5. ERG Regulates Angiogenesis through Wnt/ β -Catenin Signaling

(A) In vitro Brdu incorporation in control and ERG-deficient HUVEC treated in presence or absence of LiCl (n = 4).

(B–D) (B) Representative images of EC sprouts on fibrin gel beads using siCtrl or siERG-treated HUVEC in the presence or absence of LiCl; (C) quantification of numbers of sprouts; and (D) tube length (n = 20).

(E) (Top) Representative whole mount images of E10.5 *Erg*^{fl/fl} and *Erg*^{IEC-KO} embryo yolk sacs from pregnant female mice treated with either NaCl (left) or LiCl (right) at E8.5 and E9.5. Scale bar, 1 mm (n = 5). (Middle and bottom panels) Endomucin staining of yolk sac vasculature; scale bar, 100 μ m.

(F) Quantification of yolk sac vitelline vessel diameter.

(G) qPCR analysis of LiCl-treated *Erg*^{fl/fl} and *Erg*^{IEC-KO} embryo yolk sacs. Data are expressed as fold change versus NaCl-treated *Erg*^{fl/fl} and are \pm SEM from at least three mice per group. All graphical data are \pm SEM, *p < 0.05, **p < 0.01, and ***p < 0.001. See also [Figure S5](#).

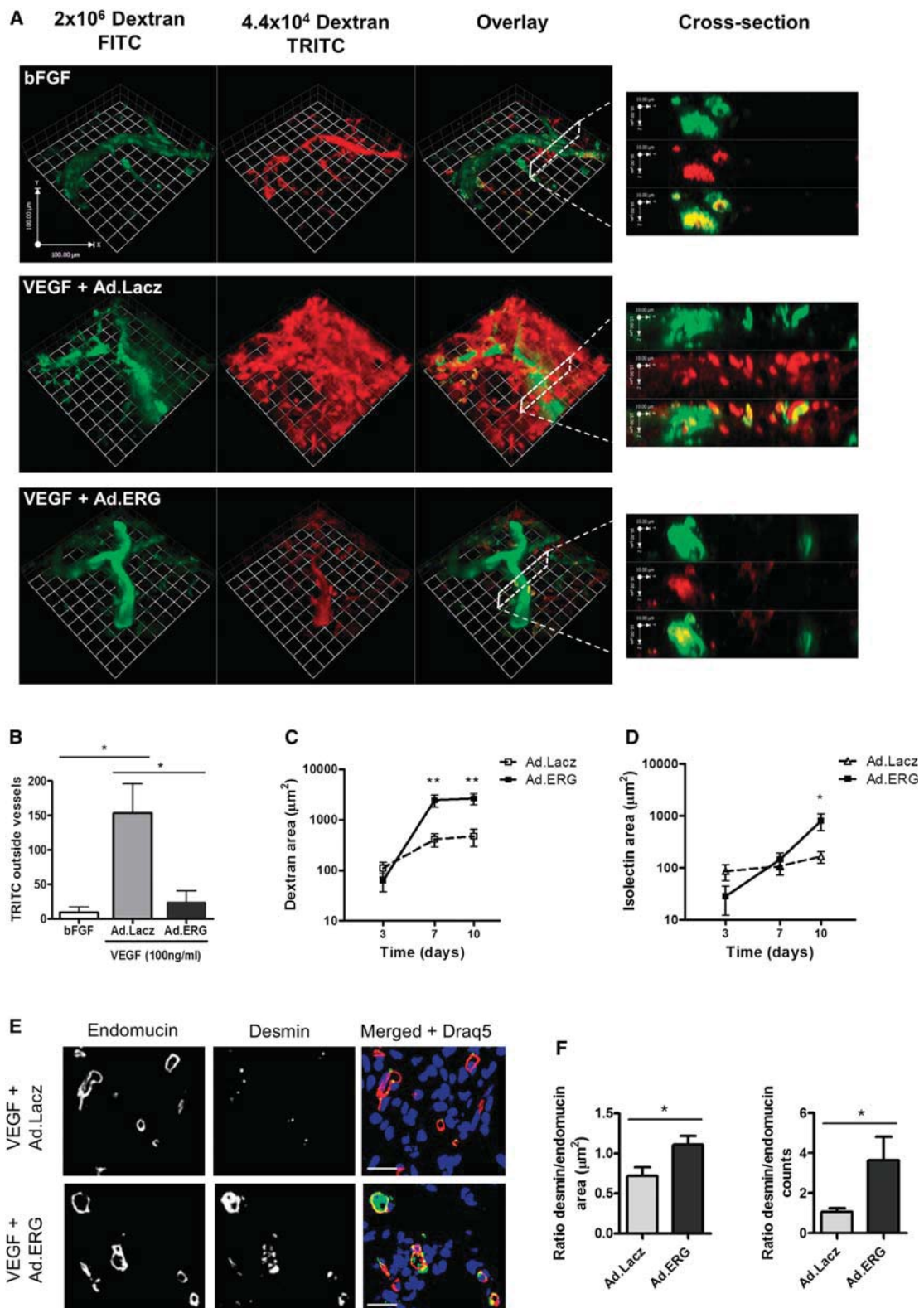


Figure 6. ERG Stabilizes Angiogenesis In Vivo

Matrigel containing bFGF or VEGF with adenovirus expressing either Lacz (Ad.Lacz) or ERG (Ad.ERG) was injected into C57BL6 mice. There were two labeled dextran molecules of different molecular weights, 2×10^6 MW (FITC, green) and 4.4×10^4 MW (TRITC, red), that were injected intravenously 15 min prior to harvesting plugs.

243

(legend continued on next page)

the FITC-dextran tracer (intravascular) from the signal corresponding to the TRITC-dextran tracer (intravascular + extravascular).

Isolation of Mouse Lung Endothelial Cells

Primary mouse lung EC were isolated from control *Erg^{fl/fl}* and *Erg^{cEC-het}* mice as described (Reynolds et al., 2002). Rat APC-CD31, anti-ICAM-2, and anti-rat PE antibodies (all BD Biosciences) were used to assess the EC purity by flow cytometric analysis using a Cyan flow cytometer (Beckman Coulter).

Cell Culture

Primary HUVEC were harvested from umbilical cords (Birdsey et al., 2008). Human *ERG* expression was inhibited using either GeneBloc antisense oligonucleotides (Silence Therapeutics) (McLaughlin et al., 2001) or siRNA against *ERG* (Hs_ERG_7); both denoted as siERG in the text. Control GeneBloc antisense or AllStars Negative Control siRNA (QIAGEN) are denoted as siCtrl.

ChIP-qPCR

ChIP was performed using ChIP-IT express (Active Motif) as previously described (Birdsey et al., 2012).

Plasmid Transfections and Reporter Assays

For Fzd4 transactivation assays, a 1,010-bp region of the Fzd4 promoter (SwitchGear, Active Motif) was cloned into the pGL4 Luciferase Reporter Vector (Promega). TCF reporter constructs TOPFLASH and FOPFLASH were used to measure the transcriptional activity of β -catenin/TCF (Korinek et al., 1997). In some experiments, cells were cotransfected with a pCMV6-Fzd4 expression construct, purchased from (Origene). Reporter assays were performed using the Dual-Luciferase Reporter Assay System (Promega).

BrdU In Vitro Proliferation Assay

Cell proliferation was determined in vitro using a BrdU proliferation ELISA kit (Roche) according to the manufacturer's instructions.

Fibrin Gel Bead Assay

The 3D in vitro model of angiogenesis was performed as described previously (Nakatsu et al., 2007).

Statistical Analysis

Values are presented as means \pm SEM. Statistical significance was determined by using unpaired two-tailed Student's *t* test. Differences were considered significant with a *p* value $<$ 0.05.

SUPPLEMENTAL INFORMATION

Supplemental Information includes Supplemental Experimental Procedures, six figures, and two movies and can be found with this article online at <http://dx.doi.org/10.1016/j.devcel.2014.11.016>.

AUTHOR CONTRIBUTIONS

G.M.B. designed, carried out, and supervised in vivo and in vitro experiments, analyzed and interpreted results, and wrote the manuscript. A.V.S. designed and carried out in vitro experiments, analyzed, interpreted, and conceptualized results, and wrote the manuscript. N.D. designed and performed in vivo experiments, analyzed, and interpreted results. B.G. provided advice on bioinformatic analysis and interpretation and contributed to scientific discussion; Y.Y. performed bioinformatic analysis and interpretation; and L.R. and K.H.D. performed and supervised the tumor angiogenesis experiments, analyzed re-

sults, and contributed to scientific discussion. L.O.A. and S.T.K. performed experiments and analyzed results. I.M.A. provided advice on retina isolation and optimized ERG retinal staining; E.D. provided reagents and contributed to scientific discussion; J.C.M. contributed to scientific discussion; H.G. provided advice and contributed to scientific discussion; R.H.A. assisted in the design of the transgenic mice, provided reagents, advice, and contributed to scientific discussion; and A.M.R. provided funding, conceived, designed, and supervised the study, interpreted results, and wrote the manuscript.

ACKNOWLEDGMENTS

We thank M. Pitulescu (Max Planck Institute for Molecular Biomedicine, Münster, Germany) for advice; H. Clevers (Hubrecht Institute for Developmental Biology and Stem Cell Research, Utrecht, Netherlands) for providing the TOPFLASH TCF reporter and control FOPFLASH plasmids; F.W. Luscin-skas (Harvard Medical School, Boston, MA) for providing the VE-cadherin GFP adenovirus; L. Lawrence (Imperial College London, UK) for technical assistance; G. Cossu (University of Manchester, UK) for critical reading of the manuscript; and A. Taddei (Cancer Research UK, London, UK), M. Johns (Imperial College London, UK), and D. Haskard (Imperial College London, UK) for helpful discussions. This work was funded by grants from the British Heart Foundation (PG/09/096 and RG/11/17/29256). A.V.S. is a recipient of a National Lung and Heart Institute Foundation Studentship. I.M.A. is a recipient of a DOC-fORTE fellowship of the Austrian Academy of Sciences at the London Research Institute.

Received: June 13, 2014

Revised: September 24, 2014

Accepted: November 10, 2014

Published: January 12, 2015

REFERENCES

- Alastalo, T.P., Li, M., Perez, Vde.J., Pham, D., Sawada, H., Wang, J.K., Koskenvuo, M., Wang, L., Freeman, B.A., Chang, H.Y., and Rabinovitch, M. (2011). Disruption of PPAR γ / β -catenin-mediated regulation of apelin impairs BMP-induced mouse and human pulmonary arterial EC survival. *J. Clin. Invest.* 121, 3735–3746.
- Baltzinger, M., Mager-Heckel, A.M., and Remy, P. (1999). XI erg: expression pattern and overexpression during development plead for a role in endothelial cell differentiation. *Dev. Dyn.* 216, 420–433.
- Birdsey, G.M., Dryden, N.H., Amsellem, V., Gebhardt, F., Sahnun, K., Haskard, D.O., Dejana, E., Mason, J.C., and Randi, A.M. (2008). Transcription factor Erg regulates angiogenesis and endothelial apoptosis through VE-cadherin. *Blood* 111, 3498–3506.
- Birdsey, G.M., Dryden, N.H., Shah, A.V., Hannah, R., Hall, M.D., Haskard, D.O., Parsons, M., Mason, J.C., Zvelebil, M., Gottgens, B., et al. (2012). The transcription factor Erg regulates expression of histone deacetylase 6 and multiple pathways involved in endothelial cell migration and angiogenesis. *Blood* 119, 894–903.
- Birney, E., Stamatoyannopoulos, J.A., Dutta, A., Guigó, R., Gingeras, T.R., Margulies, E.H., Weng, Z., Snyder, M., Dermitzakis, E.T., Thurman, R.E., et al.; ENCODE Project Consortium; NISC Comparative Sequencing Program; Baylor College of Medicine Human Genome Sequencing Center; Washington University Genome Sequencing Center; Broad Institute; Children's Hospital Oakland Research Institute (2007). Identification and analysis of functional elements in 1% of the human genome by the ENCODE pilot project. *Nature* 447, 799–816.

(A) 3D rendering of confocal microscopy images of whole-mount Matrigel plugs perfused with the dextran tracers. Cross sectioning through neovessels (right) shows localization of the tracers.

(B) Vessel permeability was quantified by measuring the amount of dextran-TRITC present outside of the dextran-FITC positive vessels, arbitrary units (*n* = 3).

(C) Perfused vessels were quantified by measuring the area of dextran-FITC within the Matrigel plug after 3, 7, and 10 days (*n* = 4).

(D) Vessel density was quantified by measuring the area of isolectin B4 within the Matrigel plug after 3, 7, and 10 days (*n* = 4).

(E) Endomucin (red), desmin-positive pericytes (green), and Draq5 (blue) staining of cryosections from Matrigel plugs implanted for 7 days; scale bar, 20 μ m.

(F) Quantification of pericyte coverage, pixel intensity (*n* = 8). All graphical data are \pm SEM, **p* < 0.05, and ***p* < 0.01. See also Figure S6.

- Bussolati, B., Ahmed, A., Pemberton, H., Landis, R.C., Di Carlo, F., Haskard, D.O., and Mason, J.C. (2004). Bifunctional role for VEGF-induced heme oxygenase-1 in vivo: induction of angiogenesis and inhibition of leukocytic infiltration. *Blood* 103, 761–766.
- Cattellino, A., Liebner, S., Gallini, R., Zanetti, A., Balconi, G., Corsi, A., Bianco, P., Wolburg, H., Moore, R., Oreda, B., et al. (2003). The conditional inactivation of the beta-catenin gene in endothelial cells causes a defective vascular pattern and increased vascular fragility. *J. Cell Biol.* 162, 1111–1122.
- Corada, M., Nyqvist, D., Orsenigo, F., Caprini, A., Giampietro, C., Taketo, M.M., Iruela-Arispe, M.L., Adams, R.H., and Dejana, E. (2010). The Wnt/ β -catenin pathway modulates vascular remodeling and specification by upregulating Dll4/Notch signaling. *Dev. Cell* 18, 938–949.
- Dejana, E. (2010). The role of wnt signaling in physiological and pathological angiogenesis. *Circ. Res.* 107, 943–952.
- Franco, C.A., Liebner, S., and Gerhardt, H. (2009). Vascular morphogenesis: a Wnt for every vessel? *Curr. Opin. Genet. Dev.* 19, 476–483.
- Gerhardt, H., Wolburg, H., and Redies, C. (2000). N-cadherin mediates pericytic-endothelial interaction during brain angiogenesis in the chicken. *Dev. Dyn.* 218, 472–479.
- Giampietro, C., Taddei, A., Corada, M., Sarra-Ferraris, G.M., Alcalay, M., Cavallaro, U., Orsenigo, F., Lampugnani, M.G., and Dejana, E. (2012). Overlapping and divergent signaling pathways of N-cadherin and VE-cadherin in endothelial cells. *Blood* 119, 2159–2170.
- Giles, R.H., van Es, J.H., and Clevers, H. (2003). Caught up in a Wnt storm: Wnt signaling in cancer. *Biochim. Biophys. Acta* 1653, 1–24.
- Goodwin, A.M., and D'Amore, P.A. (2002). Wnt signaling in the vasculature. *Angiogenesis* 5, 1–9.
- Goodwin, A.M., Sullivan, K.M., and D'Amore, P.A. (2006). Cultured endothelial cells display endogenous activation of the canonical Wnt signaling pathway and express multiple ligands, receptors, and secreted modulators of Wnt signaling. *Dev. Dyn.* 235, 3110–3120.
- Gory, S., Dalmon, J., Prandini, M.H., Kortulewski, T., de Launoit, Y., and Huber, P. (1998). Requirement of a GT box (Sp1 site) and two Ets binding sites for vascular endothelial cadherin gene transcription. *J. Biol. Chem.* 273, 6750–6755.
- Griffin, C.T., Curtis, C.D., Davis, R.B., Muthukumar, V., and Magnuson, T. (2011). The chromatin-remodeling enzyme BRG1 modulates vascular Wnt signaling at two levels. *Proc. Natl. Acad. Sci. USA* 108, 2282–2287.
- Gupta, S., Iljin, K., Sara, H., Mpindi, J.P., Mirtti, T., Vainio, P., Rantala, J., Alanen, K., Nees, M., and Kallioniemi, O. (2010). FZD4 as a mediator of ERG oncogene-induced WNT signaling and epithelial-to-mesenchymal transition in human prostate cancer cells. *Cancer Res.* 70, 6735–6745.
- Hellström, M., Gerhardt, H., Kalén, M., Li, X., Eriksson, U., Wolburg, H., and Betsholtz, C. (2001). Lack of pericytes leads to endothelial hyperplasia and abnormal vascular morphogenesis. *J. Cell Biol.* 153, 543–553.
- Jain, R.K. (2003). Molecular regulation of vessel maturation. *Nat. Med.* 9, 685–693.
- Jho, E.H., Zhang, T., Domon, C., Joo, C.K., Freund, J.N., and Costantini, F. (2002). Wnt/ β -catenin/Tcf signaling induces the transcription of Axin2, a negative regulator of the signaling pathway. *Mol. Cell Biol.* 22, 1172–1183.
- Kisanuki, Y.Y., Hammer, R.E., Miyazaki, J., Williams, S.C., Richardson, J.A., and Yanagisawa, M. (2001). Tie2-Cre transgenic mice: a new model for endothelial cell-lineage analysis in vivo. *Dev. Biol.* 230, 230–242.
- Korinek, V., Barker, N., Morin, P.J., van Wichen, D., de Weger, R., Kinzler, K.W., Vogelstein, B., and Clevers, H. (1997). Constitutive transcriptional activation by a beta-catenin-Tcf complex in APC^{-/-} colon carcinoma. *Science* 275, 1784–1787.
- Korn, C., Scholz, B., Hu, J., Srivastava, K., Wojtarowicz, J., Arnsperger, T., Adams, R.H., Boutros, M., Augustin, H.G., and Augustin, I. (2014). Endothelial cell-derived non-canonical Wnt ligands control vascular pruning in angiogenesis. *Development* 141, 1757–1766.
- Li, Y., Kong, D., Wang, Z., Ahmad, A., Bao, B., Padhye, S., and Sarkar, F.H. (2011). Inactivation of AR/TMPRSS2-ERG/Wnt signaling networks attenuates the aggressive behavior of prostate cancer cells. *Cancer Prev. Res. (Phila.)* 4, 1495–1506.
- Liebner, S., Corada, M., Bangsow, T., Babbage, J., Taddei, A., Czupalla, C.J., Reis, M., Felici, A., Wolburg, H., Fruttiger, M., et al. (2008). Wnt/ β -catenin signaling controls development of the blood-brain barrier. *J. Cell Biol.* 183, 409–417.
- Liu, F., and Patient, R. (2008). Genome-wide analysis of the zebrafish ETS family identifies three genes required for hemangioblast differentiation or angiogenesis. *Circ. Res.* 103, 1147–1154.
- Loughran, S.J., Kruse, E.A., Hacking, D.F., de Graaf, C.A., Hyland, C.D., Willson, T.A., Henley, K.J., Ellis, S., Voss, A.K., Metcalf, D., et al. (2008). The transcription factor Erg is essential for definitive hematopoiesis and the function of adult hematopoietic stem cells. *Nat. Immunol.* 9, 810–819.
- Masckauchan, T.N., Shawber, C.J., Funahashi, Y., Li, C.M., and Kitajewski, J. (2005). Wnt/ β -catenin signaling induces proliferation, survival and interleukin-8 in human endothelial cells. *Angiogenesis* 8, 43–51.
- McLaughlin, F., Ludbrook, V.J., Cox, J., von Carlowitz, I., Brown, S., and Randi, A.M. (2001). Combined genomic and antisense analysis reveals that the transcription factor Erg is implicated in endothelial cell differentiation. *Blood* 98, 3332–3339.
- Mochmann, L.H., Bock, J., Ortiz-Tánchez, J., Schlee, C., Bohne, A., Neumann, K., Hofmann, W.K., Thiel, E., and Baldus, C.D. (2011). Genome-wide screen reveals WNT11, a non-canonical WNT gene, as a direct target of ETS transcription factor ERG. *Oncogene* 30, 2044–2056.
- Nakatsu, M.N., Davis, J., and Hughes, C.C. (2007). Optimized fibrin gel bead assay for the study of angiogenesis. *J. Vis. Exp.* 186.
- Phng, L.K., Potente, M., Leslie, J.D., Babbage, J., Nyqvist, D., Lobov, I., Ondr, J.K., Rao, S., Lang, R.A., Thurston, G., and Gerhardt, H. (2009). Nrarp coordinates endothelial Notch and Wnt signaling to control vessel density in angiogenesis. *Dev. Cell* 16, 70–82.
- Pitulescu, M.E., Schmidt, I., Benedito, R., and Adams, R.H. (2010). Inducible gene targeting in the neonatal vasculature and analysis of retinal angiogenesis in mice. *Nat. Protoc.* 5, 1518–1534.
- Randi, A.M., Sperone, A., Dryden, N.H., and Birdsey, G.M. (2009). Regulation of angiogenesis by ETS transcription factors. *Biochem. Soc. Trans.* 37, 1248–1253.
- Reginato, S., Gianni-Barrera, R., and Banfi, A. (2011). Taming of the wild vessel: promoting vessel stabilization for safe therapeutic angiogenesis. *Biochem. Soc. Trans.* 39, 1654–1658.
- Reis, M., and Liebner, S. (2013). Wnt signaling in the vasculature. *Exp. Cell Res.* 319, 1317–1323.
- Reynolds, L.E., Wyder, L., Lively, J.C., Taverna, D., Robinson, S.D., Huang, X., Sheppard, D., Hynes, R.O., and Hodivala-Dilke, K.M. (2002). Enhanced pathological angiogenesis in mice lacking beta3 integrin or beta3 and beta5 integrins. *Nat. Med.* 8, 27–34.
- Roose, J., Huls, G., van, B.M., Moerer, P., van der Horn, K., Goldschmeding, R., Logtenberg, T., and Clevers, H. (1999). Synergy between tumor suppressor APC and the beta-catenin-Tcf4 target Tcf1. *Science* 285, 1923–1926.
- Shtutman, M., Zhurinsky, J., Simcha, I., Albanese, C., D'Amico, M., Pestell, R., and Ben-Ze'ev, A. (1999). The cyclin D1 gene is a target of the beta-catenin/LEF-1 pathway. *Proc. Natl. Acad. Sci. USA* 96, 5522–5527.
- Sperone, A., Dryden, N.H., Birdsey, G.M., Madden, L., Johns, M., Evans, P.C., Mason, J.C., Haskard, D.O., Boyle, J.J., Paleolog, E.M., and Randi, A.M. (2011). The transcription factor Erg inhibits vascular inflammation by repressing NF- κ B activation and proinflammatory gene expression in endothelial cells. *Arterioscler. Thromb. Vasc. Biol.* 31, 142–150.
- Stambolic, V., Ruel, L., and Woodgett, J.R. (1996). Lithium inhibits glycogen synthase kinase-3 activity and mimics wingless signalling in intact cells. *Curr. Biol.* 6, 1664–1668.
- Vijayaraj, P., Le Bras, A., Mitchell, N., Kondo, M., Juliao, S., Wasserman, M., Beeler, D., Spokes, K., Aird, W.C., Baldwin, H.S., and Oettgen, P. (2012). Erg is a crucial regulator of endocardial-mesenchymal transformation during cardiac valve morphogenesis. *Development* 139, 3973–3985.

- Wang, X., Xiao, Y., Mou, Y., Zhao, Y., Blankesteyn, W.M., and Hall, J.L. (2002). A role for the beta-catenin/T-cell factor signaling cascade in vascular remodeling. *Circ. Res.* **90**, 340–347.
- Wang, Y., Nakayama, M., Pitulescu, M.E., Schmidt, T.S., Bochenek, M.L., Sakakibara, A., Adams, S., Davy, A., Deutsch, U., Lüthi, U., et al. (2010). Ephrin-B2 controls VEGF-induced angiogenesis and lymphangiogenesis. *Nature* **465**, 483–486.
- Wu, L., Zhao, J.C., Kim, J., Jin, H.J., Wang, C.Y., and Yu, J. (2013). ERG is a critical regulator of Wnt/LEF1 signaling in prostate cancer. *Cancer Res.* **73**, 6068–6079.
- Wythe, J.D., Dang, L.T., Devine, W.P., Boudreau, E., Artap, S.T., He, D., Schachterle, W., Stainier, D.Y., Oettgen, P., Black, B.L., et al. (2013). ETS factors regulate Vegf-dependent arterial specification. *Dev. Cell* **26**, 45–58.
- Xu, Q., Wang, Y., Dabdoub, A., Smallwood, P.M., Williams, J., Woods, C., Kelley, M.W., Jiang, L., Tasman, W., Zhang, K., and Nathans, J. (2004). Vascular development in the retina and inner ear: control by Norrin and Frizzled-4, a high-affinity ligand-receptor pair. *Cell* **116**, 883–895.
- Ye, X., Wang, Y., Cahill, H., Yu, M., Badea, T.C., Smallwood, P.M., Peachey, N.S., and Nathans, J. (2009). Norrin, frizzled-4, and Lrp5 signaling in endothelial cells controls a genetic program for retinal vascularization. *Cell* **139**, 285–298.
- Yuan, L., Nikolova-Krstevska, V., Zhan, Y., Kondo, M., Bhasin, M., Varghese, L., Yano, K., Carman, C.V., Aird, W.C., and Oettgen, P. (2009). Antiinflammatory effects of the ETS factor ERG in endothelial cells are mediated through transcriptional repression of the interleukin-8 gene. *Circ. Res.* **104**, 1049–1057.
- Yuan, L., Le Bras, A., Sacharidou, A., Itagaki, K., Zhan, Y., Kondo, M., Carman, C.V., Davis, G.E., Aird, W.C., and Oettgen, P. (2012). ETS-related gene (ERG) controls endothelial cell permeability via transcriptional regulation of the claudin 5 (CLDN5) gene. *J. Biol. Chem.* **287**, 6582–6591.
- Zachary, I., and Morgan, R.D. (2011). Therapeutic angiogenesis for cardiovascular disease: biological context, challenges, prospects. *Heart* **97**, 181–189.
- Zhang, L., Gao, X., Wen, J., Ning, Y., and Chen, Y.G. (2006). Dapper 1 antagonizes Wnt signaling by promoting dishevelled degradation. *J. Biol. Chem.* **281**, 8607–8612.

Appendix 2: Permission for third party copyright works

Page Number	Type of work:	Source work	Copyright holder & year	Permission to re-use
27	Figure	Nature. 2011 May 19;473(7347):298-307	© 2011 Nature Publishing Group	✓
33	Figure	Nat Rev Mol Cell Biol. 2004 Apr;5(4):261-70	©2004 Nature Publishing Group	✓
39	Figure	Nat Rev Mol Cell Biol. 2001 Nov;2(11):827-37	©2001 Nature Publishing Group	✓
45	Figure	Gene. 2004 Jan 7;324:65-77	© 2003 Elsevier	✓
54	Figure	Circ Res. 2008 Nov 7;103(10):1147-54	© 2008 Wolters Kluwer Health	✓
141	Figure	Oncogene. 2008 Sep 1;27(38):5148-67	© 2008 Nature Publishing Group	✓
142	Figure	Nat Rev Mol Cell Biol. 2006 Sep;7(9):678-89	© 2006 Nature Publishing Group	✓
147	Figure	Cell. 2009 Jun 12;137(6):1124-35	© 2009 Elsevier	✓

NATURE PUBLISHING GROUP LICENSE TERMS AND CONDITIONS

Dec 30, 2014

This is a License Agreement between Aarti V Shah ("You") and Nature Publishing Group ("Nature Publishing Group") provided by Copyright Clearance Center ("CCC"). The license consists of your order details, the terms and conditions provided by Nature Publishing Group, and the payment terms and conditions.

License Number	3535301257593
License date	Dec 24, 2014
Licensed content publisher	Nature Publishing Group
Licensed content publication	Nature
Licensed content title	Molecular mechanisms and clinical applications of angiogenesis
Licensed content author	Peter Carmeliet, Rakesh K. Jain
Licensed content date	May 18, 2011
Volume number	473
Issue number	7347
Type of Use	reuse in a dissertation / thesis
Requestor type	academic/educational
Format	print and electronic
Portion	figures/tables/illustrations
Number of figures/tables/illustrations	1
High-res required	no
Figures	Figure 2: Molecular basis of vessel branching.
Author of this NPG article	no
Your reference number	None
Title of your thesis / dissertation	The transcription factor ERG mediates multiple endothelial signalling pathways required for angiogenesis
Expected completion date	Jan 2015
Estimated size (number of pages)	200
Total	0.00 GBP

NATURE PUBLISHING GROUP LICENSE TERMS AND CONDITIONS

Dec 30, 2014

This is a License Agreement between Aarti V Shah ("You") and Nature Publishing Group ("Nature Publishing Group") provided by Copyright Clearance Center ("CCC"). The license consists of your order details, the terms and conditions provided by Nature Publishing Group, and the payment terms and conditions.

License Number	3535310014353
License date	Dec 24, 2014
Licensed content publisher	Nature Publishing Group
Licensed content publication	Nature Reviews Molecular Cell Biology
Licensed content title	Endothelial cell-cell junctions: happy together
Licensed content author	Elisabetta Dejana
Licensed content date	Apr 1, 2004
Volume number	5
Issue number	4
Type of Use	reuse in a dissertation / thesis
Requestor type	academic/educational
Format	print and electronic
Portion	figures/tables/illustrations
Number of figures/tables/illustrations	1
High-res required	no
Figures	Figure 1 The organization of endothelial cell-cell junctions.
Author of this NPG article	no
Your reference number	None
Title of your thesis / dissertation	The transcription factor ERG mediates multiple endothelial signalling pathways required for angiogenesis
Expected completion date	Jan 2015
Estimated size (number of pages)	200
Total	0.00 USD

NATURE PUBLISHING GROUP LICENSE TERMS AND CONDITIONS

Dec 30, 2014

This is a License Agreement between Aarti V Shah ("You") and Nature Publishing Group ("Nature Publishing Group") provided by Copyright Clearance Center ("CCC"). The license consists of your order details, the terms and conditions provided by Nature Publishing Group, and the payment terms and conditions.

License Number	3535310592235
License date	Dec 24, 2014
Licensed content publisher	Nature Publishing Group
Licensed content publication	Nature Reviews Molecular Cell Biology
Licensed content title	The ETS-domain transcription factor family
Licensed content author	Andrew D. Sharrocks
Licensed content date	Nov 1, 2001
Volume number	2
Issue number	11
Type of Use	reuse in a dissertation / thesis
Requestor type	academic/educational
Format	print and electronic
Portion	figures/tables/illustrations
Number of figures/tables/illustrations	1
Figures	Figure 1 Structure of the ETS domain and pointed domain of Ets-1.
Author of this NPG article	no
Your reference number	None
Title of your thesis / dissertation	The transcription factor ERG mediates multiple endothelial signalling pathways required for angiogenesis
Expected completion date	Jan 2015
Estimated size (number of pages)	200
Total	0.00 USD

ELSEVIER LICENSE TERMS AND CONDITIONS

Dec 30, 2014

This is a License Agreement between Aarti V Shah ("You") and Elsevier ("Elsevier") provided by Copyright Clearance Center ("CCC"). The license consists of your order details, the terms and conditions provided by Elsevier, and the payment terms and conditions.

Supplier	Elsevier Limited The Boulevard, Langford Lane Kidlington, Oxford, OX5 1GB, UK
Registered Company Number	1982084
Customer name	Aarti V Shah
Customer address	ICTEM Level 5, NHLI, Imperial College London, W12 ONN
License number	3535320711891
License date	Dec 24, 2014
Licensed content publisher	Elsevier
Licensed content publication	Gene
Licensed content title	Detailed mapping of the ERG-ETS2 interval of human chromosome 21 and comparison with the region of conserved synteny on mouse chromosome 16
Licensed content author	C.M. Owczarek, K.J. Portbury, M.P. Hardy, D.A. O'Leary, J. Kudoh, K. Shibuya, N. Shimizu, I. Kola, P.J. Hertzog
Licensed content date	7 January 2004
Licensed content volume number	324
Number of pages	13
Start Page	65
End Page	77
Type of Use	reuse in a thesis/dissertation
Intended publisher of new work	other
Portion	figures/tables/illustrations
Number of figures/tables/illustrations	1
Format	both print and electronic
Original figure numbers	Figure 3 Structure of the human ERG gene
Title of your thesis/dissertation	The transcription factor ERG mediates multiple endothelial signalling pathways required for angiogenesis
Expected completion date	Jan 2015

WOLTERS KLUWER HEALTH LICENSE TERMS AND CONDITIONS

Dec 30, 2014

This is a License Agreement between Aarti V Shah ("You") and Wolters Kluwer Health ("Wolters Kluwer Health") provided by Copyright Clearance Center ("CCC"). The license consists of your order details, the terms and conditions provided by Wolters Kluwer Health, and the payment terms and conditions.

License Number	3535320886220
License date	Dec 24, 2014
Licensed content publisher	Wolters Kluwer Health
Licensed content publication	Circulation Research
Licensed content title	Genome-Wide Analysis of the Zebrafish ETS Family Identifies Three Genes Required for Hemangioblast Differentiation or Angiogenesis
Licensed content author	Feng Liu, Roger Patient
Licensed content date	Nov 7, 2008
Volume Number	103
Issue Number	10
Type of Use	Dissertation/Thesis
Requestor type	Individual
Portion	Figures/table/illustration
Number of figures/tables/illustrations	1
Figures/tables/illustrations used	Figure 6 G-I erg and flil1 are additively required for angiogenesis
Author of this Wolters Kluwer article	No
Title of your thesis / dissertation	The transcription factor ERG mediates multiple endothelial signalling pathways required for angiogenesis
Expected completion date	Jan 2015
Estimated size(pages)	200
Billing Type	Invoice
Billing Address	Aarti V Shah ICTEM Level 5, NHLI, Imperial College Hammersmith Campus Du Cane Road London, United Kingdom W12 0NN Attn: Aarti V Shah
Total	0.00 USD

NATURE PUBLISHING GROUP LICENSE TERMS AND CONDITIONS

Dec 30, 2014

This is a License Agreement between Aarti V Shah ("You") and Nature Publishing Group ("Nature Publishing Group") provided by Copyright Clearance Center ("CCC"). The license consists of your order details, the terms and conditions provided by Nature Publishing Group, and the payment terms and conditions.

License Number	3535321032113
License date	Dec 24, 2014
Licensed content publisher	Nature Publishing Group
Licensed content publication	Oncogene
Licensed content title	The many facets of Notch ligands
Licensed content author	B D'Souza, A Miyamoto and G Weinmaster
Licensed content date	Sep 1, 2008
Volume number	27
Issue number	38
Type of Use	reuse in a dissertation / thesis
Requestor type	academic/educational
Format	print and electronic
Portion	figures/tables/illustrations
Number of figures/tables/illustrations	1
High-res required	no
Figures	Figure 1 Protein structure of the DSL family of ligands
Author of this NPG article	no
Your reference number	None
Title of your thesis / dissertation	The transcription factor ERG mediates multiple endothelial signalling pathways required for angiogenesis
Expected completion date	Jan 2015
Estimated size (number of pages)	200
Total	0.00 USD

NATURE PUBLISHING GROUP LICENSE TERMS AND CONDITIONS

Dec 30, 2014

This is a License Agreement between Aarti V Shah ("You") and Nature Publishing Group ("Nature Publishing Group") provided by Copyright Clearance Center ("CCC"). The license consists of your order details, the terms and conditions provided by Nature Publishing Group, and the payment terms and conditions.

License Number	3536661129685
License date	Dec 26, 2014
Licensed content publisher	Nature Publishing Group
Licensed content publication	Nature Reviews Molecular Cell Biology
Licensed content title	Notch signalling: a simple pathway becomes complex
Licensed content author	Sarah J. Bray
Licensed content date	Sep 1, 2006
Volume number	7
Issue number	9
Type of Use	reuse in a dissertation / thesis
Requestor type	academic/educational
Format	print and electronic
Portion	figures/tables/illustrations
Number of figures/tables/illustrations	1
High-res required	no
Figures	Figure 1 The core Notch pathway
Author of this NPG article	no
Your reference number	None
Title of your thesis / dissertation	The transcription factor ERG mediates multiple endothelial signalling pathways required for angiogenesis
Expected completion date	Jan 2015
Estimated size (number of pages)	200
Total	0.00 GBP

ELSEVIER LICENSE TERMS AND CONDITIONS

Dec 30, 2014

This is a License Agreement between Aarti V Shah ("You") and Elsevier ("Elsevier") provided by Copyright Clearance Center ("CCC"). The license consists of your order details, the terms and conditions provided by Elsevier, and the payment terms and conditions.

Supplier	Elsevier Limited The Boulevard, Langford Lane Kidlington, Oxford, OX5 1GB, UK
Registered Company Number	1982084
Customer name	Aarti V Shah
Customer address	ICTEM Level 5, NHLI, Imperial College London, W12 ONN
License number	3535321140087
License date	Dec 24, 2014
Licensed content publisher	Elsevier
Licensed content publication	Cell
Licensed content title	The Notch Ligands Dll4 and Jagged1 Have Opposing Effects on Angiogenesis
Licensed content author	Rui Benedito, Cristina Roca, Inga Sørensen, Susanne Adams, Achim Gossler, Marcus Fruttiger, Ralf H. Adams
Licensed content date	12 June 2009
Licensed content volume number	137
Licensed content issue number	6
Number of pages	12
Start Page	1124
End Page	1135
Type of Use	reuse in a thesis/dissertation
Intended publisher of new work	other
Portion	figures/tables/illustrations
Number of figures/tables/illustrations	1
Format	both print and electronic
Original figure numbers	Figure 7 A-B Regulation of Sprouting Angiogenesis by Dll4 and Jagged1
Title of your thesis/dissertation	The transcription factor ERG mediates multiple endothelial signalling pathways required for angiogenesis
Expected completion date	Jan 2015
Estimated size (number of pages)	200